INFORMATION TO USERS

This manuscript has been reproduced from the microfilm master. UMI films the text directly from the original or copy submitted. Thus, some thesis and dissertation copies are in typewriter face, while others may be from any type of computer printer.

The quality of this reproduction is dependent upon the quality of the copy submitted. Broken or indistinct print, colored or poor quality illustrations and photographs, print bleedthrough, substandard margins, and improper alignment can adversely affect reproduction.

In the unlikely event that the author did not send UMI a complete manuscript and there are missing pages, these will be noted. Also, if unauthorized copyright material had to be removed, a note will indicate the deletion.

Oversize materials (e.g., maps, drawings, charts) are reproduced by sectioning the original, beginning at the upper left-hand corner and continuing from left to right in equal sections with small overlaps.

Photographs included in the original manuscript have been reproduced xerographically in this copy. Higher quality 6" x 9" black and white photographic prints are available for any photographs or illustrations appearing in this copy for an additional charge. Contact UMI directly to order.

ProQuest Information and Learning
300 North Zeeb Road, Ann Arbor, MI 48106-1346 USA
800-521-0600

Université d'Ottawa · University of Ottawa

The Life and Times of Germanium and Tin Complexes Ligated by Amidinates and Guanidinates

and

Exploratory Studies in the use of these Ligands in the Formation of Iron Complexes

Stephen R. Foley

Thesis submitted to the
School of Graduate Studies and Research
University of Ottawa
In partial fulfillment of the requirements for the
Ph.D. degree in the
Ottawa-Carleton Chemistry Institute

Candidate

Stephen R. Foley

Supervisor

Professor Darrin Richeson

In Memory of my Father
Robert James Foley
Among his many gifts
Was his continual support for me in all my pursuits

and

Dedicated to my Mother
Alma Foley
Whose courage, intelligence and compassion far surpass my own
and of whom I have always been immensely proud

Abstract

The overall objectives in the creation of this work were to investigate the structure and reactivity of the group 14 elements germanium and tin supported by amidinates and guanidinates. Prior to our work in the area, no amidinato complexes of germanium had been reported and no investigations into the reactivity of tin amidinates had ever been performed. We envisioned that amidinates could offer kinetic and thermodynamic stabilizing features that could allow the formation of unusual functions such as heteronuclear multiple bonds in the heavy main group and the formation of rare chalcogenido complexes. We further proposed to use these species in the study of metal mediated single chalcogen atom exchange reactions and to extend the reactivity of these group 14 chalcogenido complexes through explorations of their catalytic potential. Ultimately, the scope of this work was broadened to the use of amidinates and guanidiantes in the formation of Fe(II/III) species.

Chapter One outlines features of the supporting ligation used throughout the thesis.

Chapter Two describes the first characterized amidinate complexes of Ge using alkylamidinates as ancillary ligands. Spectroscopic and structural characterization of the two complexes, $(CyNC(Me)NCy)_2Ge^{II}$ and $(CyNC(^tBu)NCy)_2Ge^{II}$ (Cy = cyclohexyl), revealed that the Ge coordination geometry is distorted tetrahedral in which one of the vertices is occupied by a lone pair of electrons. Both complexes exhibited one bidentate and one monodentate ("dangling") ligand. Rapid oxidative addition of chalcogen atom sources (styrene sulfide and Se) to these complexes resulted in a series of rare terminal chalcogenido complexes with formulae $(CyNC(R)NCy)_2Ge{=}Ch$ [R = Me; Ch = S, Se; R = ^{t}Bu; Ch = S, Se]. Mixed amidinato-amido analogues were similarly obtained. For example, $[(CyNC(R)NCy)Ge^{II}[N(SiMe_3)_2]$, (R = Me, ^{t}Bu) react to yield the corresponding terminal chalcogenido complexes.

Chapter Three represents the first comprehensive study of a heteronuclear intermetal two-electron sulfur atom transfer between Sn and Ge. Complete sulfur atom exchange between amidinate complexes of tin and germanium was achieved through the reaction of $(CyNC(^tBu)NCy)_2Sn{=}S$ with $(CyNC(^tBu)NCy)_2Ge$ to form the corresponding germanium sulfide (Ge=S) and stannylene. This process can be readily monitored by NMR. The amidinato ligand system provides excellent spectroscopic handles to monitor the progress of the reaction. Rate constants for sulfur atom transfer reactions were found to vary from 1.18×10^{-3} to 2.14×10^{-2} $M^{-1}s^{-1}$ at temperature ranges from 25 to 65°C. The temperature dependence yielded activation parameters $\Delta H^{\ddagger}$= 17.6 kcal/mol and $\Delta S^{\ddagger}$= -14.4 cal$(mol\cdot K)^{-1}$. Rapid chalcogen atom exchange from P to Ge was also observed when

the chalcogen was selenium, however no reaction was observed when the chalcogen was sulfur.

Chapter Four is concerned with the cleavage of chalcogen-chalcogen bonds as routes to the formation of rare chalcogenolates of tin and germanium.

Unusual cyclic tin tetrasulfido complexes $\{(CyNC(R)NCy)[N(SiMe_3)_2]\}MS_4$ (M = Sn, R = Me, ^{t}Bu; M = Ge, R = Me) were prepared by the reaction of elemental sulfur with the divalent group 14 starting materials $[CyNC(R)NCy]M[N(SiMe_3)_2]$ (M = Sn, R = Me, tBu; M = Ge, R = Me). The tin tetrasulfido complexes were further converted to dimeric bridging sulfido complexes, $\{(CyNC(R)NCy)[N(SiMe_3)_2]Sn(\mu\text{-}S)\}_2$ (R = Me, tBu) which can also be derived from the oxidative addition of sulfur atom sources (e.g. propylene sulfide) to the respective divalent starting materials. The germanium tetrasufido analogue undergoes no such conversion however it does react with phenyl isothiocyanate to generate the polyhedral sesquisulfide complex $[(Me_3Si)_2NGeE_{1.5}]_4$.

Oxidative addition of diphenyldichalcogenides, PhE-EPh (E = S, Se) to Ge(II) and Sn(II) amidinate complexes is also reported. In the case of the bis(alkylamidinato)Ge complexes, $Ge(CyNC(R)NCy)_2$ (R = Me, ^{t}Bu), the six-coordinate Ge(IV) compounds $(PhE)_2Ge(CyNC(R)NCy)_2$ were isolated and characterized. Mixed amidinato-amido species, $M(CyNC(R)NCy)[N(SiMe_3)_2]$ (M = Ge, Sn; R = Me, ^{t}Bu), react in a similar manner to yield novel bis(phenylchalcogenolate) complexes of Sn and Ge. Spectroscopic features and single crystal structural analysis indicate that this ligand environment appears to favor Ge(IV) complexes with a strong disposition towards a tetrahedral geometry. In these cases, a five coordinate environment for the metal center is avoided by one of the amidinate ligands exhibiting a monodentate coordination mode, which preserves the pseudotetrahedral metal coordination geometry. These observations contrast with the Sn(II/IV) analogues which exhibit no such tendency. For example the single crystal structure of $(PhS)_2Sn(CyNC(Me)NCy)[N(SiMe_3)_2]$ displays a bidentate ligand and a five coordinate metal coordination geometry.
$(PhSe)_2Ge(CyNC(Me)NCy)[N(SiMe_3)_2]$ reacts with elemental Se to generate the terminal germanium selenide and regenerate PhSeSePh. Concomitant with this reaction is a rearrangement of the previously monodentate amidinate ligand to a bidentate coordination mode.

In **Chapter Five** mixed amidinato amido complexes $[Me_3SiNC(^tBu)NSiMe_3]M[N(SiMe_3)_2]$ (M = Sn, Ge) were prepared by the reaction of $[Me_3SiNC(^tBu)NSiMe_3]Li$ with $SnCl_2$ and $GeCl_2$(dioxane) in ether. The $N(SiMe_3)_2$ ligand in these compounds is derived from the rearrangement of the $[Me_3SiNC(^tBu)NSiMe_3]^-$ anion with extrusion of ^{t}BuCN. The susceptibility of $[Me_3SiNC(^tBu)NSiMe_3]^-$ to rearrangement appears to be dependent on reaction solvent and on the coordinated metal center. Replacement of Me for ^{t}Bu in the ligand allowed $[Me_3SiNC(Me)NSiMe_3]_2Sn^{II}$ to be isolated. This indicates that steric factors also play a role in the stability of $[Me_3SiNC(^tBu)NSiMe_3]^-$.

The focus of **Chapter Six** is on the catalytic cyclotrimerization of isocyanates to perhydro-1,3,5-triazine-2,4,6-triones (isocyanurates) at room temperature.

The cyclic tin and germanium tetrasulfido complexes from Chapter Four as well as the (alkylamidinato)(amido)M(II) species from Chapter Five function as outstanding catalysts for the rapid and selective catalytic cyclotrimerization of aryl isocyanates to yield isocyanurates. The tetrasulfido complex $\{(CyNC(Me)NCy)[N(SiMe_3)_2]\}SnS_4$ catalyzes the trimerization of phenyl isocyanate quantitatively and purely within minutes of addition of complex to neat isocyanate. For example, with 2 mol % catalyst a 95% isolated yield of pure triphenyl isocyanurate is obtained within 12 minutes at room temperature.

The germanium tetrasulfido species is even more active than its tin analogue where catalysis of PhNCO is complete in under 30 seconds. In contrast, $[Me_3SiNC(Me)NSiMe_3]_2Sn^{(II)}$ catalytically reacts with phenyl isocyanate to produce isocyanate dimer and trimer in a 52:35 ratio.

In **Chapter Seven**, we investigate the use of monoanionic N,N',N"-trisubstituted guanidinates as well as the anion of 1,3,4,6,7,8-hexahydro-2H-pyramido[1,2-a]pyramidine (Hhpp) in the formation of both Sn(II) and Sn(IV) complexes.

The reaction of triisopropyl guanidine with one equivalent $SnCl_4$ proceeds smoothly at room temperature to give $[(^iPrN)_2CN(H)^iPr]SnCl_3$. Reaction of tin halides with a lithium guanidinate offers an alternative metathical route for introduction of guanidinate anions. Lithium N,N',N"-tricyclohexyl guanidinate reacts with 0.5 equiv of $SnCl_2$ to give $[(CyN)_2C(HNCy)]_2Sn^{II}$. The first hpp complexes of tin were also prepared through addition of hppLi to tin halides. Contrary to reported transition metal complexes, the bis-hpp complexes $(hpp)_2Sn^{II}$ and hpp_2SnCl_2 were mononuclear with bidentate hpp ligands. Reducing the coordination number and steric bulk about tin by preparing the mono hpp Sn(II) complex $(hppSnCl)_2$ resulted in the formation of a dinuclear species with bridging hpp ligands.

Chapter Eight deals with investigations into the formation of amidinate and guanidinate complexes of both Fe(II) and Fe(III). Presented in this Chapter are results regarding the use of N, N'-dicyclohexylformamidinate as a ligand with Fe(II) to yield $Fe_4(\mu_4\text{-}O)(\mu\text{-}Br)_2(\mu\text{-}CyNCHNCy)_4$. When the bulky alkyl amidinate $CyNC^tBuNCy^-$ is employed with Fe(II), the only known mononuclear Fe(II) alkylamidinate species $Fe(CyNC^tBuNCy)_2$ results. This chemistry is further extended by introducing the $CyNC^tBuNCy^-$ into the coordination sphere of Fe(III) to form the monomeric species $(CyNC^tBuNCy)_2FeCl$.

The application of guanidinates as ligands with Fe(II) and (III) has led to a range of complexes. For example, the use of trisubstituted guanidinates as ligands resulted in the formation of the dinuclear Fe(II) species $[\mu\text{-}(RN)_2C(HNR)]_2Fe_2[(RN)_2C(HNR)]_2$, R = iPr, Cy as well as $[\mu\text{-}(CyN)_2C(HNCy)]_2Fe_2Br_2$. With Fe(III), the mononuclear species $[(^iPrN)_2C(HN^iPr)]_2FeCl$ is formed. The use of bulky tetrasubstituted guanidinates resulted in the formation of mononuclear species $[(^iPrN)_2C(N(SiMe_3)_2)]_2Fe$. Subsequent alkylation attempts resulted in the formation of dianionic guanidinate complexes $[(^iPrN)_2C{=}N^iPr]_2Fe_2[(^iPrN)_2C(HN^iPr)Li]_2$ and $Li_2(THF)Fe[(^iPrN)_2CN^iPr](CH_2SiMe_3)_2$ as well as the rearrangement product $[\mu\text{-}(^iPrNCN^iPr)_2(HN^iPr)]Fe_2[(^iPrN)_2C(HN^iPr)]_2$.

What the critics are saying...

"It is a sick, sick world when the confidence and investment of an astute scholarly institute is justified by a work of unparalleled depravity. The majority of the literate public will be relieved that only reviewers are obliged to look at any of it."

- *The Globe and Mail*

"Satisfyingly complex...finishes in a rollercoaster of twists...absorbing & intriguing...prepare for no sleep...genuine suspense, realistic emotion, and a concluding payoff that makes the effort worthwhile...a provocative debut."

- Heather Pettit, *The Village Voice*

"As a piece of writing, this thesis soars to the level of mediocrity. Perhaps it is all a joke, meant to fool the literary world into respect for rubbish."

- *The Sun*

"If I was stranded on a desert island with just one person and just one book, I would choose Stephen Foley and this thesis. And then I would beat one to death with the other."

- Seán Barry, *The Harvard Press*

"...geoff went to the zoo to tend to the llmas named steve. They were all named steve and they babbled all the time about the elusive ubiquitous ligand, what the hell...those damn llamas always ranting."

– Kitty, *The Montasourri News*

"It reads like a good chemical sleuth story... but it is not fiction. It is a painstakingly detailed history of four years worth of sweat and tears... It rivals in power and intensity to Truman Capote's *In Cold Blood.*"

-*Chicago Tribune*

A wild read. Its like god is your copilot and satan is keeping your foot on the gas.

-*Rolling Stone*

"A thin skin of insight for such a huge sausage of redundancy. Perhaps an easily wrapped gift for the 13th day of the alchemists Christmas, but not yet a patchcord between the guitar of curiosity and the amplifier of life.

Therefore,.....sadly, ...we conclude that Mr. Foley is more adept at 4:00 a.m. chess than he is at challenging the low-brow world of academic H's and O_2's."

-Joff Ward, *The Benign Chronicles*

Acknowledgments

There are many people I have to thank over the course of my existence at the University of Ottawa. First and foremost would be Darrin Richeson. A better supervisor could not be had. His support, dedication, intellect, wit and habitual anecdotes have made the experience that much more worthwhile.

There are other professors from whom I have attained or appropriated a greater understanding of chemistry and am indebted to. Sandro "Mr. 16 Chin-ups" Gambarotta for years of insults and frequent gems of knowledge. His tact and savvy are without equal and whose template I can only aspire to one day base my own. Susannah Scott for being so gracious and supporting (despite the occasional derisive remark). Christian Detellier because among other things he is The Dean. Deryn Fogg because... she's Deryn Fogg.

Numerous other individuals about the department have helped me immeasurably. Glenn Yap for all the lithium bromide structures as well as the more useful ones. Glenn Facey for introducing me to albino Jamaicans and with Raj Capoor for performing the NMR experiments that were necessary for my research. Annette, Lise, Monique and Linda for negotiating me through the mounds of red tape that engulf the university.

There are also the many grad students and post docs that I have had the fortune to encounter and work with. In particular, special attention should be called to Yarn Saber, Tan Baptize, Quick Madmen Inferno, Fund Beatify and Gaston Lafleche.

Many thanks to all my friends without whom my life would be very dull. Heather for continually being there. Ump and Oop who live inside my head and keep me in spirits. My sister Christina who has been and continues to go to places I have not even read about.

Publications

Foley, S.R.; Yap, G.P.; Richeson, D.S., "Iron Guanidinate Complexes of a Novel Dinuclear Fe(II) Species with a Dianionic Biguanidinate Ligand", *J. Chem. Soc., Chem. Commun.* **2000**, *in press.*

Foley, S.R.; Richeson, D.S., "Chalcogen Atom Transfer Reactions. Kinetics of Terminal Bonded Sulfur Atom Transfer between Main Group Metal Centers", *J. Chem. Soc., Chem. Commun.* **2000**, *in press.*

Foley, S.R.; Yap, G.P.; Richeson, D.S., "Oxidative Addition to M(II) (M = Ge, Sn) Amidinate Complexes: Routes to Group 14 Chalcogenolates with Hypervalent Coordination Environments", *J. Chem. Soc., Dalton Trans.* **2000**, *10*, 1663.

Foley, S.R.; Zhou, Y.; Yap, G.P.; Richeson, D.S., "Synthesis of M(II)[N(SiMe3)2][Me3SiNC(tBu)NSiMe3] (M = Sn, Ge) From Amidinate Precursors: Active Catalysts for Phenyl Isocyanate Cyclization", *Inorg. Chem.* **2000**, *39*, 924.

Foley, S.R.; Yap, G.P.; Richeson, D.S., "Formation of Novel Tetrasulfido Tin Complexes and Their Ability to Catalyze the Cyclotrimerization of Aryl Isocyanates", *Organometallics* **1999**, *18*, 4700.

Foley, S.R.; Bensimon,C.; Richeson, D.S., "Facile Formation of Rare Terminal Chalcogenido Germanium Complexes with Alkylamidinates as Supporting Ligands", *J. Am. Chem. Soc.* **1997**, *119*, 10359.

My So Called Life In Chemistry

Contents

List of Common Abbreviations

1. Chemicals and Ligands

Bu	butyl (^{t}Bu, tertiary-butyl)
Bz	benzyl
Ch	chalcogen
Cp	cyclopentadiene, C_5H_5
Cp*	pentamethylcyclopentadiene, C_5Me_5
Cy	cyclohexyl
DPhF	diphenylformamidinate anion
E	element
Et	ethyl
HDPhF	diphenylformamidine
Hhpp	1 ,3,4,6,7,8-hexahydro-2H-pyrimido-[1,2-a]-pyrimidine
hpp	the anion of Hhpp
L	ligand
M	central atom (usually a metal) in a compound
Me	methyl
Mes	mesityl
Ph	phenyl, C_6H_5
^{i}Pr	iso-propyl
R	alkyl or aryl group
Tbt	2,4,6-[$(SiMe_3)_2CH]_3C_6H_2$

THF or thf	tetrahydrofuran
Tip	2,4,6-$[(CH_3)CH]_3C_6H_2$
Tp^{tBu_2}	(3,5-di-tert-butylpyrazolyl)hydroborate
TPP	tetraphenylporphyrinato dianion
TTP	*meso*-tetra-*p*-tolylporphyrinato dianion
UAL	Universal Ancillary Ligand
X	halogen

2. Miscellaneous

Å	angstrom unit, 10^{-10}m
BM	Bohr magneton
cm^{-1}	wavenumber
eq	equation
FT	Fourier transform
h	Plank's constant
Hz	hertz
IR	infrared
Mp	melting point
NMR or nmr	nuclear magnetic resonance
ppm	parts per million
R	gas constant
μ	magnetic moment in Bohr magnetons

List of Figures

List of Tables

THE LOSER

Mama said I'd lose my head
If it wasn't fastened on.
Today I guess it wasn't
'Cause while playing with my cousin
It fell off and rolled away
And now it's gone.

And I can't look for it
'Cause my eyes are in it,
And I can't call to it
'Cause my mouth is on it
(Couldn't hear me anyway
'Cause my ears are on it),
Can't even think about it
'Cause my brain is in it.
So I guess I'll sit down
On this rock
And rest for just a minute. . . .

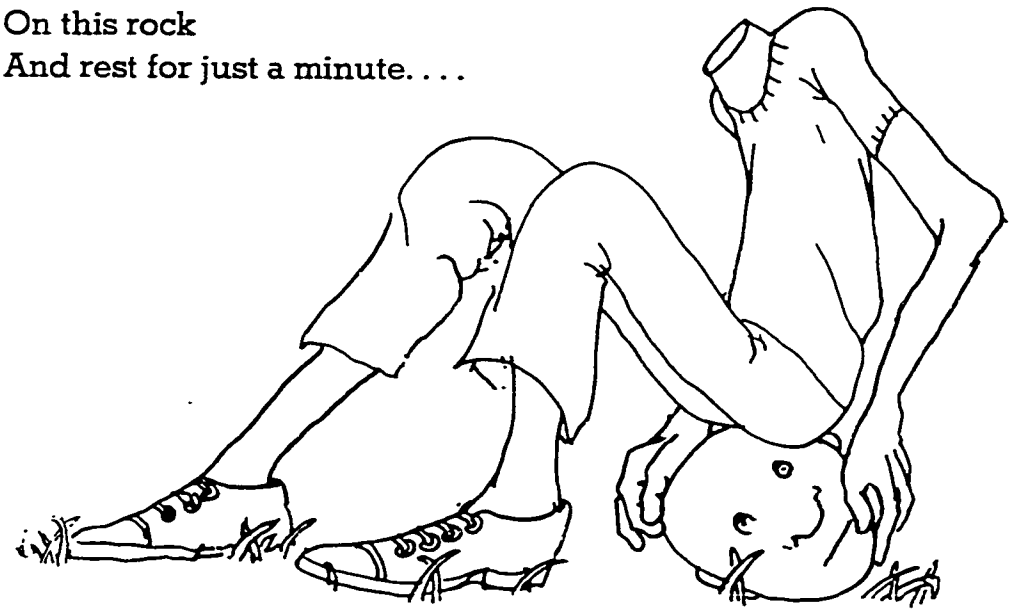

Shel Silverstein

1

The Quest for the Universal Ancillary Ligand

"I know what yer thinking..."

Chapter One

Introduction

Such a great diversity of organometallic and coordination compounds exist that any simple classification scheme would be hopelessly blurred. Metal complexes range from simple hydrated metal ions to complicated metalloenzymes, but one common theme that they all share is a reliance on supporting ligands. Ligands affect coordination number and geometry about a metal center. This in turn influences stereochemistry, magnetic and optical properties as well as electronic and physical properties. In a broad sense, ligands exert influence through steric and electronic features. These two facets allow manipulation of the reactivity and physical properties (i.e. solubility, volatility) of the complex in question.

The focus of this chapter is to introduce the concept of ligand design and how this notion evolved into the ligand set that is employed throughout this work. A chapter is devoted to the subject of ligands to reduce redundancy throughout the remaining chapters.

Given the general influence exerted by ligands on metal complexes, many organometallic and inorganic chemists embark on a quest for the Universal Ancillary Ligand (UAL); a ligand that can be used across the periodic table resulting in complexes that perform a multitude of transformations including activation of small molecules,

organic transformations and the stabilization of rare or heretofore thought impossible species.

A successful UAL would exhibit several features. Among these are: (1) they have to be Lewis bases, (2) they have to be inert (spectator) ligands and (3) they should possess an ease of synthesis including ease of steric and electronic variation. The ability to tune ligand sterics arises from the last point. In order to prevent oligomerization which leads to poor solubility and catalytically inactive species, variability of ligand sterics is desirable.

Examples of commonly employed ligands that meet one or more of these requirements are provided by CO, phosphines, olefins and carboxylates. CO has enjoyed a very rich life in d-block chemistry since the discovery of nickeltetracarbonyl in 1890 due to the fact that CO is a very weak σ base, but an excellent π acid.[1] Other common ligands that are isoelectronic with CO include CN^-, CS and NO^+.[2] These ligands differ significantly from CO and are rarely good analogues usually due to their weak π acid character. As well, no steric or electronic variation can be incorporated into these ligands.

Phosphines can behave as π acceptor ligands, but their strength lies in the fact that they are much better Lewis bases than CO and thus usually form complexes where the π acidity of the phosphorus center plays little or no role. Phosphines can also be sterically and electronically modified by altering the alkyl or aryl substituents on the phosphorus center.[3]

While olefins represent an interesting ligand class, it is really dienes and more specifically cyclopentadiene (Cp) that have become dominant examples of UAL's. As with CO, olefins act as π acceptor ligands as well as donating electron density to σ-type

acceptor orbitals on a metal. From diolefins emerged cyclopentadienyl (Cp) based ligands which went on to be a very popular ligand set of the transition metals. In fact, the quest for other UAL's truly began in earnest with the discovery of the stable organometallic compound ferrocene in 1951 which captured the imagination of chemists. Ferrocene defied conventional bonding description and ignited the development of d-block and f-block organometallic chemistry. Its importance was further underscored when Ernst Fischer and Geoffrey Wilkinson were awarded the Nobel Prize in 1973 for their contributions to organometallic chemistry. A colossal effort has gone into derivatizing the Cp ligand. One of the more popular derivatives is the pentamethyl cyclopentadienyl anion (Cp*) discovered in 1980. The use of Cp* resulted in greater stability than the unsubstituted cyclopentadiene due to the increase in steric bulk as well as avoiding C-H cleavage. Cp* is also more electron rich forming stronger metal-ligand bonds. One has only to look at any volume of Comprehensive Organometallic Chemistry to bear witness the enormous production of Cp based complexes.[4]

Cp chemistry did not enjoy the same success in the main group. The ligand had a tendency to exhibit structural peculiarities. For example, the ligand could be monohapto instead of pentahapto such as in the Ge(IV) complex $Ge(\eta^1\text{-}C_5H_5)(CH_3)_3$. This complex exhibits "ring whizzing" where the Ge atom hops around the ring in a series of 1,2-shifts.

While CO and Cp faded into obscurity in the p-block, carboxylates prevailed across the periodic table. Part of the versatility offered by carboxylates is the variety of bonding modes they exhibit. They can be monodentate, chelating or bridging two metal centers as illustrated in Chart 1.1. However, carboxylates suffer from a poor ability to

modify electronic (and especially) steric effects of the ligand due to a lack of substituents on the oxygen atoms.[5]

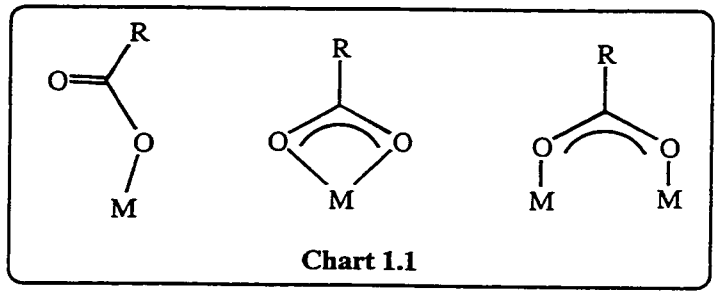

Chart 1.1

Over the past decade, an intense search has developed for new generation ligands which has resulted in a synthetic trend away from carbon based ligands. Nitrogen based ligands have emerged as promising systems for a variety of applications.[6]

Amidinates as Ancillary Ligands

The genesis of this thesis was based on a quest for a ligand which could stabilize low valent group 14 complexes and provide enough steric bulk to prevent undesired side reactions while at the same time providing routes to the stabilization of rare and unusual functionalities. We were looking for our own version of a Universal Ancillary Ligand.

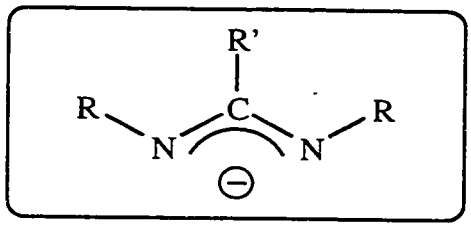

Amidinates are bidentate, three atom bridging ligands with the general formula $RNC(R')NR^{-}$. They are monoanionic ligands that are formally four electron (σ) donors. Amidinates are the nitrogen analogues of (and are isoelectronic with) carboxylates (Scheme 1.1). They are easy to synthesize and impart excellent solubility properties to the complexes formed. As with carboxylates, they also exhibit a variety of bonding modes including monodentate, chelating or bridging modes.

An inherent advantage of amidinates lies in their potential to be rationally modified. Through modification of the organic substituents on the nitrogen atoms and at the bridge position, the sterics and to a lesser extent electronics can be purposefully altered, in effect allowing the ligand to be tuned to stabilize desired structural and reactivity characteristics. Steric analysis of this ligand system places it between the Cp and Cp* ligand systems.[7] Amidinate complexes may exhibit enhanced electrophilic behaviour relative to Cp analogues. Amidinates satisfy the ancillary ligand criteria.

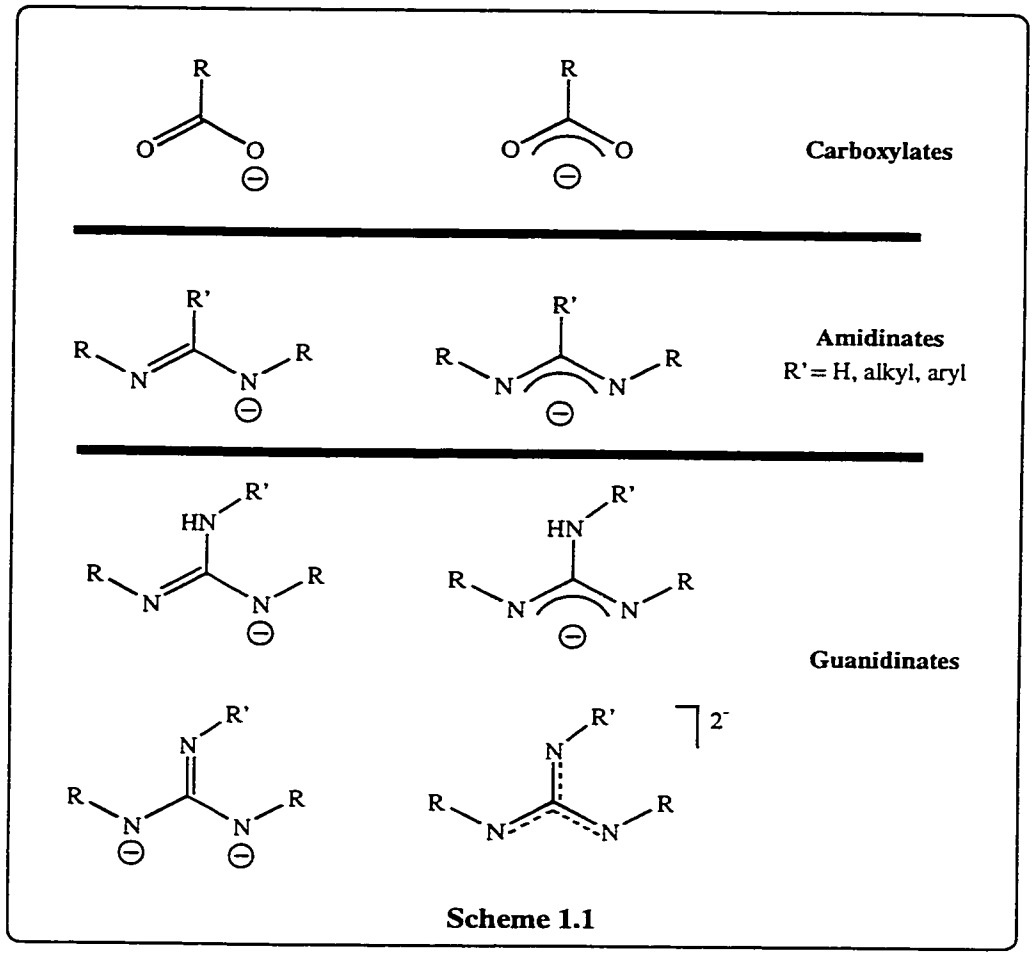

Scheme 1.1

Amidinato complexes were made widely accessible in 1990 with the synthesis of lithium and sodium salts of N-silylated benzamidinate anions according to eq. 1.1.[7a]

$$RC_6H_4CN + LiN(SiMe_3)_2 \rightarrow Li[RC_6H_4C(NSiMe_3)_2] \qquad \textbf{1.1}$$

$$R = H, Me, MeO, CF_3, Me_2N, NO_2$$

Prior to 1994, amidinato complexes consisted for the most part of N,N'-bis(trimethylsily)benzamidinates. Excellent reviews have been written summarizing the published literature.[8] Since 1994, a greater variety of organic substituents on both nitrogen atoms and on the central carbon atom has been reported arousing increased interest in amidinate chemistry.[9] Amidinates are now well established as versatile and flexible ligand systems for a variety of transition metal and main group metal centers. For example, formamidinate ligands of type **I** have been used extensively in early transition metals in the formation of M_2(formamidinato)$_4$ or so called paddle wheel (or lantern) compounds resulting in the formation of metal-metal bonds of varying degrees as illustrated by **II**.[10] Success is measured by the fact that more elements are known to form metal-metal compounds with amidinate bridges than with the classical carboxylates or any other electronically similar ligand. Amidinates have also been incorporated into cationic aluminum alkyl complexes resulting in transition metal-free ethylene polymerization catalysts.[11] From a theoretical context, the bonding properties of amidinate complexes of group 14 elements have recently been studied with

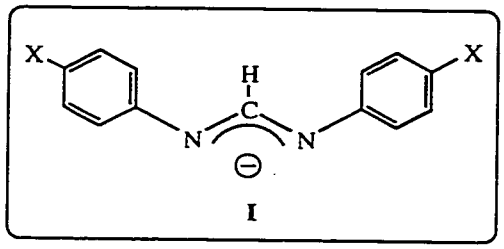

I

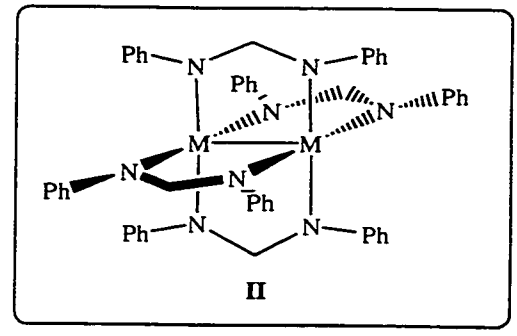

II

quantum chemical methods.[12] Some examples of amidinate ligands developed since 1994 are illustrated in Chart 1.2.[13]

Chart 1.2

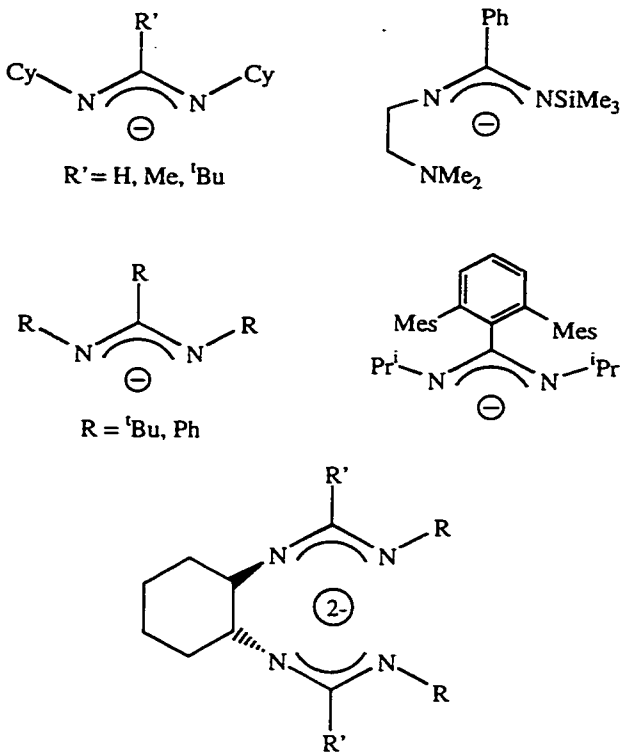

In our search of amidinato systems, we desired greater ease of synthesis and modification potential of the ligand backbone. Specifically, we were interested in modifying the steric environment about the ligand to investigate any subsequent change in the coordination environment about a metal center.

The overall objectives in the creation of this work were to investigate the synthesis and coordination chemistry of bulky amidinates with regards to the group 14 elements germanium and tin in both their divalent and tetravalent oxidation states. Prior to our work in the area, no amidinato complexes of germanium had been reported and no investigations into the reactivity of tin amidinates had ever been performed. We envisioned that amidinates could offer kinetic and thermodynamic stabilizing features that could allow the formation of unusual functions such as heteronuclear multiple bonds in the heavy main group and the formation of rare chalcogenido complexes. We further proposed to use these species in the study of metal mediated single chalcogen atom

exchange reactions and to extend the reactivity of these group 14 chalcogenido complexes through explorations of their catalytic potential. No investigations have ever been performed studying the kinetics of heteronuclear single chalcogen atom exchange reactions within the main group. As this investigation progressed, we expanded it to include other ligand sets while still preserving the basic N-C-N ligand backbone that has made this chemistry a success.

Guanidinates as Ancillary Ligands

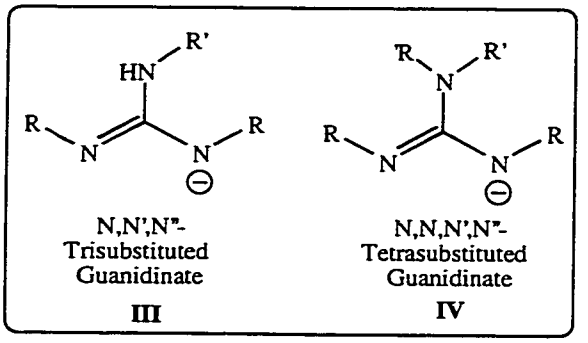

Guanidinates fall into the general class of 1,3-nitrogen ligands to which amidinates belong and upon which this thesis is based. In contrast to amidinates, guanidinates have received limited attention with transition metal and main group elements.

As with amidinates, guanidinates offer kinetic (e.g. steric) and thermodynamic (e.g. electronic) features to stabilize metal complexes. They possess all of the coordination properties of amidinates and may be stronger donor ligands as well. The presence of a third nitrogen center can further play a role in the coordination of guanidinate ligands. The third nitrogen can bear either one or two substituents resulting in either trisubstituted (**III**) or tetrasubstituted (**IV**) guanidinates.

In the trisubstituted version, the additional third nitrogen center can be further deprotonated to afford a dianionic ligand. This dianionic species may exhibit π

delocalization (Y conjugation) of the lone pairs on the sp^2 hybridized nitrogen centers making it an analogue of the trimethylene methane dianion (**V**).

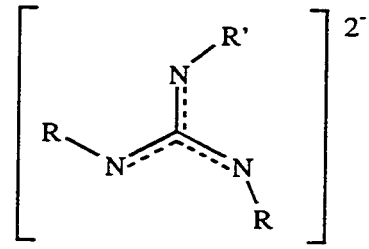

(Y conjugation)

V

The presence of a lone pair on the ancillary nitrogen NR'_2 or N(H)R of the monoanion either on the trisubstituted or the tetrasubstituted guanidinate also allows for consideration of the resonance structure **VI** (scheme 1.2). In order for this particular zwitterionic resonance structure to be considered important, the ancillary third nitrogen atom must not only be planar sp^2 hybridized, with the lone pair of electrons localized in a p orbital, but there must be substantial overlap of this p orbital with the π system of the N-C-N moiety. For this to occur, there must be a minimal dihedral angle between the planes defined by the CN(H)R' (or CNR'_2) and that defined by the chelating NCN portion of the ligand. Due to steric effects, the tetrasubstituted ligand would probably have a larger dihedral angle thus discouraging this resonance contribution.

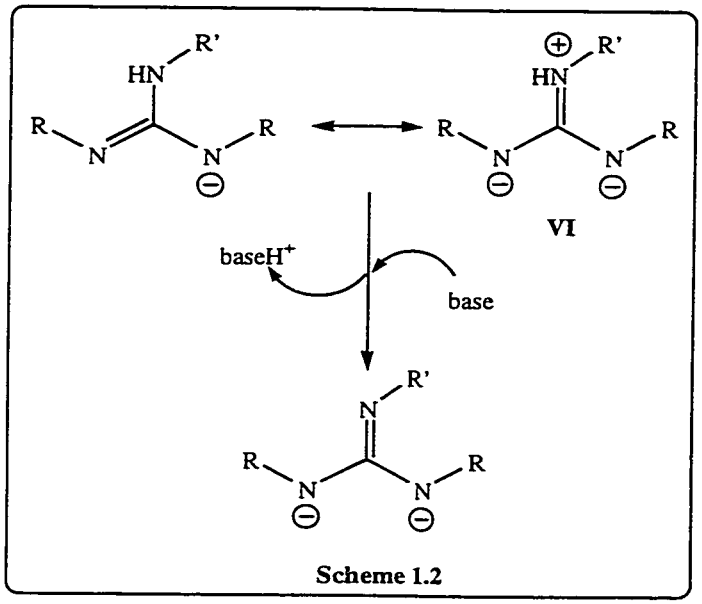

Scheme 1.2

As previously mentioned, guanidinates have received limited attention in coordination chemistry. In fact, the only main group complexes of trisubstituted guanidinate anions that have been discovered and structurally characterized are

$[(^{i}PrN)_2(NH^{i}Pr)][(^{i}PrN)_2(N^{i}Pr)]Sb$[14] along with the dianionic lithium salts, $Li_2(C(NPh)_3)$[15] and $Li_2(C(N^{t}Bu)_3)$.[16] The antimony complex, $[(^{i}PrN)_2(NH^{i}Pr)][(^{i}PrN)_2(N^{i}Pr)]Sb$, is prepared from the reaction of 1,2,3-triisopropyl guanidine with 1 equiv of $Sb(NMe_2)_3$. It formally possesses one dianionic and one monoanionic guanidinate.

Scheme 1.3

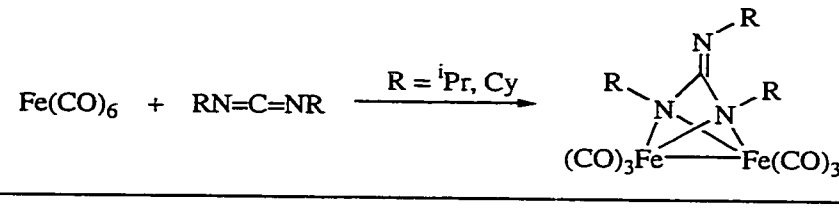

The first example of a transition metal guanidinato species was a diiron complex formed by the reaction of dicyclohexylcarbodiimide with $Fe(CO)_5$ resulting in the formation of a guanidinate dianion bridging two metal centers (Scheme 1.3).[17] In fact prior to 1996, it was the only dianionic guanidinate coordinated to a transition metal center. The second was the monomeric metal complex Pt[(NPh)2C=NPh](cod), cod = cyclooctadiene, which appeared sixteen years after the iron complex.[18]

The objectives of this thesis extend into the investigation of the synthesis and coordination chemistry of both monoanionic and dianionic guanidinate ligands of group 14 elements. Ultimately, this work was further extended into iron chemistry.

Chapter one outlines features of the supporting ligation used throughout the thesis. A lack of a synthetic base required the development of a preparative methodology both for synthesis of the ligands themselves and their introduction to metal centers. All amidinates were prepared *in situ* by simple reaction of a carbodiimide with the appropriate lithium reagent. The lithium salts of the amidinates were then introduced to

metal centers via metathesis with the corresponding metal halides. Tetrasubsituted guanidinate complexes were prepared in the same manner via addition of a lithium amide to a carbodiimide. Preparation of trisubstituted guanidinate complexes was somewhat more involved. The parent guanidine (either N,N',N''-triisopropyl or tricyclohexyl guanidine) had to first be synthesized by addition of the amine to the corresponding carbodiimide at elevated temperatures for extended reaction times. The subsequent introduction of the ligand was performed by one of two routes. The first was by direct addition of the neutral guanidine to a metal chloride, while the other was the *in situ* formation of the lithium salt of the guanidine followed by addition of the metal halide. The former approach has an inherent disadvantage in that an additional equivalent of guanidine is consumed to deprotonate the ligand. Thus, the latter technique was more commonly employed. The metal halides themselves were all commercially available except for the carbene analogue, $GeCl_2$(dioxane) which was prepared through reduction of $GeCl_4$ by Bu_3SnH in the presence of dioxane.[19]

Chapters two through six describe the synthetic methodology developed in the synthesis of a series of germanium and tin amidinato complexes. These complexes were used in the stabilization of rare chalcogenido species. The further reactivity of these complexes was investigated by performing heteronuclear single atom transfer reactions as well as investigating the catalytic trimerization of isocyanates.

Chapter seven extends this chemistry to the preparation of guanidinato complexes. It is intended to be an exploratory excursion into the formation of guanidinato and related species.

Chapter eight focuses on the formation of amidinato and guanidinato complexes of Fe(II) and Fe(III). It illustrates the differences that can arise in the reactivity and coordination environments of amidinates versus guanidinates with this metal center.

References for Chapter One

[1] Ellis, J.E.; Beck, W. *Angew. Chem. Int. Ed. Engl.* **1995**, *34*, 2489 and references therein

[2] Richter-Addo, G.B.; Legzdins, P. *Metal Nitrosyls*, Oxford University Press, London **1992**

[3] Brown, T.L.; Lee, K.J. *Coord. Chem. Rev.* **1993**, *128*, 89

[4] Abel, E.W.; Stone, F.G.A.; Wilkinson, G. *Comprehensive Organometallic Chemistry*, Pergamon **1997**

[5] Appleton, T.G.; *Inorg. Chem.* **1995**, *34*, 5646; Mak, T.C.W. *Polyhedron* **1997**, *16*, 897 and references therein

[6] Britovsek, G.J.P.; Gibson, V.C.; Wass, D.F. *Angew. Chem. Int. Ed. Engl.* **1999**, *38*, 428

[7] a) Wedner, M; Knosel, F.; Noltemeyer, M; Edelmann, F.T. *J Organomet. Chem.* **1990**, *338*, 21
b) Duchateau, R.; van Wee, C.T.; Meetsma, A.; van Duijnen, P.T.; Teuben, J.H. *Organometallics* **1996**, *15*, 2279
c) Edelmann, F.T. *J Organomet. Chem* **1992**, *426*, 295

[8] a) Edelmann, F.T. *Coord. Chem. Rev.* **1994**, *137*, 403
b) Barker, J.; Kilner, M. *Coord. Chem. Rev.* **1994**, *133*, 219

[9] Jordan, R.F.; Dagorne, S. *Organometallics* **1999**, *18*, 4619. Decker, J.M.; Geib, S.J.; Meyer, T.Y. *Organometallics* **1999**, *18*, 4417. Sita, L.R.; Babcock, J.R. *Organometallics* **1998**, *17*, 5228. Zhou, Y.; Richeson, D.S. *Inorg. Chem.* **1996**, *35*, 1423. Berno, P.; Hao, S.; Minhas, R.; Gambarotta, S. *J. Am. Chem. Soc.* **1994**, *116*, 7417 and references therein.

[10] Cotton, F.A.; Walton, R.A. *Multiple Bonds Between Metal Atoms*, Oxford University Press, Oxford, 2nd edn., **1993**. Cotton, F.A.; Daniels, L.M.; Matonic, J.H.; Murillo, C.A.;Wang, X. *Polyhedron* **1997**, *16*, 1177. Cotton, F.A.; Daniels, L.M.; Murillo, C.A.;Wang, X. *Inorg. Chem.* **1997**, *36*, 896 and references therein.

[11] Jordan, R.F.; Coles, M.P. *J Am. Chem. Soc.* **1997**, *119*, 8125

[12] Schoeller, W.W.; Sundermann, A.; Reiher, M. *Inorg. Chem.* **1999**, *38*, 29

[13] a) Zhou, Y.; Richeson, D.S. *Inorg. Chem.* **1996**, *35*, 2448
b) Brandsma, M.J.R.; Brussee, E.A.C.; Meetsma, A.; Hessen, B.; Teuben, J.H. *Eur. J. Inorg. Chem.* **1998**, 1867
c) Hagadorn, J.R.; Arnold, J. *Angew. Chem. Int. Ed. Engl.* **1998**, *37*, 1729

d) Schmidt, J.A.R.; Arnold, J. *Chem. Commun.* **1999**, *021*, 2149

[14] Bailey, P.J.; Gould, R.O.; Harmer, C.N.; Pace, S.; Steiner, A.; Wright, D.S. *Chem. Commun.* **1997**, 1161

[15] Bailey, P.J.; Blake, A.J.; Kryszczuk, M.; Parsons, S.; Reed, D. *J. Chem. Soc., Chem. Commun.*, **1995**, 1647

[16] Chivers, T.; Parvez, M., Schatte, G. *J. Organomet. Chem.* **1998**, *550*, 213

[17] Bremer, N.J.; Cutcliffe, A.B.; Farona, M.F. *Chem. Commun.* **1970**, 932.

[18] Dinger, M.B.; Henderson, W. *Chem. Commun.* **1996**, 212.

[19] Fjeldberg, T.; Haaland, A.; Schilling, B. E. R.; Lappert, M. F.; Thorne, A. J. *J. Chem. Soc., Dalton Trans.* **1986**, 1551

Amidinate Complexes of Germanium as Precursors for the Facile Formation of Rare Terminal Chalcogenides

2

"did he fire..."

Chapter Two

Introduction

Multiple bonding plays a prominent role in the chemistry of the second period p-block elements, carbon, nitrogen and oxygen. This leads to the formation of olefins, alkynes, aromatics, carbonyls and nitriles which comprise important and fundamental classes of compounds. In contrast, complexes that exhibit multiple bonding to the heavier congeners of these elements are much less common. The compounds were so elusive that they were believed to be non-existent. This led to the formulation of the so-called "classical double bond rule" which essentially stated that compounds with double bonds between heavier main group elements would not be stable due to weak π bonding. In 1975, the classical double bond rule was described as "elements having a principle quantum number greater than 2 should not be able to form (p-p)π bonds to themselves or with other elements".[1] The rule is now hopelessly outdated, but there remains some controversy as to who originally introduced the term. There are often references to the "classical double bond rule", but it appears the term itself may never have been published as an original contribution.

What is a double bond is a question commonly posed by chemists and non-chemists alike questioning the possibility (or impossibility) of multiple bonding in the heavy main group. One answer to this would be to look at the definition of a chemical bond provided by Linus Pauling which stated: "there is a chemical bond between two atoms or groups of atoms in case that the forces acting on them are such as to lead to an

aggregate of sufficient stability to make it convenient for the chemist to consider it as an independent molecular species".[2] This simple definition can be extended by saying that in essence a double bond exists if it is justified by the chemical and physical behaviour of the complex in contention.

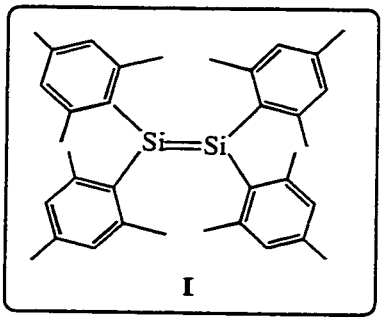

I

Perhaps goaded by the double bond rule, the stabilization of heavier main group element-element multiple bonds has been a central research theme in organometallic chemistry for almost thirty years. The area exploded in 1981 with the discovery of the first Si=Si double bond illustrated in **I**.[3] This introduced the notion of using very bulky substituents to prevent oligomerization and stabilize multiply bonded species. It should be noted that for the purposes of this thesis, complex stability refers to a complex that is stable in both solution and solid state at room temperature.

Stable Multiply Bonded Germanium Species with groups 14 and 15

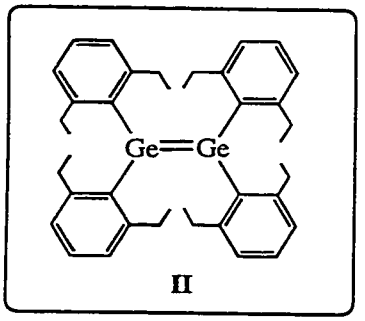

II

The first compound with a homonuclear germanium-germanium double bond, $R_2Ge=GeR_2$ (R = 2,6-diethylphenyl), was synthesized in 1984 (**II**).[4] An interesting feature of compounds with the formula $R_2M=MR_2$ (M = Si, Ge, Sn or Pb, R = organo group) is how they differ from carbon-carbon double bonds. They tend to adopt nonplanar, trans-bent structures with progressively weaker element-element bonding going down the group. The first complex with a germanium-carbon double bond was isolated in 1987 (**III**).[5] It was made by the

reaction of a cryptocarbene with a germylene. The first germaimine was also made in 1987 (**IV**).[6]

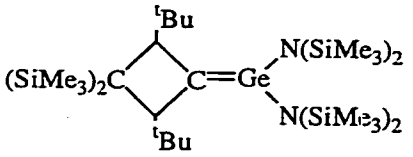

III

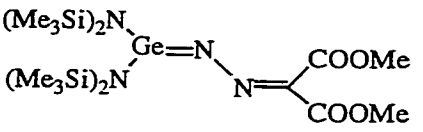

IV

Stable Germanium-Chalcogenido Multiple Bonds

The formation of germanium-chalcogenido multiple bonds proved much more elusive. Prior to 1989, the chemistry was essentially that of reactive intermediates. Attempts to isolate terminal chalcogenido complexes of germanium failed, even with sterically demanding ligands on the germanium center. In fact, stable multiply bonded terminal chalcogenido complexes of the entire heavy main group are extremely rare. Stabilization of compounds with the formula $L_2Ge{=}E$ (E = O, S, Se, Te) is much more difficult than the stabilization of compounds of the type $L_2Ge{=}EL$ (E = N, P) or $L_2Ge{=}EL_2$ (E = C, Ge) since there is no substituent on the E element to sterically shield it and prevent oligimerization.

Scheme 2.1

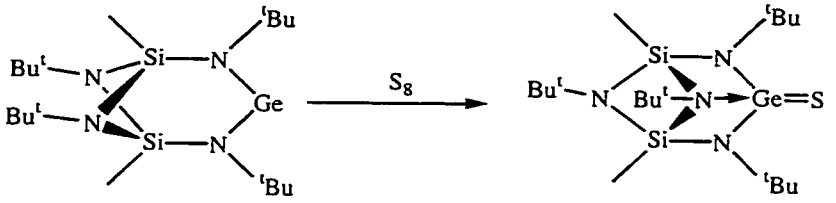

The first terminal chalcogenido complex of germanium was isolated and structurally characterized in 1989.[7] The complex was a germanium sulfide made by oxidative addition of elemental sulfur to a divalent precursor according to scheme 2.1.

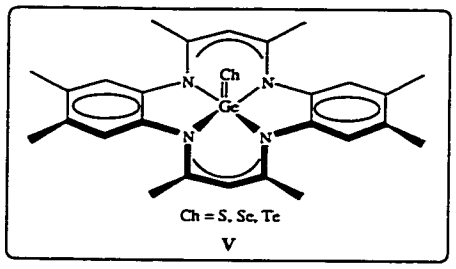

This discovery introduced the notion that complexation of the germanium center by a Lewis base might be required to stabilize a terminal chalcogenide. The first series of terminal chacogenides (S, Se, Te) was reported five years later using the versatile supporting ligand, octamethyldibenzotetraaza[14]annulene (Me_8taa^{2-}). (**V**).[8] The complexes were prepared by direct addition of the chalcogen to the divalent precursor. Another series of terminal chalcogenides was prepared with the formula (Tbt)(Tip)Ge=Ch, Ch = O[9], S[10], Se[11], Te[12] (**VI**). The importance of these compounds is that the bulky Tbt and Tip aryl ligands stabilize the three coordinate terminal chalcogenido complexes in the absence of a coordinating base. The oxo complex has not been isolated and its characterization is based on trapping reactions. These compounds summarize the published material prior to our involvement in the field. Since our contributions to this area, the series of compounds bis[(2-pyridyl)bis(trimethylsilyl)methyl]Ge=E (E = S, Se, Te) has been reported and the Se and Te derivatives structurally characterized (**VII**).[13]

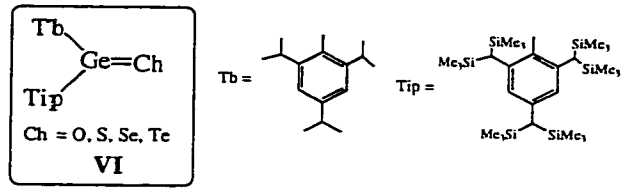

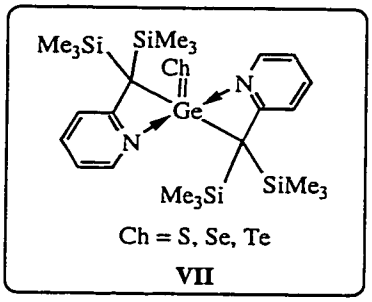

A number of reviews have been written with regard to multiply bonded germanium species[14], multiply bonded group 14 species[15], and more comprehensive reviews covering multiply bonded main group complexes.[16]

Amidinato Complexes of Germanium and Tin

Along with our interest in the formation of multiple bonds between the heavy main group elements, we are exploring the effects of ligand geometry on the coordination environments of group 14 metals. Part of this systematic study is based on the use of amidinate ligands. Specifically, we have been exploring the ability of these ligands to stabilize unusual structures and functions in Ge(II/IV) and Sn(II/IV) complexes. Amidinate anions exhibit versatility in binding modes and, through changes of substituents, should present a flexible system for tuning the effects of changes in steric bulk and electronic properties of the supporting ligand on the product compounds (see chapter 1). Using this methodology, bulky alkyl amidinate ligands have been demonstrated to provided the supporting environment for a structurally characterized terminal Sn=S complex, $S{=}Sn(CyNC(^{t}Bu)NCy)_2$, which is unique in the absence of macrocyclic supporting ligation.[17] Reducing the steric bulk of the ligand by replacing the ^{t}Bu group with a methyl functionality results in the formation of the sulfur bridged dimer, $[(CyNC(Me)NCy)_2SnS]_2$ (Scheme 2.2).

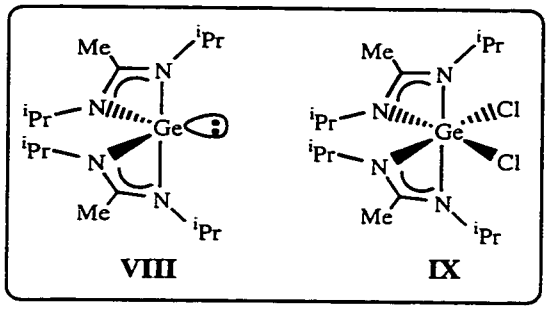

VIII **IX**

Amidinato complexes of tin have been prepared with the metal in both the divalent and tetravalent oxidation states.[18] However, prior to our work in the area, there were no germanium analogues. With regards to tin, all amidinato complexes have been limited to use of N,N'-bis(trimethylsilyl)benzamidinate based ligands, $[Me_3SiNC(C_6H_4R)NSiMe_3]$. (Since our contribution to the area, one other series of amidinato complexes of germanium has been published (**VIII** and **IX**).[19]) We

were interested in the possibility of overcoming this limitation and investigating the effects of changing the various substituents. Our investigation of the coordination chemistry of amidinate anions relies on their generation by the addition of alkyl lithium reagents to carbodiimides.

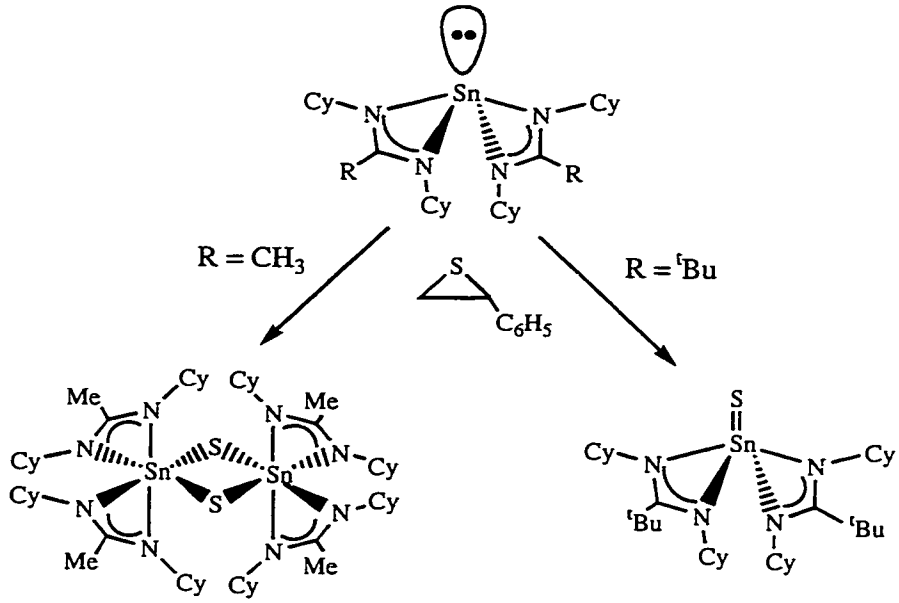

Scheme 2.2

In this chapter we describe the synthesis of a unique family of bis(amidinato) Ge(II) and mixed (amidinato)(amido) Ge(II) species. These compounds are easily converted to terminal germanium chalcogenido complexes (Ge=Ch; Ch = S, Se) through oxidation with chalcogen atom sources. These results contribute to the limited number of structurally characterized terminal chalcogenido complexes and the addition of these new species may help to delineate the features which stabilize and effect the reactivity of such species.

Results and Discussion

Ge(II) and Ge(IV) complexes of the (CyNC(R)NCy) anions (R = CH_3, CMe_3):

The *in situ* preparation of (CyNC(R)NCy)Li (R = Me, ^{t}Bu; Cy = cyclohexyl) followed by subsequent addition of 0.5 equivalents of $GeCl_2$(dioxane) generated the Ge(II) complexes **1** and **2** in excellent isolated yields (Scheme 2.3). Both of these compounds have been characterized by spectroscopic means, microanalysis, subsequent reactivity and single crystal X-ray analysis.

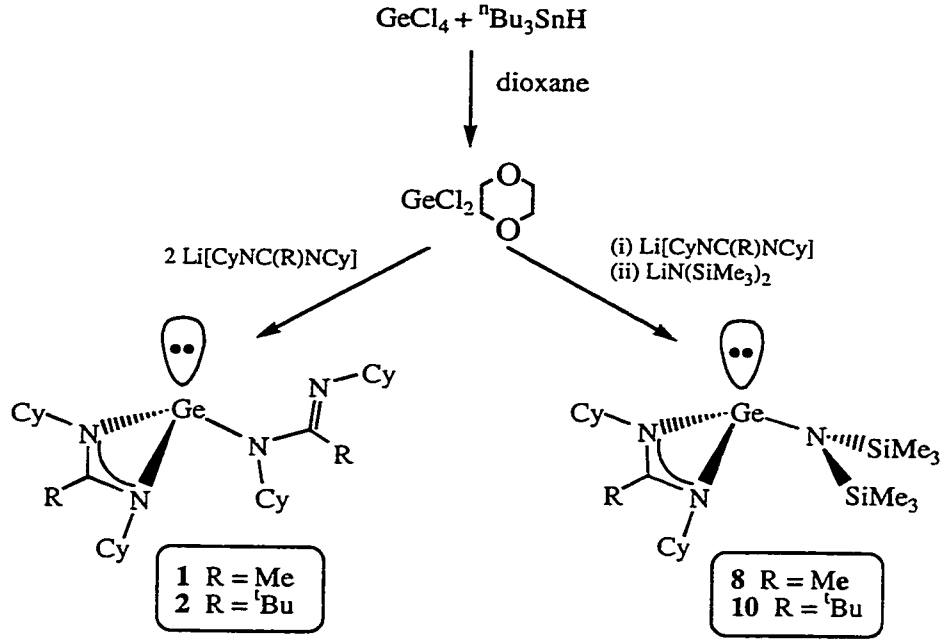

Scheme 2.3

The first indication that these compounds were not isostructural with the previously reported Sn(II) analogues shown in Scheme 2.2 was provided by the room temperature ^{1}H NMR spectrum of **2**. Unlike Sn[CyNC(^{t}Bu)NCy]$_2$ which displayed one environment for both the Cy and ^{t}Bu groups, Ge[CyNC(^{t}Bu)NCy]$_2$ gave three multiplets for the cyclohexyl protons α to nitrogen in a 1:2:1 ratio and two well-separated singlets in

a 1:1 ratio for the ^{t}Bu groups. No coalescence of these signals was observed in the ^{1}H NMR spectra of **2** up to 375K.

In contrast, the NMR spectrum for the methyl analogue, Ge[CyNC(Me)NCy]$_2$, exhibited a single environment for both the Cy and Me protons. In this case, a variable temperature ^{1}H NMR study for **1** over the temperature range 200-300K showed only a small amount of line broadening which could be attributed to solvent viscosity effects.

Table 2.1. Crystal data and structure refinement for Ge[CyNC(Me)NCy]$_2$ (**1**), for Ge[CyNC(^{t}Bu)NCy]$_2$ (**2**) and [CyNC(^{t}Bu)NCy]GeCl$_3$ (**3**).

	1	**2**	**3**
empirical formula	$GeN_4C_{28}H_{50}$	$GeN_4C_{34}H_{62}$	$C_{17}H_{30}Cl_3GeN_2$
formula weight	515.31	597.46	441.37
temp (K),	120	120	203(2)
λ (Å)	1.54056	1.54056	0.71073
crystal class / space group	monoclinic, $P2_1/c$	monoclinic, Pc	triclinic, P-1
a (Å)	15.1666(6)	17.2075(21)	9.696(5)
b (Å)	11.5652(4)	11.055	10.628(5)
c (Å)	16.0374(6)	18.223(3)	11.522(6)
α (deg)	90	90	96.126(8)
β (deg)	99.856(3)	97.029(12)	106.645(7)
γ (deg)	90	90	112.271(7)
Z	4	2	2
d_{calc} (g/cm^3),	1.235	1.157	1.435
μ (mm^{-1})	1.62	1.37	1.893
R1[a]	0.052	0.043	0.0672
wR2[b]	0.074	0.057	0.0928

[a] $R1 = \sum \| F_o | - | F_c \| / \sum | F_o |$.

[b] $wR2 = \left(\sum w (| F_o | - | F_c |)^2 / \sum w | F_o |^2 \right)^{1/2}$

Due to these apparently conflicting results, X-ray diffraction studies were undertaken to clarify the geometry of both **1** and **2** (Table 2.1). Compounds **1** and **2** possess similar geometries which are based on distorted tetrahedra in which one of the vertices is occupied by a stereochemically active lone pair of electrons. There were no anomalously short intermolecular contacts. The molecular geometry and atom-

numbering scheme are shown in Figures 2.1 and 2.2 with corresponding bond distances and angles provided in Tables 2.2 and 2.3. In contrast to the previously reported $Sn[CyNC(^tBu)NCy]_2$ in which both amidinates were bidentate, **1** and **2** exhibited one bidentate and one monodentate ("dangling") ligand. The free imine nitrogen does not exhibit any obvious interaction with an adjacent metal center.

Taking into account the smaller radius of Ge, the structural features within the bidentate ligand are similar to reported Sn(II) and Sn(IV) complexes of related ligands: the two nitrogens and bridging carbon atoms for the amidinate ligand lie in a plane which includes the Ge atom with comparable internal angles. The slight differences between the methyl (**1**) and tert-butyl (**2**) analogues (e.g. the angles around N1 and N2) appear to be consistent with the bulk of the group on the methyne carbon.

The Ge-N3 (mondentate ligand) distances are consistently shorter than the Ge-N distances of the bidentate ligand.

The results of these analyses clearly explain the ^1H NMR results for **2** and indicate that although **1** exhibits three distinct Cy groups in the solid state, the solution structure is fluxional. Although the mechanism for interconversion of the amidinate groups in complex **1** is not yet clear, it appears that substitution of the methyl group in **1** with a tertiary butyl group substantially slows this process.

Scheme 2.4

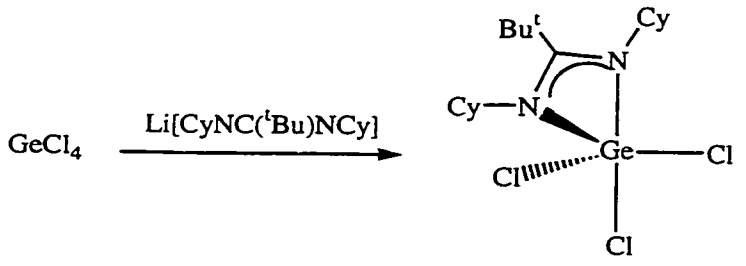

Based on these results, we set out to prepare a five coordinate amidinato germanium species to investigate the effects of coordination geometry on the

binding mode of the ligand. To this end, one equivalent of the *in situ* prepared (CyNC(^{t}Bu)NCy)Li was reacted with $GeCl_4$ according to Scheme 2.4 to generate the monoamidinate Ge(IV) complex (CyNC(^{t}Bu)NCy)$GeCl_3$, **3**. The ^{1}H NMR spectrum for **3** displayed two separate environments for the two cyclohexyl groups. To ascertain if the complex was indeed five coordinate or if it was four coordinate with a dangling amidinate, X-ray diffraction studies were undertaken (Table 2.1). Complex **3** possesses a geometry based on a distorted trigonal bipyramid as illustrated in Figure 2.3 where the coordination sphere of the Ge(IV) center is comprised of one bidentate amidinate ligand spanning axial/equatorial sites and three chloride ligands. Selected bond distances and angles are given in Table 2.4. The pseudo-equatorial plane is defined by N(1) of the amidinate ligand, the Ge atom, and Cl(1) and Cl(3). The sum of the angles of these ligands around Ge is 357° indicating these groups do indeed form a plane. The Cl(2)-Ge-N(2) angle of 165.29(14)° is defined as the pseudo-axial vector. Consistant with the formulation for a trigonal bipyramid, the axial Cl(2)-Ge distance of 2.2383(19)Å is longer than the equatorial Cl(1)-Ge and Cl(3)-Ge distances of 2.144(2) and 2.162(2)Å respectively. Likewise, the axial N(2)-Ge of 2.132(5)Å distance is longer than the equatorial N(1)-Ge distance of 1.892(5)Å. The pseudo-trigonal bipyramidal geometry about the germanium center resulting from the presence of the bidentate amidinate ligand is contrary to complexes **1** and **2** where trigonal bipyramidal geometries (counting the lone pair as a coordination site) are disfavoured in favour of tetrahedral geometries. At first this suggests that sterics rather than electronics plays the dominant factor in deciding if the dangling ligand effect will present itself but the results that will be described in Chapter 4 indicate that electronic factors obviously play a large role as well.

Figure 2.1. Molecular structure and atom numbering scheme for $[CyNC(Me)NCy]_2Ge$ (**1**) (Cy=cyclohexyl). Hydrogen atoms have been omitted for clarity.

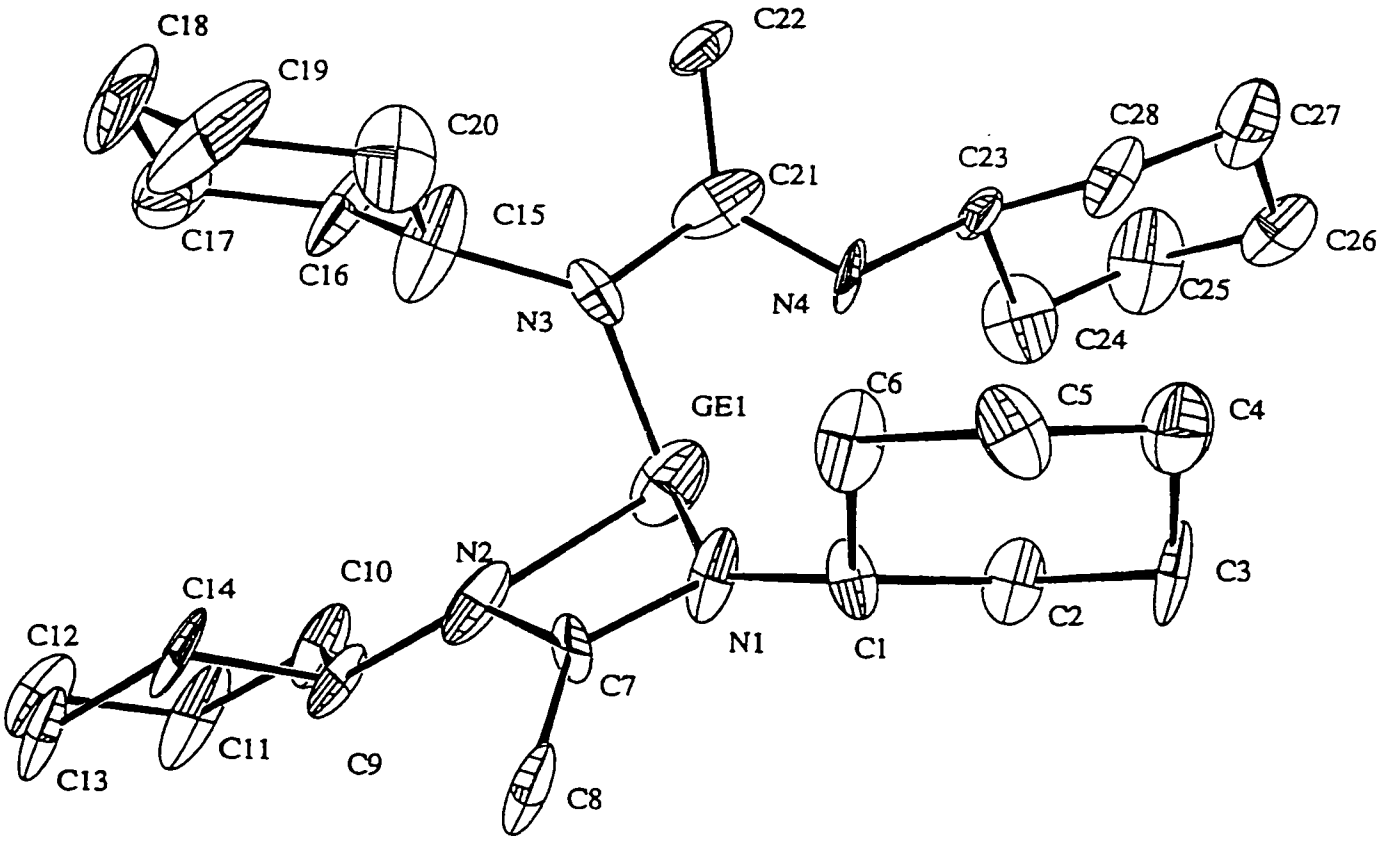

Table 2.2. Selected bond lengths(Å) and angles(°) for complex **1**

Distances			
Ge1-N1	2.037(11)	N2-C7	1.329(18)
Ge1-N2	2.158(13)	N3-C21	1.364(20)
Ge1-N3	1.935(12)	N4-C21	1.327(18)
N1-C7	1.302(19)		

Angles			
N1-Ge1-N2	62.4(4)	Ge1-N3-C15	128.1(10)
N1-Ge1-N3	101.2(5)	Ge1-N3-C21	104.4(9)
N2-Ge1-N3	96.0(4)	N1-C7-N2	111.6(13)
Ge1-N1-C1	137.3(10)	Ge1-N1-C7	95.6(9)
Ge1-N2-C7	89.4(9)	N3-C21-N4	111.4(12)
Ge1-N2-C9	139.0(9)		

Figure 2.2. Molecular structure and atom numbering scheme for one of the two molecules in the asymmetric unit for the structure of $[CyNC(^tBu)NCy]_2Ge$ (**2**) (Cy=cyclohexyl). Hydrogen atoms have been omitted for clarity.

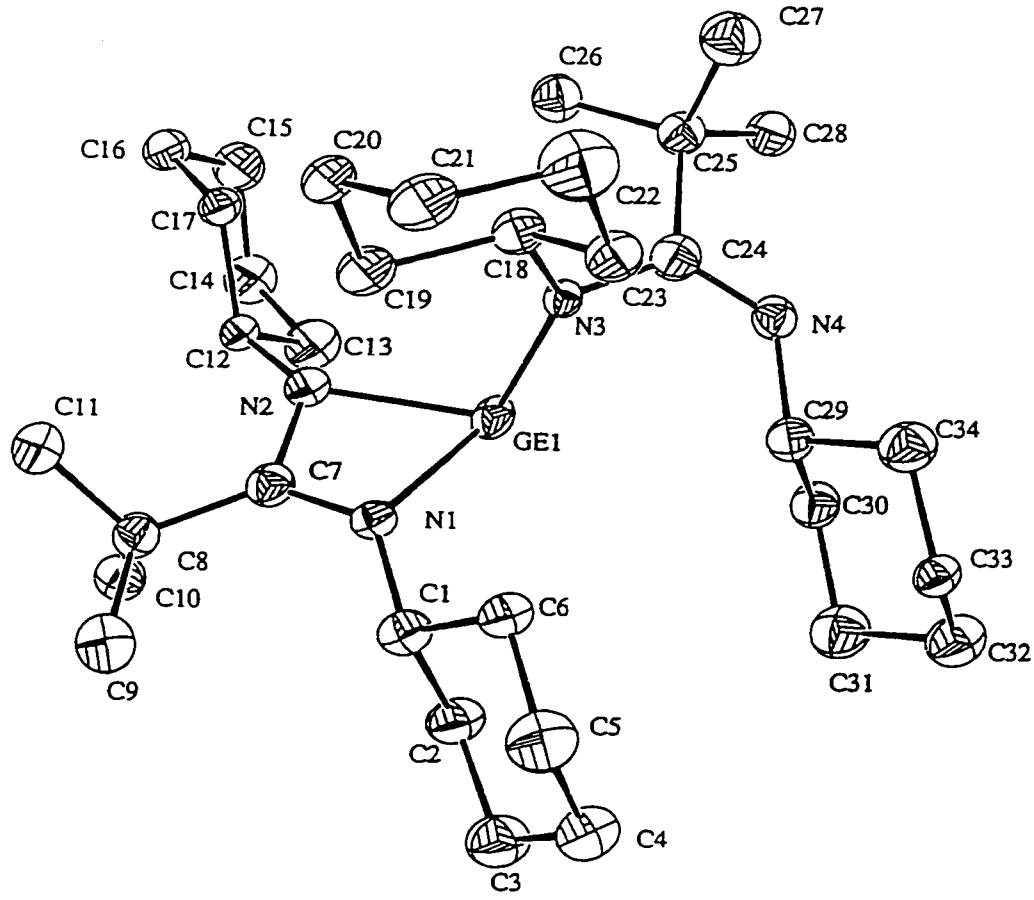

Table 2.3. Selected bond lengths(Å) and angles(°) for complex **2**

Distances			
Ge1-N1	2.040(9)	N1-C7	1.299(15)
Ge1-N2	1.993(10)	N2-C7	1.420(15)
Ge1-N3	1.903(9)	N3-C24	1.419(15)
Ge2-N5	2.043(9)	N4-C24	1.282(16)
Ge2-N6	2.090(9)	Ge2-N7	1.898(9)

Angles			
N1-Ge1-N2	65.6(4)	Ge1-N2-C12	135.7(7)
N1-Ge1-N3	107.0(4)	Ge1-N3-C18	133.6(7)
N2-Ge1-N3	108.1(4)	Ge1-N3-C24	112.5(7)
Ge1-N1-C1	129.7(7)	N1-C7-N2	106.8(10)
Ge1-N1-C7	93.4(7)	N3-C24-N4	125.0(11)
Ge1-N2-C7	91.8(7)		

Figure 2.3. Molecular structure and atom numbering scheme for [CyNC(^{t}Bu)NCy]$GeCl_3$ (**3**) (Cy=cyclohexyl).

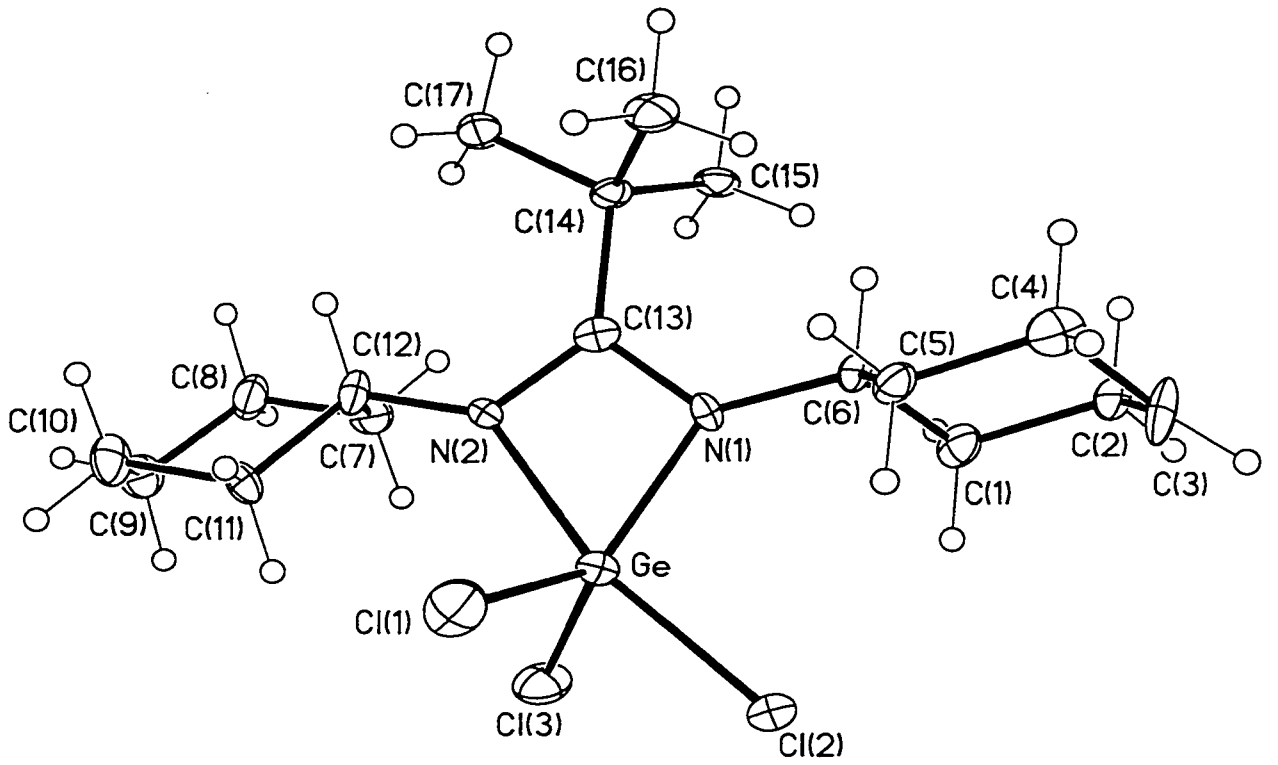

Table 2.4. Selected bond lengths(Å) and angles(°) for complex **3**

Distances			
Ge-N(1)	1.892(5)	Ge-C(13)	2.460(6)
Ge-N(2)	2.032(5)	N(1)-C(13)	1.378(6)
Ge-Cl(1)	2.144(2)	N(2)-C(13)	1.331(6)
Ge-Cl(3)	2.162(2)	C(13)-C(14)	1.523(8)
Ge-Cl(2)	2.2383(19)		

Angles			
N(1)-Ge-N(2)	66.55(19)	Cl(2)-Ge-C(13)	132.72(16)
N(1)-Ge-Cl(1)	118.31(16)	C(13)-N(1)-C(6)	128.9(5)
N(2)-Ge-Cl(1)	94.61(14)	C(13)-N(1)-Ge	96.3(4)
N(1)-Ge-Cl(3)	125.85(16)	C(6)-N(1)-Ge	134.4(4)
N(2)-Ge-Cl(3)	94.56(15)	C(13)-N(2)-C(12)	130.8(5)
Cl(1)-Ge-Cl(3)	113.23(9)	C(13)-N(2)-Ge	91.6(4)
N(1)-Ge-Cl(2)	98.87(16)	C(12)-N(2)-Ge	137.1(4)
N(2)-Ge-Cl(2)	165.29(14)	N(2)-C(13)-N(1)	105.5(5)
Cl(1)-Ge-Cl(2)	94.26(8)	N(2)-C(13)-C(14)	130.0(5)
Cl(3)-Ge-Cl(2)	92.69(7)	N(1)-C(13)-C(14)	124.5(5)
N(1)-Ge-C(13)	33.85(18)	N(2)-C(13)-Ge	55.7(3)
N(2)-Ge-C(13)	32.74(17)	N(1)-C(13)-Ge	49.9(3)
Cl(1)-Ge-C(13)	108.04(14)	C(14)-C(13)-Ge	174.3(5)
Cl(3)-Ge-C(13)	114.20(15)		

Terminal S and Se complexes of Ge:

Treatment of the two new complexes **1** and **2** with chalcogen sources (e.g. styrene sulfide or Se) followed the redox pathway outlined in Scheme 2.5. In both cases the reaction was rapid and complete. Spectroscopic and microanalytical data for both products confirmed the formulae for compounds **4-7.** Specifically, the ^{1}H NMR spectra of $[CyNC(Me)NCy]_2GeS$ (**4**) and $[CyNC(Me)NCy]_2GeSe$ (**6**) compared favorably to the parent **1.** Similarly, the NMR spectra of $[CyNC(^{t}Bu)NCy]_2GeS$ (**5**) and $[CyNC(^{t}Bu)NCy]_2GeSe$ (**7**) indicated similar coordination of the amidinate ligands as was observed above for **2.** Furthermore, both COSY and heteroatom ($^{13}C/^{1}H$) correlation NMR experiments for **5** were consistent with the structure proposed in Scheme 2.5.

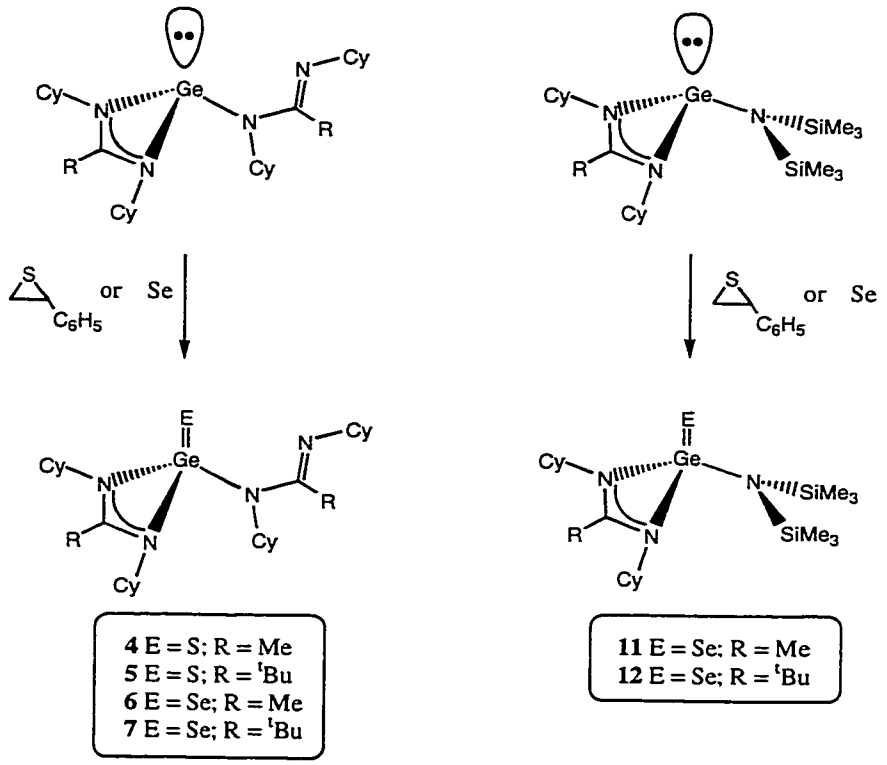

Scheme 2.5

Finally, the ^{77}Se NMR (δ = 1023.8 vs. Me_2Se) of **7** is comparable to that of a structurally characterized germaselenone, (Tbt)(Tip)Ge=Se, which appeared at δ = 940.6.[11]

In order to validate the terminal Ge=Ch bond in these materials we undertook an investigation of the structure of **7** by single crystal X-ray diffraction (Table 2.5). The corresponding bond distances and angles are shown in Table 2.6. From Figure 2.4 it is clear that the most outstanding structural feature in this molecule is the terminal Ge=Se bond. The Ge-Se bond length of 2.196Å correlates favorably with the comparable reports in the literature of 2.247Å and 2.180Å.[9,11]

Table 2.5. Crystal data and structure refinement for [CyNC(^{t}Bu)NCy]$_2$GeSe (**7**) and [CyNC(Me)NCy]$_2$Ge[N(SiMe$_3$)$_2$]Se (**11**)

	7	**11**
empirical formula	$SeGeN_4C_{34}H_{62}$	$GeSeSi_2N_3C_{20}H_{43}$
formula weight	678.43	533.29
temp (K),	120	120
λ (Å)	1.54056	0.07093
crystal class / space group	monoclinic, $P2_1/c$	monoclinic, $P2_1/c$
a (Å)	17.806(3)	8.8803(1)
b (Å)	9.900(2)	16.5932(1)
c (Å)	20.425(5)	18.2614(3)
α (deg)	90	90
β (deg)	94.920(16)	97.186(1)
γ (deg)	90	90
Z	4	4
d_{calc} (g/cm^3),	1.256	1.327
μ (mm^{-1})	2.52	2.61
R1	0.087	0.024
wR2	0.111	0.027

The distorted tetrahedral Ge coordination geometry in this complex is similar to that of the Ge(II) starting material (**2**) with Ge-Se vector residing in the site previously occupied by the lone electron pair. The coordination sphere of Ge is completed by the nitrogen atoms of one bidentate (N3, N4) and one monodentate amidinate (N1). The gross features (e.g. internal angles of the Ge-N3-C24-N4 cycle) of both amidinate ligands

and their relative disposition are very similar to **2**. Not surprisingly, the three Ge(IV)-N bonds for **7** are shorter than those of the Ge(II) starting material. The Se-Ge-N angles range from 120.0(5)° to 122.3(4)°.

Ge(II) complexes with mixed ligand systems:

The observation that one of the amidinate ligands in both the Ge(II) complexes and the terminal Ge^{IV}=Ch complexes is monodentate prompted us to consider substitution of this ligand with a simple amido ligand. Complexes **1, 2** and **4-7** appear to be essentially equal to mixed amidinato amido species. Based on accessibility and the previous synthesis of $Ge^{II}[N(SiMe_3)_2]_2$, we chose to investigate the substitution of the dangling amidinate with $N(SiMe_3)_2$ moiety. It should be noted that reaction of $Ge^{II}[N(SiMe_3)_2]_2$ with chalcogen is rapid and yields the expected bridging system $(\mu\text{-Ch})_2\{Ge[N(SiMe_3)_2]_2\}_2$.[20]

The mixed ligand species **8** and **10** were obtained by the stepwise reaction of $GeCl_2$(dioxane) with one equivalent of lithium amidinate followed by addition of one equivalent of lithium amide (Scheme 2.3). Only in the case of CyNC(^{t}Bu)NCy]2GeCl (**9**) was the intermediate species isolated and characterized. The ^{1}H NMR spectrum of $CyNC(^tBu)NCy]_2GeN(SiMe_3)_2$ (**10**) displays a broadened singlet for the trimethylsilyl groups relative to that of $CyNC(Me)NCy]GeN(SiMe_3)_2$ (**8**) indicative of hindered rotation of the amido ligand.

Figure 2.4. Molecular structure and atom numbering scheme for $[CyNC(^tBu)NCy]_2Ge{=}Se$ (**7**) (Cy=cyclohexyl). Hydrogen atoms have been omitted for clarity.

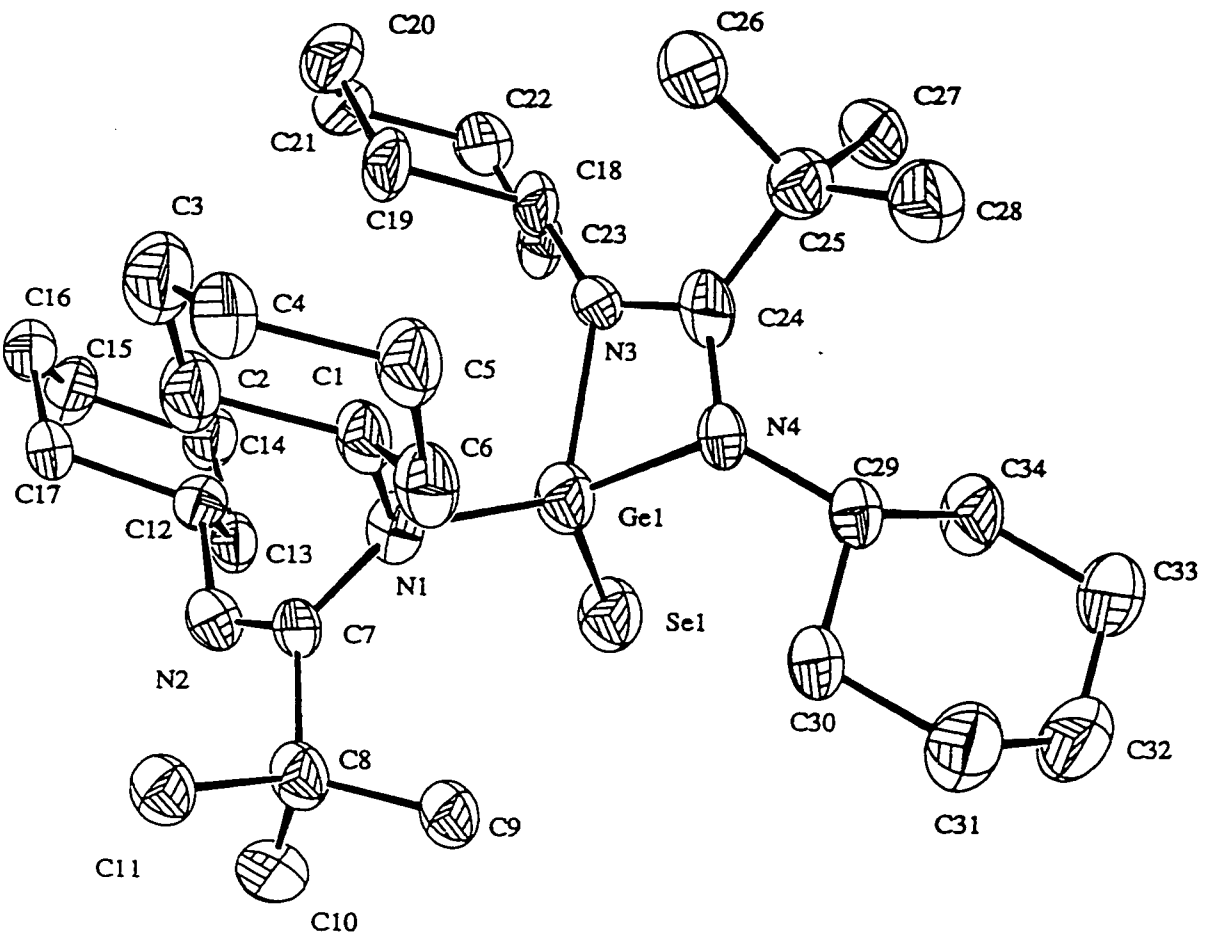

Table 2.6. Selected bond lengths(Å) and angles(°) for complex **7**

Distances			
Ge-Se	2.196(4)	N1-C7	1.42(2)
Ge-N1	1.86(1)	N2-C7	1.27(2)
Ge-N3	2.01(1)	N3-C24	1.29(2)
Ge1-N4	1.99(1)	N4-C24	1.35(2)
Angles			
N1-Ge-N3	106.4(6)	Ge-N4-C24	91.7(11)
N1-Ge-N4	108.9(6)	N3-C24-N4	109.9(16)
N3-Ge-N4	65.6(6)	Se1-Ge1-N1	120.0(5)
Ge-N1-C7	119.8(11)	Se1-Ge1-N3	122.3(4)
C1-N1-C7	123.9(13)	Se1-Ge1-N4	121.4(4)
Ge-N3-C24	92.4(11)		

Figure 2.5. Molecular structure and atom numbering scheme for $[C_6H_{11}NC(Me)NC_6H_{11}]Ge[N(SiMe_3)_2]Se$ (**11**) (Cy=cyclohexyl).

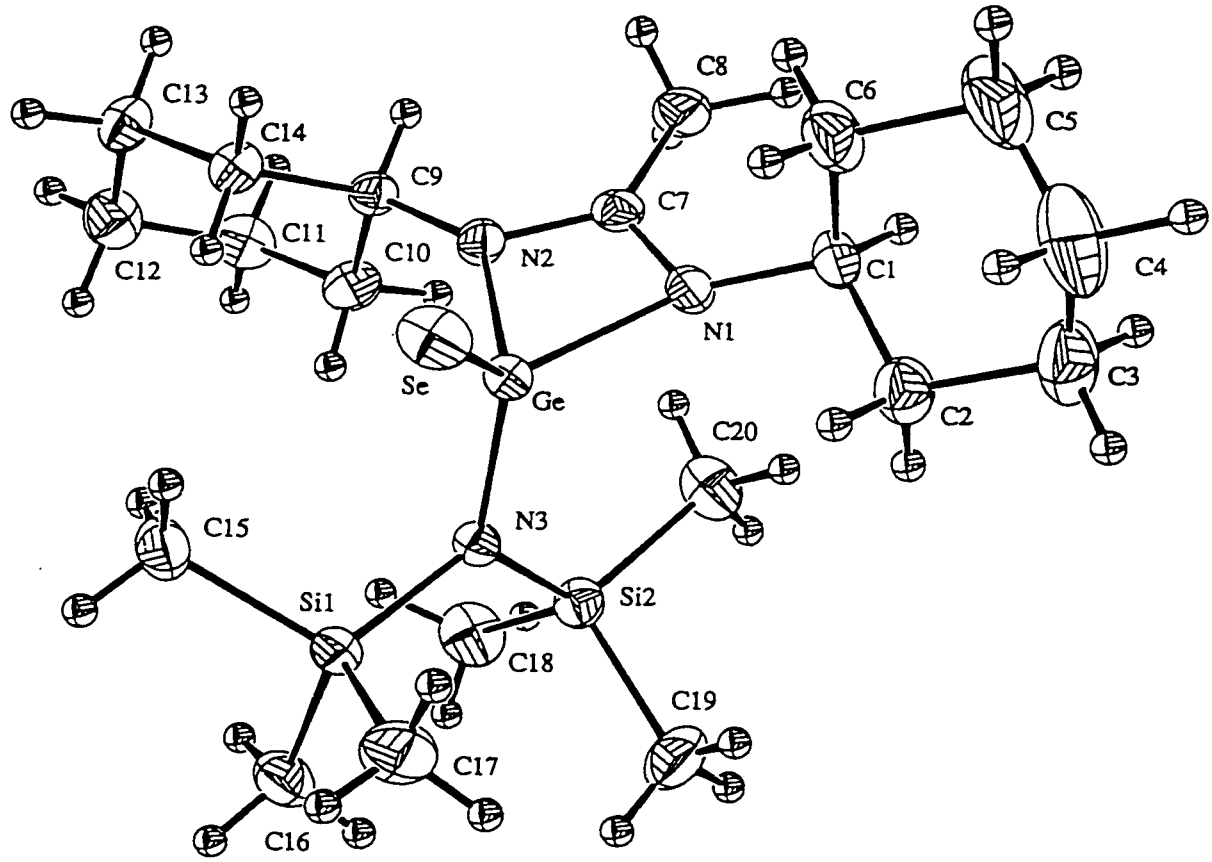

Table 2.7. Selected bond lengths(Å) and angles(°) for complex **11**

Distances			
Ge-Se	2.2212(3)	N1-C7	1.3367(24)
Ge-N1	1.9946(15)	N2-C7	1.3209(24)
Ge-N2	1.9572(15)	N3-Si1	1.7723(15)
Ge-N3	1.8410(15)	N3-Si2	1.7542(15)
Angles			
Se-Ge-N1	115.18(5)	N2-Ge-N3	107.42(6)
Se-Ge-N2	121.03(5)	Ge-N1-C7	92.12(11)
Se-Ge-N3	120.52(5)	Ge-N2-C7	92.06(11)
N1-Ge-N2	67.14(6)	N1-C7-N2	108.54(16)
N1-Ge-N3	114.05(6)		

These Ge(II) species also readily react with elemental selenium to yield chalcogenido complexes $[CyNC(Me)NCy]_2Ge[N(SiMe_3)_2]Se$ (**11**) and $[CyNC(^tBu)NCy]_2Ge[N(SiMe_3)_2]Se$ (**12**). Both COSY and heteroatom ($^{13}C/^1H$) correlation NMR experiments for **12** were consistent with the connectivity shown in Scheme 2.5. As in the case of **10,** the NMR spectrum of **12** indicates that there is hindered rotation around Ge-$N(SiMe_3)_2$ bond. The appearance of a ^{77}Se NMR resonance at $\delta = 1115.6$ vs. Me_2Se in **11** is similar to **7** and appropriate for a terminal function.[11]

A single crystal X-ray diffraction analysis provided the detailed connectivity of **11** (Table 2.5). From Figure 2.5 it is clear that **11**, like **7**, is a terminal Ge chalcogenido species (for selected bond distances and angles, see Table 2.7). Again, the Ge coordination geometry in this complex is that of a distorted tetrahedron with the Ge-Se vector residing on one of the vertices at a slightly longer distance (2.2212(3)Å) than in **7** but comparable to literature species.[9,11] The coordination sphere of Ge is completed by the nitrogen atoms of one bidentate (N1, N2) amidinate and the bis(trimethylsilyl)amido nitrogen (N3). The internal angles of the planar Ge-N1-C7-N2 cycle are reminiscent of those in the bidentate ligands in **1**, **2**, and **7**. The amido nitrogen (N3) is planar with the plane of this ligand rotated out of the plane of the amidinate ligand (torsional angles: N1-Ge-N3-Si1 165.2°, N1-Ge-N3-Si2 = -9.04°, Se-Ge-N3-Si1 21.72°). The three Ge(IV)-N bonds are very similar to those of **7** and the Se-Ge-N are slightly smaller and range from 115.18(5)° to 121.03(5)°.

Conclusion:

Terminal chalcogenido germanium complexes have been prepared from a unique family of bis(amidinato) Ge(II) and mixed (amidinato)(amido) Ge(II) compounds. These results add significantly to the limited number of structurally characterized terminal chalcogenido complexes. These new species will help to delineate the steric and electronic features which stabilize and influence the reactivity of such species.

The structural studies presented above show that Ge(II) and Ge(IV) complexes with these ligand environments have a strong disposition towards a tetrahedral coordination geometry. This tendency leads to the systematic observation of dangling ligands in the bis(amidinate) systems. This contrasts with reported Sn(II/IV) analogues. However, in the monoamidinate Ge(IV) complex (CyNC(^{t}Bu)NCy)$GeCl_3$, a trigonal bipyramidal environment exists in favour of a tetrahedral coordination geometry. Sterics rather than electronics in this example could provide an explanation for deciding if the dangling ligand effect will present itself. An investigation to examine these geometric effects is described in Chapter 4. In conclusion, amidinate anions have been shown to be excellent ancillary ligands for Ge complexes with fairly well-defined structural features.

Preparation of these relatively stable Ge=Ch species is allowing a thorough study of their reactivity. Chapter three focuses on terminal chalcogen atom exchange reactions involving germanium, tin and phosphorus chalcogenides.

Experimental for Chapter Two

General Considerations: All manipulations were carried out in a Vacuum Atmospheres Company dry box or on a vacuum line using standard Schlenk techniques. Solvents were distilled under nitrogen from Na/K alloy. $GeCl_2$(dioxane)[21] was prepared by literature procedures. ^tBuLi, MeLi, $LiN(SiMe_3)_2$ and dicyclohexylcarbodiimide were used as received from Aldrich Chemical Company.

NMR spectra were run on a Gemini 200 MHz or Bruker 500MHz spectrometer with deuterated benzene as a solvent and internal standard. All elemental analyses were run on a Perkin Elmer PE CHN 4000 elemental analysis system. Satisfactory CHN microanalysis was obtained for all products.

$Ge[C_6H_{11}NC(Me)NC_6H_{11}]_2$ (1)

To a solution of dicyclohexylcarbodiimide (0.889 g, 4.32 mmol) in diethyl ether (40 ml) was added MeLi (3.08 ml, 1.4M, 4.32 mmol). After 30 min., $GeCl_2$(diox) (0.50 g, 2.16 mmol) was added. The solution was stirred for 12 hrs, filtered to remove the white LiCl precipitate and evaporated to dryness. Colorless crystals were obtained from hexanes at -34 °C (1.73g, 78% yield). Spectroscopic data: ^1H NMR (C_6D_6, ppm) 3.29 (br, C_6H_{11}, 4H); 2.02-1.16 (m, C_6H_{11}, 40H); 1.64 (s, Me, 6H). ^{13}C NMR (C_6D_6, ppm) 163.0 (s, NCN); 56.3, 35.8, 26.5, 26.3 (4s, C_6H_{11}); 12.6 (s, Me).

$Ge[C_6H_{11}NC(CMe_3)NC_6H_{11}]_2$ (2)

To a solution of dicyclohexylcarbodiimide (1.24 g, 6.00 mmol) in diethyl ether (50 ml) was added ^tBuLi (3.55 ml, 1.7M, 6.00 mmol). After 30 min., $GeCl_2$(diox) (0.700 g, 3.00 mmol) was added. The solution was stirred for 12 hrs, filtered to remove the white LiCl precipitate and evaporated to dryness. Pale yellow crystals were obtained from a.50:50 mixture of hexamethyldisiloxane / hexanes at -34 °C (3.05g, 85% yield). Spectroscopic data: ^1H NMR (C_6D_6, ppm) 4.10 (br, C_6H_{11}, 1H); 3.77 (br, C_6H_{11}, 2H); 3.50 (br, C_6H_{11}, 1H); 2.35-1.17 (m, C_6H_{11}, 40H); 1.61 (s, CMe_3, 9H); 1.17 (s, CMe_3, 9H).

$(C_6H_{11}NC(^tBu)N\ C_6H_{11})GeCl_3$ (3)

To a solution of dicyclohexylcarbodiimide (0.400 g, 1.94 mmol) in toluene (20 ml) was added ^tBuLi (1.14 ml, 1.7M, 1.94 mmol). After 30 min., the solution was added to 1 eq. $GeCl_4$ (0.416 g, 1.94 mmol) in toluene (20 ml). The solution was stirred for 16 hrs, filtered, and the solvent removed *in vacuo*. Colourless crystals were obtained from ether (0.76g, 88% yield). Spectroscopic data: ^1H NMR ($CDCl_3$, ppm) 3.68 (br, C_6H_{11}, 2H); 2.24-1.05 (m, C_6H_{11}, 20H); 1.47 (s, CMe_3, 9H). ^{13}C NMR (C_6D_6, ppm) 57.9, 33.3, 29.5, 25.5 (4s, C_6H_{11}); 26.7 (s, $\underline{C}Me_3$).

$[C_6H_{11}NC(Me)NC_6H_{11}]_2GeS$ (4)

To a solution of **1** (0.152 g, 0.30 mmol) in hexanes (5 ml) was added styrene sulfide (0.061 g, 0.45 mmol). Product slowly precipitated out of solution. The solution was stirred for 12 hrs, filtered, and crystallized from ether at -34 °C (0.12g, 75% yield of

colorless crystals of **3**). Spectroscopic data: ^{1}H NMR (C_6D_6, ppm) 3.27 (br, C_6H_{11}, 4H); 2.12-1.04 (m, C_6H_{11}, 40H); 1.49 (s, Me, 6H).

$[C_6H_{11}NC(CMe_3)NC_6H_{11}]_2GeS$ (5)

To a solution of **2** (0.110 g, 0.184 mmol) in hexanes (5 ml) was added styrene sulfide (0.037 g, 0.28 mmol). Product slowly precipitated out of solution. The solution was stirred for 12 hrs, filtered, and crystallized from ether at -34 °C (0.087g, 75% yield of colorless crystals of **4**). Spectroscopic data: ^{1}H NMR (C_6D_6, ppm) 4.07 (br, C_6H_{11}, 1H); 3.71 (br, C_6H_{11}, 2H); 3.22 (br, C_6H_{11}, 1H); 2.67-0.90 (m, C_6H_{11}, 40H); 1.70 (s, CMe3, 9H); 1.07 (s, CMe3, 9H).

$[C_6H_{11}NC(Me)NC_6H_{11}]_2GeSe$ (6)

To a solution of **1** (1.00 g, 1.94 mmol) in ether (15 ml) was added 1 eq. selenium (0.154 g, 1.94 mmol). The solution was stirred for 12 hrs and evaporated to dryness. Colorless rystals were obtained from ether at -34 _C (1.02g, 89% yield). Spectroscopic data: ^{1}H NMR (C_6D_6, ppm) 3.30 (br, C_6H_{11}, 4H); 2.15-0.85 (m, C_6H_{11}, 40H); 1.50 (s, Me, 6H).

$[C_6H_{11}NC(CMe_3)NC_6H_{11}]_2GeSe$ (7)

To a solution of **2** (0.300 g, 0.500 mmol) in ether (10 ml) was added 1 eq. selenium (0.040 g, 0.500 mmol). The solution was stirred for 12 hrs and evaporated to dryness. Crystals were obtained from ether at -34 _C (0.25g, 85% yield of colorless crystals of **6**). Spectroscopic data: ^{1}H NMR (C_6D_6, ppm) 4.03 (br, C_6H_{11}, 1H); 3.75 (br, C_6H_{11}, 2H);

3.23 (br, C_6H_{11}, 1H); 2.70-0.90 (m, C_6H_{11}, 40H); 1.71 (s, CMe_3, 9H); 1.07 (s, CMe_3, 9H). ^{13}C NMR (C_6D_6, ppm) 178.7 (s, NCN); 162.5 (s, NCN); 32.2 (s, Me); 28.6 (s, Me). ^{77}Se NMR (C_6D_6, ppm vs. Me_2Se) 1023.8 (s, GeSe).

$[C_6H_{11}NC(Me)NC_6H_{11}]GeN(SiMe_3)_2$ (8)

To a solution of dicyclohexylcarbodiimide (0.445 g, 2.16 mmol) in diethyl ether (25 ml) was added MeLi (1.54 ml, 1.4M, 2.16 mmol). After 30 min., the solution was added to 1 eq. $GeCl_2$(diox) (0.500 g, 2.16 mmol) in diethyl ether (25 ml). The solution was stirred for 6 hrs and 1 eq. of lithium bis(trimethylsilylamide) (0.361 g) was then added. The solution was stirred for another 12 hrs and filtered to remove the white LiCl precipitate. The solvent was removed under vacuum at which point an intractable yellow oil was observed as the sole product (0.90g, 92% yield). Spectroscopic data: ^1H NMR (C_6D_6, ppm) 3.05 (br, C_6H_{11}, 2H); 2.00-1.02 (m, C_6H_{11}, 20H); 1.29 (s, Me, 3H); 0.46 (s, $SiMe_3$, 18H).

$[C_6H_{11}NC(CMe_3)NC_6H_{11}]GeCl$ (9)

To a solution of dicyclohexylcarbodiimide (0.267 g, 1.30 mmol) in diethyl ether (20 ml) was added ^tBuLi (0.76 ml, 1.7M, 1.30 mmol). After 30 min., 1 eq. $GeCl_2$(diox) (0.300 g, 1.30 mmol) was added. The solution was stirred for 12 hrs, filtered to remove the white LiCl precipitate and evaporated to dryness to give a white solid. Spectroscopic data: ^1H NMR (C_6D_6, ppm) 3.62 (br, C_6H_{11}, 2H); 2.12-0.90 (m, C_6H_{11}, 20H); 1.20 (s, CMe_3, 9H).

$[C_6H_{11}NC(CMe_3)NC_6H_{11}]GeN(SiMe_3)_2$ (10)

To a solution of **8** (0.130 g, 0.350 mmol) in ether (10 ml) was added 1 eq. lithium bis(trimethylsilylamide) (0.217 g, 0.350 mmol). The solution was stirred for 12 hrs, filtered, and evaporated to dryness. White crystals were obtained from ether at RT (0.13g, 77% yield). Spectroscopic data: ^1H NMR (C_6D_6, ppm) 3.72 (br, C_6H_{11}, 2H); 2.20-0.95 (m, C_6H_{11}, 20H); 1.11 (s, CMe_3, 9H); 0.50 (br s, $SiMe_3$, 18H).

$[C_6H_{11}NC(Me)NC_6H_{11}]Ge[N(SiMe_3)_2]Se$ (11)

To a solution of **7** (0.98 g, 2.15 mmol) in diethyl ether (30 ml) was added 1eq selenium (0.17g, 2.15 mmol). The solution was stirred for 24 hrs and evaporated to dryness leaving behind a yellow powder. Clear, colorless crystals were obtained from 75:25 diethyl ether / hexanes at -34 °C (0.85g, 74% yield). Spectroscopic data: ^1H NMR (C_6D_6, ppm) 2.98 (br, C_6H_{11}, 2H); 2.10-0.85 (m, C_6H_{11}, 20H); 1.16 (s, Me, 3H); 0.53 (s, $SiMe_3$, 18H). ^{13}C NMR (C_6D_6, ppm) 170.0 (s, NCN); 55.3, 35.1, 33.6, 25.4 (4s, C_6H_{11}); 11.8 (s, Me); 6.1 (s, $SiMe_3$). ^{77}Se NMR (C_6D_6, ppm vs. Me_2Se) 1115.6 (s, GeSe).

$[C_6H_{11}NC(CMe_3)NC_6H_{11}]Ge[N(SiMe_3)_2]Se$ (12)

To a solution of **9** (0.050 g, 0.101 mmol) in C_6D_6 (0.5 ml) was added 1 eq. selenium (0.008 g, 0.101 mmol). Spectroscopic data: ^1H NMR (C_6D_6, ppm) 3.67 (br, C_6H_{11}, 2H); 2.75-0.90 (m, C_6H_{11}, 20H); 1.11 (s, CMe_3, 9H); 0.84 (b, $SiMe_3$, 9H); 0.33 (b, $SiMe_3$, 9H). ^{13}C NMR (C_6D_6, ppm) 175.7 (s, NCN); 57.7, 37.1, 34.3, 25.9, 25.4 (5s, C_6H_{11}); 38.1 (s, CMe_3); 28.0 (s, Me); 7.0, 5.8 (br s, $SiMe_3$).

References for Chapter Two

[1] Jutzi, P. Angew. *Chem. Int. Ed. Engl.* **1975**, *14*, 232

[2] Pauling, L. *The Nature of the Chemical Bond*, Cornell University Press, Ithica, New York, 3rd edn., **1960**

[3] West, R.; Fink, M.J.; Michl, J. *Science* **1981**, *214*, 1343

[4] Snow, J.T.; Murakami, S.; Masumune, S.; Williams, D.J. *Terahedron Lett.* **1984**, *25*, 4191. *The digermene II was synthesized by photolysis of tetrakis(2,6-ethylphenyl)cyclotrigermane.

[5] Meyer, H.; Baum, G.; Massa, W.; Berndt, A. *Angew. Chem., Int. Ed. Engl.* **1987**, *26*, 798

[6] Glidewell, C.; Lloyd, D.; Lumbard, K.W.; McKechnie, J.S. *Tetrahedron Lett.* **1987**, *28*, 343

[7] Veith, M.; Becker, S.; Huch, V. *Angew. Chem., Int. Ed. Engl.* **1989**, *28*, 1237

[8] Kuchta, M.C.; Parkin, G. *J. Chem. Soc., Chem. Commum.* **1994**, 1351

[9] Matsumoto, T.; Tokitoh, N.; Okazaki, R. . *J. Chem. Soc., Chem. Commum.* **1997**, 1553

[10] Tokitoh, N.; Matsumoto, T.; Manmaru, K.; Okazaki, R. *J. Am. Chem. Soc.* **1993**, *115*, 8855

[11] Matsumoto, T.; Tokitoh, N.; Okazaki, R. *Angew. Chem., Int. Ed. Engl.* **1994**, *33*, 2316

[12] Tokitoh, N.; Matsumoto, T.; Okazaki, R. *J. Am. Chem. Soc.* **1997**, *119*, 2337

[13] Ossig, G.; Meller, A.; Bronneke, C.; Muller, O.; Schafer, M.; Herbst-Irmer, R. *Organometallics* **1997**, *16*, 2116

[14] Barrau, J.; Escudie, J.; Satge, J. *Chem. Rev.* **1990**, *90*, 283. Escudie, J.; Couret, C.; Satge, J. *Coord. Chem. Rev.* **1994**, *130*, 427

[15] Kuchta, M.C.; Parkin, G. *Coord. Chem. Rev.* **1998**, *176*, 323

[16] Norman, N.C. Polyhedron **1993**, *12*, 2431. Stone, F.G.A.; West, R. *Adv. Organomet. Chem.* **1996**, *39*, 1. Power, P.P. *J. Chem. Soc., Dalton Trans.* **1998**, 2939

[17] Zhou, Y.; Richeson, D. S. *J. Am. Chem. Soc.* **1996**, *118*, 10850

[18] Dehnicke, K.; Ergezinger, C.; Hartmann, E.; Zinn, A.; Hösler, K. *J. Organomet. Chem.* **1988**, *352*, C1. Roesky, H. W.; Meller, B.; Noltemeyer, M.; Schmidt, H.-G.; Scholz, U.; Sheldrick, G. M. *Chem. Ber.* **1988**, *121*, 1403. Ergezinger, C.; Weller, F.; Dehnicke, K. *Z. Naturforsch.* **1988**,*43B*, 1621. Kidea, J. D.; Hiller, W.; Borgsen, B.; Dehnicke, K. *Z. Naturforsch.* **1989**,*44B*, 889. Appel, S.; Weller, F.; Dehnicke, K. *Z. Anorg. Allg. Chem.* **1990**,*583*, 7. Borgsen, B.; Dehnicke, K.; Fenske, D.; Baum, G. *Z. Anorg. Allg. Chem.* **1991**,*596*, 133. Kilimann, U.; Noltemeyer, M.; Edelmann, F. T. *J. Organomet. Chem.* **1993**, *443*, 35.

[19] Karsch, H.H.; Schluter, P.A.; Reisky, M. *Eur. J. Inorg. Chem.* **1998**, 433

[20] Hitchcock, P. B.; Jang, E.; Lappert, M. F. *J. Chem. Soc., Dalton Trans.* **1995**, 3179. Hitchcock, P. B.; Jasim, H. A.; Lappert, M. F.; Leung, W-P. Rai, A. K.; Taylor, R. E. *Polyhedron* **1991**, *10*, 1203

[21] Fjeldberg, T.; Haaland, A.; Schilling, B. E. R.; Lappert, M. F.; Thorne, A. J. *J. Chem. Soc., Dalton Trans.* **1986**, 1551

Study of Single Chalcogen Atom Transfer Reactions Involving Tin and Germanium

"six shots or only five?"

Chapter Three

Introduction

Atom exchange reactions are an important area of fundamental research due to their manifest pertinence in redox processes. The result of many oxidation reactions can be formally described as the transfer of single atoms such as oxygen or sulfur. It is nevertheless rarely facile to obtain mechanistic evidence for the involvement of transient activated complexes. There have been a large number of examples involving oxygen atom transfer between metal centers however relatively few studies have been performed on the heavier chalcogens. Most chalcogen atom studies involve transfer of an oxygen atom from (i) a non-metal species to a low valent transition metal center[1], (ii) from a transition metal oxo species to a phosphine[2] or (iii) between two homonuclear transition metal species[3]. Oxygen atom transfer reactions are of importance in the d-block for example due to the use of transition metal complexes as catalysts for epoxidation of hydrocarbons[4]. In the main group however, few intermetal single chalcogen atom transfer reactions have been observed.

The only reported observation of a single sulfur or selenium atom transfer from tin to germanium has been described by Parkin[5] using terminal sulfido and selenido complexes of the macrocyclic tin [η^4-Me_8taa]SnE (E = S, Se; Me_8taa = octamethyldibenzotetraazaannulene) to the corresponding Ge(II) species (eq 3.1).

$$[\eta^4\text{-Me}_8\text{taa}]\text{SnE} + [\eta^4\text{-Me}_8\text{taa}]\text{Ge}^{II} \rightarrow [\eta^4\text{-Me}_8\text{taa}]\text{Sn}^{II} + [\eta^4\text{-Me}_8\text{taa}]\text{GeE} \quad (\mathbf{3.1})$$

The poor solubility of $[\eta^4\text{-Me}_8\text{taa}]$GeE made the establishment of kinetic parameters impractical in this system.

Parkin has more recently extended this work by preparing terminal selenido complexes of gallium and indium supported by tris(3,5-di-tert-butylpyrazolyl)hydroborato (Tp^{tBu_2}) ligation and has observed selenium atom transfer from indium to gallium (eq 3.2).[6]

$$[Tp^{tBu_2}]\text{InSe} + [Tp^{tBu_2}]\text{Ga}^{I} \rightarrow [Tp^{tBu_2}]\text{In}^{I} + [Tp^{tBu_2}]\text{GaSe} \quad (\mathbf{3.2})$$

Only one comprehensive study has been reported demonstrating single atom transfer reactions with a group 14 element and the heavier chalcogens. The study involved the reversible transfer of sulfur and selenium atoms between tin porphyrin complexes using *meso*-tetraphenylporphyrinato (TPP) and *meso*-tetra-*p*-tolylporphyrinato (TTP) tin species (eq 3.3).[7]

$$(\text{TTP})\text{Sn}^{II} + (\text{TPP})\text{Sn=Ch} \rightleftharpoons (\text{TTP})\text{Sn=Ch} + (\text{TPP})\text{Sn}^{II} \quad (3.3)$$

Kinetic measurements on eq 3.3 (Ch = S) at temperatures ranging from 30 to 60°C resulted in k_f values from 0.40 to 2.39 $M^{-1}s^{-1}$ where $\Delta H^{\ddagger}$= 10.9 kcal/mol and $\Delta S^{\ddagger}$= -24.1 cal$(mol{\cdot}K)^{-1}$.

It is also worthwhile to note that an oxygen atom transfer metathesis reaction from a Re(VII) complex to germanium has been observed[8] (eq 3.4).

$$(\eta^5\text{-}C_5H_5)ReO_3 + GeCl_2(diox) \rightarrow (\eta^5\text{-}C_5H_5)ReOCl_2 + GeO_2 \quad (3.4)$$

I have been studying the effects of amidinate ligands on the coordination environments and chemistry of group 14 metals. Coincident with this is my interest in the formation of multiple bonds between main group elements and the subsequent reactivity of these multiple bonds.[9]

Amidinates have been used extensively as ligands for transition metals as well as main group elements. Amidinato complexes of tin have been prepared with the metal in both the tetravalent and divalent oxidation states however very few reactivity studies have been carried out with tin specifically and I have only recently prepared the first amidinato complexes of germanium. The synthesis and structural characterization of the terminal sulfido complex[10] of Sn, $(CyNC(^tBu)NCy)_2Sn{=}S$ $[(Cy^{tBu})_2Sn{=}S]$, and the terminal sulfido and selenido complexes[11] of germanium, $(CyNC(^tBu)NCy)_2Ge{=}E$ $\{[(Cy^{tBu})_2Ge{=}E]$; E = S, Se$\}$ by oxidative addition of styrene sulfide or elemental selenium to the corresponding M(II) precursors, $(CyNC(^tBu)NCy)_2M$ $\{[(Cy^{tBu})_2M]$; M = Ge, Sn$\}$ was described in Chapter Two. I was, unfortunately, unable to synthesize the terminal selenido complex of tin and thus unable to study the selenium atom exchange reactions.

This chapter reports the first comprehensive study of heteronuclear intermetal sulfur atom transfer reactions. Results of chalcogen atom exchange reactions involving germanium and phosphine chalcogenides will also be presented and discussed.

Results and Discussion

Complete sulfur atom exchange between amidinate complexes of tin and germanium can be achieved according to eq 3.5.

$$(Cy^{tBu})_2Sn{=}S + (Cy^{tBu})_2Ge^{II} \rightarrow (Cy^{tBu})_2Sn^{II} + (Cy^{tBu})_2Ge{=}S \quad \textbf{(3.5)}$$

The reaction of $(Cy^{tBu})_2Sn{=}S$ with $(Cy^{tBu})_2Ge$ in C_6D_6 can be monitored by ^1H NMR. The proton shifts are consistent with the transfer of a terminally bonded sulfur atom from tin to germanium. The ^{t}Bu moiety of the amidinate ligands provides a convenient spectroscopic handle to monitor the reaction. For example, as the reaction progresses, new ^{t}Bu resonances appear at 1.35 ppm signifying the formation of $(Cy^{tBu})_2Sn$ while the ^{t}Bu resonances of $(Cy^{tBu})_2Sn{=}S$ at 1.17 ppm correspondingly decrease in intensity.

The ^{t}Bu resonances for the germanium complexes are slightly more complicated. Instead of having both amidinate ligands bidentate as with tin, the complexes exhibit one bidentate and one monodentate ("dangling") ligand, where the Ge center prefers to be in a distorted tetrahedral environment rather than the expected trigonal bipyramidal based geometry (Scheme 3.1). This phenomenon has been shown both structurally and spectroscopically in both $(Cy^{tBu})_2Ge$ and $(Cy^{tBu})_2Ge{=}S$ as well as in a number of other germanium amidinate complexes I have prepared (Ch. 2 and 4). Due to the inequivalence of the two amidinate ligands, two separate ^{t}Bu signals are observed for both $(Cy^{tBu})_2Ge$ and $(Cy^{tBu})_2Ge{=}S$. Thus, new ^{t}Bu resonances appear at 1.70 and 1.07 ppm signifying the

formation of $(Cy^{tBu})_2Ge{=}S$ while the resonances of $(Cy^{tBu})_2Ge$ at 1.61 and 1.16 correspondingly decrease in intensity.

By comparing the integration of the ^tBu resonances of either $(Cy^{tBu})_2Ge{=}S$ or $(Cy^{tBu})_2Sn$ to that of the starting materials, the progress of the reaction can be monitored.

In all kinetic runs, the data for the atom transfer reaction (Scheme 3.1) was found to obey an integrated rate law for second order reactions. Plots of reciprocal concentration vs time were linear for at least 2 half lives. A typical kinetic curve for $[Ge(Cy^{tBu})_2]$ and the corresponding 1/c plot are illustrated in Figure 3.1.

Rate constants for eq 3.5 were determined over a 40°C temperature range. A summary of the data is given in Table 3.1. Temperature ranges from 25 to 65°C resulted in k values from 1.18×10^{-3} to 2.14×10^{-2} $M^{-1}s^{-1}$ with resulting half lives of 18 hours to 31 minutes. The thermal decomposition of $(Cy^{tBu})_2Ge{=}S$ precluded further studies at higher temperatures. The temperature dependence of the rate constants yielded activation parameters $\Delta H^{\ddagger}= 17.6 \pm 0.2$ kcal/mol and $\Delta S^{\ddagger}= -14.4 \pm 0.3$ cal$(mol\cdot K)^{-1}$ derived from the Eyring equation. An Eyring plot of ln(k/T) vs. 1/T is a straight line as shown in Figure 3.3.

Pseudo-first order conditions were imposed by having $(Cy^{tBu})_2Sn{=}S$ in large excess compared to $(Cy^{tBu})_2Ge$ indicating the contribution of $(Cy^{tBu})_2Ge$ and subsequent formation of $(Cy^{tBu})_2Ge{=}S$ was first order. A plot of the natural logarithm of the concentration versus time is linear as illustrated in Figure 3.2. At 35°C, the rate constant k_1 was found to be $(2.09 \pm 0.49)\times10^{-4}$ s^{-1}.

Scheme 3.1

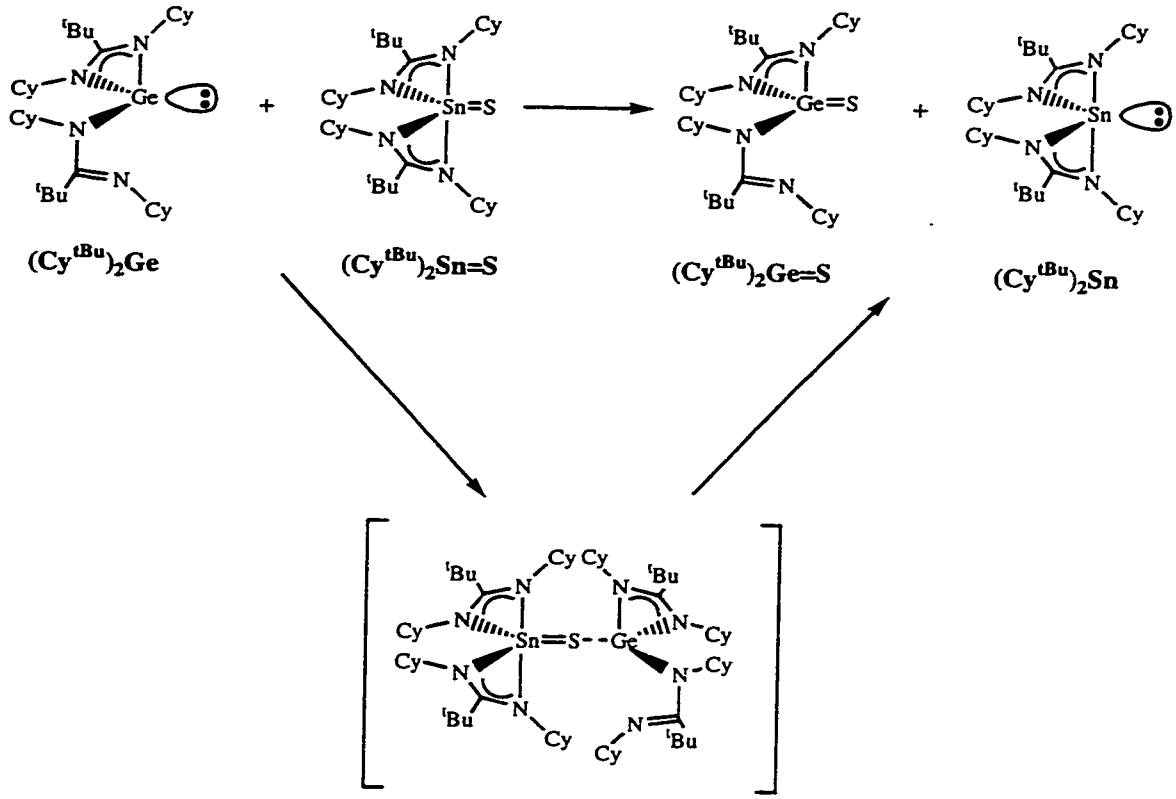

Table 3.1. Rate constants for eq 3.5 in C_6D_6

Temp (°C)	k ($M^{-1}s^{-1}$)
25	(6.28±0.84) x 10^{-4}
35	(1.46±0.13) x 10^{-3}
45	(4.19±0.06) x 10^{-3}
55	(1.08±0.04) x 10^{-2}
60	(1.53±0.06) x 10^{-2}
65	(2.14±0.05) x 10^{-2}

The reaction probably proceeds via an inner sphere mechanism mediated by attack of the chalcogen atom on tin to the Ge(II) center resulting in a sulfur bridged intermediate $[(Cy^{tBu})_2Sn{=}S{\cdots}Ge(Cy^{tBu})_2]$. The proposed sulfur bridged intermediate necessary for an inner sphere mechanism is not observed by NMR, however the negative entropy of activation ($\Delta S^{\ddagger}$= -14.4 cal(mol·K)$^{-1}$) is consistent with an associative type reaction involving atom transfer via a sulfido bridged intermediate. As well, the low $\Delta H^{\ddagger}$ value suggests that significant bond formation occurs ($Sn^{IV}{=}S{\cdots}Ge^{II}$).

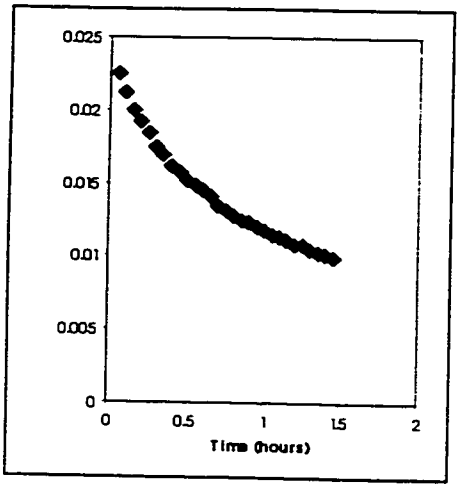

(a)

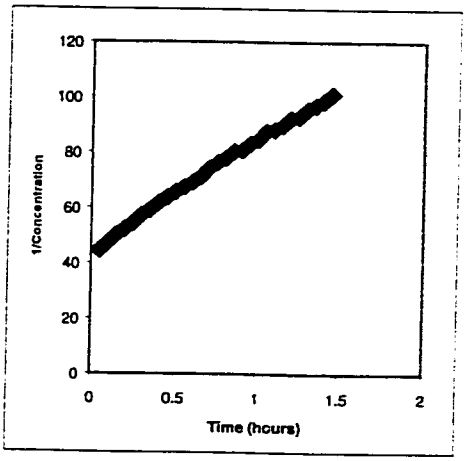

(b)

Figure 3.1
Representative plot of:
(a) Concentration $[Ge(Cy^{tBu})_2]$ vs time for eq 3.5 at 55°C
(b) corresponding 1/concentration plot

The atom exchange reaction studied here demonstrates that Ge=S interactions are significantly stronger than the corresponding Sn=S interactions. This is consistent with the notions that both the tendency to engage in multiple bonding and the stability of M(IV) *vs* M(II) decreases for the heavier congeners of the group 14 elements (Ge > Sn > Pb). This is further supported by the fact that the π-bond energy associated with the Sn=S

bond has been estimated to be 31.8 kcal/mol which is considerably lower than that of the Ge=S bond at 40.0 kcal/mol.[12]

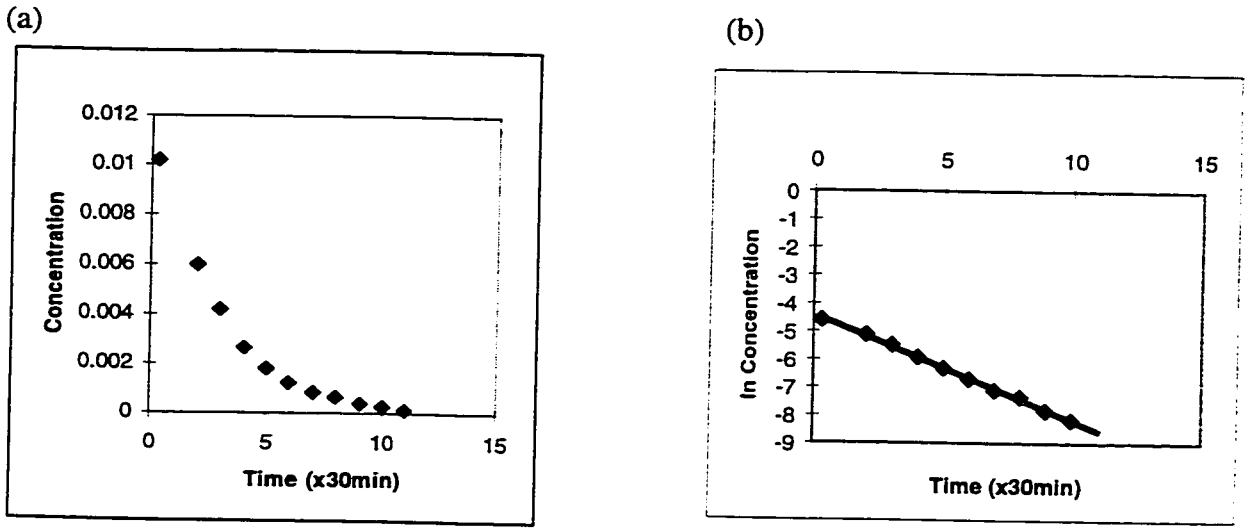

Figure 3.2.
(a) plot of concentration [$Ge(Cy^{tBu})_2$] vs time for eq. 3.5 under pseudo first order conditions at 35°C
(b) corresponding ln C plot

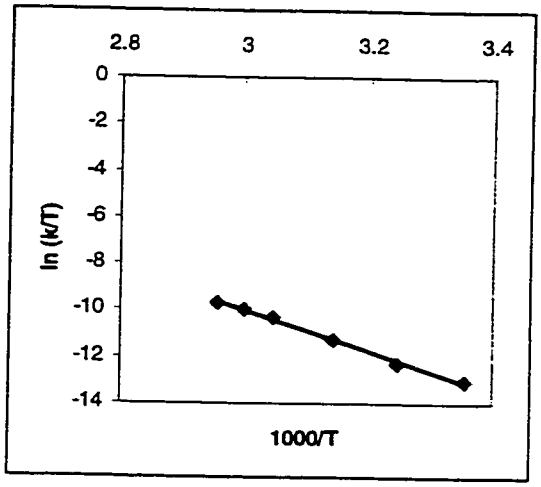

Figure 3.3. Eyring plot derived from $k = (k_bT/hC^{\theta})e^{\Delta S/R}e^{-\Delta H/RT}$

Chalcogen atom exchange reactions involving germanium and phosphine chalcogenides were also studied according to Scheme 3.2. $(Cy^{tBu})_2Ge$ was allowed to react with 1 equiv triphenylphosphine selenide in C_6D_6. It was found that complete selenide atom exchange was achieved from the phosphorus to the germanium in less than four minutes at room temperature. ^1H NMR showed complete conversion of $(C_6H_5)_3P{=}Se$ to $(C_6H_5)_3P$ while the germylene was converted to $(Cy^{tBu})_2Ge{=}Se$.

However, when the same reaction was performed with triphenylphosphine sulfide in place of the selenide, no reaction was observed with $(Cy^{tBu})_2Ge$ even at elevated temperatures. This is consistent with decreasing covalent bond energies on going to the heavier congeners of group 16. The relative rate of selenium versus sulfur atom exchange is expected to be much higher. For example, in equation 3.3, the relative rate of selenium to sulfur atom exchange is 218:1 at 30°C.[7]

Scheme 3.2

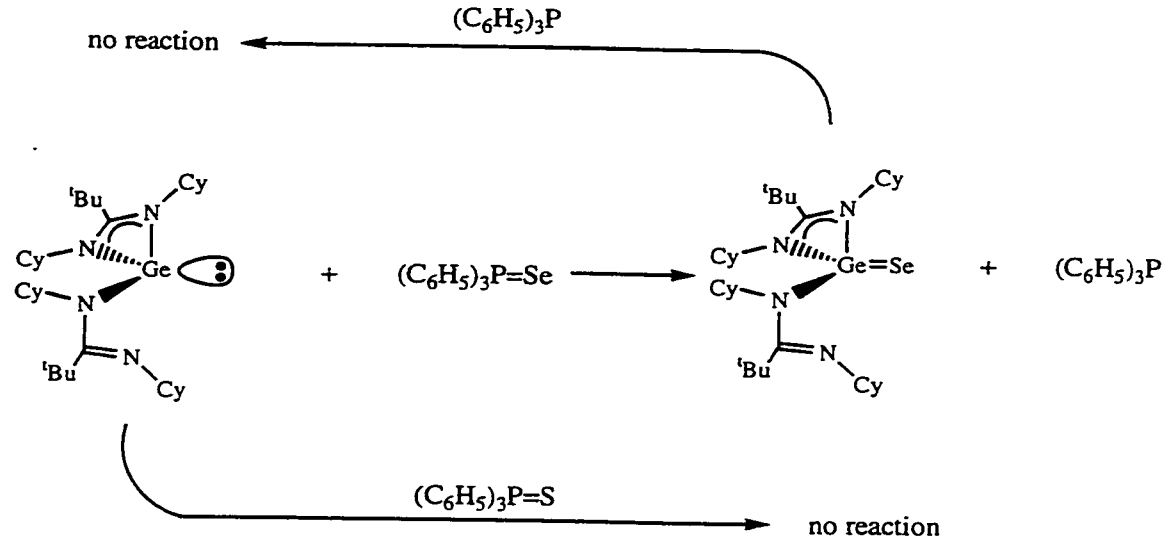

Conclusion

We have found complete sulfur atom exchange between tin and germanium amidinates can be achieved. This chapter represents the first comprehensive study of a heteronuclear intermetal two-electron sulfur atom transfer between Sn and Ge. This process can be readily monitored by NMR. The amidinato ligand system provides excellent spectroscopic handles to monitor the progress of the reaction. Rate constants for sulfur atom transfer in equation 3.5 were found to vary from 1.18×10^{-3} to 2.14×10^{-2} $M^{-1}s^{-1}$ at temperature ranges from 25 to 65°C. This contrasts sharply with the only previously reported sulfur atom exchange reaction between two tin centers (eq. 3.3) where k_f values were found to vary from 0.40 to 2.39 $M^{-1}s^{-1}$. The temperature dependence for equation 3.5 yielded activation parameters $\Delta H^{\ddagger}$= 17.6 kcal/mol and $\Delta S^{\ddagger}$= -14.4 $cal(mol \cdot K)^{-1}$. These activation parameters are similar in both value and sign to that reported for equation 3.3 ($\Delta H^{\ddagger}$= 10.9 kcal/mol and $\Delta S^{\ddagger}$= -24.1 $cal(mol \cdot K)^{-1}$). Rapid chalcogen atom exchange from P to Ge was observed when the chalcogen was selenium, however no reaction was observed when the chalcogen was sulfur.

Experimental For Chapter Three

All NMR experiments were performed on a Bruker 500 MHz or a Gemini 200 MHz spectrometer. Benzene-d_6 was distilled from Na/K alloy and used as solvent and internal standard. $(CyNC(^tBu)NCy)_2Sn{=}S$ and $(CyNC(^tBu)NCy)_2Ge$ were prepared according to literature procedures.[10,11]

Kinetic Measurements: Reactions were initiated by mixing equal volumes of 0.050 M solutions of $(CyNC(^tBu)NCy)_2Sn{=}S$ and $(CyNC(^tBu)NCy)_2Ge$ in C_6D_6 so that the concentrations of both reactants was initially 0.025 M. Samples were monitored in a temperature controlled NMR probe for at least 2 half lives. Remote ^1H NMR experiments were set up so that spectra were obtained from every 45 min for the 35°C experiments to every 3 min for the 65°C experiments. Due to the slow rate of the reaction at 25°C, a temperature controlled water bath set at 25.0°C was used where spectra were recorded manually every 2 hours for 60 hours. Rate constants were determined by comparing integrated ^1H NMR peak ratios over time and using standard integrated rate laws for second order reactions.

Pseudo first order conditions were investigated at 35°C where the initial concentrations were: $[(CyNC(^tBu)NCy)_2Sn{=}S] = 0.075$ M and $[(CyNC(^tBu)NCy)_2Ge] = 0.011$ M. Remote ^1H NMR experiments were set up so that spectra were obtained every 30 min at 35°C. Rate constants were determined by comparing integrated ^1H NMR peak ratios over time and using standard integrated rate laws for first order reactions.

$(C_6H_5)_3P{=}Se$ was prepared by dissolving triphenyl phosphine (2.038g, 7.78mmol) in 35ml THF followed by addition of excess elemental selenium (1.023g, 13mmol). The mixture was stirred for 24hrs and filtered. The product was subsequently recrystallized from THF in 66% yield (1.66g).

References for Chapter Three

[1] Holm, R.H.; Donahue, J.P. *Polyhedron* **1993**, *12*, 571-589

[2] Lorber, C.; Plutino, M.R.; Elding, L.I.; Nordlander, E. *J. Chem. Soc., Dalton Trans.* **1997**, 3997-4003

[3] Holm, R.H.; *Chem. Rev.* **1997**, *87*, 1401-1449

[4] Jorgensen, K.A. *Chem. Rev.* **1989**, *89*, 431-455

[5] Kuchta, M.C.; Parkin, G. *Inorg. Chem.* **1994**, *116*, 8372-8373

[6] Kuchta, M.C.; Parkin, G. *Inorg. Chem.* **1997**, *36*, 2492-2493

[7] Berreau, L.M.; Woo, K.L. *J. Am. Chem. Soc.* **1995**, *117*, 1314-1317

[8] Herrmann, W.A.; Floel, M.; Kulpe, J.; Felixberger, J.K., Herdtweck, E. *J. Organomet. Chem.* **1988**, *355*, 297-313

[9] For reviews of multiple bonding to Ge and Sn :
(a) Kuchta, M.C.; Parkin, G. *Coord. Chem. Rev.* **1998**, *176*, 323-372
(b) Baines, K.M.; Stibbs, W.G. *Adv. Organomet. Chem.* **1996**, *39*, 275-324.
(c) Escudie, J.; Couret, C.; Ranaivonjatovo; Satge, J. *Coord. Chem. Rev.***1994**, *130*, 427-480

[10] Zhou, Y; Richeson, D.S. *J. Am. Chem. Soc.* **1996**, *118*, 10850

[11] Foley, S.R.; Bensimon,C.; Richeson, D.S. *J. Am. Chem. Soc.* **1997**, *119*, 10359-10363

[12] Matsuhashi, Y.; Tokitoh, N.; Okazaki, R.; Goto, M. *Organometallics* **1993**, *12*, 2573-2583.

Cleavage of Chalcogen-Chalcogen Bonds: Routes to Rare Hypervalent Chalcogenolates of Sn and Ge

4

'Frankly in all the confusion...'

Chapter Four

Introduction

Our efforts to elucidate the factors that lead to unusual structural features and consequently to remarkable reactivity for the p-block metals have focused on employing amidinate anions as potentially tunable supporting ligands in complexes of these elements. For example, in Chapter two we demonstrated that bulky trialkyl amidinates provide the environment for the preparation of novel terminal chalcogenido complexes of group 14 metals {e.g. $S{=}Sn(C_6H_{11}NC(^tBu)NC_6H_{11})_2$, $Se{=}Ge[C_6H_{11}NC(Me)NC_6H_{11}][N(SiMe_3)_2]\}$.[1,2]

Amidinato complexes of tin have been reported with the metal in both the tetravalent and divalent oxidation states.[3] However, the first amidinato complexes of germanium were only recently discovered (Chapter Two). Some of these complexes have stimulated theoretical interest.[4] However, very few reactivity studies have appeared for these compounds. While our primary focus has been centered on the ability of these ligands to stabilize rare functionalities and unusual structural features, we have observed interesting reactivity for some of these complexes. For example, the M(II) (M = Ge, Sn) species are susceptible to oxidation by elemental chalcogens and many of these complexes are excellent catalyst for the cyclization of arylisocyanates (Chapter Six).

The focus of this chapter is on the oxidative cleavage of chalcogen-chalcogen bonds resulting in the formation of structurally rare cyclotetrasulfides as well as sulfur bridged dimers and other chalcogenolates.

Results and Discussion

Sulfido Complexes

Cyclic polychalcogenido ligands generally refer to chelating bidentate S_4^{2-} and S_5^{2-} ligands. A rich variety of cyclic polychalcogenido transition metal complexes such as Cp_2TiS_5[5], Cp_2VS_5[6], Cp_2MoS_4[7] and Cp_2WS_4[8] are known.[9,10] In contrast, main group analogues are relatively rare. The first main group cyclic polychalcogenide was discovered in 1991 and was the silicon-based compound **I** formed according to Scheme 4.1.[11,12] Since then, the employment of similar bulky aryl substituents has resulted in the formation of the only known mononuclear cyclic polychalcogenido complexes of the remaining heavy group 14 elements, e.g. Tbt(Mes)MS_4 (M = Ge, Sn; X = S, Se; Mes = mesityl; Tbt = 2,4,6-$[(SiMe_3)_2CH]_3C_6H_2$) and Tbt(Tip)MS_4 (M = Si, Ge, Sn, Pb; Tip = 2,4,6-$[(CH_3)CH]_3C_6H_2$).[13] The stability of these species has been attributed to the efficient steric protection offered by the Tbt ligand. These compounds serve as precursors to both stable and transient terminal sulfido complexes via chalcogen atom abstraction routes.[14] It should be noted that the bis(amido) complexes, M(II)$[N(SiMe_3)_2]_2$ (M = Ge, Sn), undergo rapid reaction with chalcogens (Ch = S, Se, Te) to yield the bridged dimers $(\mu\text{-Ch})_2\{M[N(SiMe_3)_2]_2\}_2$ (**II**).[15] In

Scheme 4.1

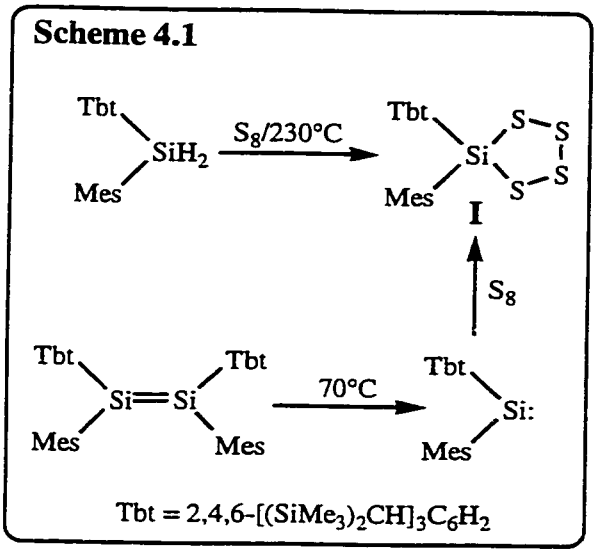

Tbt = 2,4,6-$[(SiMe_3)_2CH]_3C_6H_2$

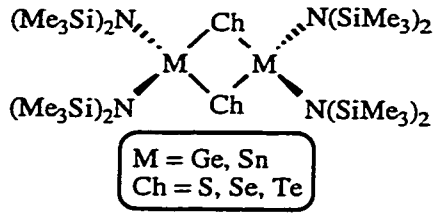

II

the remainder of the p-block, only the tris(pyrazolylborate)InS_4 complex has been reported.[16] Germanium and tin complexes with the formula $(C_6H_5)_2M(S_4)$ (M = Ge, Si) have also been described but are reported to be stable only below -20°C.[17]

The observation of terminal chalcogenido species for Ge compounds having a combination of amido and amidinato ligands prompted our investigation of the Sn(II) analogues. The first part of this chapter describes the synthesis of new cyclic tin and germanium tetrasulfido complexes derived from the oxidation of (alkylamidinato)(amido)M(II) species with elemental sulfur. These novel compounds function as outstanding catalysts for the rapid and selective catalytic cyclotrimerization of aryl isocyanates to yield isocyanurates. The trimerization of isocyanates constitutes the basis of Chapter Six.

Sn(II) complexes with mixed ligand systems

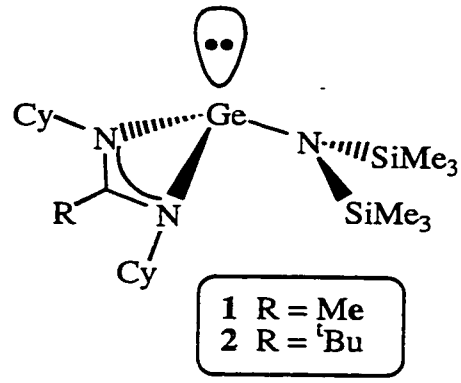

As with the mixed ligand Ge(II) species **1** and **2** described in Chapter two, the mixed ligand Sn(II) species **3** and **4** were obtained by the stepwise reaction of $SnCl_2$ with one equivalent of lithium amidinate followed by addition of one equivalent of lithium amide (Scheme 4.2). Both complexes have been characterized by spectroscopic means, microanalysis, and subsequent reactivity. In particular, the ^1H and ^{13}C NMR spectra of these species are consistent with our

formulation and reminiscent of the Ge analogues [CyNC(R)NCy]GeN(SiMe$_3$)$_2$ (R = Me. ^{t}Bu).

Scheme 4.2

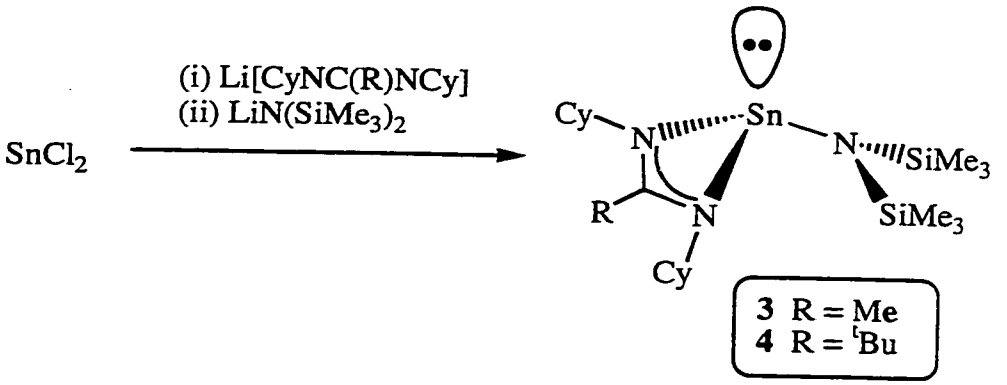

In the case of **4**, X-ray structural analysis (Table 4.1) revealed that the Sn coordination geometry is as depicted in Scheme 4.2 and consisted of the nitrogen centers of one bidentate amidinate and the bis(trimethylsilyl)amido nitrogen. Figure 4.1 provides the molecular geometry and atom numbering schemes for **4** and shows that the metal center resides in a distorted tetrahedral-based environment with one vertex occupied by a stereochemically active lone pair of electrons. Bond distances and angles are provided in Table 4.2. The result is an overall pyramidal ligand array around the M(II) center. The planarity of the amidinate ligand is confirmed by the fact that the sum of the internal angles for the four membered Sn-amidinate ring is 358.2(4)°. The corresponding C13-N1 and C13-N2 bond lengths (average 1.34Å) are consistent with delocalization of the π bond in the N-C-N unit of the ligand. This complex exhibits two slightly different M-N(amidinate) bond distances with values that are in line with those observed for reported complexes of these ligands.[1,18] The Sn-N(amido) distance (2.134(4)Å) is only slightly longer than in Sn[N(SiMe$_3$)$_2$]$_2$ (2.09(1)Å).[19]

The structural features of these complexes are similar to the Ge analogues which generated terminal chalcogenido complexes upon reaction with elemental chalcogens.

Figure 4.1. Molecular structure and atom numbering scheme for $(CyNC(^tBu)NCy)Sn[N(SiMe_3)_2]$ (**4**) (Cy=cyclohexyl). Hydrogen atoms have been omitted for clarity.

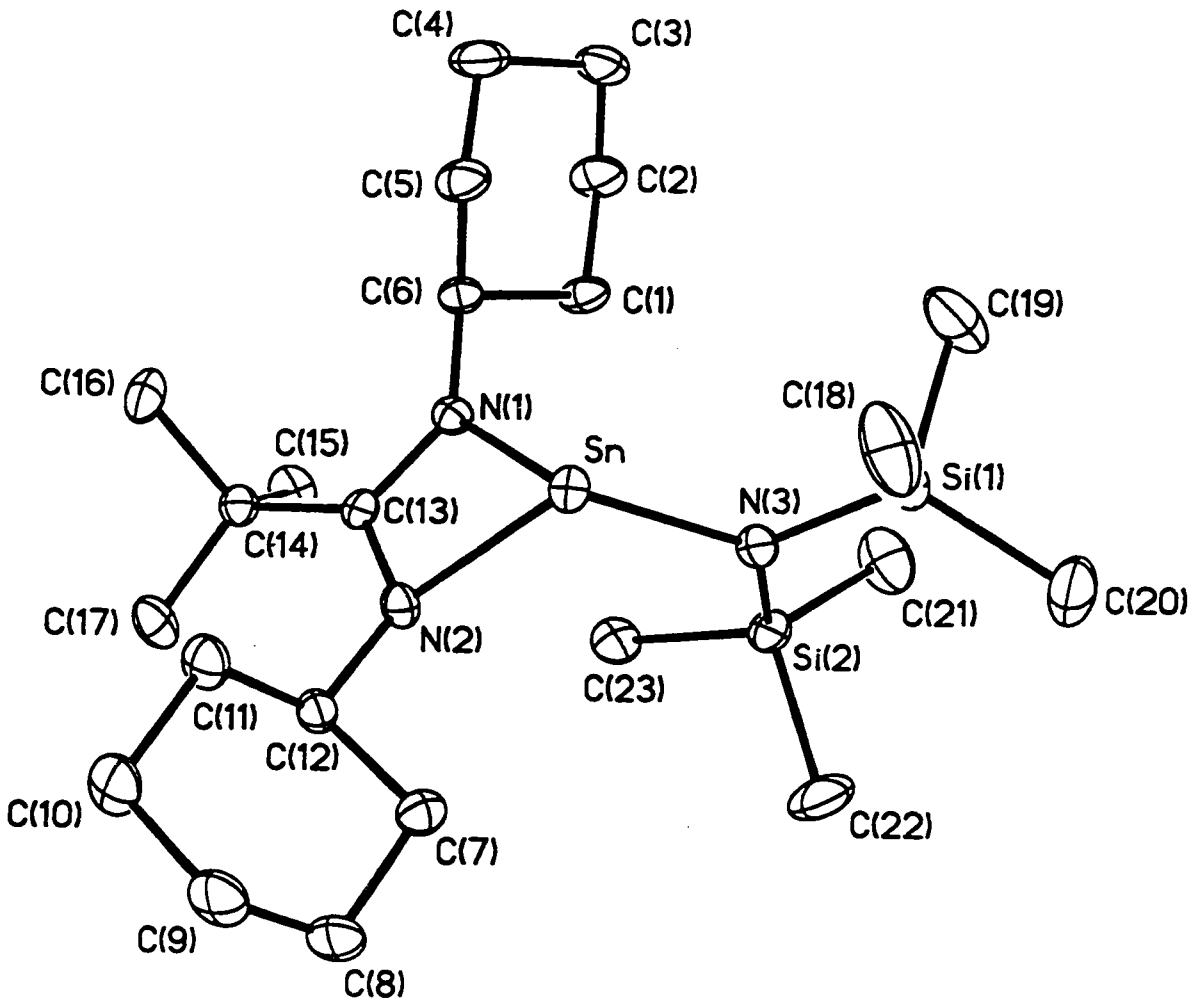

Cyclic polychalcogenido complexes of Sn amidinates

Reactions of **3** and **4** with elemental sulfur proceeded efficiently, as shown in Scheme 4.3, to yield complexes **5** and **6** with chelating bidentate S_4^{2-} ligands.

Scheme 4.3

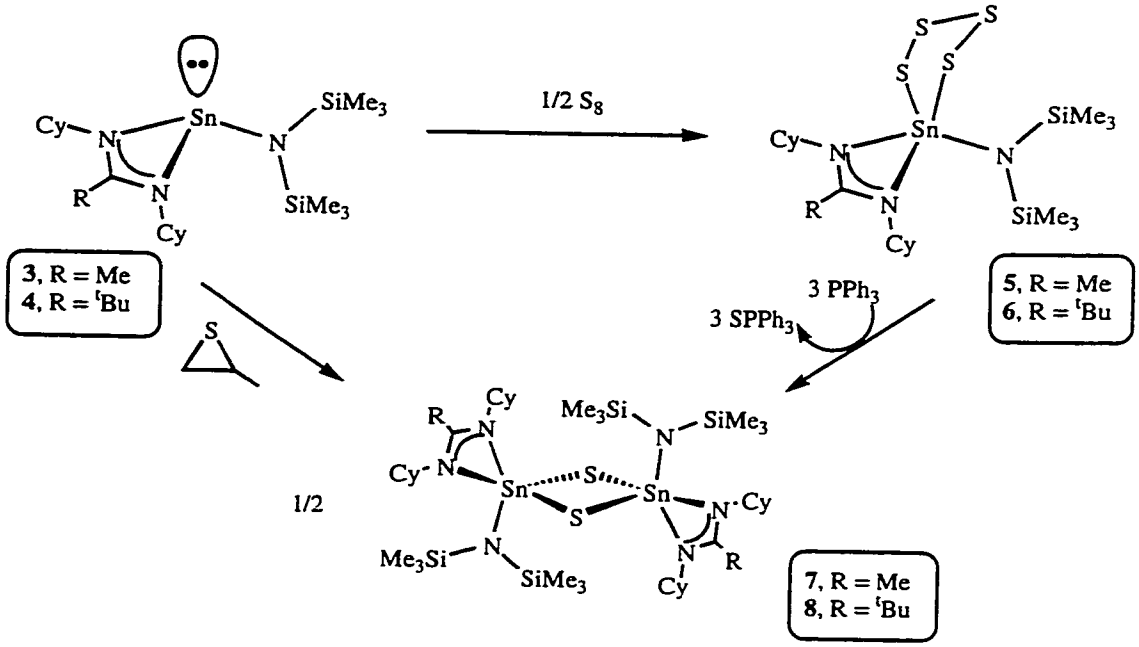

The structural details of **6** are displayed in Figure 4.2 as provided by a single crystal X-ray diffraction study (Table 4.1). Bond distances and angles are given in Table 4.3. This complex exhibits the Sn(IV) center in a distorted five coordinate geometry consisting of a bidentate amidinate, the bis(trimethylsilyl)amido ligand and the S1 and S4 centers of a chelating tetrasulfido ligand. The five-membered SnS_4 ring is in a distorted half-chair conformation with S2 and S3 deviating on either side of the S1-Sn-S4 plane by 0.707 and 0.500Å respectively. The S1-Sn-S4 angle of 93.77(3)° is similar to structurally characterized SnS_4 rings. The S-S bond distances exhibit distinct alternation (S1-S2

2.0610(14)Å, S2-S3 2.0450(16)Å, S3-S4 2.0622(16)Å) with the average being slightly shorter than the 2.050Å average S-S bond observed for orthorhombic sulfur.[20]

Figure 4.2. Molecular structure and atom numbering scheme for {(CyNC(^{t}Bu)NCy)[N(SiMe$_3$)$_2$]}SnS$_4$ (**6**) (Cy=cyclohexyl). Hydrogen atoms have been omitted for clarity.

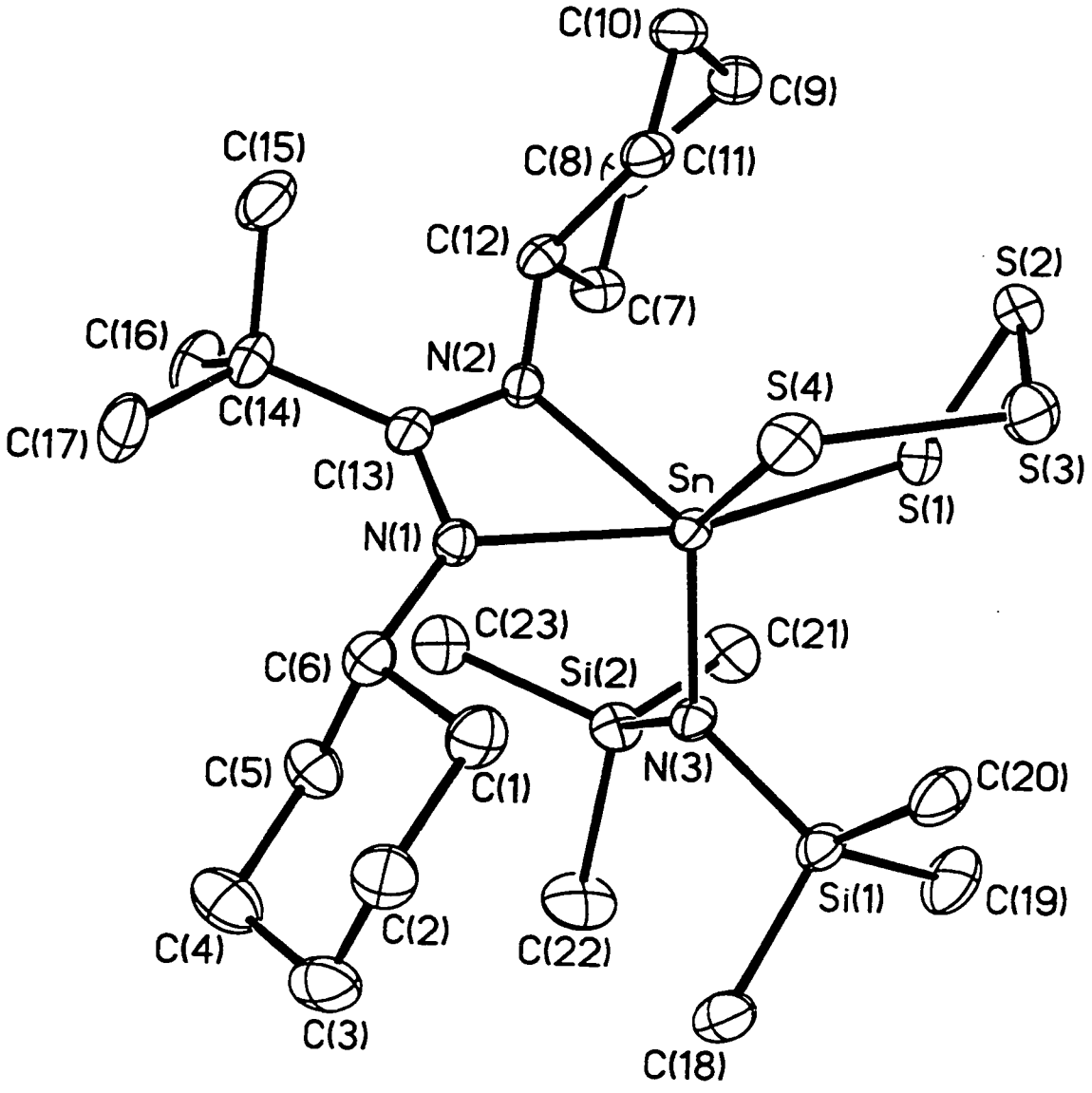

As anticipated, reaction of **5** or **6** with PPh_3 lead to abstraction of ring sulfur atoms with the ultimate products being complexes **7** and **8**. Spectroscopic and microanalytical data for **7** and **8** allowed confirmation of their constitutions and single crystal X-ray diffraction studies revealed that these compounds are dimers of presumed transient terminal sulfido intermediate complexes. A molecular structure for **8** is shown in Figure 4.3 with bond distances and angles given in Table 4.4. From this figure it is clear that **8** is a dimeric species with bridging sulfido ligands resulting in a planar four-membered $[Sn(\mu\text{-}S)]_2$ unit. The coordination sphere of the Sn atom is completed by amido and bidentate amidinato ligands which are arranged in a *trans* orientation relative to the $[Sn(\mu\text{-}S)]_2$ core. Compounds **7** and **8** could also be prepared in a rapid and complete reaction of **3** and **4** with sulfur atom sources (e.g. styrene sulfide, propylene sulfide) following the redox pathway outlined in Scheme 4.3. These same species could not be obtained in a clean manner by direct reaction of the Sn(II) starting material (**3** or **4**) with elemental sulfur. Tin sulfides can exhibit a range of aggregation, the degree of which is known to depend on the steric bulk of the supporting ligands bonded to tin and the availability of intramolecular bases for coordination to the metal center.[15, 21,22, 23,24]

The fact that the reported Sn compounds favor singly bonded, bridging sulfur centers while the Ge analogues were found to be terminal is consistent with the steric observations made in our previous investigations.[1] Furthermore, the fact that unlike their Ge analogues, **3** and **4** did not react with elemental Se is consistent with the relative stabilities of Sn(II) and Ge(II) toward oxidation.

Figure 4.3. Molecular structure and atom numbering scheme for $\{(CyNC(^tBu)NCy)[N(SiMe_3)_2]Sn(\mu\text{-}S)\}_2$ (**8**). Hydrogen atoms have been omitted for clarity.

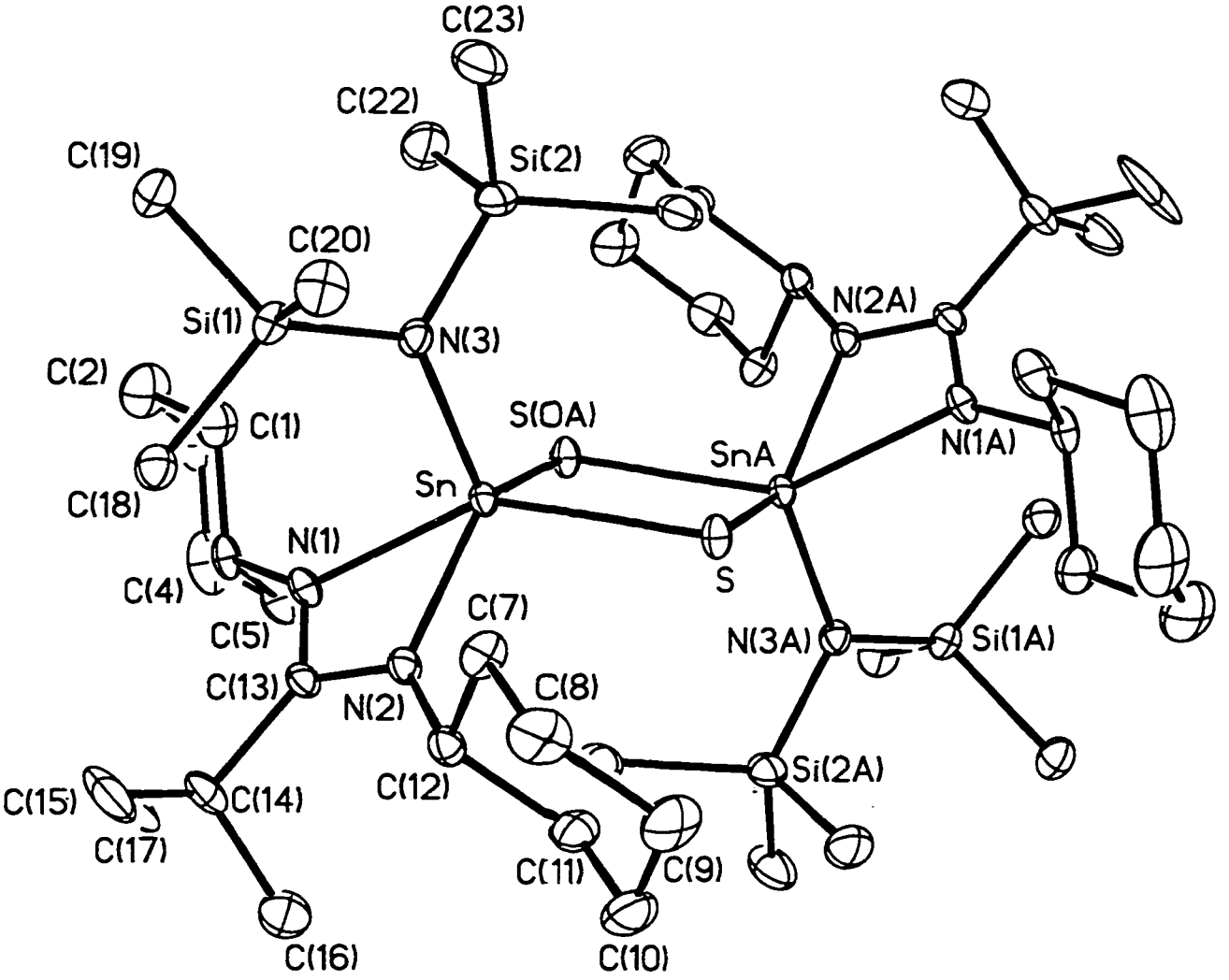

Cyclic polychalcogenido complexes of Ge amidinates

As with the Sn(II) complex **3**, the germanium analogue **1** readily reacts with elemental sulfur as shown in Scheme 4.4, to yield complex **9** with a chelating bidentate S_4^{2-} ligands.

Scheme 4.4

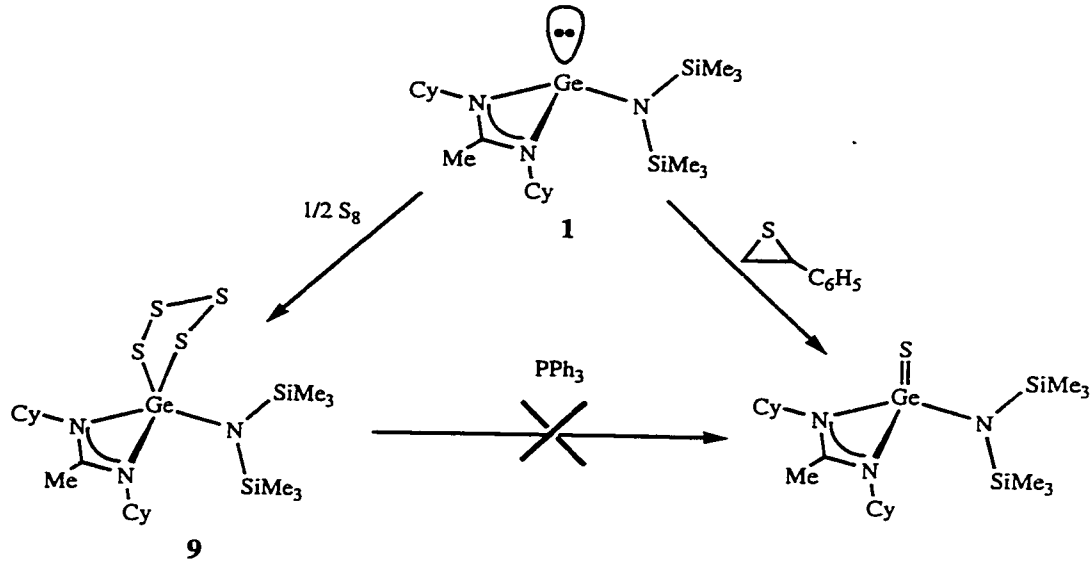

The structural details of **9** are displayed in Figure 4.4 as provided by a single crystal X-ray diffraction study (Table 4.1). Bond distances and angles are given in Table 4.5. A somewhat surprising feature is that this complex exhibits the Ge(IV) center in a distorted five coordinate geometry consisting of a bidentate amidinate, the bis(trimethylsilyl)amido ligand and the S1 and S4 centers of a chelating tetrasulfido ligand. This is contrary to other Ge(II)/(IV) amidinato complexes we have discovered where, rather than the expected five coordinate geometry, the amidinate ligand "backs off" and becomes monodentate thus preserving a four coordinate environment. All of these Ge(IV) species that we have previously observed favor pseudo-tetrahedral based geometries even in the presence of a pendant base from the "dangling" amidinate nitrogen

and in spite of the increased oxidation state and associated Lewis acidity of the Ge center. Similarly, the geometry of the Sn(II) complexes is maintained upon oxidation to Sn(IV). We have never observed the monodentate amidinate ligand for Sn. The only other five coordinate example we have found with germanium is the monoamidinate Ge(IV) complex (CyNC(^{t}Bu)NCy)$GeCl_3$ (Chapter two).

Figure 4.4. Molecular structure and atom numbering scheme for {(CyNC(Me)NCy)[$N(SiMe_3)_2$]}GeS_4 (**9**) (Cy=cyclohexyl). Hydrogen atoms have been omitted for clarity.

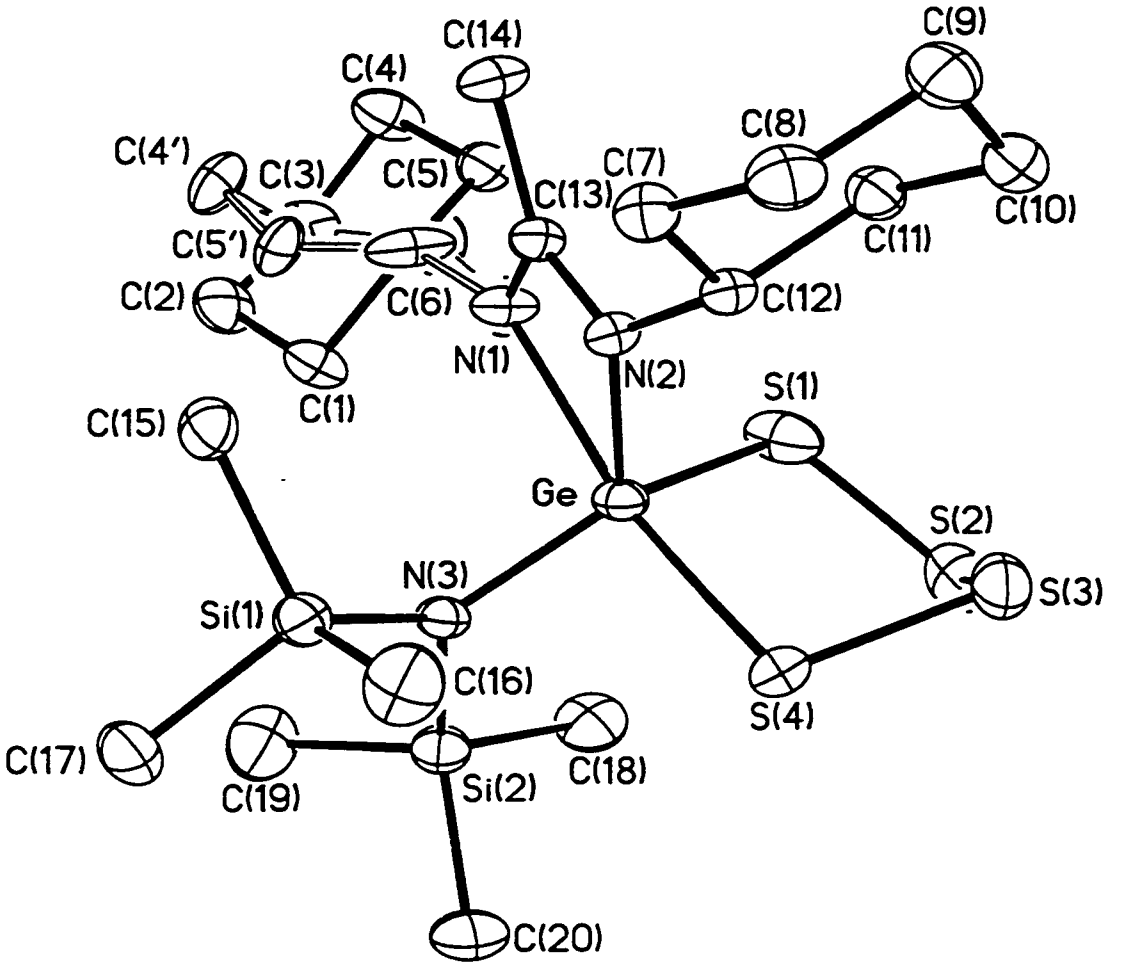

The five-membered GeS_4 ring in **9** is in a distorted half-chair conformation. The S1-Ge-S4 angle of 98.57(3)° is similar to structurally characterized GeS_4 rings.[13] The S-S bond distances do not exhibit the distinct alternation that is present in the Sn analogue **4** (S1-S2 2.0687(13)Å, S2-S3 2.0556(14)Å, S3-S4 2.0494(11)Å). Instead the bond distances decrease with the average of 2.058Å being slightly longer than the 2.050Å average S-S bond observed for orthorhombic sulfur.[20]

In further contrast to the Sn analogue, the reaction of **9** with PPh_3 does not lead to abstraction of ring sulfur atoms and thus does not provide a route to the corresponding terminal sulfido complex (Scheme 4.4).

The next section of this chapter focuses on the oxidative cleavage of the chalcogen-chalcogen bonds of diphenyldichalcogen compounds (PhE-EPh, E = S, Se) with bis(alkylamidinato) Ge(II) complexes, Ge(CyNC(R')NCy) (Cy = cyclohexyl; R' = Me, ^{t}Bu), and mixed amidinato-amido species, M(CyNC(R')NCy)[$N(SiMe_3)_2$] (M = Ge, Sn; R = Me, ^{t}Bu), to yield novel bis(phenylchalcogenolate) complexes of Sn and Ge. We include some observations on the effects of ligand variation on the structure and reactivity of these species.

*Oxidative addition of diphenyldichalcogenides to Ge(II) amidinate complexes **10** and **11***

Among the M(II) (M = Ge, Sn) species that we have isolated by employing bulky alkylamidinate ligands are those shown in Chart 4.1. The bis(amidinato)Ge(II) complexes (**10** and **11**) were shown through NMR spectroscopic measurements and by single crystal X-ray diffraction studies to possess one bidentate and one monodentate ("dangling")

amidinato ligand and to have geometries based on distorted tetrahedra in which one of the vertices is occupied by a stereochemically active lone pair of electrons (Chapter two). In contrast, the bis(amidinato)Sn(II) analogues (**12**,and **13**) displayed distorted trigonal bipyramidal geometries with one of the vertices occupied by a lone pair of electrons. We have attributed these differences to the smaller ionic radius of Ge(II) relative to Sn(II) and to the ability of Sn to more readily accommodate an expanded octet. The observation that one of the amidinate ligands in the Ge(II) complexes was monodentate provided some motivation to prepare the previously mentioned mixed ligand species (**1-4**).

Chart 4.1

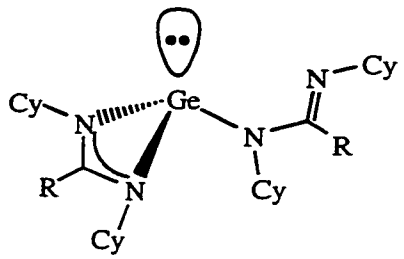

R = Me (**10**)
R = ^{t}Bu (**11**)

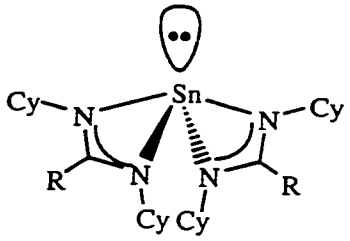

R = Me (**12**)
R = ^{t}Bu (**13**)

Oxidative addition of diphenyldisulfide and diphenyldiselenide occurs rapidly to complexes **10** and **11**. The products of these reactions are the result of cleavage of the chalcogen-chalcogen bond and formation of the corresponding bis(phenylchalcogenolate) M(IV) complexes **14-16** in high yields (Scheme 4.5). The most obvious change in the NMR spectra for the products of these reactions is the appearance of aromatic signals with integrated intensities consistent with the formulation of the products. Diphenylditelluride does not react with **10** or **11**, even at elevated temperatures, a feature that is likely due to the weaker oxidizing power of this reagent.

Scheme 4.5

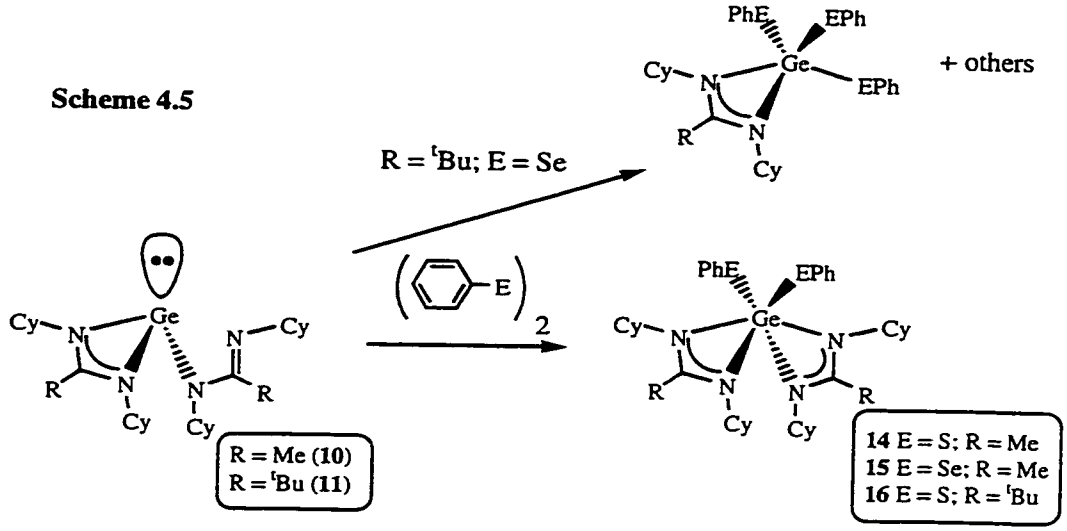

Observation of single Me groups and single Cy functions in the ^{1}H and ^{13}C NMR spectra of **14** and **15** is consistent with our previously reported findings and indicative of fluxional species (Chapter two). However, similar observations with the ^{t}Bu analogue, **16**, were at odds with our prior observations that Ge complexes of this ligand exhibit hindered internal motion and reduced fluxionality compared with their Me analogues.

In order to clarify the geometry of these complexes, a crystallographic study was performed on **15** (Figure 4.5, Table 4.6). This analysis revealed a monomeric Ge(IV) species in a distorted octahedral coordination sphere that included the four nitrogen atoms of the two chelating amidinate anions and was completed by two *cis*-phenylselenolate ligands. Table 4.7 presents a summary of selected bond distances and angles for **15**. The unusual six coordinate geometry exhibited by the Ge center in this complex contrasts with our previous observations for bis(amidinate) germanium complexes.

The two amidinate ligands in **15** are only very slightly different and in both cases the two nitrogen atoms and the bridging carbon atoms of the ligands lie in a plane which includes the Ge atom (Σ internal angles = 360°). Ligand bite angles of 64.1(4)° and

64.4(3)° are similar to the corresponding angles in our previous germanium amidinates. The equivalence of the C-N bond lengths within N-C-N frameworks of the amidinates as well as their magnitudes (range from 1.322(12)Å to 1.310(14)Å) indicate that the π electrons within the ligands are delocalized.

Figure 4.5. Molecular structure of $[C_6H_{11}NC(Me)NC_6H_{11}]_2Ge[SeC_6H_5]_2$ (**15**). Hydrogen atoms have been omitted for clarity.

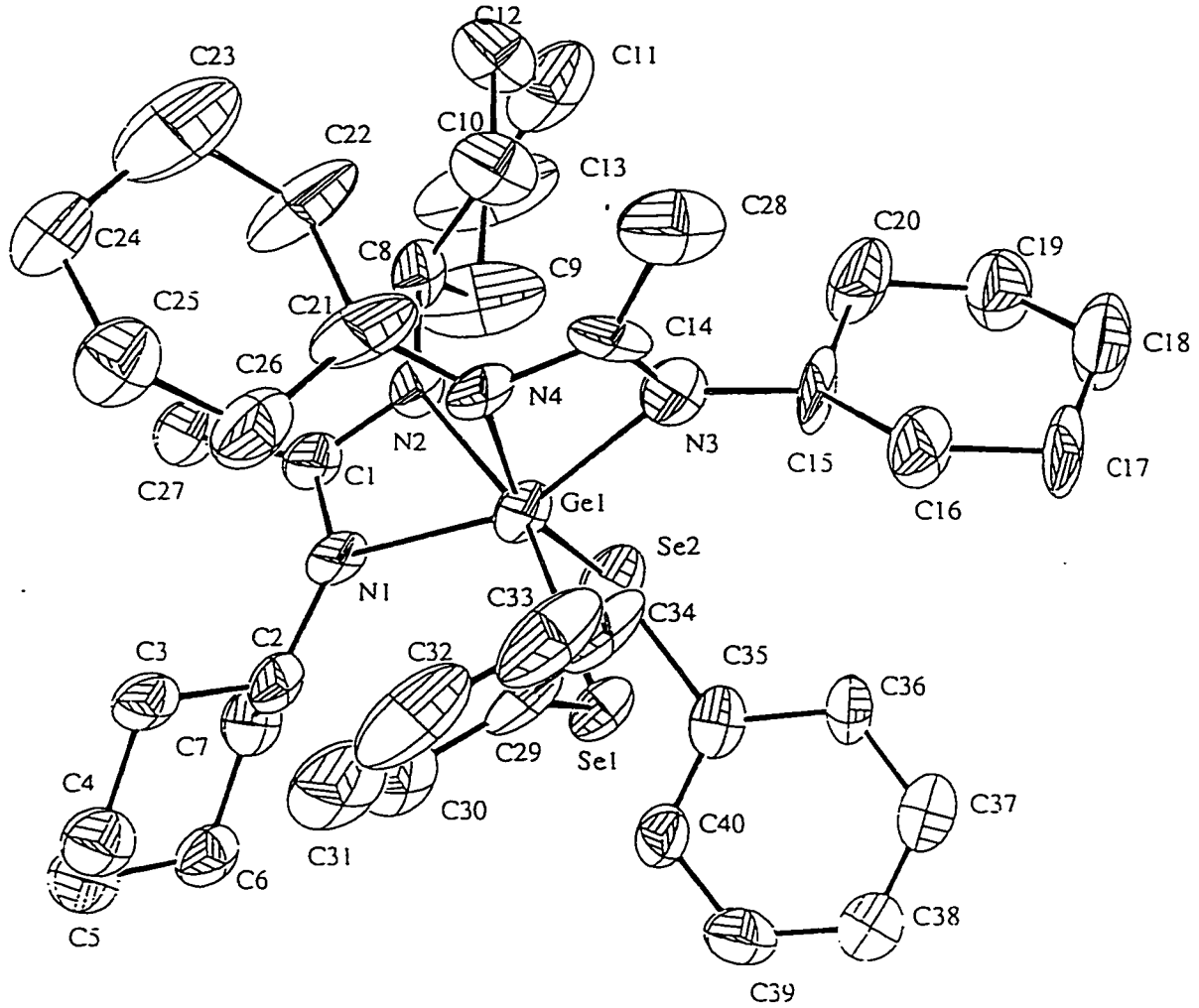

The termini of the amidinate ligand can be divided into two types, the *cis*-NCy groups (N(2), N(3)) and *trans*-NCy groups (N(1), N(4)). The *cis*-GeN bond lengths (Ge-N(3) 2.062(9) Å, Ge-N(2) 2.105(7)Å) are slightly longer than the *trans*-GeN distances (Ge-N(1) 1.955(7)Å,Ge-N(4) 1.978(8)Å). This feature is likely due to a combination of the relative steric congestion experienced by the two groups and the effect of the *trans* oriented SePh groups.

The few reported Ge^{IV} complexes with phenyl(selenolate) ligands all exhibit four coordinate geometries.[25] In **15,** the nearly equal Ge-Se bond lengths of 2.4698(14)Å and 2.4790(17)Å are longer than in the reported complexes (range 2.34-2.39Å) and the angles around two Se centers (C(34)-Se(1)-Ge 105.7(2)°, C(40)-Se(2)-Ge 106.3(2)°) are larger than in these compounds. Both of these observations are consistent with the sterically crowded six coordinate Ge center that was observed for **15**.

We found the appearance of a six coordinate Ge center in **15** all the more surprising given the increased steric congestion of this geometry compared to that of **10** and to other reported complexes of these ligands. In contrast to the solid state structural observation of distinct Cy groups, the Cy moieties appear to be equivalent in the room temperature ^{1}H and ^{13}C NMR spectra thus indicating that complex **15** has a fluxional solution structure.

While diphenydisulfide and diphenyldiselenide react readily with complex **10** to form **14** and **15** and the corresponding Ge(IV) bis(phenylthiolato) complex **16** can be prepared by reaction of **11** with diphenyldisulfide, the reaction of **11** with diphenyldiselenide follows a different course. This reaction generates a mixture of products from which we have been able to isolate only $(CyNC(^{t}Bu)NCy)Ge(SePh)_3$. The

low and unreliable yield of this compound as well as the difficulty in separating it from the other reaction products has so far prohibited spectroscopic and microanalytical characterization of this material. We have confirmed the identity of this product with a preliminary crystallographic study (Figure 4.6).

This result, while still under investigation, seems to indicate that the increase steric bulk provided by the substitution of a Me for ^{t}Bu in the amidinate ligand can have substantial effects on the reactivity and stability of complexes of this anion.

Figure 4.6. Preliminary molecular structure of (CyNC(^{t}Bu)NCy)Ge(SePh)$_3$. Hydrogen atoms have been omitted for clarity.

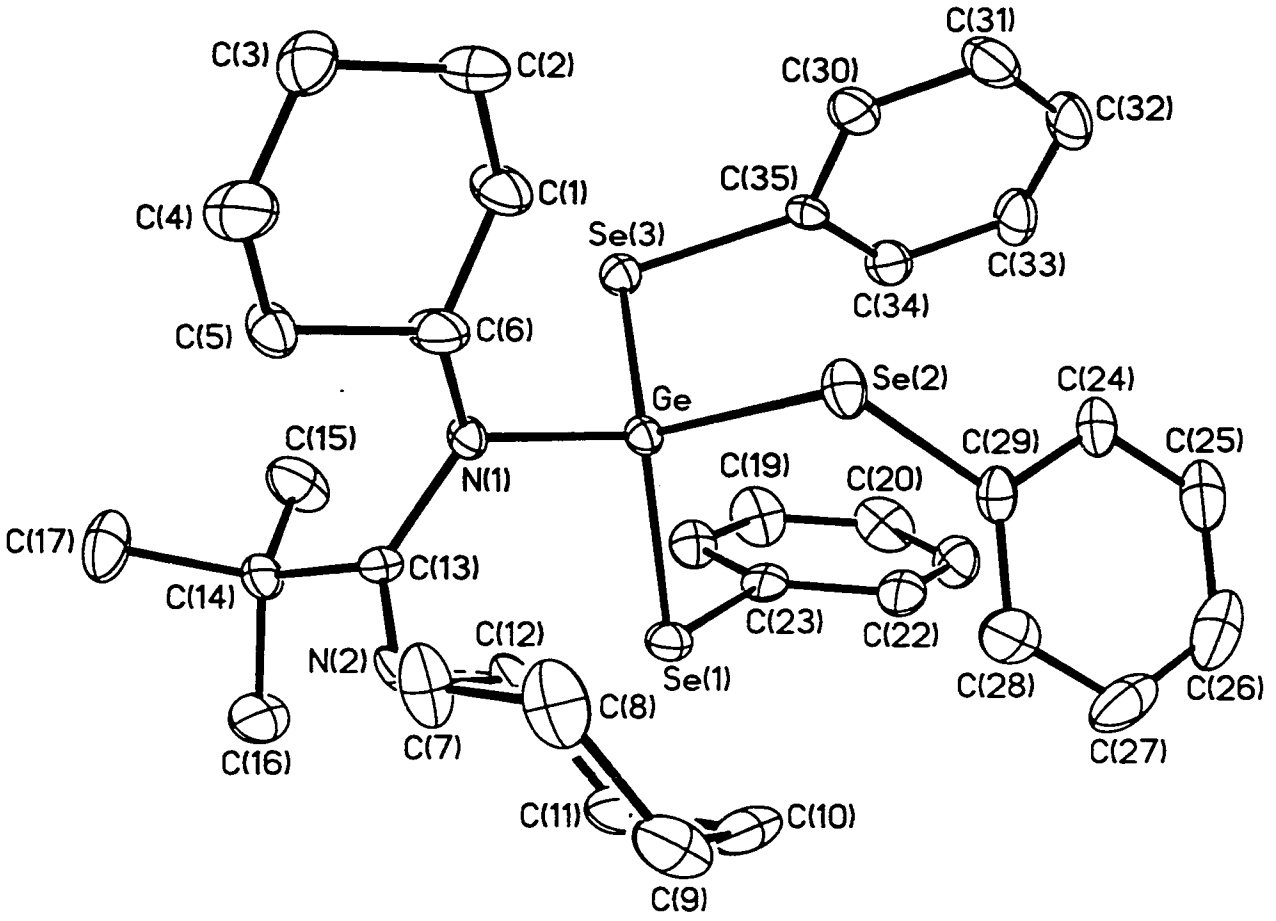

Oxidative addition of diphenyldichalcogenides to Ge(II) and Sn(II) amidinate complexes 5 and 7:

Diphenydisulfide and diphenyldiselenide also add rapidly to the mixed ligand complexes **1** and **3** according to Scheme 4.6. Again the products of these reactions complexes **17-20** are M(IV) species with two phenyl(chalcogenolate) ligands derived from the cleavage of the chalcogen-chalcogen bonds. Compounds **17-20** display very similar NMR spectral data with the key features being the appearance of equivalent phenyl groups and with the amidinate providing a single set of resonances for the Cy groups. While these observations suggest similar structures for **17-20**, the fluxionality that has been observed for similar complexes prompted us to investigate the solid state structures of **18** and **19** by single crystal X-ray crystallography (Table 4.6).

Complex **18** crystallized with two independent molecules in the asymmetric unit, each of which displayed similar bonding parameters. Consistent with our proposals, the structural analysis of **18** (Figure 4.7) revealed it to be a monomeric species which, in contrast to **15**, displayed the characteristic "dangling" amidinate ligand. Coordination of the amidinate ligand in a monodentate fashion preserves a metal coordination environment based on a pseudotetrahedral geometry rather than achieving the five coordinate environment possible via bidentate coordination. The coordination sphere of Ge is completed by a bis(trimethylsilyl)amido group and two phenylselenolate moieties. The observed pseudotetrahedral Ge coordination geometry (average interligand angle of 109.4°) is consistent with our previous observations for Ge complexes of alkylamidinates. A summary of bond distances and angles for **18** is provided in Table 4.8.

Figure 4.7. Molecular structure for one of the independent molecules of $[C_6H_{11}NC(Me)NC_6H_{11}]Ge[N(SiMe_3)_2][SeC_6H_5]_2$ (**18**). Hydrogen atoms have been omitted for clarity.

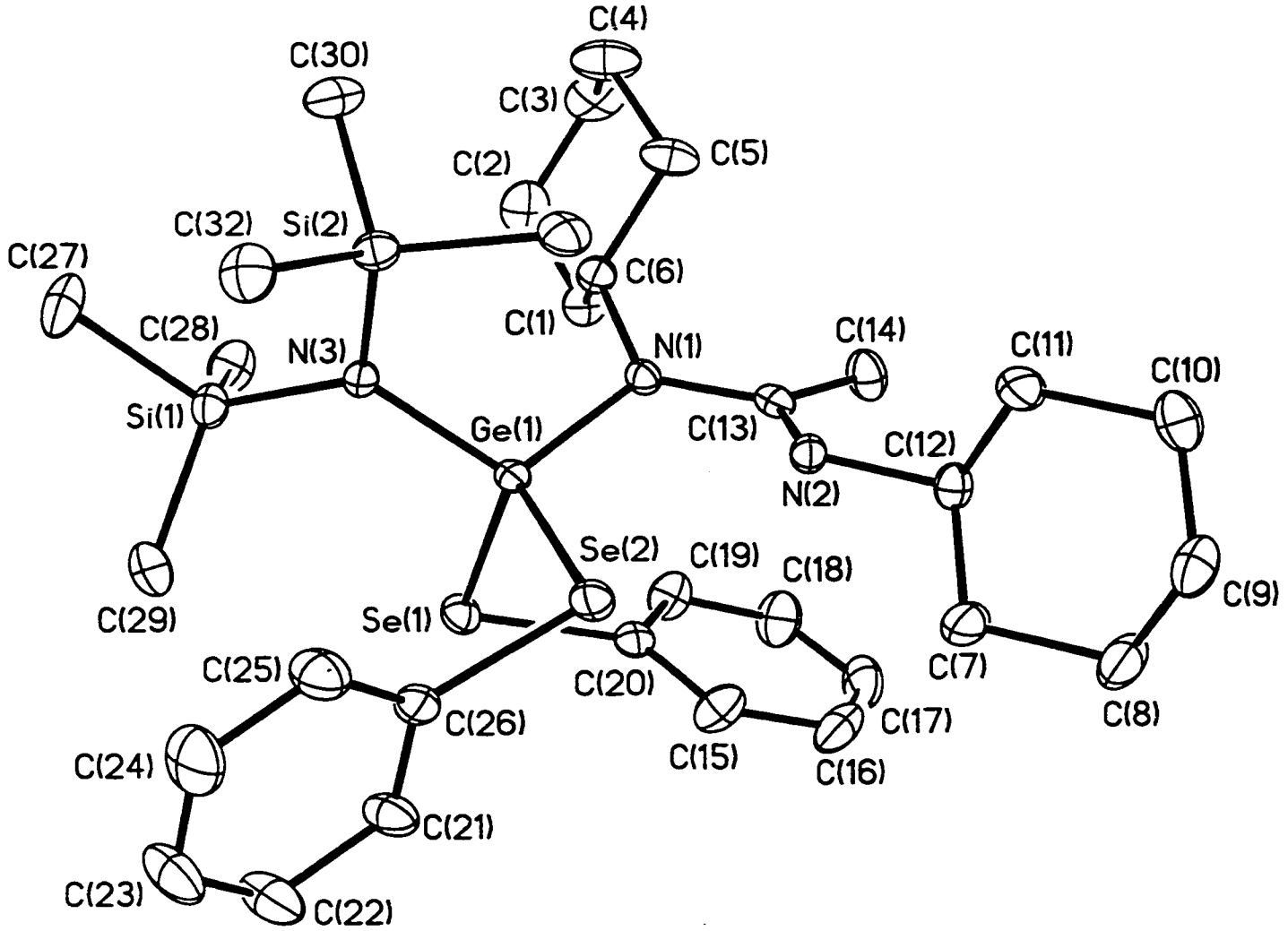

Scheme 4.6

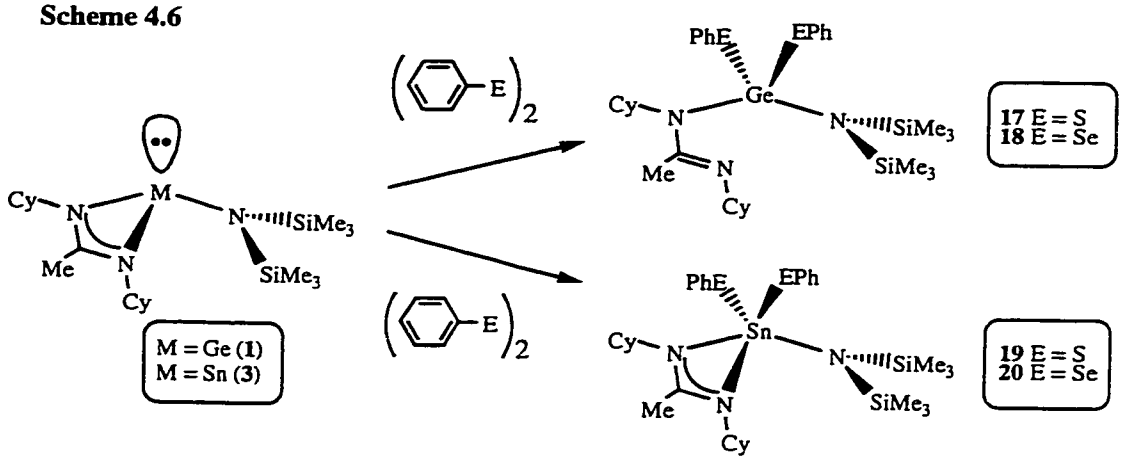

The Ge-N bond lengths are similar for both the amido and monodentate amidinato ligands. Furthermore, the pertinent nitrogen centers (N(1), N(3)) are planar (sum to 360°). Consistent with the localized valence structure for **18** presented in Scheme 4.6, the bond lengths (N(2)-C(13), 1.272(3)Å) and one defining angle (C(13)-N(2)-C(12), 121.5(3)°) for the uncoordinated nitrogen atom support the imine formulation for this center. The phenylselenolate ligands exhibit bonding parameters that are similar to the few reported Ge complexes possessing these ligands with an average Ge-Se distance of 2.373Å and an average Ge-Se-Ph angle of 97.98°.

Complex **19** also crystallized with two independent molecules in the asymmetric unit and with no significant differences in metrical parameters between these two species (Figure 4.8). While the Sn coordination sphere in **19** is comprised of a similar ligand set as **18**, **19** exhibited a bidentate amidinate ligand rather than the monodentate coordination observed in **18**. The result is a distorted trigonal bipyramidal environment for the Sn(IV) center in **19**.

A selection of bond distances and angles for **19** is provided in Table 4.9. Examination of this data confirms that the amidinate ligands bind asymmetrically to the

Sn(IV) centers and suggest an assignment of N(1) as pseudo-axial and N(2) as pseudo-equatorial. The relative Sn-N bond distances (i.e. axial greater than equatorial) are consistent with this formulation. Based on this arrangement the other pseudo-axial group is a phenylthiolato ligand (S(2)). The equatorial plane is then defined by the amido nitrogen, one amidinate nitrogen and the second phenylthiolato ligand. The angles within this plane are irregular but sum to 358° in the case of Sn(1) and 356° for Sn(2). The expected bond length difference between the pseudo-axial and pseudo-equatorial groups is reflected in the two Sn-S distances of each molecule. The Sn-S distances correlate favorably with the few comparable structural reports of bis(phenylthiolato) with five coordinate geometries.[26]

Figure 4.8. Molecular structure for one of the independent molecules of $[C_6H_{11}NC(Me)NC_6H_{11}]Sn[N(SiMe_3)_2][SC_6H_5]_2$ (**19**). Hydrogen atoms have been omitted for clarity.

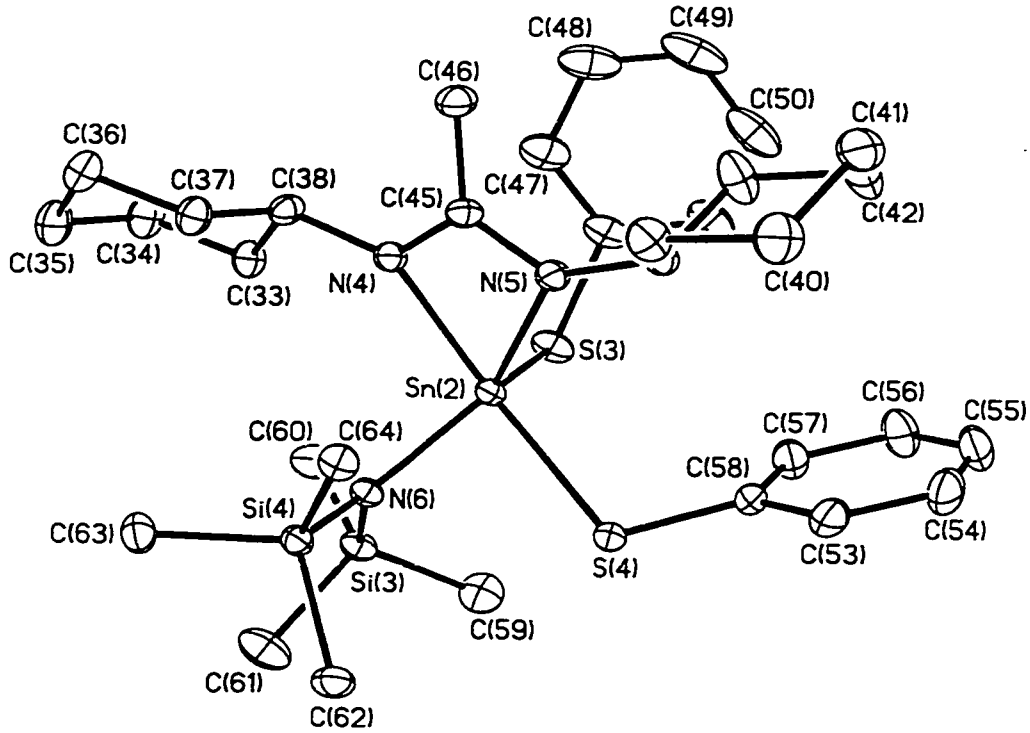

The amidinate ligands form planar metallocycles with the Sn centers (Σ internal angles = 360°). As anticipated for the bidentate coordination mode, the alkyl amidinate ligands exhibit a delocalized π bond over the N-C-N backbone as reflected in the CN bond lengths ranging from 1.303(4)Å to 1.336(4)Å.

Exchange reactions of bis(phenylchalcogenolato)Ge(IV) complexes

The mixed ligand bis(phenylselenolato) Ge(IV) complex **18** exhibits ligand exchange reactivity as shown in Scheme 4.7. Complex **18** reacts cleanly with elemental selenium to form the corresponding terminal selenide, with elimination of diphenyldiselenide. This reaction provides a qualitative measure of the relative stabilities of the terminal selenido species versus the bis(diphenylselenido) complex. Concomitant with this reaction is a rearrangement of the amidinate ligand around the Ge(IV) center. The previously monodentate amidinate ligand now becomes bidentate and the pseudotetrahedral geometry of the Ge center remains intact.

Scheme 4.7

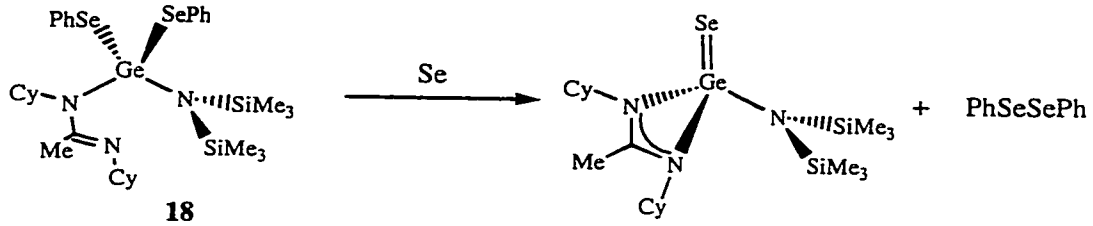

18

The corresponding bis(phenylthiolato) complex **17** $(CyNC(Me)NCy)_2Ge(SPh)_2$ however, does not react with elemental Se or styrene sulfide at room temperature. The

relative oxidizing power and Ge-E bond strength of Se versus S may rationalize the lack of reactivity with Se but the fact that styrene sulfide did not react with **17** is still under investigation.

Reactivity of cyclotetrasulfide complexes with heterocumulenes

Both germanium and tin cyclotetrasulfide complexes **6** and **9** are excellent catalysts for the trimerization of aryl isocyanates to the corresponding isocyanurates. The details of this reaction are presented in full detail in Chapter six. This observation prompted us to investigate the reactivity of other heterocumulenes with the hope that a similar reaction may be observed or that an intermediate might be isolated which would help elucidate the mechanism of isocyanate trimerization.

The tin cyclotetrasulfide complex **6** does not react with phenyl isothiocyanate. However the germanium analogue **9** undergoes a surprising rearrangement upon exposure to PhNCS. There is complete extrusion of the amidinate ligand resulting in the formation of the polyhedral sesquisulfide complex **21** possessing four equivalent vertices with each germanium center ligated by three bridging sulfides and a bistrimethylsilylamido moiety (Scheme 4.8).

Scheme 4.8

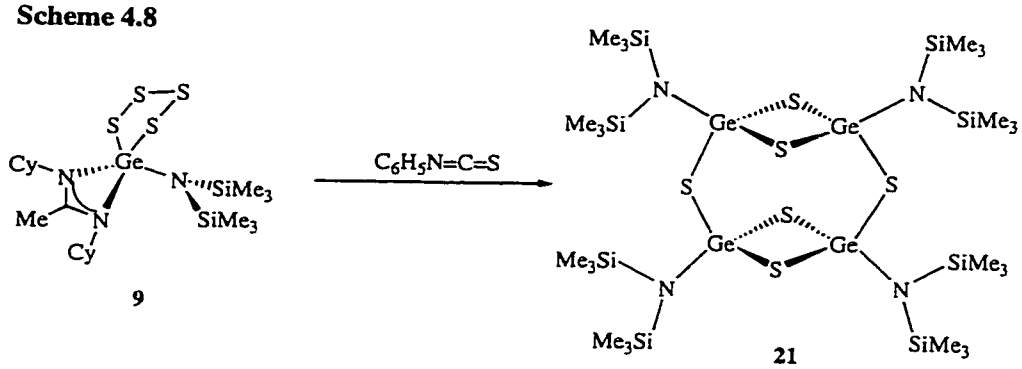

Sesquichalcogenides like complex **21** are characterized by polyhedral cagelike frameworks.[27] Two possible structures exist for tetragermachalcogenanes with the general formula $(RGeE_{1.5})_4$: adamantane-like cages of type **III** and "double-decker"-like cages of type **IV**. Prior to 1992 only adamantane type structures were known to exist. The first "double-decker" type tetragermachalcogenane was the sesquisulfide **V**.[28] The formation of adamantane cages is much more likely than double-decker structures due to ring strain considerations, thus double decker tetragermachalcogenanes are quite rare.[29] Double-decker structures have been shown to isomerize to adamantane type systems at high temperatures according to scheme 4.9.[29]

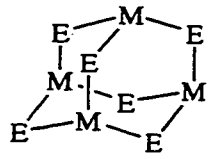

III

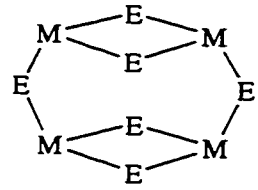

IV

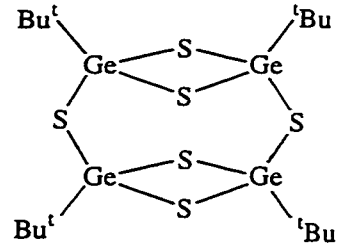

V

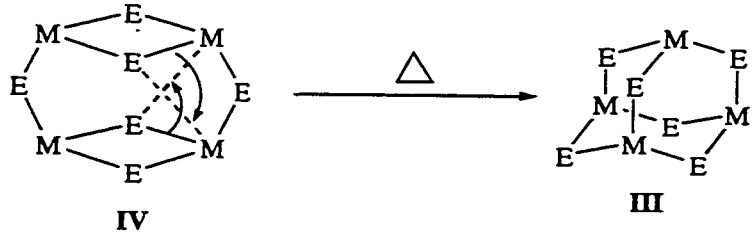

IV **III**

Scheme 4.9

Tetragermachalcogenane **21** shows only one signal in its ^1H NMR spectrum. X-ray structure analysis of **21** confirms a double-decker structure where the Ge_4S_6 core consists of two planar Ge_2S_2 rings which are linked by two bridging sulfur atoms (Table

4.10). The structural details of **10** are displayed in Figure 4.9 with bond distances and angles provided in Table 4.11. The Ge-S bond lengths are all very similar (range = 2.22 – 2.23Å) and show no differences between the four-membered rings and the eight membered rings. The average Ge-S bond length of 2.22Å is similar to that of **V** (2.23Å).

Figure 4.9. Molecular structure and atom numbering scheme for $[(Me_3Si)_2NGeE_{1.5}]_4$ (**21**). Hydrogen atoms have been omitted for clarity.

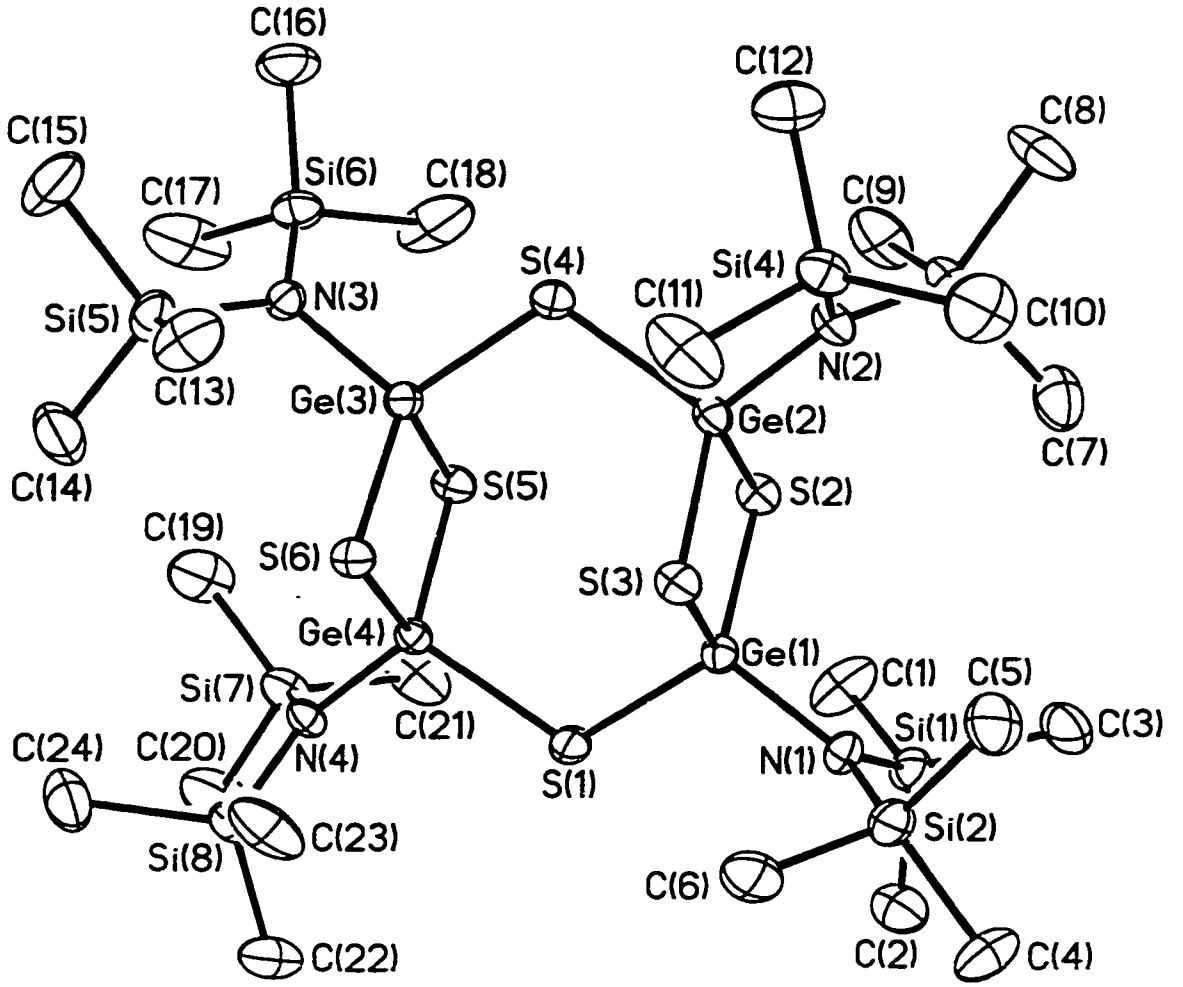

Conclusion

In summary, these results add significantly to the limited number of structurally characterized main group cyclopolychalcogenido complexes and will help to delineate the steric and electronic features which stabilize and influence the reactivity of such species. The reactivity of **3** and **4** contrasts with the reported Ge(II/IV) analogues yielding cyclic tetrasulfido species (**5** and **6**) and μ-sulfido complexes (**7** and **8**) rather than terminal species. The cyclo-SnS_4 complexes are interesting and very effective catalysts for isocyanate trimerization (see Chapter Six).

As well, a series of bis(phenylchalcogenolate) complexes of Ge and Sn have been prepared through the oxidative addition of diphenyldisulfide and diphenyldiselenide to a family of bis(amidinato) Ge(II) and mixed amidinato-amido Ge(II) and Sn(II) complexes. Structural studies confirm the geometric features of these species and indicate that this ligand environment appears to favor Ge(IV) complexes with a strong disposition towards either a tetrahedral or an octahedral geometry. In most observed cases a five coordinate environment is avoided by one of the amidinate ligands exhibiting a monodentate coordination mode thus preserving a pseudotetrahedral metal coordination geometry. This contrasts with the Sn(II/IV) analogues which exhibit no such tendency.

Experimental for Chapter Four

General Procedure. All manipulations were carried out in either a Vacuum Atmospheres drybox or under nitrogen using standard Schlenk-line techniques. Diethyl ether, hexane, toluene, benzene and deuterated benzene were distilled under nitrogen from Na/K alloy. MeLi (1.4 M in diethyl ether), ^{t}BuLi (1.7 M in pentane), $SnCl_2$, dicyclohexylcarbodiimide, $LiN(SiMe_3)_2$, Diphenyldisulfide, diphenyldiselenide, diphenylditelluride, elemental selenium and propylene sulfide were purchased from Aldrich and used without further purification. S_8 was recrystallized from toluene. NMR spectra were run on a GEMINI 200 MHz spectrometer with deuterated benzene as a solvent and internal standard. All elemental analyses were run on a Perkin-Elmer PE CHN 4000 elemental analysis system.

$[C_6H_{11}NC(Me)NC_6H_{11}]Sn[N(SiMe_3)_2]$ (3). To a solution of dicyclohexylcarbodiimide (0.653g, 3.16mmol) in diethyl ether (60ml) was added MeLi (2.26ml, 1.4M, 3.16mmol). After 30 min, 1 equiv of $SnCl_2$ (0.600g, 3.15mmol) was added to this mixture which was stirred for 1.5 h. Lithium bis(trimethylsilylamide) (0.530g, 3.16mmol) was then added to the reaction mixture. The solution was stirred for another 12 h and filtered to remove the white LiCl precipitate. The solvent was removed under vacuum, at which point a yellow oil was observed as the sole product (1.49g, 94% yield). ^{1}H NMR (C_6D_6, ppm) : 3.09 (br, C_6H_{11}, 2H); 1.97-1.02 (m, C_6H_{11}, 20H); 1.35 (s, Me, 3H); 0.47 (s, $SiMe_3$, 18H). ^{119}Sn NMR (C_6D_6, ppm *vs.* $SnMe_4$): 17.6.

$[C_6H_{11}NC(^tBu)NC_6H_{11}]Sn[N(SiMe_3)_2]$ (4). To a solution of dicyclohexylcarbodiimide (0.816g, 3.97mmol) in diethyl ether (60ml) was added ^{t}BuLi (2.33ml, 1.7M, 3.96mmol). After 15 min, 1 equiv of $SnCl_2$ (0.750g, 3.96mmol) was added to this mixture which was stirred for 2 h. Lithium bis(trimethylsilylamide) (0.663g, 3.96mmol) was then added to the reaction mixture. The solution was stirred for another 14 h, filtered to remove the white LiCl precipitate and evaporated to dryness. White crystals were obtained from diethyl ether at –34°C (2.010g, 94% yield). Mp 82-84°C. ^{1}H NMR (C_6D_6, ppm) : 3.87 (br, C_6H_{11}, 2H); 2.16-0.92 (m, C_6H_{11}, 20H); 1.16 (s, ^{t}Bu, 9H); 0.48 (s, $SiMe_3$, 18H). ^{13}C NMR (C_6D_6, ppm) : 173.5 (s, N$\underline{C}^t$BuN); 55.6, 41.0, 35.7, 25.9 (4s, C_6H_{11}); 41.8 (s, $\underline{C}(CH_3)_3$); 29.5 (s, $C(\underline{C}H_3)_3$); 5.3 (s, $SiMe_3$). ^{119}Sn NMR (C_6D_6, ppm *vs.* $SnMe_4$): 10.3. Anal. Calcd for $C_{23}H_{49}N_3Si_2Sn$: C 50.92; H 9.10; N 7.75. Found: C 50.73; H 8.88; N 7.41.

$[C_6H_{11}NC(Me)NC_6H_{11}]Sn[N(SiMe_3)_2]S_4$ (5). To a solution of **3** (0.230g, 0.460mmol) in diethyl ether (5ml) was added 0.5 equiv of S_8 (0.060g, 0.234mmol). The solution was allowed to react for 3 h. A small amount of insoluble white precipitate formed which was filtered off. Yellow crystals were obtained from diethyl ether at –34°C (0.19g, 66% yield). Mp 133°C (dec). ^{1}H NMR (C_6D_6, ppm) : 3.30 (br, C_6H_{11}, 2H); 1.87-0.96 (m, C_6H_{11}, 20H); 1.23 (s, Me, 3H); 0.40 (s, $SiMe_3$, 18H). ^{13}C NMR (C_6D_6, ppm) : 168.3 (s, N$\underline{C}$MeN); 56.2, 35.4, 25.7, 12.3 (4s, C_6H_{11}); 26.0 (s, C$\underline{C}H_3$); 5.3 (s, $SiMe_3$). ^{119}Sn NMR (C_6D_6, ppm *vs.* $SnMe_4$): 156.5. Anal. Calcd for $C_{20}H_{43}N_3Si_2S_4Sn$ C 38.21; H 6.89; N 6.68. Found: C 37.12; H 6.63; N 6.09.

$[C_6H_{11}NC(^tBu)NC_6H_{11}]Sn[N(SiMe_3)_2]S_4$ (6). To a solution of **4** (0.450g, 0.829mmol) in diethyl ether (20ml) was added 0.5 equiv of S_8 (0.106g, 0.415mmol). The solution was allowed to react for 18 h. A small amount of insoluble white precipitate formed which was filtered off. Yellow crystals

were obtained from diethyl ether at –34°C (0.38g, 68% yield). Mp 79-81°C. ^{1}H NMR (C_6D_6, ppm) : 3.72 (br, C_6H_{11}, 2H); 2.15-0.83 (m, C_6H_{11}, 20H); 1.08 (s, ^{t}Bu, 9H); 0.43 (s, $SiMe_3$, 18H). ^{119}Sn NMR (C_6D_6, ppm *vs.* $SnMe_4$): 154.8. Anal. Calcd for $C_{23}H_{49}N_3Si_2S_4Sn$ C 41.18; H 7.36; N 6.26. Found: C 40.31; H 7.06; N 5.53.

{[$C_6H_{11}NC(Me)NC_6H_{11}$]Sn[$N(SiMe_3)_2$]S}$_2$ (7). To a solution of **3** (0.300g, 0.600mmol) in toluene (5 ml) was added excess propylene sulfide (0.180g). The homogeneous solution was allowed to react for 5 days after which sparingly soluble white crystals were obtained at room temperature (0.285g, 89% yield). mp 172-173°C. ^{1}H NMR ($CDCl_3$, ppm) : 3.30 (br, C_6H_{11}, 2H); 1.97-1.05 (m, C_6H_{11}, 20H); 1.52 (s, Me, 3H); 0.43 (s, $SiMe_3$, 18H). Anal. Calcd for $C_{20}H_{43}N_3Si_2SnS$: C 45.11; H 8.14; N 7.89. Found: C 45.46; H 7.95; N 7.60.

{[$C_6H_{11}NC(^tBu)NC_6H_{11}$]Sn[$N(SiMe_3)_2$]S}$_2$ (8). To a solution of **4** (0.288g, 0.531mmol) in diethyl ether (4 ml) was added excess styrene sulfide (0.144g). The homogeneous solution was allowed to react for 2 days after which sparingly soluble white crystals were obtained at room temperature (0.276g, 90% yield). mp 168-170°C. ^{1}H NMR ($CDCl_3$, ppm) : 3.65 (br, C_6H_{11}, 2H); 2.10-0.90 (m, C_6H_{11}, 20H); 1.39 (s, Me, 3H); 0.38 (s, $SiMe_3$, 18H). Anal. Calcd for $C_{23}H_{49}N_3Si_2SnS$: C 48.08; H 8.60; N 7.31. Found: C 47.71; H 8.79; N 7.61.

[$C_6H_{11}NC(Me)NC_6H_{11}$]Ge[$N(SiMe_3)_2$]$S_4$ (9). To a solution of **1** (0.400g, 0.880mmol) in diethyl ether (10ml) was added 0.5 equiv of S_8 (0.113g, 0.440mmol). The solution was stirred for 12h. Yellow crystals were obtained from diethyl ether at –34°C (0.35g, 68% yield). ^{1}H NMR (C_6D_6, ppm) : 2.95 (br, C_6H_{11}, 2H); 1.92-0.95 (m, C_6H_{11}, 20H); 1.18 (s, Me, 3H); 0.52 (s, $SiMe_3$, 18H).

^{13}C NMR (C_6D_6, ppm) : 170.5 (s, N$\underline{C}$MeN); 55.0, 35.0, 33.8, 11.6 (4s, C_6H_{11}); 25.4 (s, C$\underline{C}H_3$); 5.8 (s, $SiMe_3$). Anal. Calcd for $C_{20}H_{43}N_3Si_2S_4Ge$: C 41.23; H 7.44; N 7.21. Found: C 41.70; H 7.64; N 7.25.

Reaction of 5 with PPh_3 to form 7. To a solution of **5** (0.150g, 0.239mmol) in ether (5 ml) was added 3 equiv triphenylphosphine (0.188g, 0.718mmol). Complex **7** slowly crystallized out of solution over 12 hrs. Crystals were isolated and washed with toluene (3x 5 ml) and dried in vacuo (0.132g, 98% yield).

Reaction of 6 with PPh_3 to form 8. To a solution of **6** (0.150g, 0.224mmol) in ether (5 ml) was added 3 equiv triphenylphosphine (0.176g, 0.672mmol). Complex **8** slowly crystallized out of solution over 12 hrs. Crystals were isolated and washed with toluene (3x 5 ml) and dried in vacuo (0.117g, 91% yield).

$[C_6H_{11}NC(Me)NC_6H_{11}]_2Ge[SC_6H_5]_2$ (14). To a solution of **10** (0.300g, 0.583mmol) in diethyl ether (25ml) was added 1 equiv of diphenyldisulfide (0.127g). The solution was allowed to react for 12 h and evaporated to dryness. White crystals were obtained from hexane at –34°C (0.33g, 78% yield). ^1H NMR (C_6D_6, ppm) : 7.72, (m, C_6H_5, 4H); 7.08 (m, C_6H_5, 6H); 3.39 (br, C_6H_{11}, 4H); 2.16-0.89 (m, C_6H_{11}, 40H); 1.57 (s, Me, 6H). ^{13}C NMR (C_6D_6, ppm) : 161.6 (s, N$\underline{C}$MeN); 136.8, 136.2, 129.2, 125.5 (4s, C_6H_5); 56.0, 34.1, 26.9, 25.5 (4s, C_6H_{11}); 13.0 (s, C$\underline{C}H_3$). Anal. Calcd for $C_{40}H_{60}N_4GeS_2$: C 65.49; H 8.24; N 7.64. Found: C 65.87; H 8.54; N 7.06.

$[C_6H_{11}NC(Me)NC_6H_{11}]_2Ge[SeC_6H_5]_2$ (15). To a solution of **10** (0.187g, 0.363mmol) in diethyl ether (20ml) was added 1 equiv of diphenyldiselenide (0.113g). The solution was allowed to react for 12 h and evaporated to dryness. Yellow crystals were obtained from diethyl ether at –34°C (0.27g, 90% yield). ^{1}H NMR (C_6D_6, ppm) : 7.89, (m, C_6H_5, 4H); 7.04 (m, C_6H_5, 6H); 3.42 (br, C_6H_{11}, 4H); 2.05-0.95 (m, C_6H_{11}, 40H); 1.59 (s, Me, 6H). ^{13}C NMR (C_6D_6, ppm) : 162.4 (s, N$\underline{C}$MeN); 138.5, 135.0, 127.9, 126.4 (4s, C_6H_5); 56.1, 34.5, 27.2, 26.6 (4s, C_6H_{11}); 13.5 (s, C$\underline{C}H_3$). Anal. Calcd for $C_{40}H_{60}N_4GeSe_2$: C 58.06; H 7.31; N 6.77. Found: C 57.72; H 7.75; N 6.67.

$[C_6H_{11}NC(^tBu)NC_6H_{11}]_2Ge[SC_6H_5]_2$ (16). To a solution of **11** (0.098g, 0.164mmol) in hexane (4ml) was added 1 equiv of diphenyldisulfide (0.036g). The solution was allowed to react for 1 h and evaporated to dryness. White crystals were obtained from hexane at –34°C (0.12g, 91% yield). ^{1}H NMR (C_6D_6, ppm) : 7.95, (m, C_6H_5, 4H); 7.05 (m, C_6H_5, 6H); 3.98 (br, C_6H_{11}, 4H); 2.25-0.98 (m, C_6H_{11}, 40H); 1.32 (s, ^{t}Bu, 18H). ^{13}C NMR (C_6D_6, ppm) : 168.0 (s, N$\underline{C}$(CH_3)N); 135.8, 129.3, 128.1, 125.6 (4s, C_6H_5); 58.3, 34.0, 26.8, 26.0 (4s, C_6H_{11}); 30.7 (s, C($\underline{C}H_3$)$_3$); 15.8 (s, $\underline{C}$(CH_3)$_3$). Anal. Calcd for $C_{46}H_{72}N_4GeS_2$: C 67.56; H 8.87; N 6.85. Found: C 67.70; H 8.90; N 6.629.

$[C_6H_{11}NC(Me)NC_6H_{11}]Ge[N(SiMe_3)_2][SC_6H_5]_2$ (17). To a solution of **1** (0.126g, 0.277mmol) in hexane (5ml) was added 1 equiv of diphenyldisulfide (0.061g). The solution was allowed to react for 2.5 h and evaporated to dryness. White crystals were obtained from hexane at –34°C (0.14g, 72% yield). ^{1}H NMR (C_6D_6, ppm) : 7.78 (m, C_6H_5, 4H); 7.02 (m, C_6H_5, 6H); 3.35 (br, C_6H_{11}, 2H); 1.92-0.81 (m, C_6H_{11}, 20H); 1.71 (s, Me, 3H); 0.38 (s, $SiMe_3$, 18H). ^{13}C NMR (C_6D_6, ppm) : 158.5 (s, N$\underline{C}$MeN); 136.1, 135.9, 134.0, 127.5 (4s, C_6H_5); 57.6, 34.4, 26.6, 26.3 (4s, C_6H_{11}); 16.6 (s, C$\underline{C}H_3$); 6.2 (s, $SiMe_3$). Anal. Calcd for $C_{32}H_{53}N_3Si_2GeS_2$: C 57.14; H 7.94; N 6.25. Found: C 57.14; H 7.83; N 6.27.

$[C_6H_{11}NC(Me)NC_6H_{11}]Ge[N(SiMe_3)_2][SeC_6H_5]_2$ (18). To a solution of **1** (0.400g, 0.881mmol) in hexane (10ml) was added 1 equiv of diphenyldiselenide (0.275g). The solution was allowed to react for 4 h and evaporated to dryness. White crystals were obtained from hexane at –34°C (0.60g, 84% yield). ^{1}H NMR (C_6D_6, ppm) : 7.90 (m, C_6H_5, 4H); 7.05 (m, C_6H_5, 6H); 3.40 (br, C_6H_{11}, 2H); 1.97-0.82 (m, C_6H_{11}, 20H); 1.66 (s, Me, 3H); 0.38 (s, $SiMe_3$, 18H). ^{13}C NMR (C_6D_6, ppm) : 159.1 (s, N$\underline{C}$MeN); 136.9, 130.7, 128.8, 127.6 (4s, C_6H_5); 57.2, 34.6, 26.7, 26.2 (4s, C_6H_{11}); 16.2 (s, C$\underline{C}H_3$); 6.3 (s, $SiMe_3$). Anal. Calcd for $C_{32}H_{53}N_3Si_2GeSe_2$: C 50.14; H 6.92; N 5.48. Found: C 50.57; H 7.07; N 5.36.

$[C_6H_{11}NC(Me)NC_6H_{11}]Sn[N(SiMe_3)_2][SC_6H_5]_2$ (19). To a solution of **3** (0.225g, 0.450mmol) in hexane (6ml) was added 1 equiv of diphenyldisulfide (0.098g). The solution was allowed to react for 12 h and evaporated to dryness. White crystals were obtained from hexane at –34°C (0.24g, 74% yield). ^{1}H NMR (C_6D_6, ppm) : 7.76, (m, C_6H_5, 4H); 6.98 (m, C_6H_5, 6H); 3.01 (br, C_6H_{11}, 2H); 1.72-0.98 (m, C_6H_{11}, 20H); 1.28 (s, Me, 3H); 0.46 (s, $SiMe_3$, 18H). ^{13}C NMR (C_6D_6, ppm) : 165.8 (s, N$\underline{C}$MeN); 136.0, 135.7, 128.5, 126.6 (4s, C_6H_5); 56.2, 34.4, 25.7, 13.4 (4s, C_6H_{11}); 26.3 (s, C$\underline{C}H_3$); 6.0 (s, $SiMe_3$). Anal. Calcd for $C_{32}H_{53}N_3Si_2SnS_2$: C 53.47; H 7.43; N 5.85. Found: C 53.64; H 7.45; N 5.78.

$[C_6H_{11}NC(Me)NC_6H_{11}]Sn[N(SiMe_3)_2][SeC_6H_5]_2$ (20). To a solution of **3** (0.200g, 0.400mmol) in hexane (6ml) was added 1 equiv of diphenyldiselenide (0.125g). The solution was allowed to react for 12 h and evaporated to dryness. Yellow crystals were obtained from hexane at –34°C (0.27g, 82% yield). ^{1}H NMR (C_6D_6, ppm) : 7.78, (m, C_6H_5, 4H); 6.95 (m, C_6H_5, 6H); 3.01 (br, C_6H_{11}, 2H); 1.75-0.97 (m, C_6H_{11}, 20H); 1.30 (s, Me, 3H); 0.48 (s, $SiMe_3$, 18H). ^{13}C NMR (C_6D_6, ppm) : 166.0 (s, N$\underline{C}$MeN); 137.9, 130.4,

129.1, 128.9 (4s, C_6H_5); 56.4, 34.9, 26.3, 14.1 (4s, C_6H_{11}); 26.8 (s, $C\underline{C}H_3$); 6.6 (s, $SiMe_3$). Anal. Calcd for $C_{32}H_{53}N_3Si_2SnSe_2$: C 47.30; H 6.57; N 5.17. Found: C 47.42; H 6.64; N 5.10.

Formation of $[C_6H_{11}NC(Me)NC_6H_{11}][N(SiMe_3)_2]Ge{=}Se$ from $[C_6H_{11}NC(Me)NC_6H_{11}]Ge[N(SiMe_3)_2][SeC_6H_5]_2$. To a solution of $[C_6H_{11}NC(Me)NC_6H_{11}]Ge[N(SiMe_3)_2][SeC_6H_5]_2$ (0.055g, 0.072mmol) in 0.5 ml C_6D_6 was added elemental selenium (11mg, 0.14mmol). The reaction was complete after 2 hrs at 60°C. Identity of the product was confirmed by comparison of NMR spectra of authentic samples of $[C_6H_{11}NC(Me)NC_6H_{11}][N(SiMe_3)_2]Ge{=}Se$ and $(C_6H_5Se)_2$. No other species were observed.

Reaction of $[C_6H_{11}NC(Me)NC_6H_{11}]Ge[N(SiMe_3)_2][SC_6H_5]_2$ with Se. To a solution of $[C_6H_{11}NC(Me)NC_6H_{11}]Ge[N(SiMe_3)_2][SC_6H_5]_2$ (0.055g, 0.082mmol) in 0.5 ml C_6D_6 was added elemental selenium (26mg, 0.33mmol). The sample was heated to at 60°C for 12 hours and monitored by ^1H NMR. No change in the starting material was observed.

Reaction of $[C_6H_{11}NC(Me)NC_6H_{11}]Ge[N(SiMe_3)_2][SC_6H_5]_2$ with Styrene Sulfide. To a solution of $[C_6H_{11}NC(Me)NC_6H_{11}]Ge[N(SiMe_3)_2][SC_6H_5]_2$ (0.040g, 0.059mmol) in 0.5 ml C_6D_6 was added styrene sulfide (32mg, 0.24mmol). The sample was heated to at 60°C for 2 days and monitored by ^1H NMR. No change in the starting material was observed.

$[(Me_3Si)_2NGeE_{1.5}]_4$ (21). To a solution of **9** (0.250g, 0.430mmol) in 4 ml toluene was added two equivalents phenyl isothiocyanate (116mg, 0.859mmol). Yellow crystals slowly precipitated from the orange reaction mixture over 24 hours (0.33mg, 28% yield). ^{1}H NMR (C_6D_6, ppm): 0.42 (s, $SiMe_3$). ^{13}C NMR (C_6D_6, ppm): 5.2 (s, $SiMe_3$).

Data Tables for Chapter Four

Table 4.1. Crystallographic Data for $[C_6H_{11}NC(^tBu)NC_6H_{11}]Sn[N(SiMe_3)_2]$ **(4)**, $[C_6H_{11}NC(^tBu)NC_6H_{11}]Sn[N(SiMe_3)_2]S_4$ **(6)**, $\{[C_6H_{11}NC(^tBu)NC_6H_{11}]Sn[N(SiMe_3)_2]S\}_2$ **(8)** and $[C_6H_{11}NC(Me)NC_6H_{11}]Ge[N(SiMe_3)_2]S_4$ **(9)**.

Compound	**4**	**6**	**8**	**9**
Empirical formula	$C_{23}H_{49}N_3Si_2Sn$	$C_{23}H_{49}N_3S_4Si_2Sn$	$C_{46}H_{98}N_6S_2Si_4Sn_2$	$C_{20}H_{43}N_3S_4Si_2Ge$
Formula weight	542.52	670.76	1149.16	582.56
Temperature (K)	203(2)	203(2)	203(2)	203(2)
Wavelength Å	0.71073	0.71073	0.71073	0.71073
Crystal system,	Triclinic,	Triclinic,	Triclinic,	Monoclinic,
Space Group	P-1	P-1	P-1	C2/c
Unit cell dimensions (Å)	a =11.266(3) b =12.173(3) c =12.877(4)	a =10.5767(7) b =10.7715(7) c =15.255(1)	a =10.842(1) b =12.040(1) c =13.492(1)	a =24.1704(16) b =17.4466(12) c =18.2381(12)
(deg)	α =67.321(4) β =66.285(4) γ =70.237(4)	γ =84.472(1) β =85.874(1) γ =68.747(1)	α =71.051(2) β =69.605(2) γ =63.381(2)	α =90 β =131.339(1) γ =90
Volume ($Å^3$)	1456.4(7)	1610.9(2)	1445.6(3)	5774.4(7)
Z	2	2	1	8
Density(calc.) (Mg/m^3)	1.237	1.383	1.320	1.340
Absorption coefficient (mm^{-1})	0.973	1.144	1.054	1.447
F(000)	572	700	604	2464
Goodness-of-fit on F^2	1.109	1.003	1.016	1.039
Final R indices [I>2σ(I)]	R1 = 0.0444, wR2 = 0.1236	R1 = 0.0359, wR2 = 0.0743	R1 = 0.0345, wR2 = 0.0601	R1 = 0.0376, wR2 = 0.0639
R indices (all data)	R1 = 0.0491, wR2 = 0.1254	R1 = 0.0457, wR2 = 0.0815	R1 = 0.0528, wR2 = 0.0612	R1 = 0.0802, wR2 = 0.0682

$$R1 = \sum \left| |F_o| - |F_c| \right| / \sum |F_o| . \quad wR2 = \left(\sum w \left(|F_o| - |F_c| \right)^2 / \sum w |F_o|^2 \right)^{1/2}$$

Table 4.2. Selected bond distances (Å) and angles (°) for $[C_6H_{11}NC(^tBu)NC_6H_{11}]Sn[N(SiMe_3)_2]$ (**4**)

Distances			
Sn-N(3)	2.134(4)	N(1)-C(13)	1.330(5)
Sn-N(1)	2.192(4)	N(1)-C(6)	1.465(5)
Sn-N(2)	2.216(4)	N(2)-C(13)	1.354(6)
Si(1)-N(3)	1.728(4)	N(2)-C(12)	1.443(5)
Si(2)-N(3)	1.732(4)		

Angles			
N(3)-Sn-N(1)	101.3(1)	C(13)-N(2)-Sn	93.9(2)
N(3)-Sn-N(2)	105.3(1)	C(12)-N(2)-Sn	124.3(3)
N(1)-Sn-N(2)	59.4(1)	Si(1)-N(3)-Si(2)	120.7(2)
C(13)-N(1)-C(6)	131.8(4)	Si(1)-N(3)-Sn	110.4(2)
C(13)-N(1)-Sn	95.7(3)	Si(2)-N(3)-Sn	128.8(2)
C(6)-N(1)-Sn	131.5(3)	N(1)-C(13)-N(2)	109.2(4)
C(13)-N(2)-C(12)	130.4(4)	N(1)-C(13)-C(14)	123.1(4)
N(2)-C(13)-C(14)	127.7(4)		

Table 4.3. Selected bond distances (Å) and angles (°) for $[C_6H_{11}NC(^tBu)NC_6H_{11}]Sn[N(SiMe_3)_2]S_4$ (**6**)

Distances			
Sn-N(3)	2.065(2)	Sn-C(13)	2.644(3)
Sn-N(2)	2.136(2)	S(1)-S(2)	2.0610(14)
Sn-N(1)	2.217(3)	S(2)-S(3)	2.0450(16)
Sn-S(4)	2.4637(9)	S(3)-S(4)	2.0622(16)
Sn-S(1)	2.5230(10)		

Angles			
N(3)-Sn-N(2)	119.05(10)	N(2)-Sn-S(1)	105.94(7)
N(3)-Sn-N(1)	98.57(10)	N(1)-Sn-S(1)	165.80(7)
N(2)-Sn-N(1)	60.53(9)	S(4)-Sn-S(1)	93.77(3)
N(3)-Sn-S(4)	131.89(8)	S(2)-S(1)-Sn	101.15(5)
N(2)-Sn-S(4)	105.03(7)	S(3)-S(2)-S(1)	102.00(6)
N(1)-Sn-S(4)	86.34(7)	S(2)-S(3)-S(4)	102.96(6)
N(3)-Sn-S(1)	91.94(8)	S(3)-S(4)-Sn	103.16(5)

Table 4.4. Selected bond distances (Å) and angles (°) for $\{[C_6H_{11}NC(^tBu)NC_6H_{11}]Sn[N(SiMe_3)_2]S\}_2$**(8).**

Distances			
Sn-N(3)	2.068(2)	Si(2)-N(3)	1.759(3)
Sn-N(2)	2.169(3)	Si(2)-C(21)	1.855(3)
Sn-N(1)	2.218(3)	Si(2)-C(23)	1.871(4)
Sn-S#1	2.4373(8)	Si(2)-C(22)	1.880(4)
Sn-S	2.4685(8)	Si(1)-C(20)	1.878(3)
Si(1)-N(3)	1.739(2)	Si(1)-C(19)	1.882(3)
Si(1)-C(18)	1.852(3)		

Angles			
N(3)-Sn-N(2)	111.48(10)	C(13)-N(1)-Sn	95.27(19)
N(3)-Sn-N(1)	104.48(10)	C(6)-N(1)-Sn	132.0(2)
N(2)-Sn-N(1)	59.35(9)	C(13)-N(2)-Sn	96.65(19)
N(3)-Sn-S#1	111.08(7)	C(12)-N(2)-Sn	132.6(2)
N(2)-Sn-S#1	134.01(7)	Si(1)-N(3)-Sn	125.55(15)
N(1)-Sn-S#1	93.66(7)	Si(2)-N(3)-Sn	117.74(12)
N(3)-Sn-S	108.18(7)	S#1-Sn-S	88.40(3)
N(2)-Sn-S	94.34(7)	Sn#1-S-Sn	91.60(3)
N(1)-Sn-S	144.04(7)		

Table 4.5. Selected bond distances (Å) and angles (°) for $[C_6H_{11}NC(Me)NC_6H_{11}]Ge[N(SiMe_3)_2]S_4$ **(9).**

Distances			
Ge-N(3)	1.851(2)	Ge-S(1)	2.3213(8)
Ge-N(2)	1.896(2)	S(1)-S(2)	2.0687(13)
Ge-N(1)	2.208(2)	S(2)-S(3)	2.0556(14)
Ge-S(4)	2.2616(8)	S(3)-S(4)	2.0494(11)

Angles			
N(3)-Ge-N(2)	116.50(8)	N(2)-Ge-S(1)	105.97(6)
N(3)-Ge-N(1)	95.39(8)	N(1)-Ge-S(1)	81.04(6)
N(2)-Ge-N(1)	63.90(8)	S(4)-Ge-S(1)	98.57(3)
N(3)-Ge-S(4)	95.99(7)	S(2)-S(1)-Ge	102.92(4)
N(2)-Ge-S(4)	102.38(7)	S(3)-S(2)-S(1)	101.44(4)
N(1)-Ge-S(4)	165.20(6)	S(2)-S(3)-S(4)	98.16(5)
N(3)-Ge-S(1)	130.57(7)	S(3)-S(4)-Ge	100.34(4)

Table 4.6. Crystal data for compounds $[C_6H_{11}NC(Me)NC_6H_{11}]_2Ge[SeC_6H_5]_2$ (**15**), $[C_6H_{11}NC(Me)NC_6H_{11}]Ge[N(SiMe_3)_2][SeC_6H_5]_2$ (**18**), and $[C_6H_{11}NC(Me)NC_6H_{11}]Sn[N(SiMe_3)_2][SC_6H_5]_2$ (**19**)

Empirical formula	$C_{40}H_{60}GeN_4Se$ (**15**)	$C_{32}H_{53}GeN_3Se_2Si_2$ (**18**)	$C_{32}H_{53}N_3S_2Si_2Sn$ (**19**)
Formula weight	827.43	766.46	718.76
Temperature (K)	163(2)	203(2)	203(2)
λ (Å)	0.71073	0.71073	0.71073
Space group	$P2_1/c$	$P2_1/c$	P-1
Unit cell dimensions (Å, deg)	a = 10.953(2) b = 19.181(4) c = 18.909(4) β = 94.72(3)	a = 10.828(1) b = 25.140(3) c = 26.674(3) β = 98.304(2)	a = 13.234(2) b = 15.834(2) c = 19.023(2) α= 88.728(2) β = 80.465(2) γ = 67.232(2)
Volume ($Å^3$)	3959(1)	7185(1)	3621.0(7)
Z	4	8	4
Density (Mg/m^3) (calculated)	1.388	1.417	1.318
Absorption coefficient (mm^{-1})	2.645	2.971	0.912
R (F_o)	0.0708	0.0366	0.0393
R_w (F_o^2)	0.1931	0.0610	0.0791

Table 4.7. Selected bond lengths [Å] and angles [deg] for $[C_6H_{11}NC(Me)NC_6H_{11}]_2Ge[SeC_6H_5]_2$ (**15**).

Distances			
Se(1)-Ge	2.4698(14)	N(1)-C(13)	1.322(12)
Se(2)-Ge	2.4790(17)	N(1)-C(6)	1.466(12)
Se(1)-C(34)	1.926(5)	N(2)-C(13)	1.313(12)
Se(2)-C(40)	1.940(5)	N(2)-C(12)	1.465(12)
Ge-N(1)	1.955(7)	N(3)-C(27)	1.313(14)
Ge-N(4)	1.978(8)	N(3)-C(20)	1.468(14)
Ge-N(3)	2.062(9)	N(4)-C(27)	1.310(14)
Ge-N(2)	2.105(7)	N(4)-C(26)	1.472(14)
Ge-C(27)	2.467(10)	C(13)-C(14)	1.515(14)
Ge-C(13)	2.468(9)	C(27)-C(28)	1.520(15)

Angles			
C(34)-Se(1)-Ge	105.7(2)	C(13)-N(1)-Ge	95.8(6)
C(40)-Se(2)-Ge	106.3(2)	C(6)-N(1)-Ge	130.0(6)
N(1)-Ge-N(4)	154.9(4)	C(13)-N(2)-C(12)	124.1(8)
N(1)-Ge-N(3)	96.5(3)	C(13)-N(2)-Ge	89.3(6)
N(4)-Ge-N(3)	64.1(4)	C(12)-N(2)-Ge	146.6(6)
N(1)-Ge-N(2)	64.4(3)	C(27)-N(3)-C(20)	121.6(10)
N(4)-Ge-N(2)	98.2(3)	C(27)-N(3)-Ge	91.2(7)
N(3)-Ge-N(2)	89.9(3)	C(20)-N(3)-Ge	145.5(8)
N(1)-Ge-Se(1)	99.8(2)	C(27)-N(4)-C(26)	131.0(10)
N(4)-Ge-Se(1)	98.5(2)	C(27)-N(4)-Ge	95.0(7)

N(3)-Ge-Se(1)	97.5(2)	C(26)-N(4)-Ge	131.0(8)
N(2)-Ge-Se(1)	163.3(2)	N(2)-C(13)-N(1)	110.5(8)
N(1)-Ge-Se(2)	96.6(2)	N(2)-C(13)-C(14)	124.0(9)
N(4)-Ge-Se(2)	99.2(3)	N(1)-C(13)-C(14)	125.4(9)
N(3)-Ge-Se(2)	161.0(2)	N(4)-C(27)-N(3)	109.6(9)
N(2)-Ge-Se(2)	83.5(2)	N(4)-C(27)-C(28)	125.7(12)
Se(1)-Ge-Se(2)	93.71(6)	N(3)-C(27)-C(28)	124.6(12)
C(13)-N(1)-C(6)	127.8(8)		

Table 4.8. Selected bond lengths [Å] and angles [deg] for one of the independent molecules of $[C_6H_{11}NC(Me)NC_6H_{11}]Ge[N(SiMe_3)_2][SeC_6H_5]_2$ (**18**).

Distances			
Ge(1)-N(3)	1.840(2)	N(1)-C(13)	1.395(4)
Ge(1)-N(1)	1.859(2)	N(1)-C(6)	1.489(3)
Ge(1)-Se(2)	2.3522(5)	N(2)-C(13)	1.272(3)
Ge(1)-Se(1)	2.4009(5)	N(2)-C(12)	1.467(4)
Se(1)-C(20)	1.925(3)	C(13)-C(14)	1.514(4)
Se(2)-C(26)	1.934(3)		

Angles			
N(3)-Ge(1)-N(1)	108.87(11)	C(13)-N(2)-C(12)	121.5(3)
N(3)-Ge(1)-Se(2)	111.98(7)	Si(1)-N(3)-Si(2)	120.99(14)
N(1)-Ge(1)-Se(2)	113.81(7)	Si(1)-N(3)-Ge(1)	121.12(14)
N(3)-Ge(1)-Se(1)	110.26(7)	Si(2)-N(3)-Ge(1)	117.88(13)
N(1)-Ge(1)-Se(1)	104.13(8)	N(2)-C(13)-N(1)	117.3(3)
Se(2)-Ge(1)-Se(1)	107.484(17)	N(2)-C(13)-C(14)	124.2(3)
C(20)-Se(1)-Ge(1)	96.23(9)	N(1)-C(13)-C(14)	118.4(3)
C(26)-Se(2)-Ge(1)	99.67(9)	C(45)-N(5)-C(44)	121.3(3)
C(13)-N(1)-C(6)	123.8(2)	Si(4)-N(6)-Si(3)	120.84(14)
C(13)-N(1)-Ge(1)	118.45(18)	Si(4)-N(6)-Ge(2)	121.65(13)
C(6)-N(1)-Ge(1)	117.60(19)		

Table 4.9. Selected bond lengths [Å] and angles [deg] for one of the independent molecules of $[C_6H_{11}NC(Me)NC_6H_{11}]Sn[N(SiMe_3)_2][SC_6H_5]_2$ (**19**).

Distances			
Sn(1)-N(3)	2.070(2)	S(2)-C(26)	1.777(4)
Sn(1)-N(2)	2.140(3)	N(1)-C(13)	1.303(4)
Sn(1)-N(1)	2.213(2)	N(1)-C(12)	1.463(4)
Sn(1)-S(1)	2.4158(10)	N(2)-C(13)	1.336(4)
Sn(1)-S(2)	2.4854(10)	N(2)-C(6)	1.468(4)
S(1)-C(20)	1.781(4)	C(13)-C(14)	1.516(4)

Angles			
N(3)-Sn(1)-N(2)	135.18(11)	C(13)-N(1)-C(12)	124.8(3)
N(3)-Sn(1)-N(1)	95.56(10)	C(13)-N(1)-Sn(1)	93.1(2)
N(2)-Sn(1)-N(1)	60.05(10)	C(12)-N(1)-Sn(1)	142.1(2)
N(3)-Sn(1)-S(1)	116.44(8)	C(13)-N(2)-C(6)	130.0(3)

N(2)-Sn(1)-S(1)	106.28(8)	C(13)-N(2)-Sn(1)	95.4(2)
N(1)-Sn(1)-S(1)	104.03(8)	C(6)-N(2)-Sn(1)	133.8(2)
N(3)-Sn(1)-S(2)	88.81(8)	Si(2)-N(3)-Si(1)	121.65(15)
N(2)-Sn(1)-S(2)	98.23(8)	Si(2)-N(3)-Sn(1)	116.18(15)
N(1)-Sn(1)-S(2)	152.35(8)	Si(1)-N(3)-Sn(1)	119.88(14)
S(1)-Sn(1)-S(2)	98.29(3)	N(1)-C(13)-N(2)	111.3(3)
N(6)-Sn(2)-N(5)	140.30(10)	N(1)-C(13)-C(14)	124.3(3)
C(20)-S(1)-Sn(1)	105.61(11)	N(2)-C(13)-C(14)	124.3(3)
C(26)-S(2)-Sn(1)	114.00(13)		

Table 4.10. Crystallographic Data for $[(Me_3Si)_2NGeE_{1.5}]_4$ **(21)**

Compound	**21**
Empirical formula	$C_{24}H_{72}N_4Si_8SGeS_6$
Formula weight	1124.3
Temperature (K)	238(2)
Wavelength Å	0.71073
Crystal system,	Triclinic,
Space Group	P-1
Unit cell dimensions (Å)	a =13.612(1) b =14.125(1) c =16.232(1)
(deg)	α =98.545(2) β =112.679(1) γ =101.298(1)
Volume ($Å^3$)	2735.7(4)
Z	2
Density(calc.) (Mg/m^3)	1.365
Absorption coefficient (mm^{-1})	2.602
F(000)	1160
Goodness-of-fit on F^2	1.002
Final R indices [I>2σ(I)]	R1 = 0.0383, wR2 = 0.0873
R indices (all data)	R1 = 0.0621, wR2 = 0.0.0908

Table 4.11. Selected bond distances (Å) and angles (°) for $[(Me_3Si)_2NGeE_{1.5}]_4$ **(21).**

Distances			
Ge(1)-N(1)	1.828(3)	Ge(3)-N(3)	1.823(3)
Ge(1)-S(1)	2.2212(10)	Ge(3)-S(4)	2.2193(10)
Ge(1)-S(3)	2.2216(10)	Ge(3)-S(6)	2.2198(11)
Ge(1)-S(2)	2.2312(11)	Ge(3)-S(5)	2.2268(9)
Ge(2)-N(2)	1.823(3)	Ge(4)-N(4)	1.828(3)
Ge(2)-S(2)	2.2184(9)	Ge(4)-S(1)	2.2185(10)
Ge(2)-S(4)	2.2186(11)	Ge(4)-S(6)	2.2227(10)
Ge(2)-S(3)	2.2328(11)	Ge(4)-S(5)	2.2259(11)
Angles			
N(1)-Ge(1)-S(1)	103.72(10)	N(3)-Ge(3)-S(5)	114.65(9)
N(1)-Ge(1)-S(3)	115.02(9)	S(4)-Ge(3)-S(5)	116.03(4)
S(1)-Ge(1)-S(3)	113.26(4)	S(6)-Ge(3)-S(5)	95.50(4)
N(1)-Ge(1)-S(2)	114.14(10)	N(4)-Ge(4)-S(1)	103.62(10)
S(1)-Ge(1)-S(2)	115.47(4)	N(4)-Ge(4)-S(1)	114.94(9)
S(3)-Ge(1)-S(2)	95.75(4)	N(4)-Ge(4)-S(1)	115.34(4)
N(2)-Ge(2)-S(2)	115.09(9)	N(4)-Ge(4)-S(1)	114.73(9)
N(2)-Ge(2)-S(4)	103.41(10)	N(4)-Ge(4)-S(1)	113.29(4)
S(2)-Ge(2)-S(4)	112.96(4)	N(4)-Ge(4)-S(1)	95.44(4)
N(2)-Ge(2)-S(3)	114.35(10)	Ge(4)-S(1)-Ge(1)	107.55(4)
S(2)-Ge(2)-S(3)	95.79(4)	Ge(2)-S(2)-Ge(1)	84.24(3)
S(4)-Ge(2)-S(3)	115.80(4)	Ge(1)-S(3)-Ge(2)	84.13(3)
N(3)-Ge(3)-S(4)	103.16(10)	Ge(3)-S(4)-Ge(2)	107.30(4)
N(3)-Ge(3)-S(6)	114.95(9)	Ge(4)-S(5)-Ge(3)	84.36(3)
S(4)-Ge(3)-S(6)	113.14(4)	Ge(3)-S(6)-Ge(4)	84.60(3)

References for Chapter Four

[1] Y. Zhou .D. S. Richeson *J. Am. Chem. Soc.* **1996**, *118*, 10850.

[2] S. Foley, C. Bensimon, D. Richeson *J. Am. Chem. Soc.* **1997**, *119*, 10359.

[3] (a) Y. Zhou, and D. S. Richeson *Inorg. Chem.* 1997, **36**, 501. (b) U. Kilimann, M. Noltemeyer, and F. T.Edelmann *J. Organomet. Chem.* 1993, **443**, 35. (c) B. Borgsen, K. Dehnicke, D. Fenske, G. Baum. *Z. Anorg. Allg. Chem.* 1991,**596**, 133. (d) S. Appel, F. Weller, K. Dehnicke *Z. Anorg. Allg. Chem.* 1990,**583**, 7. (e) J. D. Kidea, W. Hiller, B. Borgsen, K. Dehnicke *Z. Naturforsch.* 1989,**44B**, 889. (f) K. Dehnicke, C. Ergezinger, E. Hartmann, A. Zinn, and K. Hösler *J. Organomet. Chem.* 1988, **352**, C1. (g) H. W. Roesky, B. Meller, M. Noltemeyer, H.-G. Schmidt, U. Scholz, and G. M. Sheldrick, *Chem. Ber.* 1988, **121**, 1403. (h) C. Ergezinger, F. Weller, K. Dehnicke. *Z. Naturforsch.* 1988,**43B**, 1621.

[4] W.W. Schoeller, A. Sundermann, and M. Reiher *Inorg. Chem.* 1999, **38**, 29.

[5] Kopf, H.; Block, B.; Schmidt, M. *Chem Ber.* **1968**, *101*,272

[6] Kopf, H.; Wirl, A.; Kahl, W. *Angew. Chem., Int. Ed. Engl.* **1971**,*10*, 137

[7] Kopf, H.; Hazari, S.K.S.; *Z. Anorg. Allg. Chem.* **1976**, *426*, 49

[8] Kopf, H.; Wirl, A.; Kahl, W. *Angew. Chem., Int. Ed. Engl.* **1970**, *9*, 801

[9] For reviews of polysulfido complexes see: (a) Müller, A.; Diemann, E.; *Advances in Inorganic Chemistry* **1987**, *31*, 89; (b) Draganjac, M.; Rauchfuss, T. B.; *Angew Chem. Int. Ed. Engl.* **1985**, *24*, 742.

[10] For reviews of polychalcogenido complexes see: (a) Kolis, J. W. *Coord. Chem. Rev.***1990**, *105*, 195; (b) Ansari, M. A. ; Ibers, J. A. *Coord. Chem. Rev.* **1990**, *100*, 223; (c) Dubois, M. R. *Chem. Rev.***1989**, *89*, 1.

[11] Tokitoh, N.; Suzuki, H.; Matsumoto, T.; Matsuhashi, Y.; Okazaki, R.; Goto, M. *J. Am. Chem. Soc.* **1991**, *112*, 7047

[12] The molecular species $[N(Et)_4]_2\{[Sn(S_4)_3]_{0.4}[Sn(S_4)_2(S_6)]_{0.6}\}$ which consists of $[Sn(S_4)_3]^{2-}$ and $[Sn(S_4)_2(S_6)]^{2-}$ anions has been reported. Muller, A.; Schimanski, J.; Romer, M.; Bogge, H.; Baumann, F.-W.; Eltzner, W.; Krickemeyer, E.; Billerbeck, U. *Chimia*, **1985**, *39*, 25.

[13] (a) Saito, M.; Tokitoh, N.; Okazaki, R. *J. Am. Chem. Soc.* **1997**, *119*, 11124. (b) Tokitoh, N.; Kano,N.;Shibata, K.; Okazaki, R.*Organometallics* **1995**, *14*, 3121. (c) Matsumoto, T.; Tokitoh, N.; Okazaki, R *Organometallics* **1995**, *14*, 1008. (d) Matsuhashi, Y.; Tokitoh, N.; Okazaki, R.; Goto, M.; Nagase, S. *Organometallics* **1993**,

12, 1351. (e) Tokitoh, N.; Matsumoto, T.; Okazaki, R *Tetrahedron Lett.* **1992**, *33*, 2531. (f) Tokitoh, N.; Matsuhashi, Y.; Okazaki, R *Tetrahedron Lett.* **1991**, *32*, 6151.

[14] (a)Kano, N.; Tokitoh, N.; Okazaki, R. *Chemistry Letters* **1997**, 277. (b) Suzuki, H.; Tokitoh, N.; Nagase, S.; Okazaki, R. *J. Am. Chem. Soc.* **1994**, *116*, 11578.(c) Matsumoto, T.; Tokitoh, N.; Okazaki, R. *Angew. Chem. Int. Ed. Engl.* **1994**, *33*, 2316. (d) Tokitoh, N.; Matsumoto, T.; Manmaru, K.; Okazaki, R. *J. Am. Chem. Soc.* **1993**, *115*, 8855. (e) Tokitoh, N.; Matsumoto, T.; Ichida, H; Okazaki, R. *Tetrahedron Lett.* **1991**, *32*, 6877

[15] Hitchcock, P. B.; Jang, E.; Lappert, M. F. *J. Chem. Soc., Dalton Trans.* **1995**, 3179. Hitchcock, P. B.; Jasim, H. A.; Lappert, M. F.; Leung, W-P. Rai, A. K.; Taylor, R. E. *Polyhedron* **1991**, *10*, 1203.

[16] Reger, D. L.; Coan, P. S.; *Inorg. Chem* **1995**, *34*, 6226.

[17] Albertsen, J.; Steudel, , R. *Phosphorus, Sulfur, Silicon Relat. Elem.* **1992**, *65*, 165. Steudel, R. In *Chemistry of Inorganic Ring Systems*; Steudel, R., Ed.; Elsevier: Amsterdam, 1992, p. 233.

[18] Zhou, Y.; Richeson, D. S. *Inorg. Chem.* **1997**, *36*, 501 and references therein.

[19] Fjeldberg, T.: Hope, H.; Lappert, M. F.; Power, P. P.; Thorne, A. J. *J. Chem. Soc., Chem. Commun.* **1983**, 639. Lappert, M. F.; Power, P. P.; Slade, M. J.; Hedberg, L.; Hedberg, K.; Schomaker, V. *J. Chem. Soc., Chem. Commun.* **1979**, 369.

[20] Complete structural details for S_8 were measured at T = 203 K so that the average S-S distances could be compared to our systems measured at the same temperature. Crystal system: orthorhombic, Space group: Fddd; cell parameters: a = 10.402(2)Å, b = 12.771(2)Å, c = 24.400(4)Å.

[21] Puff, H.; Bertram, G.; Ebeling, B.; Franken, M.; Gattermayer, R.; Hundt, R.; Schuh, W.; Zimmer, R. *J. Organomet. Chem.* **1989**, *379*, 235 and references therein.

[22] Jung, O.-S.; Hwa, J.; Sohn, Y. S. *Polyhedron* **1989**, *8*, 2557.

[23] Jurkschat, K.; Van Dreumel, S.; Dyson, G.; Dakternieks, D.; Bastow, T. J.; Smith, M. E.; Drager, M. *Polyhedron* **1992**, *11*, 2747 and references therein.

[24] Leung, W.-P.; Kwok, W.-H.; Law, L. T. C.; Zhou, Z-Y.; Mak, T. C. W. *Chem. Commun.* **1996**, 505.

[25] B. Kersting and B. Krebs *Inorg. Chem.* 1994, **33**, 3886. H. J. Gysling, H. R. Luss *Organometallics* 1989, **8**, 363. S. Tomoda, M. Shimoda, Y. Takeuchi, and Y. Iitaka. *Chem. Lett.*1988, 535

[26] D. Dakternieks, K. Jurkschat, R. Tozer, J. Hook, E. R. T. Tiekink, *Organometallics* 1997, **16**, 3696. D. Dakternieks, G. Dyson, K. Jurkschat, R. Tozer, E. R. T Tiekink. *J. Organomet. Chem.* 1993, **485**, 29

[27] Armitage, D.A. In The chemistry of organic silicon compounds; Patai, S., Rappoport, Z., Eds.; John Wiley and Sons Ltd.; London, 1989; pp 1401-1409

[28] Ando, W.; Kadowaki, T.; Kabe, Y.; Ishii, M. *Angew. Chem. Int. Ed. Engl.* **1992**, *31*, 59

[29] Unno, M.; Kawai, Y.; Shioymaya, H.; Matsumoto, H. *Organometallics* **1997**, *16*, 4428

The Synthesis of Group 14 Amidinato Complexes via a Ligand Rearrangement

'I kinda lost track of myself.'

Chapter Five

Introduction

Recent interest in the use of amidinate ligands in the preparation of main group element compounds stems from the recognition that these complexes can exhibit catalytic activity (Chapter six) and that these species are useful for fundamental studies of the effects of ligand geometry on the coordination environments of post-transition elements.

Up to this point in the thesis our interest in this area has focused on employing alkyl amidinates in the chemistry of group 14 elements and investigating the effects of variation of R and R' on the features of these products. In general, we have relied on lithium amidinates, which have been prepared by the addition of alkyl anions to the appropriate carbodiimide, as our synthetic access for preparation of these species. The work presented in the previous four chapters has focussed solely on employment of amidinate ligands of the variety CyNC(R)NCy, R = Me, ^{t}Bu.

Motivated by a continual interest in exploring the effects of increasing the steric bulk of the amidinate ligand, the bulky amidinate $[Me_3SiNC(^tBu)NSiMe_3]^-$ was prepared by reaction of ^{t}BuLi and bis(trimethylsilyl)carbodiimide. This anion was previously employed by our group in the synthesis of In(III) and Sn(IV) compounds. The monomeric five coordinate complex, $[Me_3SiNC(^tBu)NSiMe_3]_2InCl$ (**I**),[1] was prepared by reaction of two equivalents of the *in situ* generated lithium salt of the ligand with $InCl_3$. Unlike the amidinate complex **II** shown in Scheme 5.1, complex **I** does not react with alkylating or

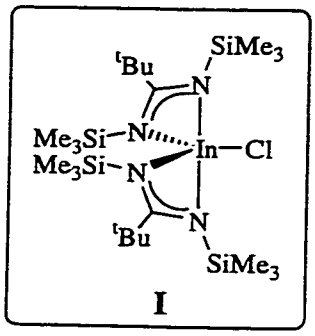

I

reducing agents and will not incorporate a third amidinate ligand. These observations were attributed to the increased bulk of the ligand which presumably prevents further metathesis or disproportionation reactions from occuring. The six-coordinate Sn(IV) complex, $[Me_3SiNC(^tBu)NSiMe_3]_2SnCl_2$, was prepared according to Scheme 5.2.[2] As with the indium complex, the Sn(IV) complex shows diminished reactivity in comparison with complexes possessing the less bulky N,N'-dicyclohexyl amidinate analogues are consistent with the increased steric demand anticipated for $[Me_3SiNC(^tBu)NSiMe_3]^-$.

Scheme 5.1

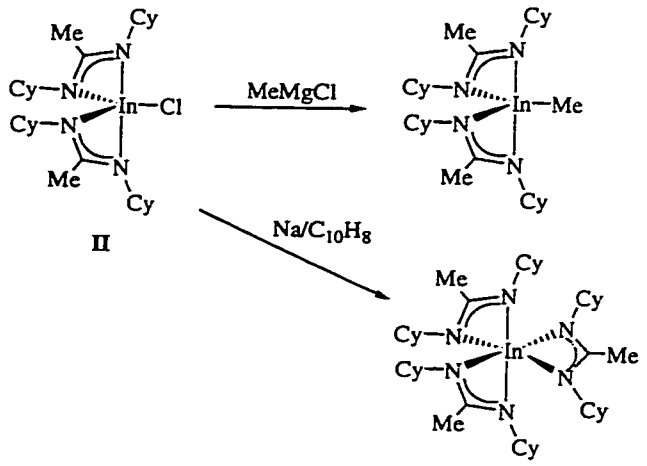

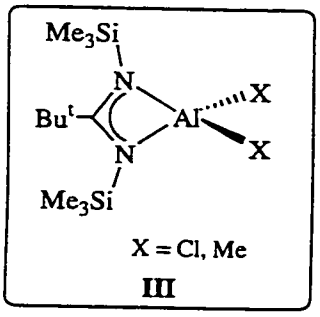

III

This same route was used also by Jordan et al. to prepare $[Me_3SiNC(^tBu)NSiMe_3]AlX_2$ (X = Cl, Me) (**III**). All attempts to isolate the lithium salt of the amidinate, $[Me_3SiNC(^tBu)NSiMe_3]Li$ (**1a**) yielded the rearrangement product $[Li(^tBuCN)\{\mu\text{-}N(SiMe_3)_2\}]_2$ (**IV**). It was concluded that the ligand had to be generated *in situ* for use in subsequent reactions.[3]

The results of this chapter stem from an interest in employing the bulky amidinate $[Me_3SiNC(^tBu)NSiMe_3]^-$ in the preparation of new Sn(II) and Ge(II) complexes. Based on our discovery that amidinate complexes of tin(IV) are excellent catalysts for the

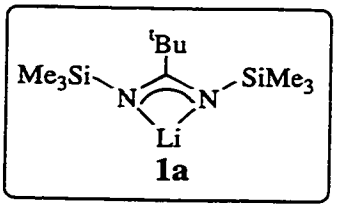

1a

cyclotrimerization of isocyanates to yield isocyanurates,[4] we extended our results in this area by applying new amidinate complexes of tin and germanium as catalysts for this reaction. The catalytic behaviour of these complexes constitutes the basis of Chapter six and will not be discussed further here. During attempts to synthesize these new bulky amidinate complexes, we observed some features of the stability of this amidinate ligand and of the lithium salt, $[Me_3SiNC(^tBu)NSiMe_3]Li$, which are pertinent for the utilization of this species. This ligand is susceptible to rearrangement that ultimately yielded, in the case of Sn(II) and Ge(II) metal centers, the mixed amidinato amido complexes $[Me_3SiNC(^tBu)NSiMe_3]M[N(SiMe_3)_2]$ (M = Sn **2**, Ge **3**). Replacement of Me for ^{t}Bu in the ligand allowed for the isolation of $[Me_3SiNC(Me)NSiMe_3]_2Sn^{(II)}$ (**4**).

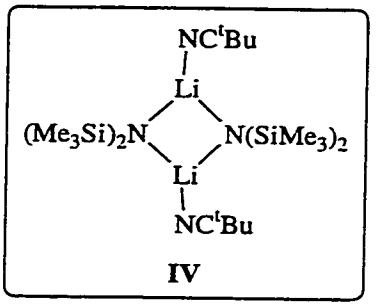

IV

Results and Discussion

The observation that *in situ* generated $[Me_3SiNC(^tBu)NSiMe_3]Li$ (**1a**) was an effective reagent for the introduction of this bulky amidinate into the coordination spheres of Sn,[2] In[1] and Al[3] along with the fact that the reactivity of $Sn(CyNC(R)NCy)_2$ (see Chapter two) depended on the nature of the R substituent provided the motivating factors that lead to our attempt to prepare and investigate the reactivity of the proposed new complex $[Me_3SiNC(^tBu)NSiMe_3]_2Sn$. All previous syntheses employing **1a** have been performed by first generating this species through the addition of ^{t}BuLi to

$Me_3SiN{=}C{=}NSiMe_3$ in ether (Equation 5.1) followed by metathesis reactions with metal halides. For example, $[Me_3SiNC(^tBu)NSiMe_3]_2SnCl_2$ was synthesized in 77% isolated

Equation 5.1

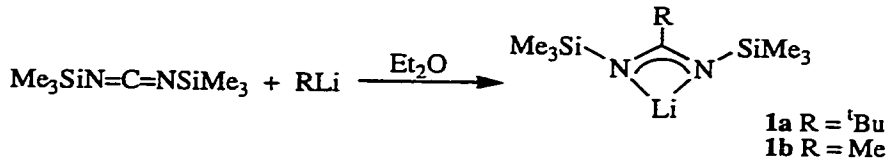

yield following the reaction of **1a** with $SnCl_4$ (Scheme 5.2).[5] Attempting to follow this procedure using a suspension of $SnCl_2$ in diethyl ether produced a material with a ^1H NMR spectrum inconsistent with the targeted species. The observed spectrum exhibited two signals assigned to trimethylsilyl functions (0.43, 0.30 ppm) and a single resonance for the ^{t}Bu group (1.04 ppm) with integrated ratios indicating four trimethylsilyl groups per *tert*-butyl moiety. On the basis of this data we proposed the connectivity for **2** as indicated in Scheme 5.2. This was subsequently confirmed by X-ray diffraction *vide infra*. On the basis of this formulation the yield of **2** from this reaction procedure is 83%.

Scheme 5.2

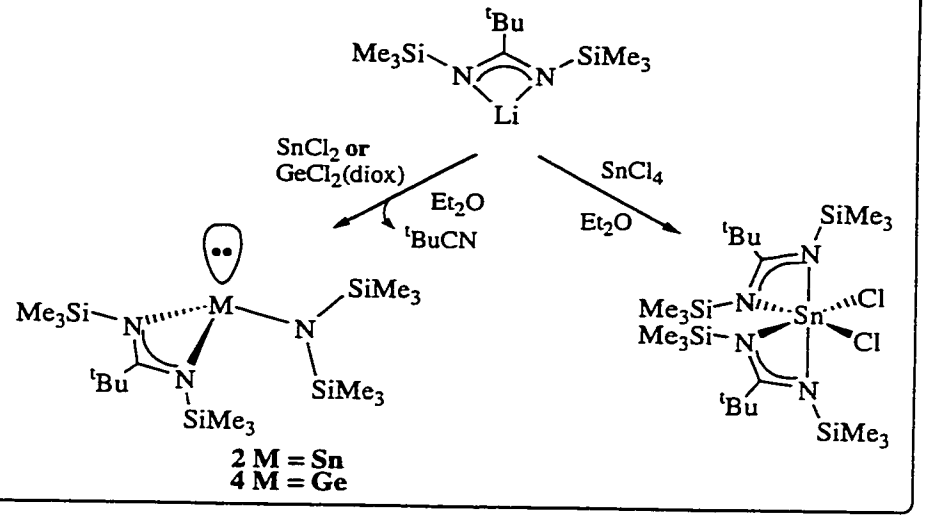

Interestingly, when this same reaction is performed in the presence of THF the yield of **2** is substantially lower (45% yield).

While the appearance of the amidinato ligand $[Me_3SiNC(^tBu)NSiMe_3]^-$ in **2** is as expected, the bis(trimethylsilyl)amido ligand was not anticipated and likely arises from a rearrangement of the amidinate anion with loss of ^{t}BuCN. A probable route for this rearrangement is a 1,3 trimethylsilyl shift to form amido and ^{t}BuCN (Scheme 5.3).

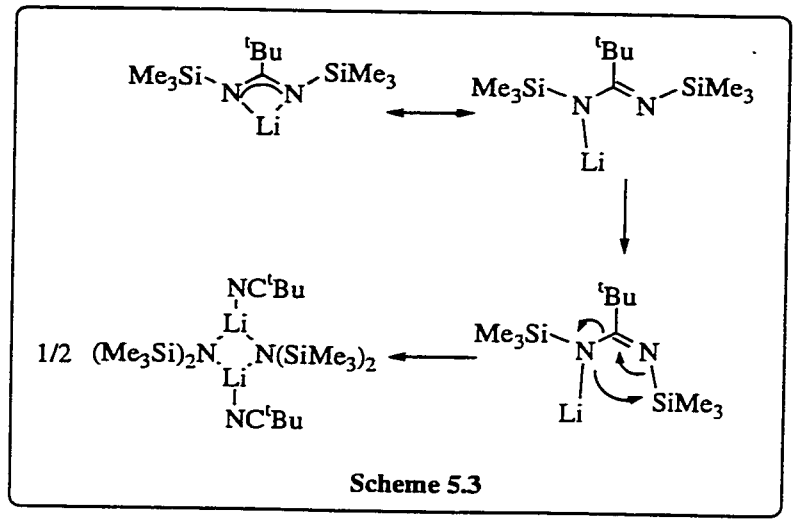

Scheme 5.3

This same transformation was proposed by Jordan et al. when, during their attempts to isolate and structurally characterize **1a,** they obtained the crystal structure of the dimeric species $[Li(^tBuCN)^+[\mu\text{-}N(SiMe_3)_2]^-]_2$ (**IV**)that consisted of $N(SiMe_3)_2^-$ units bridged by Li cations which were coordinated by ^{t}BuCN.[3] All of our attempts to isolate **1a** have so far resulted only in isolation of the identical species as confirmed by comparison of unit cell parameters with those in the literature.[3] Precedent for 1,3 trimethylsilyl shifts within the amidinate framework is provided by the common preparative routes to benzamidinate anions $[Me_3SiNC(Ar)NSiMe_3]^-$.[5] These species are generated by reaction of $LiN(SiMe_3)_2$ and ArCN, a synthetic methodology that relies on what is essentially the reverse reaction

to that proposed. These rearrangements depend on the presence of trimethylsilyl substituents (Chapter one).

Understanding the conditions that affect the stability of $[Me_3SiNC(^tBu)NSiMe_3]^-$ is a critical factor for the effective use of this ligand. Given the previous isolation of $[Me_3SiNC(^tBu)NSiMe_3]_2SnCl_2$[2], $[Me_3SiNC(^tBu)NSiMe_3]_2InCl$[1] and $[Me_3SiNC(^tBu)NSiMe_3]AlX_2$[3] (X = Cl, Me), steric factors can be ruled out as the sole reason for the observed reorganization.

We have observed that the yield of **2** exhibited a strong solvent dependence with a substantial decrease in yield in the presence of even small amounts of THF. We interpret these results as indicating that **1a** is sensitive to the coordinating ability of the reaction solvent and that in the presence of more strongly coordinated solvents (THF *vs.* diethylether) **1a** is less stable. While these observations provide evidence for the solvent-based stability of N,N'-bis(trimethylsilyl)amidinates, the previous report of the high yield syntheses of Sn(IV) and In(III) complexes of $[Me_3SiNC(^tBu)NSiMe_3]^-$ under similar reaction conditions indicate that solvent effects do not offer a complete explanation for the observation that **2** was obtained in an excellent yield as the sole isolated product from the reaction of $SnCl_2$ and **1a**.

Our results appear to indicate that the stability of the amidinate anion in **1a** is affected by interaction with the Sn(II) metal center. The possibility that complex **2** in fact arises from an insertion reaction of ^tBuCN into the the Sn-N bond of $Sn[N(SiMe_3)_2]_2$ coupled with a 1,3-trimethylsilyl shift can be excluded based on our observation that these two species do not produce **2** under the reaction conditions reported above (Equation 5.2). This observation further suggests that the *in situ* generation of **1a** by the

reaction of ^{t}BuLi and $Me_3SiNCNSiMe_3$ does indeed proceed according to Equation 5.1. Interestingly, we have also observed that **2** does not undergo further rearrangement/elimination to give ^{t}BuCN and $Sn[N(SiMe_3)_2]_2$ even under forcing conditions (100°C) or variation of the solvent.

Equation 5.2

$$Sn[N(SiMe_3)]_2 + Me_3CCN \not\longrightarrow \mathbf{2}$$

We attempted to explore the effect of the Lewis acidity of the coordinated metal center on the stability of $[Me_3SiNC(^{t}Bu)NSiMe_3]^-$ through the synthesis of Ge(II) analogues of this amidinate. Replacing $SnCl_2$ in the reaction with **1a** by $GeCl_2$(dioxane) provides a means of increasing the Lewis acidity of the metal center. Thus, reaction of an ether solution of **1a** and a suspension of $GeCl_2$(dioxane) in ether in a 2:1 ratio followed the pathway outlined in Scheme 5.2. Spectroscopic characterization of the product of this reaction, **3**, clearly indicated it to be the analogue of **2**. The smaller Ge(II) center causes the steric demands of the ligands to be more pronounced in the case of **3** which is reflected in the broadening of the ^{1}H and ^{13}C NMR resonances attributed to the $N(SiMe_3)_2$ moiety. This hindered fluxionality enables the two trimethylsilyl groups to be distinguished at 230K. Definitive confirmation of the structure of this complex was provided by single crystal X-ray analysis of **3**.

The less sterically demanding species $[Me_3SiNC(Me)NSiMe_3]Li$ (**1b**) is easily synthesized by the reaction of MeLi and $Me_3SiNCNSiMe_3$ in ether (Equation 5.1) and provides a means of exploring the role of sterics in the stability of **1a** and in the synthesis

of **2** and **3**. We employed the methyl analogue **1b** in a reaction with $SnCl_2$ as represented in Scheme 5.4. In this case, the ^1H and ^{13}C NMR spectra of the product **4** indicated no rearrangement of the amidinate and that we had isolated the bis(amidinate) complex. X-ray structural analysis of **4** confirmed these observations. The isolation of **4** suggests that $[Me_3SiNC(Me)NSiMe_3]^-$ is less susceptible to the 1,3-trimethylsilyl shift observed for the ^{t}Bu substituted species. In addition, the effective use of this species provides further evidence that the ether solutions of **1a** and **1b** do, in fact, contain the amidinate species. Interestingly, complex **4** appears to be stable to the rearrangement that was observed for the generation of **2** even when heated to greater than 70°C.

Scheme 5.4

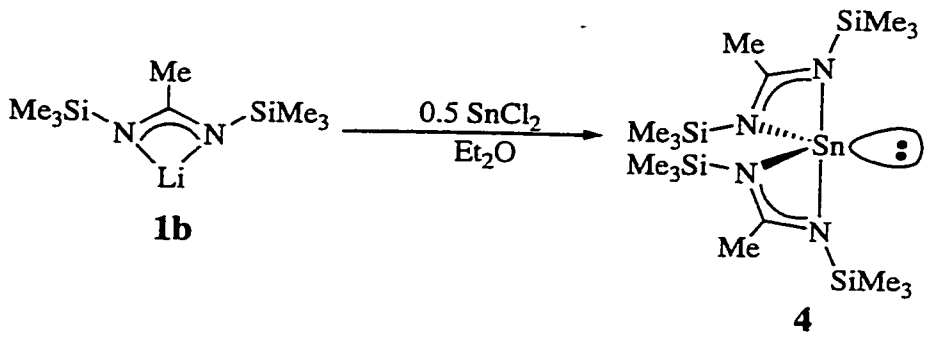

1b **4**

These results offer corroborating evidence that the coordinated metal center (Sn(II) or Ge(II)) plays a role in the stability of these bulky amidinate ligands. Furthermore, the sterics of the substituents on the methyne carbon do play a role in the stability of bis(trimethylsilyl) amidinate ligands.

Structural Studies of $[Me_3SiNC(^tBu)NSiMe_3]M[N(SiMe_3)_2]$ (M = Sn **2**, Ge **3**),

Single crystal X-ray analyses of complexes **2**, and **3** confirmed the proposed connectivities and give the structural parameters of the amidinates employed in this study. A summary of the data collections is provided in Table 5.1.

Figures 5.1 and 5.2 provide the molecular geometries and atom numbering schemes for **2** and **3** respectively and show that the two complexes adopt similar coordination geometries. Furthermore, the metal centers in these mixed ligand species are similar the previously described analogues $[(CyNC(R)NCy)Sn[N(SiMe_3)_2]$ (R = Me, ^tBu)[4] and $[(CyNC(R)NCy)Ge[N(SiMe_3)_2]$ (R = Me, ^tBu) which reside in distorted tetrahedral environments with one vertex occupied by a stereochemically active lone pair of electrons (see Chapters four and two respectively). The result is an overall pyramidal ligand array around the M(II) centers which consists of one bidentate amidinate and the bis(trimethylsilyl)amido nitrogen center.

Complexes **2** and **3** both exhibit two M-N(amidinate) bond distances (Tables 5.2 and 5.3) which are only slightly different. As expected, the average M-N(amidinate) distance is shorter for the Ge complex (**3**) with the corresponding distances in **2** (2.229(4)Å) being slightly longer than in $[(CyNC(^tBu)NCy)Sn[N(SiMe_3)_2]$ (2.204(4)Å) which is indicative of increased bulk for the amidinate ligand in **2**. The amido nitrogen atoms in both compounds have planar geometries with metal-N_{amido} distances of 2.121(5)Å for **2** and 1.9101(19)Å in **3** which are comparable when adjusted for the relative covalent radii of Ge and Sn.[6]

Figure 5.1. Molecular structure and atom numbering scheme for $[Me_3SiNC(^tBu)NSiMe_3]Sn[N(SiMe_3)_2]$ (**2**). Hydrogen atoms have been omitted for clarity. Thermal ellipsoids are drawn at 30% probability.

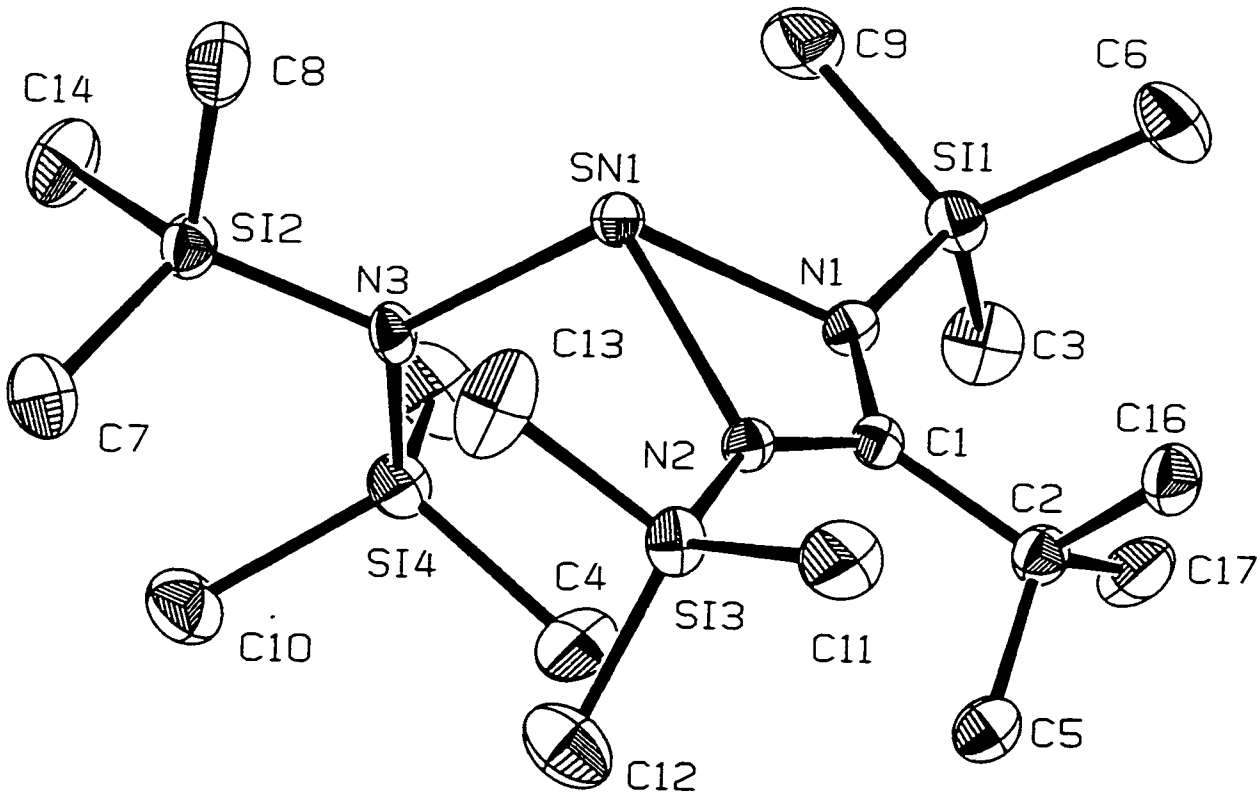

Figure 5.2. Molecular structure and atom numbering scheme for $[Me_3SiNC(^tBu)NSiMe_3]Ge[N(SiMe_3)_2]$ (**3**). Hydrogen atoms have been omitted for clarity. Thermal ellipsoids are drawn at 30% probability.

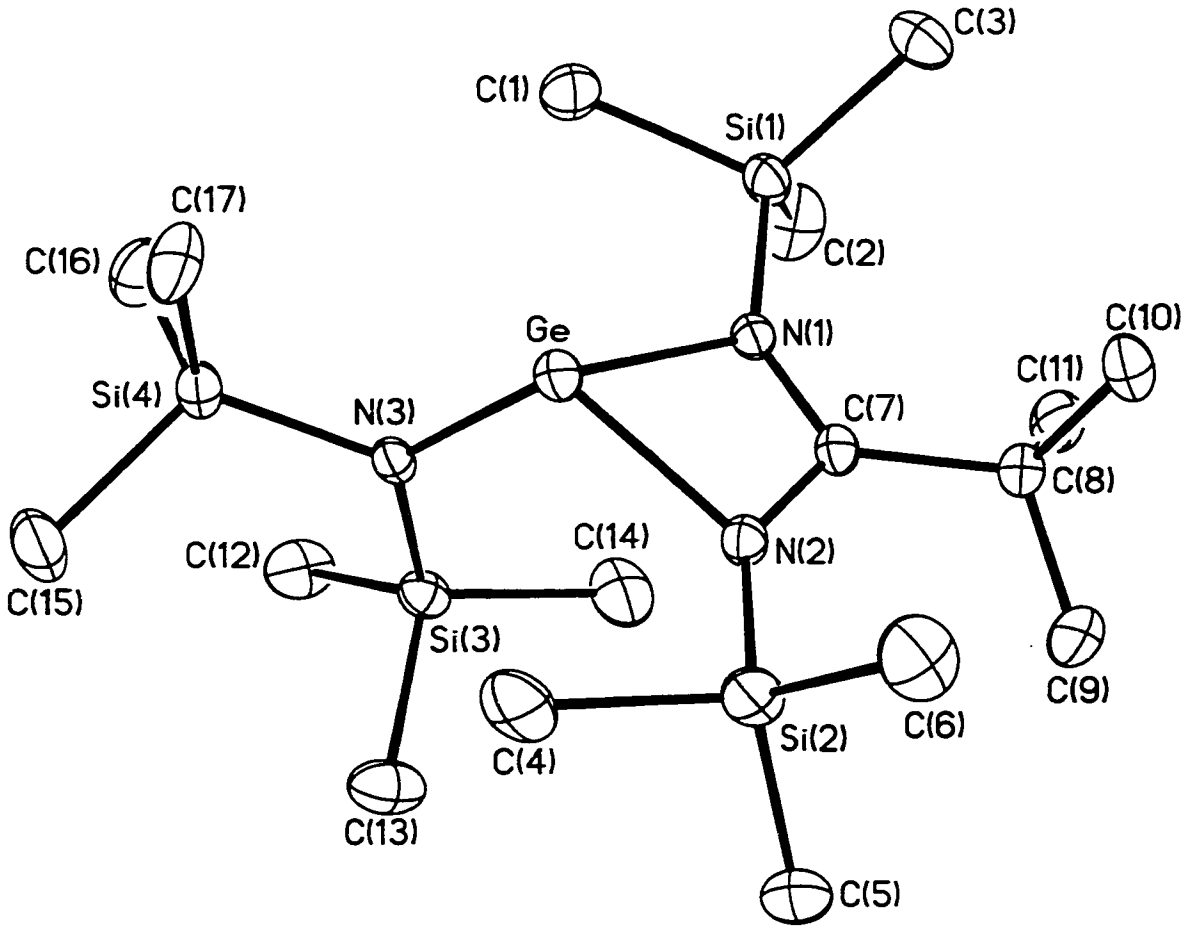

The two N atoms and central C of the amidinate frameworks are in distorted trigonal planar environments resulting in planar amidinate ligands in both **2** and **3**. The corresponding C-N bond lengths (average for both compounds 1.34(1)Å) are consistent with delocalization of the π bond in the N-C-N unit of the ligand.

Replacing the organic substitutents of the amidinate with bulkier groups leads to increased steric crowding around the metal center. A comparison of the angles around the amidinate N atoms of **2** and $[(CyNC(^tBu)NCy)Sn[N(SiMe_3)_2]$[4] supports this idea by exhibiting the effects anticipated for the relative interactions of Cy and bulkier $SiMe_3$ substituents with the central ^{t}Bu groups (Chart 5.1). These steric effects are even more pronounced in the case of **3** and help to justify the spectroscopic features noted above.

Structural Study of $[Me_3SiNC(Me)NSiMe_3]_2Sn$ (**4**)

In order to confirm the structural features of **4** and to provide metrical details for the new amidinate in this complex a single crystal X-ray study of this complex was performed. Complex **4** (Figure 5.3, Table 5.4) possesses two bidentate amidinate ligands and has a molecular geometry derived from a distorted trigonal bipyramid in which one of the pseudo-equatorial sites is occupied by a lone pair of electrons. The electron pair lies on a molecular C_2 axis making N(2)/N(2A) the pseudo-axial positions with N(1)/N(1A) the pseudo-equatorial ligands. Planarity of the amidinate rings is confirmed by the fact that the sum of the internal angles of the MNCN cycle is 360°. The axial Sn-N(2) bond lengths are slightly longer (2.397(2)Å) than the Sn-N(1) equatorial bond lengths (2.224(2)Å) a feature which is similar to the previously reported cyclohexyl analogues.[7]

Figure 5.3. Molecular structure and atom numbering scheme for $Sn[Me_3SiNC(Me)NSiMe_3]_2$ (**4**). Hydrogen atoms have been omitted for clarity. Thermal ellipsoids are drawn at 30% probability.

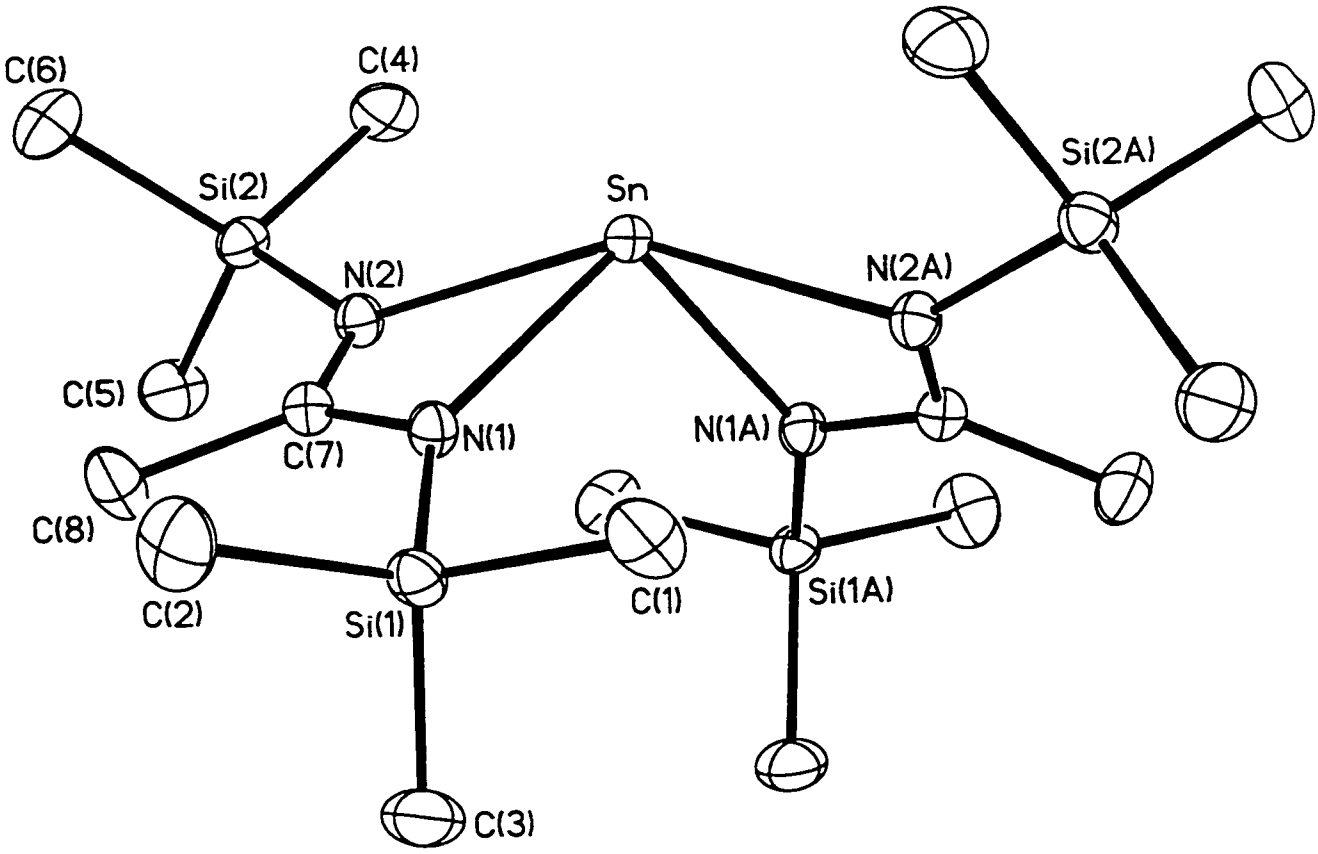

A comparison of the angles around the amidinate N atoms of **4** with those of **2**, **3**, and [(CyNC(^{t}Bu)NCy)Sn[N(SiMe$_3$)$_2$] is provided in Chart 5.1. These data clearly indicate the decreased steric demands of [Me$_3$SiNC(Me)NSiMe$_3$]$^-$ relative to the ^{t}Bu analogue and place this species as even more svelte than (CyNC(^{t}Bu)NCy)$^-$.

Chart 5.1

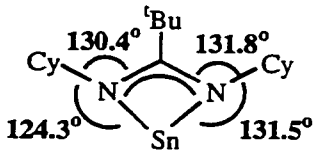

[CyNC(^{t}Bu)NCy]Sn[N(SiMe$_3$)$_2$]

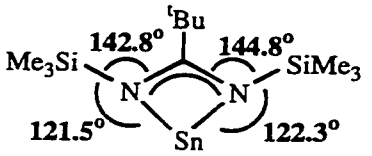

[Me$_3$SiNC(^{t}Bu)NSiMe$_3$]Sn[N(SiMe$_3$)$_2$]
2

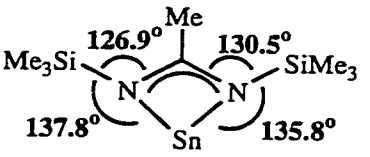

[Me$_3$SiNC(Me)NSiMe$_3$]$_2$Sn
4

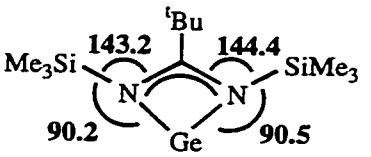

[Me$_3$SiNC(^{t}Bu)NSiMe$_3$]Ge[N(SiMe$_3$)$_2$]
3

Conclusions

The bulky amidinate [Me$_3$SiNC(^{t}Bu)NSiMe$_3$]$^-$ has been used in the preparation of novel mixed ligand Sn(II) and Ge(II) species. A rearrangement of this ligand via trimethylsilyl migration and nitrile elimination generates a bis(trimethylsilyl)amido ligand and provides ultimate products with the formulas [Me$_3$SiNC(^{t}Bu)NSiMe$_3$]M[NSiMe$_3$]. The propensity for this rearrangement is dependent on reaction solvent and on the

coordinated metal center. Furthermore, the isolation of $[Me_3SiNC(Me)NSiMe_3]_2Sn$ (**4**) indicates that steric factors also play a role in the stability of $[Me_3SiNC(^tBu)NSiMe_3]^-$.

These complexes exhibit catalytic activity toward the cyclotrimerization and cyclodimerization of isocyanates and represent unique catalysts for these transformations. This topic will be the focus of Chapter Six.

Experimental for Chapter Five

General Procedure. All reactions were carried out either in a nitrogen filled drybox or under nitrogen with standard Schlenk-line techniques. Diethyl ether, hexane and THF were distilled under nitrogen from potassium. Deuterated benzene was dried with potassium. MeLi (1.4 M in diethyl ether), ^{t}BuLi (1.7 M in hexane), $SnCl_2$ (99.99+%), 1,3-bis(trimethylsilyl)carbodiimide were purchased from Aldrich and used without further purification. $GeCl_2$(dioxane) was prepared according to a literature procedure.[8] NMR spectra were run on a GEMINI 200 MHz spectrometer with deuterated benzene as a solvent and internal standard. Variable temperature NMR spectra were run on a Brüker 500 MHz spectrometer.

[$Me_3SiNC(^{t}Bu)NSiMe_3$]Sn[$N(SiMe_3)_2$] (2). To a solution of bis(trimethylsilyl)carbodiimide (0.300g, 1.61mmol) in diethyl ether (30ml) was added ^{t}BuLi (0.95ml, 1.7M, 1.62mmol). After 30 min, 0.5 equiv of $SnCl_2$ (0.153g, 0.81mmol) was added. The solution was stirred for 12 h and filtered to remove the white LiCl precipitate. The solvent was removed under vacuum to give a pure off white powder (0.350g, 83% yield). mp 59-60°C. ^{1}H NMR (C_6D_6, ppm) : 1.04 (s, ^{t}Bu, 9H); 0.44 (s, $Si(CH_3)_3$, 18H); 0.31 (s, $Si(CH_3)_3$, 18H). ^{13}C NMR (C_6D_6, ppm) : 183.9 (s, N$\underline{C}(^{t}Bu)$N); 42.7 (s, $\underline{C}CH_3$); 29.3 (s, C$\underline{C}H_3$); 6.3 (s, $Si(CH_3)_3$); 3.7 (s, $Si(CH_3)_3$). Analysis Calcd for $C_{17}H_{45}N_3Si_4Sn$ C 39.07; H 8.68; N 8.04. Found C C 39.04; H 8.66;N 7.80.

[$Me_3SiNC(^tBu)NSiMe_3$]Ge[$N(SiMe_3)_2$] (3). To a solution of bis(trimethylsilyl)carbodiimide (0.500g, 2.68mmol) in diethyl ether (35ml) was added ^{t}BuLi (1.58ml, 1.7M, 2.69mmol). After 30 min, 0.5 equiv of $GeCl_2$(dioxane) (0.311g, 1.34mmol) was added. The solution was stirred for 12 h and filtered to remove the white LiCl precipitate. The solvent was removed under vacuum to give a white powder. Crystals were obtained from diethyl ether at –34°C (0.518g, 81% yield). ^{1}H NMR (C_6D_6, ppm, 230°K) : 1.01 (s, ^{t}Bu, 9H); 0.36 (s, $Si(CH_3)_3$, 18H); 0.58 (s, $Si(CH_3)_3$, 9H); 0.39 (s, $Si(CH_3)_3$, 9H). ^{13}C NMR (C_6D_6, ppm, 230°K) : 181.0 (s, N$\underline{C}$(^{t}Bu)N); 40.1 (s, $\underline{C}CH_3$); 28.9 (s, C$\underline{C}H_3$); 2.9 (s, $Si(CH_3)_3$) ; 5.8 (s, $Si(CH_3)_3$); 5.3 (s, $Si(CH_3)_3$). Analysis Calcd for $C_{17}H_{45}N_3Si_4Ge$ C 42.85; H 9.52; N 8.82. Found C 42.68; H 9.55;N 8.86.

Sn[$Me_3SiNC(Me)NSiMe_3$]$_2$ (4). To a solution of bis(trimethylsilyl)carbodiimide (0.500g, 2.68mmol) in diethyl ether (35ml) was added MeLi (1.90ml, 1.4M, 2.66mmol). After 30 min, 0.5 equiv of $SnCl_2$ (0.254g, 1.34mmol) was added. The solution was stirred for 12 h and filtered to remove the white LiCl precipitate. The solvent was removed under vacuum to give a pale yellow powder. Crystals were obtained from diethyl ether at –34°C (0.370g, 53% yield). mp 90°C(dec). ^{1}H NMR (C_6D_6, ppm) : 1.80 (s, Me, 3H); 0.24 (s, $Si(CH_3)_3$, 18H). ^{13}C NMR (C_6D_6, ppm) : 176.0 (s, N$\underline{C}$(Me)N); 28.3 (s, Me); 2.5 (s, $Si(CH_3)_3$). Attempts to obtain satisfactory microanalysis data for this compound have so far been unsuccessful.

Attempted reaction of Sn[$N(SiMe_3)_2$]$_2$ with ^{t}BuCN. To a solution of 0.160g (0.36mmol) of Sn[$N(SiMe_3)_2$]$_2$ in 5ml ether was added 0.060g (0.81mmol) of ^{t}BuCN.

The reaction mixture was stirred for 24 hr at room temperature. Removal of solvent under vacuum and isolation of the resultant solid yielded starting material as confirmed by ^{1}H and ^{13}C NMR. A similar reaction with 0.060g (0.14mmol) of $Sm[N(SiMe_3)_2]_2$ and 0.023g (0.31mmol) of $^{t}BuCN$ in 0.5ml C_6D_6 was carried out at 80°C. No spectral changes were observed over 24 hours.

Data Tables for Chapter Five

Table 5.1. Crystal data for compounds $[Me_3SiNC(^tBu)NSiMe_3]Sn[N(SiMe_3)_2]$ (**2**), $[Me_3SiNC(^tBu)NSiMe_3]Ge[N(SiMe_3)_2]$ (**3**), and $Sn[Me_3SiNC(Me)NSiMe_3]_2$ (**4**).

	2	**3**	**4**
Empirical formula	$C_{17}H_{45}N_3Si_4Sn$	$C_{17}H_{45}N_3Si_4Ge$	$C_{16}H_{42}N_4Si_4Sn$
Formula weight	522.59	476.51	521.59
Temperature (K)	113(1)	203(2)	203(2)
λ (Å)	0.71073	0.71073	0.71073
Space group	$P2_1/c$	$P2_1/n$	Pbcn
Unit cell dimensions (Å, deg)	a = 15.071(1) b = 10.712(1) c = 18.290(1) β = 112.12(1)	a = 14.791(1) b = 10.176(1) c = 19.542(2) β = 111.806(1)	a = 10.998(1) b = 12.154(1) c = 20.084(2)
Volume ($Å^3$)	2735.4(8)	2730.9(4)	2684.6(4)
Z	4	4	4
Density (Mg/m^3) (calculated)	1.269	1.159	1.290
Absorption coefficient (mm^{-1})	1.12	1.304	1.138
R (F_o)	0.042	0.0442	0.0362
R_w (F_o^2)	0.060	0.0886	0.0975

$$R1 = \sum \| F_o | - | F_c \| / \sum | F_o |. \quad wR2 = \left(\sum w (| F_o | - | F_c |)^2 / \sum w | F_o |^2 \right)^{1/2}$$

Table 5.2. Selected bond lengths [Å] and angles [deg] for $[Me_3SiNC(^tBu)NSiMe_3]Sn[NSiMe_3]_2$ (**2**)

Distances			
Sn-N(1)	2.236(4)	Si(2)-C(11)	1.855(7)
Sn-N(2)	2.221(4)	Si(2)-C(9)	1.861(7)
Sn-N(3)	2.121(5)	Si(2)-C(10)	1.858(7)
Si(1)-N(1)	1.748(5)	Si(4)-N(3)	1.739(5)
Si(1)-C(8)	1.850(7)	Si(4)-C(17)	1.864(7)
Si(1)-C(6)	1.862(7)	Si(4)-C(15)	1.868(7)
Si(1)-C(7)	1.878(6)	Si(4)-C(16)	1.858(7)
Si(3)-N(3)	1.726(5)	N(1)-C(1)	1.331(7)
Si(3)-C(13)	1.878(7)	N(2)-C(1)	1.355(7)
Si(3)-C(12)	1.861(7)	C(1)-C(2)	1.534(8)
Si(3)-C(14)	1.860(7)	C(2)-C(5)	1.520(9)
Si(2)-N(2)	1.730(5)	C(2)-C(4)	1.532(8)
		C(2)-C(3)	1.534(8)

Angles			
N(1)-Sn-N(2)	60.6(2)	N(3)-Si(4)-C(16)	110.9(3)
N(1)-Sn-N(3)	103.9(2)	C(17)-Si(4)-C(15)	104.6(3)
N(2)-Sn-N(3)	99.0(2)	C(17)-Si(4)-C(16)	107.6(3)
N(1)-Si(1)-C(8)	114.6(3)	C(15)-Si(4)-C(16)	106.4(3)
N(1)-Si(1)-C(6)	113.6(3)	C(1)-N(1)-Si(1)	142.8(4)
N(1)-Si(1)-C(7)	104.5(3)	C(1)-N(1)-Sn	92.6(3)
C(8)-Si(1)-C(6)	110.6(3)	Si(1)-N(1)-Sn	121.5(2)
C(8)-Si(1)-C(7)	107.2(3)	C(1)-N(2)-Si(2)	144.8(4)
C(6)-Si(1)-C(7)	105.5(3)	C(1)-N(2)-Sn	92.6(3)
N(3)-Si(3)-C(13)	111.8(3)	Si(2)-N(2)-Sn	122.3(2)
N(3)-Si(3)-C(12)	112.5(3)	Si(3)-N(3)-Si(4)	120.1(3)
N(3)-Si(3)-C(14)	112.2(3)	Si(3)-N(3)-Sn	113.5(2)
C(13)-Si(3)-C(12)	105.7(3)	Si(4)-N(3)-Sn	126.1(2)
C(13)-Si(3)-C(14)	108.8(3)	N(1)-C(1)-N(2)	113.6(5)
C(12)-Si(3)-C(14)	105.4(3)	N(1)-C(1)-C(2)	125.1(5)
N(2)-Si(2)-C(11)	116.1(3)	N(2)-C(1)-C(2)	121.3(5)
N(2)-Si(2)-C(9)	113.2(3)	C(1)-C(2)-C(5)	111.0(5)
N(2)-Si(2)-C(10)	104.4(3)	C(1)-C(2)-C(4)	108.0(5)
C(11)-Si(2)-C(9)	110.4(3)	C(1)-C(2)-C(3)	111.8(5)
C(11)-Si(2)-C(10)	105.8(3)	C(5)-C(2)-C(4)	110.1(5)
C(9)-Si(2)-C(10)	105.8(3)	C(5)-C(2)-C(3)	107.1(5)
N(3)-Si(4)-C(17)	114.1(3)	C(4)-C(2)-C(3)	108.8(5)
N(3)-Si(4)-C(15)	112.7(3)		

Table 5.3. Selected bond lengths [Å] and angles [deg] for $[Me_3SiNC(^tBu)NSiMe_3]Ge[NSiMe_3]_2$ (**3**)

Distances			
Ge-N(3)	1.9101(19)	Si(3)-C(14)	1.857(3)
Ge-N(1)	2.037(2)	Si(3)-C(13)	1.870(3)
Ge-N(2)	2.042(2)	Si(3)-C(12)	1.868(3)
Ge-C(7)	2.445(2)	Si(4)-N(3)	1.740(2)
Si(1)-N(1)	1.745(2)	Si(4)-C(17)	1.871(3)
Si(1)-C(1)	1.853(3)	Si(4)-C(16)	1.870(3)
Si(1)-C(2)	1.864(3)	Si(4)-C(15)	1.874(3)
Si(1)-C(3)	1.866(3)	N(1)-C(7)	1.334(3)
Si(2)-N(2)	1.749(2)	N(2)-C(7)	1.338(3)
Si(2)-C(4)	1.858(3)	C(7)-C(8)	1.533(3)
Si(2)-C(6)	1.858(3)	C(8)-C(9)	1.532(4)
Si(2)-C(5)	1.867(3)	C(8)-C(11)	1.537(4)
Si(3)-N(3)	1.743(2)	C(8)-C(10)	1.540(4)

Angles			
N(3)-Ge-N(1)	104.84(8)	C(17)-Si(4)-C(16)	105.86(16)
N(3)-Ge-N(2)	104.96(8)	N(3)-Si(4)-C(15)	112.03(13)
N(1)-Ge-N(2)	65.65(8)	C(17)-Si(4)-C(15)	105.94(16)
N(3)-Ge-C(7)	112.61(8)	C(16)-Si(4)-C(15)	107.80(16)
N(1)-Ge-C(7)	33.08(8)	C(7)-N(1)-Si(1)	144.41(18)
N(2)-Ge-C(7)	33.19(8)	C(7)-N(1)-Ge	90.49(15)
N(1)-Si(1)-C(1)	104.13(12)	Si(1)-N(1)-Ge	122.50(11)
N(1)-Si(1)-C(2)	114.02(14)	C(7)-N(2)-Si(2)	143.17(18)
C(1)-Si(1)-C(2)	106.96(16)	C(7)-N(2)-Ge	90.18(15)
N(1)-Si(1)-C(3)	114.24(14)	Si(2)-N(2)-Ge	121.29(11)
C(1)-Si(1)-C(3)	107.89(15)	Si(4)-N(3)-Si(3)	120.07(11)
C(2)-Si(1)-C(3)	109.06(17)	Si(4)-N(3)-Ge	112.46(10)
N(2)-Si(2)-C(4)	104.81(12)	Si(3)-N(3)-Ge	127.24(11)
N(2)-Si(2)-C(6)	112.61(13)	N(1)-C(7)-N(2)	111.6(2)
C(4)-Si(2)-C(6)	107.25(15)	N(1)-C(7)-C(8)	123.8(2)
N(2)-Si(2)-C(5)	114.30(13)	N(2)-C(7)-C(8)	124.4(2)
C(4)-Si(2)-C(5)	107.82(14)	N(1)-C(7)-Ge	56.43(12)
C(6)-Si(2)-C(5)	109.60(16)	N(2)-C(7)-Ge	56.64(12)
N(3)-Si(3)-C(14)	114.35(12)	C(8)-C(7)-Ge	166.10(17)
N(3)-Si(3)-C(13)	111.97(13)	C(9)-C(8)-C(7)	111.9(2)
C(14)-Si(3)-C(13)	107.00(17)	C(9)-C(8)-C(11)	107.5(2)
N(3)-Si(3)-C(12)	111.89(13)	C(7)-C(8)-C(11)	110.4(2)
C(14)-Si(3)-C(12)	104.57(16)	C(9)-C(8)-C(10)	109.5(2)
C(13)-Si(3)-C(12)	106.47(15)	C(7)-C(8)-C(10)	107.9(2)
N(3)-Si(4)-C(17)	111.94(12)	C(11)-C(8)-C(10)	109.6(2)
N(3)-Si(4)-C(16)	112.81(13)		

Table 5.4. Selected bond lengths [Å] and angles [deg] for $Sn[Me_3SiNC(Me)NSiMe_3]_2$ (**4**).

Distances			
Sn-N(1A)	2.224(2)	Si(1)-C(2)	1.870(3)
Sn-N(1)	2.224(2)	Si(2)-N(2)	1.734(2)
Sn-N(2A)	2.397(2)	Si(2)-C(4)	1.858(3)
Sn-N(2)	2.397(2)	Si(2)-C(5)	1.866(4)
Si(1)-N(1)	1.740(2)	Si(2)-C(6)	1.868(4)
Si(1)-C(1)	1.856(3)	N(1)-C(7)	1.345(4)
Si(1)-C(3)	1.866(3)	N(2)-C(7)	1.317(4)
		C(7)-C(8)	1.508(4)

Angles			
N(1A)-Sn-N(1)	95.36(12)	C(4)-Si(2)-C(5)	108.68(17)
N(1A)-Sn-N(2A)	158.63(8)	N(2)-Si(2)-C(6)	111.89(15)
N(1)-Sn-N(2A)	99.15(8)	C(4)-Si(2)-C(6)	108.71(18)
N(1A)-Sn-N(2)	99.15(8)	C(5)-Si(2)-C(6)	108.18(18)
N(1)-Sn-N(2)	58.63(8)	C(7)-N(1)-Si(1)	126.93(19)
N(2A)-Sn-N(2)	148.84(11)	C(7)-N(1)-Sn	95.26(17)
N(1)-Si(1)-C(1)	107.91(13)	Si(1)-N(1)-Sn	137.80(13)
N(1)-Si(1)-C(3)	110.23(15)	C(7)-N(2)-Si(2)	130.5(2)
C(1)-Si(1)-C(3)	108.58(18)	C(7)-N(2)-Sn	88.38(17)
N(1)-Si(1)-C(2)	113.11(15)	Si(2)-N(2)-Sn	135.83(13)
C(1)-Si(1)-C(2)	107.61(18)	N(2)-C(7)-N(1)	116.8(2)
C(3)-Si(1)-C(2)	109.26(18)	N(2)-C(7)-C(8)	122.2(3)
N(2)-Si(2)-C(4)	105.93(14)	N(1)-C(7)-C(8)	120.9(3)
N(2)-Si(2)-C(5)	113.32(15)		

References for Chapter Five

(1) Zhou, Y.; Richeson, D. S. *Inorg. Chem.* **1996**, *35*, 2448.

(2) Zhou, Y.; Richeson, D. S. *Inorg. Chem.* **1997**, *36*, 501.

(3) Coles, M.P.; Swenson, D.C.; Jordan, R.F.; Young V.G. *Organometallics* **1997**, *16*, 5183.

(4) Foley, S. R.; Yap, G. P. A.;Richeson, D. S. *Organometallics* **1999**, *18*, 4700

(5) Edelmann, F.T. *Coord. Chem Rev.* **1994**, *137*, 403

(6) Pauling, L. *The Nature of the Chemical Bond*, Cornell University Press: Ithaca, NY, 1960, p.224.

(7) Zhou, Y.; Richeson, D.S. *J. Am. Chem. Soc.* **1996**, *118*, 10850

(8) Fjeldberg, T.; Haaland, A.; Schilling, B. E. R.; Lappert, M. F.; Thorne, A. J. *J. Chem. Soc., Dalton Trans.* **1986**, 1551.

Active Catalysts for the Trimerization of Isocyanates

'But you gotta ask yourself...'

Chapter Six

Introduction

Isocyanates are highly unsaturated functionalities with the general formula R-N=C=O. They exhibit a high degree of reactivity and undergo a myriad of molecular transformations. For example, they react with alcohols to form urethanes and with amines to form substituted ureas. Chain propagation of these two reactions leads to the corresponding polyurethanes and polyureas. In addition, a number of reactions may take place depending the presence of different kinds of catalysts. The type of catalyst influences the formation of various types of reaction products such as the formation of allophanates (reactions between urethanes and isocyanates), biuret (reaction between substituted ureas and isocyanates), carbodiimides, uretidinediones (dimerization of isocyanates) and isocyanurates (trimerization of isocyanates). Isocyanates can also be polymerized to form 1-nylon. These reactions are illustrated in Scheme 6.1.[1,2] The focus of this chapter is on one specific transformation of isocyanates: the catalytic trimerization of isocyanates to isocyanurates.

Applications of Isocyanurates

Triaryl isocyanurates are catalysts for the continuous anionic polymerization of ε-caprolactam to nylon-6 (eq 6.1).[3] Impure isocyanurates adversely affect the quality of nylon-6, therefore efficient routes to high purity compounds are often desired.

Scheme 6.1

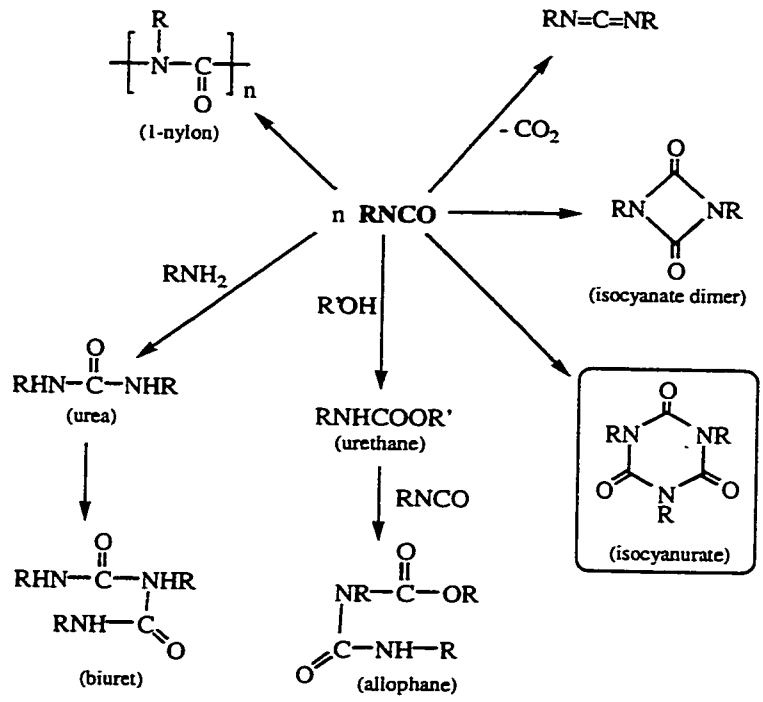

An important use of isocyanurates is in the production of urethane-modified isocyanurate foams. In addition to urethane, polyurethane contains other groups such as allophanates, biurets, or isocyanurates. Unlike allophanate or biuret cross-links in modified polyurethanes, the thermal and hydrolytic stabilities of isocyanurate crosslinks are very high. This is due to the thermal, hydrolytic, and chemical stability of the isocyanurates themselves. Isocyanurates are stable up to 400°C and thus serve as excellent crosslinking agents in the modification of polyurethane foams.[4,5]

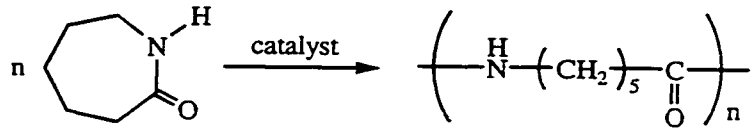

(6.1)

A search through the literature reveals that research on the applications of isocyanurates is firmly entrenched in the domains of patents. For example, triallyl isocyanurates are used to make polymers in the preparation of flame-retardant laminating materials for electrical devices.[6] They are also used in the production of co-polymer resins that are water-resistant, transparent and impact-resistant.[7] In general, isocyanurates are being widely used in the modification of polymers. The polymeric products have high thermal stability, good radiation resistance, good mechanical strength, high chemical and thermal resistance as well as reduced toxicity.[8]

Formation of Isocyanurates

Isocyanurates (i.e. hexahydro-1,3,5-triazine-2,4,6-trione) are formed by the cyclotrimerization of isocyanates according to eq 6.2.

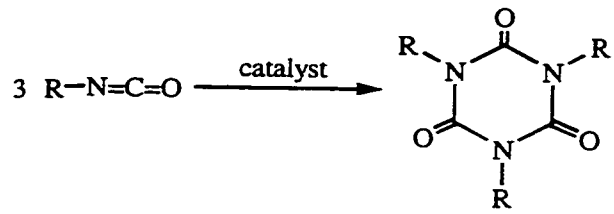

(6.2)

Since isocyanurates have been known to improve polyurethanes, a number of catalysts have been reported with the conventional catalysts being anions or neutral Lewis bases such as acid salts and tertiary amines.[9,10,11,12,13,14,15] However, some metal-based systems have been described and a Lewis acid pathway could be envisioned for these systems.[16] Conventional catalysts for isocyanurate formation suffer from low activity necessitating severe conditions, poor selectivity resulting in by-products such as dimers or carbodiimides, and difficulty in separating the catalysts from the product.

Tertiary amines can act as catalysts in the formation of isocyanurates. The catalytic efficiency of tertiary amines generally increases as the basicity of the amine increases and the steric shielding decreases. Urethanes are produced as by-products as the reactions are performed in alcohol-based solvent systems.[17]

Trialkyltin alkoxides trimerize isocyanates in good yields however, reaction times of up to 25 days are required (Table 6.1).[18]

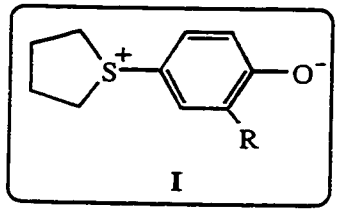

I

Cyclic sulfonium zwitterions of the general formula **I** are active catalysts for cyclotrimerization. The products are cyclic dimers and trimers as well as low molecular weight polymers.[19]

Alkoxyallenes of type **II** were found to catalyze the cyclotrimerization of phenyl isocyanates (Table 6.1). Varying the R group of **II** had little effect. The reactivity was

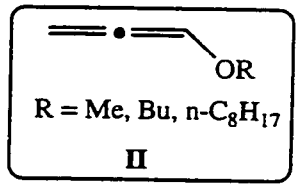

II

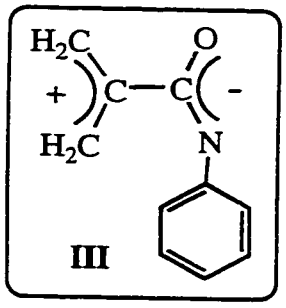

III

proposed to be due to the formation of a stable zwitterionic intermediate of type **III** in the reaction with phenyl isocyanate. Unfortunately, the spontaneous copolymerization of **II** with the isocyanate occurs concurrently with the formation of isocyanurate.[12]

Fluoride salts also serve as catalysts for the trimerization of aromatic isocyanates (Table 6.1). CsF demonstrated high reactivity but on the other hand, KF showed very low activity. It was suggested that CsF is more active because the fluoride anion interacts more loosely with the counterion.[11]

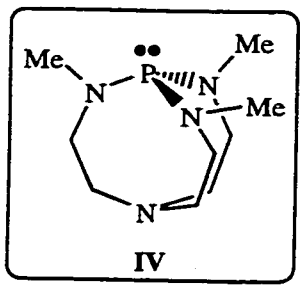

IV

An excellent catalyst is the phosphine superbase **IV** (Table 6.1). The reaction was proposed to proceed through the formation of the zwitterionic intermediate **V**. To date, **IV** is the most effective catalyst discovered for the conversion of isocyanates to isocyanurates.[9,10]

In Chapter four we described the synthesis of cyclic tin and germanium tetrasulfido complexes derived from the oxidation of (alkylamidinato)(amido)M(II) species with elemental sulfur. In Chapter five, we described the synthesis of (alkylamidinato)(amido)M(II) species derived from the rearrangement of the $[Me_3SiNC(^tBu)NSiMe_3]^-$ anion. These novel compounds function as outstanding catalysts for the rapid and selective catalytic cyclotrimerization of aryl isocyanates to yield isocyanurates.

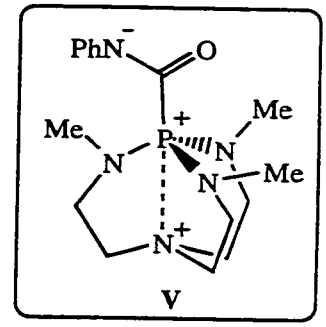

V

Results and Discussion

In an attempt to trap the presumed terminal sulfido intermediate in the reaction of **1** or **2** with PPh_3 using aryl isocyanates (Chapter four), we discovered that the tetrasulfido complexes **1** and **2** are outstanding catalysts for the cyclotrimerization of aryl isocyanates to yield triaryl isocyanurates (eq. 6.3). To our knowledge, this chapter constitutes the first application of a Sn(II) species or Ge(II/IV) in this reaction.

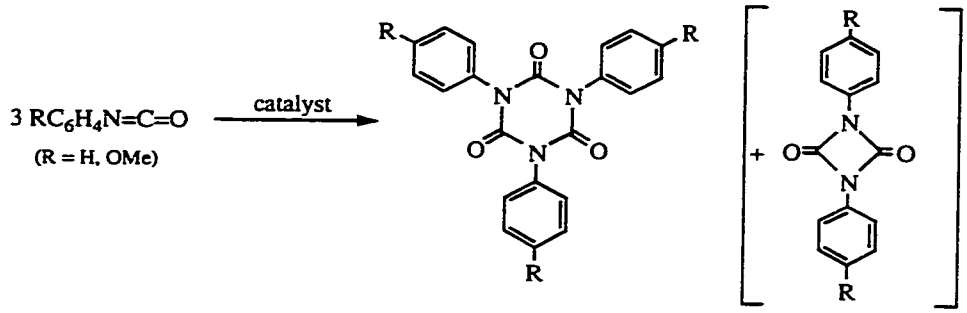

(6.3)

As described previously, conventional catalysts for isocyanurate formation suffer from low activity, poor selectivity, and difficulty in separating the catalysts from the product. Our catalyst system appears to address these difficulties.

Table 6.1. Data for the Cyclotrimerization of Aryl Isocyanates to yield Triarylisocyanurates[a]

Catalyst	Substrate	Time (min.)	Isolated yield (%)	Ref.
1	C_6H_5NCO	12	95	----
1	p-$MeOC_6H_4NCO$	14	95	----
2	C_6H_5NCO	60	68	----
2	p-$MeOC_6H_4NCO$	90	77	----
3	C_6H_5NCO	30 sec	75	----
4	C_6H_5NCO	120	93	----
5	C_6H_5NCO	210	94	----
6	C_6H_5NCO	16	98	----
7	C_6H_5NCO	10	35 (52% dimer)	----
$P(MeNCH_2CH_2)_3N$	C_6H_5NCO	2	94	10
$P(MeNCH_2CH_2)_3N$	p-$MeOC_6H_4NCO$	5	94	10
CsF	C_6H_5NCO	20	80.2 (8.8% dimer)	11
KF	C_6H_5NCO	20	1.4	11
Bu_3SnO	C_6H_5NCO	12 days	"good"	17
$H_2C{=}C{=}C(H)OMe$	C_6H_5NCO	24 hr	72	12
NEt_3	C_6H_5NCO	20	0	9
AcOK	C_6H_5NCO	20	0	

[a] All reactions carried out in neat isocyanate at room temperature.

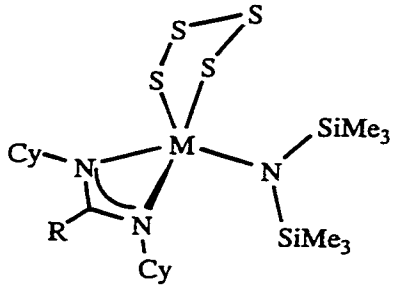

1 M = Sn; R = Me
2 M = Sn; R = ^{t}Bu
3 M = Ge; R = Me

The catalytic activity of Sn(IV) species **1** and **2** is superior to or comparable to literature species (Table 6.1). The tetrasulfido complex **1** catalyzes the trimerization of phenyl isocyanate quantitatively and purely within minutes of addition of complex to neat isocyanate. For example, with 2 mol % catalyst a 95% isolated yield of pure triphenyl isocyanurate is obtained within 12 minutes at room temperature. In fact, the purity offered by our system permitted the isolation of single crystals of isocyanurate when the reaction was carried out in benzene thus allowing for a structural determination of $(PhNCO)_3$ (Figure 6.1 and Table 6.2). Selected bond distances and angles are given in Table 6.3. It is worthwhile to note that increasing the steric bulk of the catalyst in going from **1** to **2** (from Me to ^{t}Bu on the bridgehead position of the amidinate) results in a decrease in both the rate and yield for the reaction.

A comparison with both conventional and recently reported catalysts is provided by Table 6.1. In particular it is notable that under similar experimental conditions, triethylamine and potassium acetate, commonly employed catalysts, are inactive toward triphenyl isocyanurate production. Only the phosphine superbase, $P(MeNCH_2CH_2)_3N$, gives a comparable performance to the tin tetrasulfido species.

The germanium tetrasulfido species **3** is even more active than its tin analogue where catalysis of PhNCO is complete in under 30 seconds however the yield for the reaction is only a reasonable 75%. The germanium tetrasulfido species has a high enough

activity to cyclotrimerize even alkyl isocyanates, albeit poorly. With 2 mol % catalyst, a 24% isolated yield of pure triethyl isocyanurate is obtained after 8 days at room temperature. Triethylisocyanurate slowly precipitates out of the neat solution as single crystals allowing for a structural determination of $(EtNCO)_3$ (Figure 6.2 and Table 6.2). Selected bond distances and angles are given in Table 6.4.

The tetrasulfido catalysts can be recycled without apparent loss of activity. When an active catalyst system was probed by ^1H NMR only the starting amidinate SnS_4 complex (**1** or **2**) was observed, no by-products were evident and no degradation of the starting material was noticed.

The superior catalytic nature of **1** and **2** is reflected in their ability to readily trimerize aryl isocyanates with electron donating substituents. An electron donating group on the aromatic ring of an aryl isocyanate renders the carbonyl less electrophilic, and thus more difficult to trimerize. In the case of para-methoxyphenyl isocyanate, a substrate which is noted for its reduced reactivity and difficulty in generating the corresponding isocyanurate, complex **1** displayed essentially no decrease in reactivity and produced $[p\text{-}MeO(C_6H_4)NCO]_3$ in 95% isolated yield within 14 min. at room temperature.

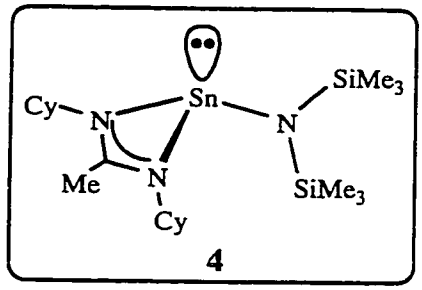

4

A comparison of the Sn(IV) catalyst **1** to its Sn(II) precursor **4** would be instructive in attempting to understand the role of the oxidation state of the metal as well as that of the tetrasulfide moiety to help elucidate a possible mechanism. Catalyst **4** effectively trimerizes

PhNCO in quantitative yields however the rate greatly decreases resulting in fifty turnovers of monomer in 120 minutes in comparison to 12 minutes for catalyst **1**.

We have discerned that amidinate complexes of germanium and tin are outstanding catalysts for the cyclotrimerization of arylisocyanates. In an effort to elucidate the generality of this observation and the features which dictate the activity and selectivity in this reaction we extended the complexes employed in this reaction to include the (alkylamidinato)(amido)M(II) species **5**, **6** and **7** derived from the rearrangement of the $[Me_3SiNC(^tBu)NSiMe_3]^-$ anion as seen in chapter five.

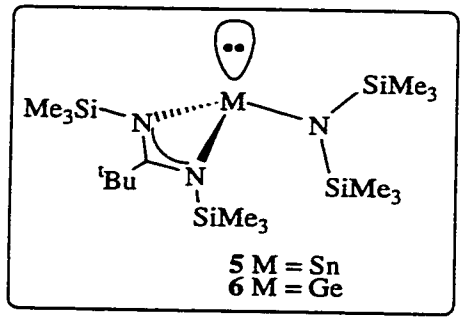

5 M = Sn
6 M = Ge

The catalytic activity of species **5-7** is presented in Table 6.1. From these data it is clear that these complexes also exhibit catalytic activity that is superior or comparable to known catalysts. For example, in the presence of 50 equivalents of isocyanate (2 mol % catalyst), Ge(II) complex **6** generates a 98% isolated yield of pure triphenyl isocyanurate within 16 minutes at room temperature. These results place this complex as one of the most active and selective species reported to catalyze Equation 6.3.

A comparison of the Sn(IV) catalyst, $[CyNC(Me)NCy]Sn[N(SiMe_3)_2]S_4$, and the Sn(II) complexes **5** and **7** is informative. While these species exhibited comparable selectivity to the Sn(IV) compound they have substantially slower reaction rates. Similarly, **5** is also much less active than the analogous Ge(II) species **6**. These two observations suggest that the Lewis acidity of the metal center plays a role in the activity of these complexes.

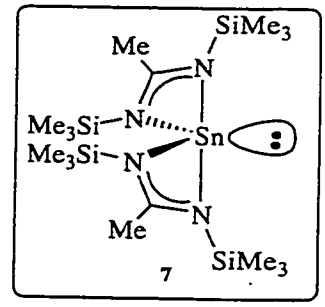

7

The metal coordination environment also appears to be a factor in the selectivity of isocyanurate formation. Our results indicate the complexes **5** and **7** exhibit a high degree of selectivity in generating only isocyanurate (95-98% yield). In contrast, the bis(amidinate) Sn(II) complex **4,** while quite active in reaction with phenylisocyanate, displayed a selectivity for the formation of phenylisocyanate dimer (Equation 6.3) with an approximate 2:3 ratio of trimer:dimer formation.

The mechanism for this catalytic transformation is a current point of contention. The possibility of a Lewis acid-based pathway may be supported by our preliminary observation that other Sn amidinate and amido complexes are effective albeit inferior isocyanurate trimerization catalysts.

Conclusion

Cyclic tin and germanium tetrasulfido complexes as well as M(II) complexes are interesting and very effective catalysts for isocyanate trimerization. Our findings suggest that increased steric bulk about the catalyst decreases reactivity. Moving from tin to the more electronegative germanium results in a more active catalyst. The oxidation state also appears to effect reactivity, with higher (thus more electrophilic) oxidation states being preferred. Finally, coordination geometry appears to effect selectivity. Four coordinate complexes might have a preference to form dimers over trimers, while three and five coordinate complexes form exclusively trimers.

These results add to our mechanistic investigation of this transformation and provide some evidence for a Lewis acid pathway and for the role of the metal coordination environment in dimer/trimer selectivity.

Experimental for Chapter Six

Typical Procedure for the Catalytic Formation of $(PhNCO)_3$. To complex **1** (0.200g, 0.318mmol) was added neat phenyl isocyanate (50eq., 1.890g, 15.9mmol). A crystalline white solid precipitated out of the yellow solution. After 12 min., the white solid was crushed into a powder and washed with 7ml of benzene for 5 repetitions, filtered and dried in vacuo to give 1.80g (95.2% yield) of $(PhNCO)_3$. ^1H NMR ($CDCl_3$, ppm) : 7.41-7.56 (m, C_6H_5). Anal. Calcd for $C_{21}H_{15}N_3O_3$: C 70.59; H 4.20; N 11.76. Found: C 70.80; H 4.50; N 11.50. mp : 281.6-282.1°C (lit. mp. 281.0-281.5°C). X-ray structural analysis confirmed the identity of this compound. Catalyst **3** was isolated by extraction with benzene and the reaction with phenyl isocyanate was repeated with a 93% yield of $(PhNCO)_3$.

$(p\text{-}MeOC_6H_4NCO)_3$ from 1. To complex **1** (0.025g, 0.040mmol) was added neat *para*-methoxyphenyl isocyanate (50eq., 0.296g, 2.00mmol). A crystalline white solid precipitated out of the yellow solution. After 14 min., the white solid was crushed into a powder and washed with 5ml of benzene for 5 repetitions, filtered and dried in vacuo to give 0.281g (95% yield) of $(p\text{-}OMePhNCO)_3$. ^1H NMR ($CDCl_3$, ppm) : 3.70 (s, 9H, OCH_3), 6.85 (d, 6H, C_6H_4; $^3J_{HH} = 9.2Hz$), 7.16 (d, 6H, C_6H_4; $^3J_{HH} = 9.2Hz$). mp : 258-259°C (lit. mp. 261°C).

Reaction of 4 with PhNCO to Yield $(PhNCO)_3$ and $(PhNCO)_2$. To complex **4** (0.034g, 0.065mmol) was added neat phenylisocyanate (50eq., 0.440g, 3.70mmol). After 10 min.

the reaction mixture solidified. The resultant white solid was crushed into a powder and extracted with ether. The remaining solid (0.154g, 35% yield) was identified as $(PhNCO)_3$ by comparison with authentic material. The extracts were combined, dried in vacuo and further washed with 5ml of benzene for 5 repetitions, filtered and dried to give 0.228g (52% yield) of $(PhNCO)_2$. The identity of $(PhNCO)_2$ was confirmed by comparison of m.p., ^1H NMR spectra[9] and unit cell parameters with literature values.[20]

Molecular Structures and Data Tables for Chapter Six

Table 6.2. Crystallographic Data for triphenylisocyanurate and triethylisocyanurate

Compound	**PhNCO**	**EtNCO**
Empirical formula	$C_{27}H_{21}N_3O_3$	$C_9H_{15}N_3O_3$
Formula weight	435.47	213.24
Temperature (K)	203(2)	203(2)
Wavelength Å	0.71073	0.71073
Crystal system,	Monoclinic	Orthrhombic
Space Group	C2/c	P2(1)2(1)2(1)
Unit cell dimensions (Å) (deg)	a =13.882(2) b =13.666(2) c =12.630(2) β =96.512(3)	a =7.856(3) b =8.183(3) c =16.852(60 β =90
Volume ($Å^3$) Z	2380.7(7) 4	1084.6(6) 4
Density(calc.) (Mg/m^3)	1.215	1.306
Absorption coefficient (mm^{-1})	0.081	0.099
Goodness-of-fit on F^2	1.031	1.022
Final R indices [I>2σ(I)]	R1 = 0.0685, wR2 = 0.1774	R1 = 0.0471, wR2 = 0.0977
R indices (all data)	R1 = 0.1305, wR2 = 0.1955	R1 = 0.0614, wR2 = 0.1004

$$R1 = \sum \| F_o | - | F_c \| / \sum | F_o |. \quad wR2 = \left(\sum w (| F_o | - | F_c |)^2 / \sum w | F_o |^2 \right)^{1/2}$$

Figure 6.1. Molecular structure and atom numbering scheme for $(PhNCO)_3$

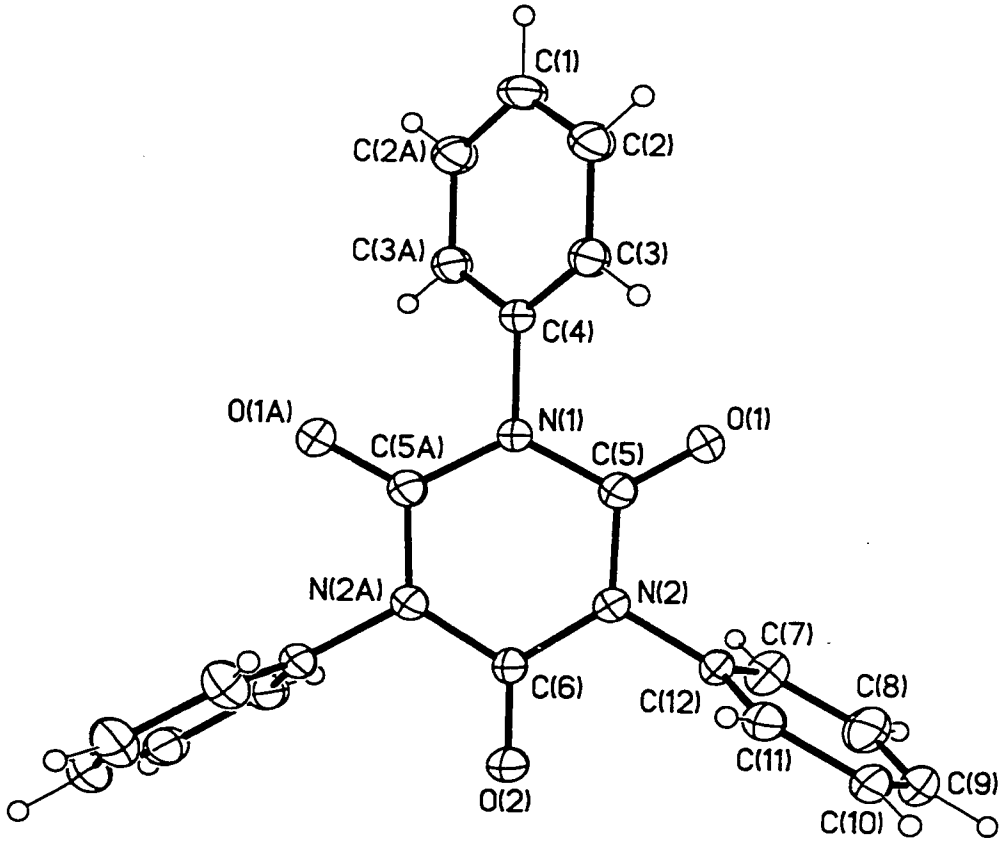

Table 6.3. Selected bond lengths [A] and angles (°) for $(PhNCO)_3$

Distances			
O(1)-C(5)	1.211(3)	N(2)-C(5)	1.387(3)
O(2)-C(6)	1.203(4)	N(2)-C(6)	1.391(3)
N(1)-C(5)	1.395(3)	N(2)-C(12)	1.455(3)
N(1)-C(5)#1	1.395(3)	C(6)-N(2)#1	1.391(3)
N(1)-C(4)	1.458(4)		

Angles			
C(5)-N(1)-C(5)#1	123.6(3)	C(3)-C(4)-N(1)	119.30(15)
C(5)-N(1)-C(4)	118.22(13)	O(1)-C(5)-N(2)	121.9(2)
C(5)- #1-N(1)-C(4)	118.22(13)	O(1)-C(5)-N(1)	122.3(2)
C(5)-N(2)-C(6)	124.7(2)	N(2)-C(5)-N(1)	115.8(2)
C(5)-N(2)-C(12)	118.15(19)	O(2)-C(6)-N(2)#1	122.46(14)
C(6)-N(2)-C(12)	117.18(19)	O(2)-C(6)-N(2)	122.46(14)
N(2) #1-C(6)-N(2)	115.1(3)		

Figure 6.2. Molecular structure and atom numbering scheme for $(EtNCO)_3$

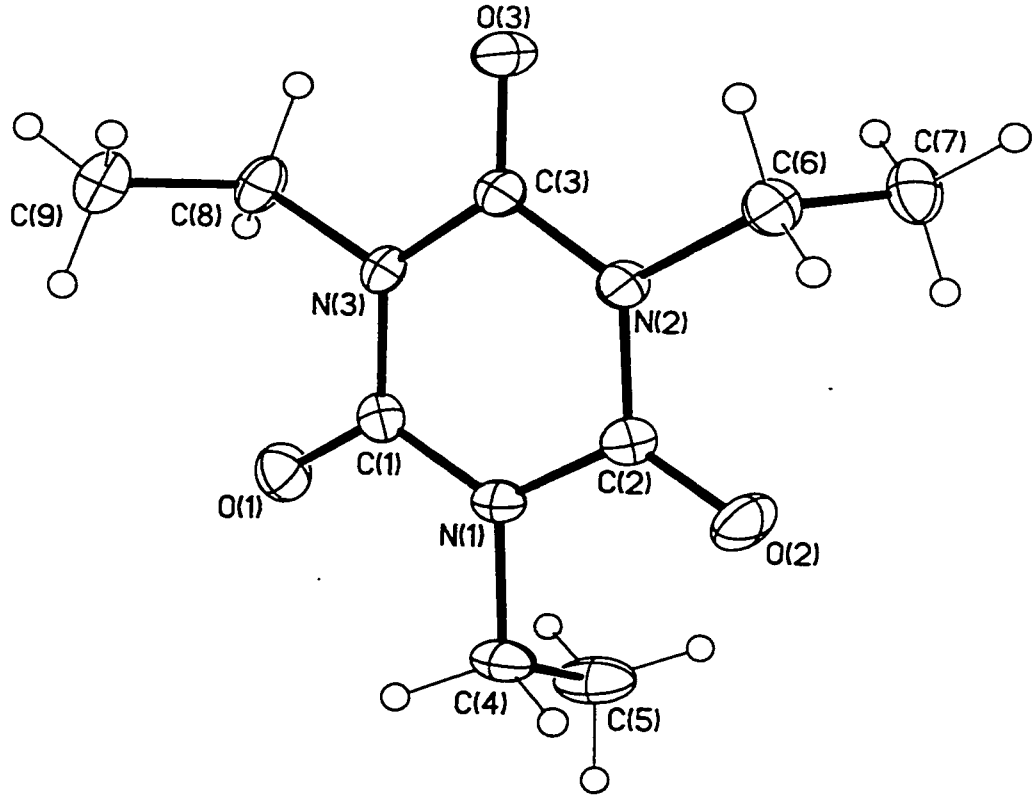

Table 6.4. Selected bond lengths [A] and angles (°) for $(EtNCO)_3$

Distances			
N(1)-C(1)	1.378(3)	N(3)-C(1)	1.373(2)
N(1)-C(2)	1.380(2)	N(3)-C(8)	1.468(2)
N(1)-C(4)	1.475(2)	O(1)-C(1)	1.209(2)
N(2)-C(2)	1.375(2)	O(2)-C(2)	1.208(2)
N(2)-C(3)	1.386(2)	O(3)-C(3)	1.205(2)
N(2)-C(6)	1.473(2)		

Angles			
C(1)-N(1)-C(2)	123.44(16)	N(3)-C(1)-N(1)	116.44(16)
C(1)-N(1)-C(4)	118.67(17)	N(2)-C(2)-N(1)	116.00(17)
C(2)-N(1)-C(4)	117.79(18)	N(3)-C(3)-N(2)	114.95(17)
C(2)-N(2)-C(3)	124.54(16)	N(1)-C(4)-C(5)	111.72(16)
C(2)-N(2)-C(6)	116.93(16)	N(2)-C(6)-C(7)	111.45(17)
C(3)-N(2)-C(6)	118.27(16)	N(3)-C(8)-C(9)	112.25(17)
C(1)-N(3)-C(3)	124.48(16)	C(3)-N(3)-C(8)	118.12(18)
C(1)-N(3)-C(8)	117.38(17)		

References for Chapter Six

[1] Wong, S.; Frisch, K.C. *J. Polym. Sci. A*, **1986**, *24*, 2867

[2] Spirkova, M.; Kubin, M.; Spacek, P.; Krakovsky, I.; Dusek, K. . *J. Appl. Polym. Sci.* **1994**, *52*, 895

[3] Malkin, A.Y.; Beghishev, P.; Bolgov, S.A. *Polymer*, **1982**, *23*, 385

[4] Kordomenos, P.I.; Kresta, J.E. Macromolecules 1981, 14, 1434

[5] Spirkova, M.; Kubin, M.; Spacek, P.; Krakovsky, I.; Dusek, K. . *J. Appl. Polym. Sci.* **1994**, *53*, 1435

[6] Misawa, H; koseki, T. JP 03,166,255 (91,166,255) (C1.C08271/1), **1991**; Chem Abstr. 1991, 115, 257582a

[7] Ishikawa, T.; Tanaka, S.; Shidara, M.; Hatsutori, I.; Takagame, H.; Mashita, K. JP 0187,651 (89,87651) (C1.C0835/06), 1898; Chem. Abstr. 1989, 111, 155203c

[8] Pavlova, M.; Draganova, M. *Polym. Commun.* **1991**, *32*, 446

[9] Tang, J.; Verkade, J. G. *Angew. Chem., Int. Ed. Engl.*, **1993**, *32*, 896

[10] Tang, J.; Mohan, T.; Verkade, J. G. *J. Org. Chem.* **1994**, *59*, 4931

[11] Nambu, Y.; Endo, T. *J. Org. Chem.* **1993**, *58*, 1932

[12] Mizura, J.; Yokozawa, T.; Endo, T. *J. Poly. Sci., Polym. Chem.* **1991**, *29*, 1545

[13] Endo, T.; Suike, J. JP 1989 01226878 A2 (Cl. C07D251/34) *Chem. Abstr.* **1990**, *112*, 77236v

[14] Tanimoto, F.; Kitano, H. JP 72 22,558 (Cl. C07D) 1972 *Chem. Abstr.* **1972**, *77*, 88546f

[15] Kitano, H.; Tanimoto, F.; Miura, J. JP 73 26,022 (Cl. C07D) 1973 *Chem. Abstr.* **1973**, *79*, 115642j

[16] Srinivas, B.; Chang, C.-C.; Chen, C.-H.; Chiang, M. Y.; Chen, I.-T.; Wang, Y.; Lee, G.-H. *J. Chem. Soc., Dalton Trans.* **1997**, 957

[17] Wong, S.; Frisch, K.C. *J. Polym. Sci. A*, **1986**, *24*, 2877

[18] Bloodworth, A. J.; Davies, A. G. *J. Chem. Soc.* **1965**, 6858

[19] Kresta, J.E.; Shen, C.S.; Hsieh, K.H.; Frisch, K.C. *Anion. Polym.* **1981**, *32*, 501

[20] Baudour, J.-L.; Delugeard, Y.; Sanquer, M. *Acta Crystallogr., Sect. B*, **1974**, *30*, 691.

Guanidinato and Pyramidinato Complexes of Tin

7

'one question...'

Chapter Seven

Introduction

Having established amidinates as versatile and flexible ligand systems for tin and germanium in the formation of interesting, rare, and catalytically active complexes (see chapters 2 through 6 and references therein), we wished to explore other ligand systems while preserving the basic N-C-N ligand framework upon which this thesis is based (chart 7.1). Guanidinates fall into this general class and, in contrast

Chart 7.1

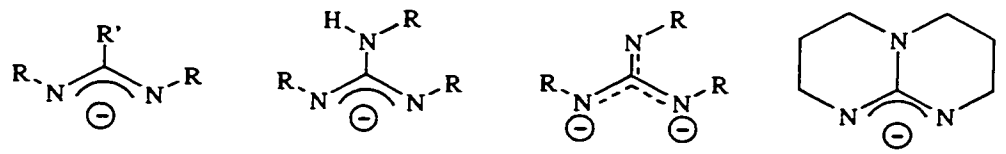

amidinate | monoanionic guanidinate | dianionic guanidinate | hexahydro pyramido pyramidinate (hpp)

to amidinates, have received limited attention with transition metal and main group elements. With regard to N,N',N''-trisubstituted guanidinate complexes of main group metals, only three examples have been reported. The only p-block complex is $[(^{i}PrN)_2(NH^{i}Pr)][(^{i}PrN)_2(N^{i}Pr)]Sb$, made from the reaction of 1,2,3-triisopropyl guanidine with 1 equiv of $Sb(NMe_2)_3$. It formally possesses one dianionic and one monoanionic guanidinate.[1] The remaining guanidinate complexes are the dianionic lithium salts, $Li_2(C(NPh)_3)$[2] and $Li_2(C(N^{t}Bu)_3)$.[3] Given the analogy of guanidinate anions to amidinate

anions as well as the additional coordination and reactivity possibilities, we felt that use of these species with group 14 metals was warranted.

The main resonance contributions to N,N',N"-trisubstituted guanidinate anions were summarized in Chapter One. Furthermore increased flexibility in the coordination properties of this ligand arises from the presence of an additional nitrogen center and two ionizable protons. This offers potential to investigate the coordination properties of the dianionic ligand in the formation of tin complexes. Guanidines are also strong bases and may be able to function in this regard by direct reaction with metal halides.

In this chapter, we investigate the use of monoanionic N,N',N"-trisubstituted guanidinates in the formation of both Sn(II) and Sn(IV) complexes. Two preparative routes are employed. The first is direct addition of the neutral guanidine with tin tetrachloride ,while the other is the *in situ* formation of the monolithium salt of the guanidine followed by addition of a either $SnCl_2$ or $SnCl_4$.

An interesting related ligand that falls into the general N-C-N framework of these studies is the anion of 1,3,4,6,7,8-hexahydro-2H-pyramido[1,2-a]pyramidine (Hhpp). The pyramidinate anion formed by deprotonation is designated as hpp^- (Chart 7.1). It resembles a tetrasubstituted guanidinate more so than an amidinate ligand given the presence of an ancillary third nitrogen. The steric bulk of the ligand is greatly restricted as a result of the tethered functionalities on the nitrogen atoms. The tethered nature of the ligand results in a small dihedral angle. Thus, a conjugated π system with the ancillary third nitrogen and that of the chelating N-C-N moiety might be expected.

In amidinate and guanidinate ligands, steric crowding between R groups on the carbon bridge and on the chelating nitrogens results in the nitrogen σ donor orbitals

extending more towards the center of the amidinate thus favouring a chelating bonding mode. However, with the hpp anion, the N-R groups are tethered away from the metal center thus projecting the σ orbitals in parallel directions (Chart 7.2).[8]

Chart 7.2

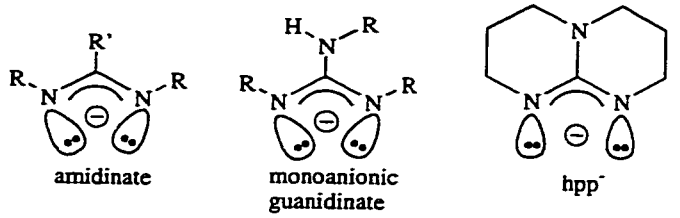

The hpp anion has had limited application in transition metal chemistry in the formation of dinuclear species of the formula $(hpp)_4M_2$ where M = V, Cr, Mo,[4] and Nb[5] as well as $M_2(hpp)_4Cl_2$ where M = Ru[6] and Ir.[7] In all cases, the hpp ligands bridge the metal atoms resulting in the formation of lantern type complexes possessing metal-metal bonds. For example, the Nb(II) complex exhibits the shortest known Nb-Nb bond distance.

The only reported main group metal complex of the hpp anion is $[(\mu\text{-hpp})AlMe_2]_2$ (Scheme 7.1).[8] As with the transition metal complexes, the aluminum complex adopts a dimeric structure in which the hpp⁻ ligands bridge two $AlMe_2$ moieties.

Scheme 7.1

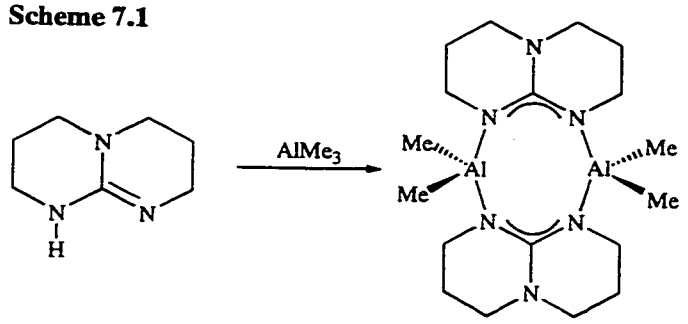

The reduction in three-dimensional steric bulk about the N-C-N framework first attracted us to this ligand. We were interested in investigating if this ligand would result in the formation of dinuclear complexes of Sn(II).

Results and discussion

Guanidinate complexes of tin :

Prior to our involvement in the area, guanidinate complexes of tin were non-existent, requiring the development of a synthetic methodology for introducing the ligand. Preparative routes to guanidinate complex of tin were examined by two methods (Schemes 7.2 and 7.3). The first method involved direct addition of the neutral guanidine to $SnCl_4$ using an additional equivalent of guanidine to deprotonate the ligand. The second method was based on a metathesis reaction between $SnCl_2$ and the monolithium salt of the guanidine.

The reaction of triisopropyl guanidine with one equivalent $SnCl_4$ proceeds smoothly at room temperature as depicted in scheme 7.2 to give complexes **1** and **2**.

Scheme 7.2

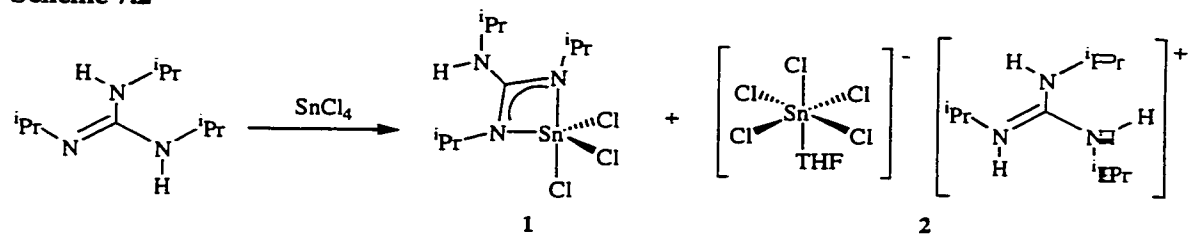

1 **2**

Complex **1**, $[(^iPrN)_2CN(H)^iPr]SnCl_3$, possesses a monoanionic ligand which is apparently derived from the deprotonation of a coordinated guanidine by a second guanidine to yield guanidinium cation and release chloride. This results in the formation of a second species $[(^iPrNH)_3C^+][SnCl_5^-]$, **2**.

As expected, the ^{1}H and ^{13}C NMR spectrum of **1** shows two sets of isopropyl resonances in a ratio of 2 :1. The most obvious change in the ^{13}C NMR for the guanidine upon deprotonation and coordination is a shift for the central sp^2 carbon, CN_3, from 148 ppm to 160 ppm. This is in accord with the formulation for **1** as a monoanionic guanidinate complex. Complex **1** is stable at temperatures over 125°C.

Further confirmation of connectivity for **1** was provided by X-ray diffraction studies (Table 7.1). The structure is shown in Figure 7.1 with corresponding values for bond distances and angles provided in Table 7.2. The results confirm the coordination environment about the Sn(IV) center is trigonal bipyramidal with one bidentate guanidinate ligand spanning axial/equatorial sites and three chloride ligands. The pseudo-equatorial plane is defined by N(1) of the guanidinate ligand and Cl(1) and Cl(2). The sum of the angles of these ligands around Sn is 357° indicating these groups do indeed form a plane. The Cl(3)-Sn-N(2) angle of 159.76(7)° is defined as the pseudo-axial vector.

The guanidinate anion is bonded to Sn through the nitrogen atoms N(1) and N(2). While the sum of the angles around the central carbon, C(7), and N(2) of the NCN framework indicate planarity, the sum of angles around N(1) is only 349° indicating it still retains some sp^3 character. The ligand does not yield a planar four-membered ring with the Sn center but is slightly distorted out of the plane by N(1).
This asymmetry is further observed in the ligand where the N(1)-C(7) distance of 1.361(4)Å is longer than the N(2)-C(7) distance of 1.341(3)Å. (Furthermore, the Sn-N(1) distance of 2.091(2)Å is shorter than that of Sn-N(2) at 2.137(2)Å.) These observations

suggest a sustantial contribution to the static structure of **1** from the localized bonding description shown in **I**.

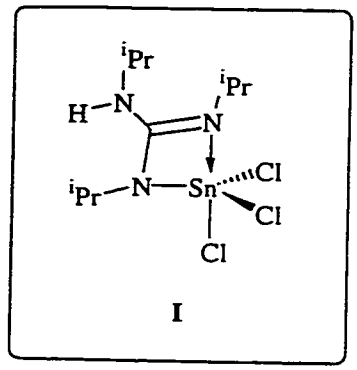

I

The third guanidinate nitrogen, N(3), lies in the plane of the ligand (Sn-C(7)-N(3) 179.1(2)°) and the C(8)-N(3)-C(7) angle of 127.3(3)° suggests sp^2 hybridization about N(3). The short N(3)-C(7) distance of 1.339(4)Å is equivalent to that of C(7)-N(2) indicating some degree of multiple bonding is indeed taking place.

Figure 7.1. Molecular structure and atom numbering scheme for $\{[(CH_3)_2CHN]_2C[NHCH(CH_3)_2]\}SnCl_3$ (**1**). Hydrogen atoms have been omitted for clarity.

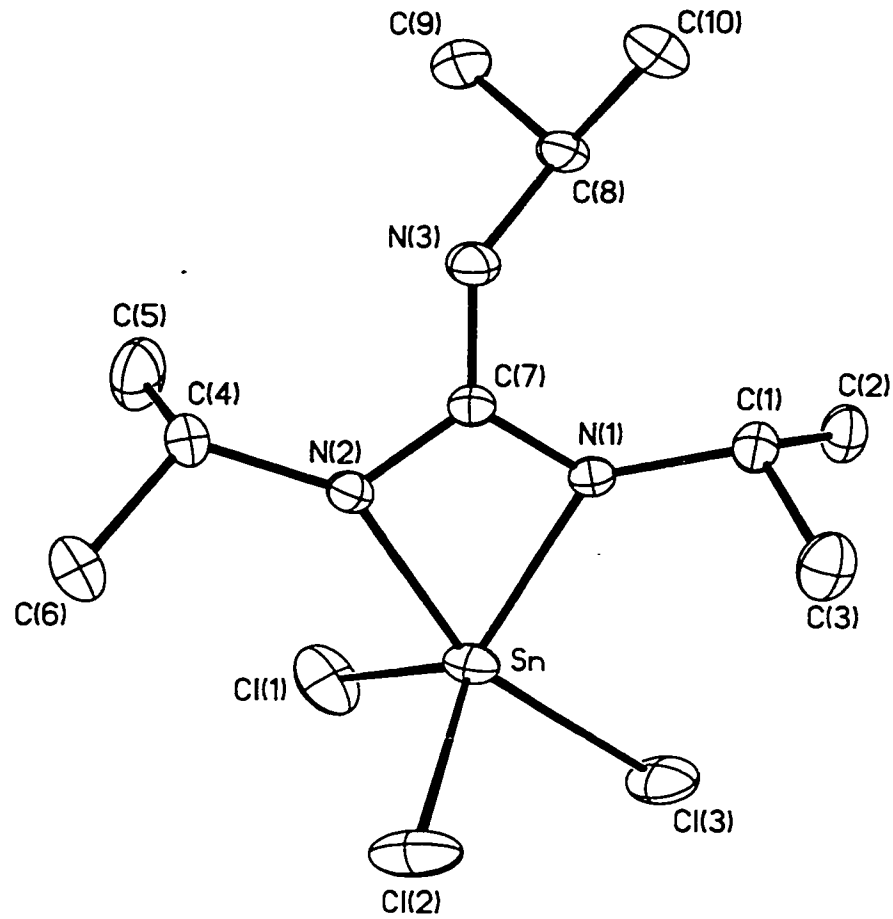

For conjugation of the p orbital of an sp^2 N(3) with the π system of the N(1)-C(7)-N(2) group, the plane defined by C(8)-N(3)-C(7) should be coincident with the plane defined by N(1)-C(7)-N(2). The observed angle between these two planes is 32.9° which, while not ideal, certainly allows some degree of π bonding between N(3) and C(7). Based on these results, a better bonding description for **1** might indeed be provided by the resonance structure shown by **II**.

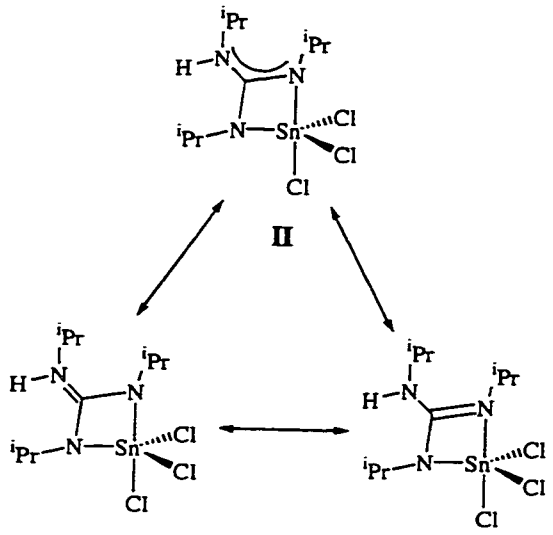

II

The identity of the ionic complex **2** was confirmed by elemental analysis and NMR. The ^{1}H and ^{13}C NMR spectrum of **2** clearly shows only one set of resonances for the protonated guanidine indicating all three ^{i}PrNH are equivalent. A preliminary crystal structure was obtained to confirm the presence of a $SnCl_5^-$ counterion and to confirm connectivity (Figure 7.2).

Reaction of tin halides with a lithium guanidinate offers an alternative metathical route for introduction of guanidinate anions. The N,N',N"-tricyclohexyl guanidinate monoanion is generated *in situ* by reaction of the guanidine with one equiv of MeLi. Subsequent addition of 0.5 equiv of $SnCl_2$ results in the formation of $[(CyN)_2C(HNCy)]_2Sn$, **3**, in 78% yield according to Scheme 7.3. When the reaction is performed with one equivalent $SnCl_2$ in an attempt to generate a monoguanidinato tin(II) chloride species ,only complex **3** forms with unreacted $SnCl_2$ remaining.

Figure 7.2. Preliminary molecular structure of $[(CH_3)_2CHNH]_3C^+ SnCl_5^-$ (**2**).

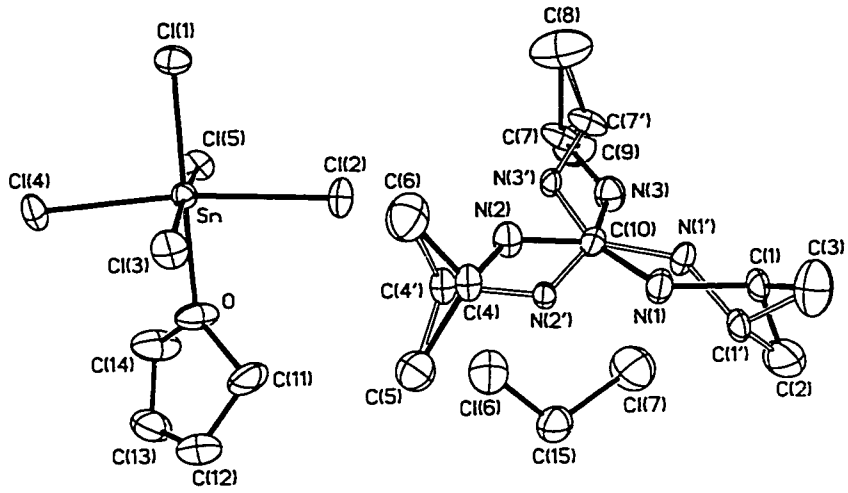

The presence of the monoanion is confirmed by ^1H NMR of **3** which shows three independent cyclohexyl groups all in a 1:1:1 ratio. This is expected for the geometry shown in Scheme 7.3. One cyclohexyl is in the pseudo-equatorial position, another in the pseudo-axial position while the third in on the ancillary third nitrogen, NCyH. The N-H proton is observed at 3.40 ppm.

Scheme 7.3

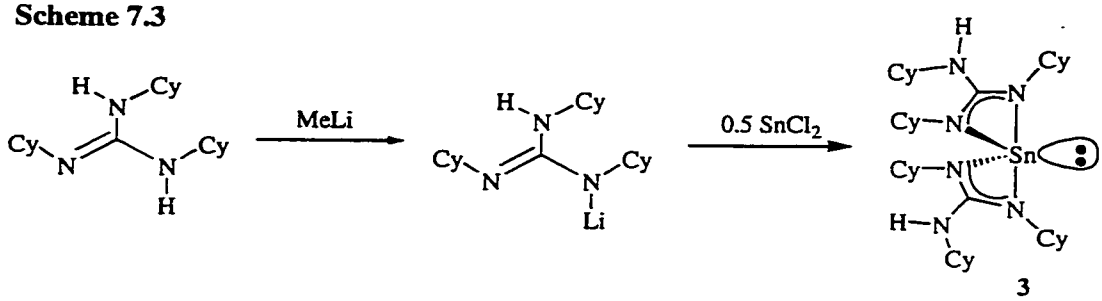

In order to clarify the guanidinate ligand coordination modes and the geometry around the metal center, an X-ray diffraction study was performed (Table 7.1). From Figure 7.3, it is clear that the environment about the Sn(II) center consists solely of two

bidentate guanidinate anions. Selected bond distances and angles corresponding to Figure 7.3 are provided in Table 7.3.

Consistent with the spectroscopic data, the geometry about the Sn center would best be described as a distorted trigonal bipyramid where two chelating guanidinate anions span axial/equatorial sites with the fifth coordination site being occupied by the lone pair of electrons. Complex **3** possesses a crystallographic C_2 axis which makes the two ligands equivalent.

Figure 7.3. Molecular structure and atom numbering scheme for $\{[(C_6H_{11})N)_2C[NHC(C_6H_{11})]\}_2Sn$ (**3**). Hydrogen atoms have been omitted for clarity.

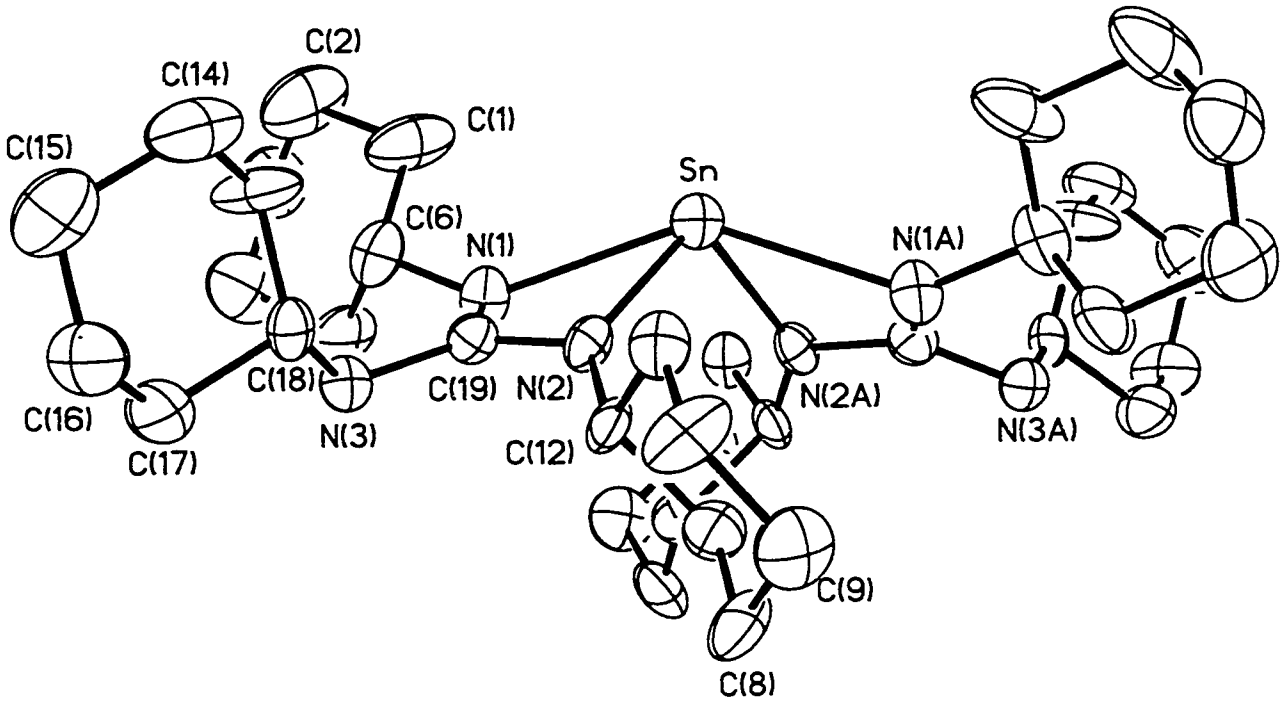

In **3**, the pseudo equatorial plane is defined by N(2) and N(2A) of the guanidinate ligands and the lone pair on tin. The N(1)-Sn-N(1A) angle of 140.4(3)° is defined as the pseudo-axial vector and is heavily distorted due to the restricted bite angle (58.1(2)°) of the ligands. The bite angle is typical of both amidinates and guanidinates.[9,10] The axial Sn-N(1) distance of 2.424(6)Å is correspondingly longer than the equatorial Sn-N distance of 2.152(6)Å. As with complex **1**, the ligand does not yield a planar four membered ring of sp^2 hybridized N and C but is distorted out of the plane due to non-planar N(1). In this case the effect is more pronounced. The sum of the angles around N(2) is 360° however, the sum of the angles around N(1) is only 344°. The N(1)-C(19) distance of 1.306(9)Å is shorter than that of N(2)-C(19) at 1.344(8)Å which is similar to that of complex **1**. The reasons why the ligand deviates so much from the plane around N(1) would probably best be attributed to sterics.

The third guanidinate nitrogen, N(3), lies in the plane of the ligand. The C(8)-N(3)-C(7) angle of 118.3(6)° at first suggests sp^2 hybridization about N(3), but the longer N(3)-C(19) distance of 1.435(9)Å indicates little π conjugation is taking place. Calculation of the angle between the two planes defined by C(18)-N(3)-C(19) and that defined by N(1)-C(19)-N(2) gives a value of 57.3°. This again indicates little π bonding between N(3) and C(19).

Pyramidinato complexes of tin :

The lithium salt of Hhpp was prepared by reaction of Hhpp with one equivalent MeLi. Subsequent reaction with $SnCl_2$ follows one of two paths depending on the

stoichiometry (Scheme 7.4). Addition of 0.5 equiv $SnCl_2$ resulted in the formation of the mononuclear complex $(hpp)_2Sn$, **4**, in 73% yield while a stoichiometric ratio of 1 :1 produced the dinuclear complex **5** in 63% yield.

Scheme 7.4

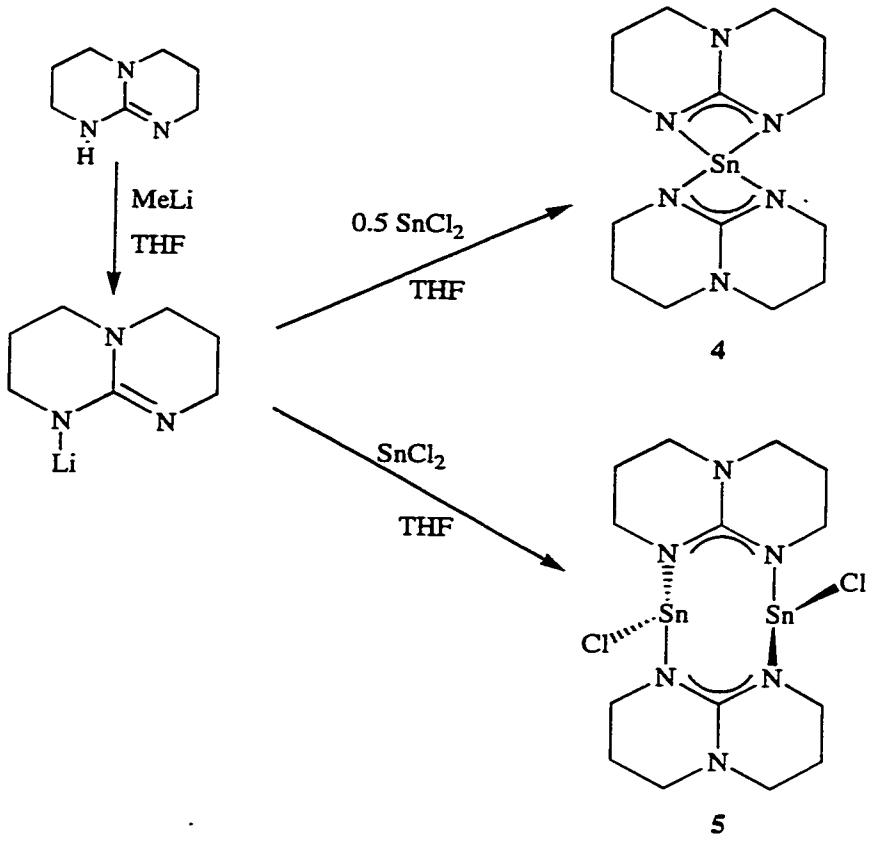

Unfortunately, NMR did not provide any definitive structural motif due to the lack of spectroscopic handles built into the ligand. ^1H NMR spectra show only two broad signals in a ratio of 2 :1. X-ray diffraction studies had to be performed to confirm both level of aggregation and connectivity (Table 7.4). Structures are shown in Figure 7.4 and 7.5 with corresponding values for selected bond distances and angles of **4** and **5** provided in Table 7.5 and 7.6.

Contrary to all previous structures involving hpp ligands, the Sn(II) complex **4** is mononuclear with two chelating bidentate hpp anions. As in **3**, the Sn center resides in a distorted trigonal bipyramidal environment with the fifth coordination site being occupied by a lone pair of electrons.[11]

Figure 7.4. Molecular structure and atom numbering scheme for $\{CN[N(CH_2)_3]_2\}_2Sn$ (**4**). Hydrogen atoms have been omitted for clarity.

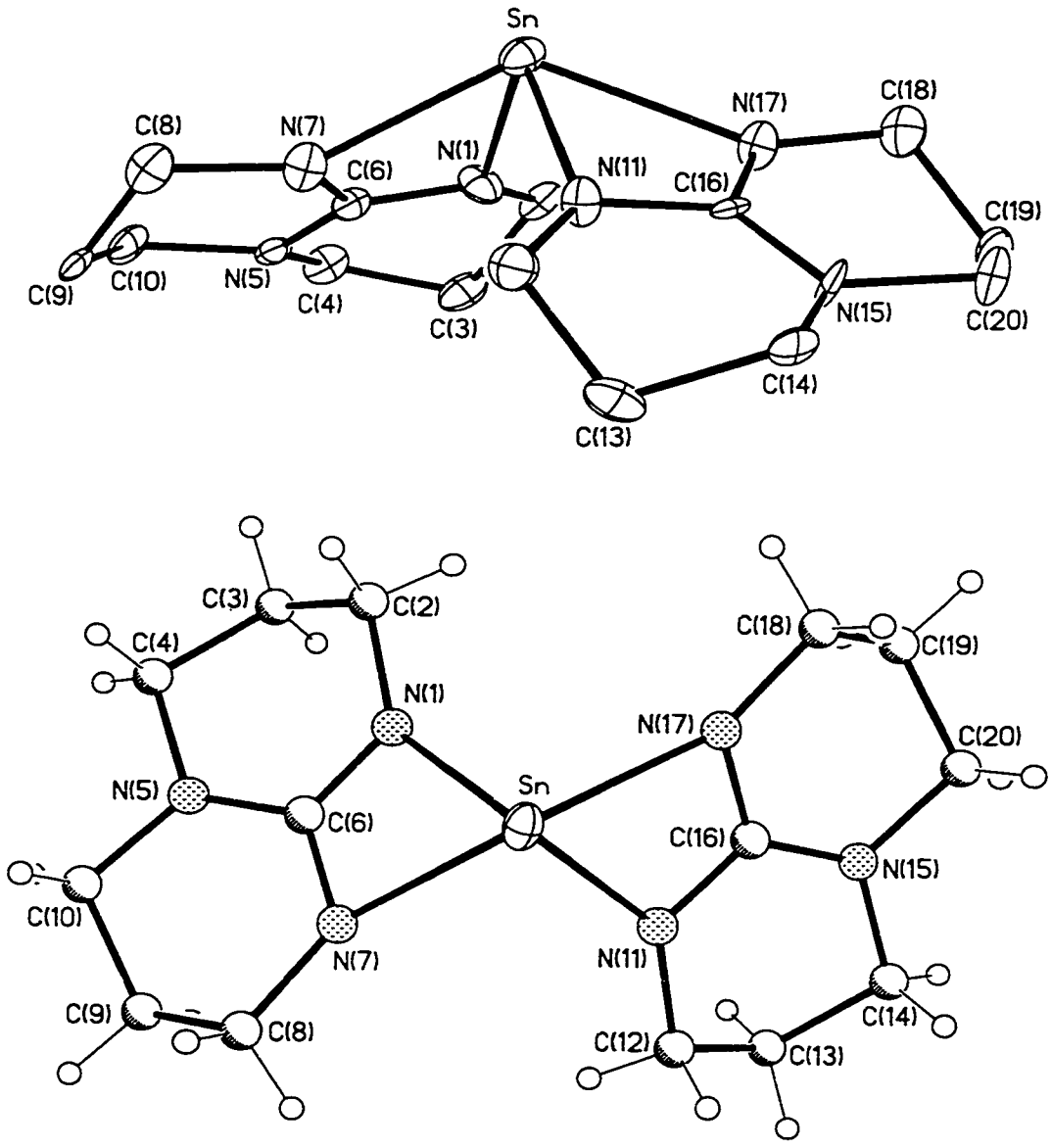

Figure 7.5a. Molecular structure and atom numbering scheme for $\{CN[N(CH_2)_3]_2SnCl\}_2$ (**5**) showing one of the unique molecules in the unit cell. Hydrogen atoms have been omitted for clarity.

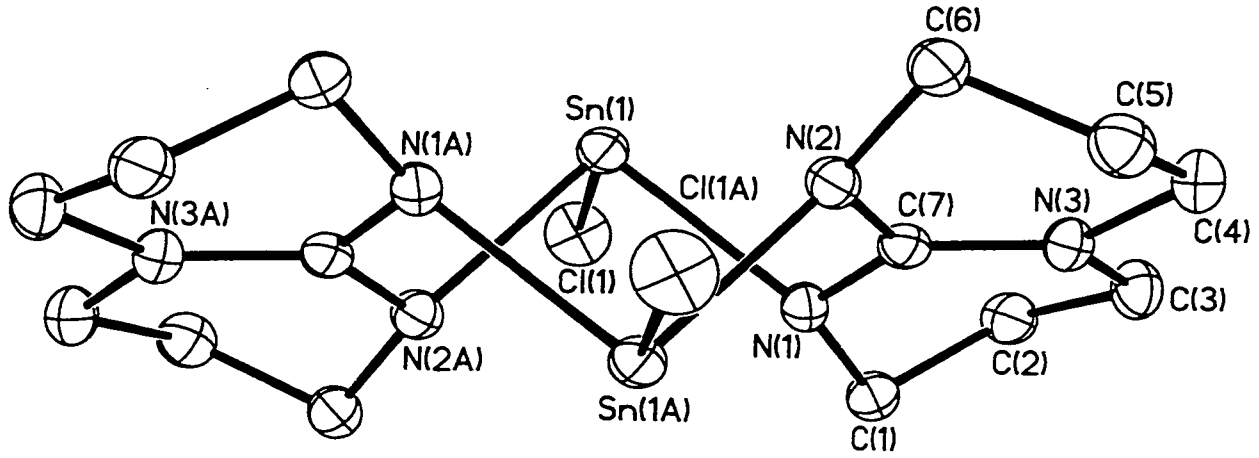

Figure 7.5b. Molecular structure and atom numbering scheme for $\{CN[N(CH_2)_3]_2SnCl\}_2$ (**5**) showing one of the unique molecules in the unit cell. Hydrogen atoms have been omitted for clarity.

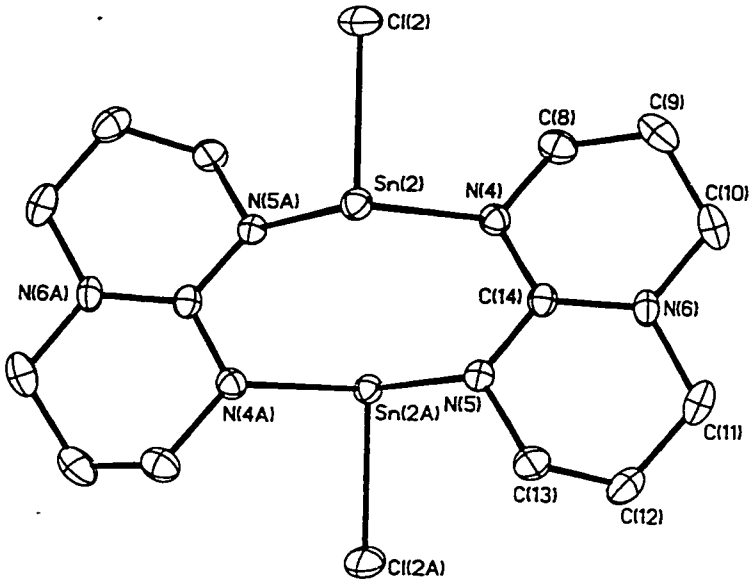

The N(7)-Sn-N(17) angle of 129.6(3)° defines the pseudo-axial vector. The axial vector is extremely distorted due to the bidentate nature of the hpp ligands. As expected, this pseudo-axial angle is more distorted than that of the bis(guanidinate) complex **3** (140.4(3)°) due to the tethered nature of the hpp ligand. The restricted bite angle of the ligand, N(2)-Sn-N(1), at 58.1(2)° is typical of both amidinates and guanidinates and is in fact the same as that of the bis(guanidinate) complex **3**.

The sum of angles around all three nitrogen centers of the ligand varies only slightly from 356-358° suggesting sp^2 character. The three C-N bond distances on each ligand from the central sp^2 carbon varies from 1.30-1.37Å. This indicates that all three nitrogen atoms in each ligand participate to some degree in π bonding to the central sp^2 carbon [C(6) or C(16)]. The π bond is thus not delocalized between only the two nitrogen atoms bonded to the tin center but is instead delocalized between all three nitrogen atoms and the central carbon.

The formation of a mononuclear hpp tin complex was disappointing but in hindsight not unexpected given the relative large size of tin. To extend this chemistry further, we were curious if reducing both the coordination number and the steric bulk about the tin center might promote the formation of a dinuclear hpp complex.

To this end, $SnCl_2$ was reacted with one equivalent of hppLi in THF which resulted in the production of the dinuclear complex $(hppSnCl)_2$, **5** (Scheme 7.4). Again, X-ray diffraction studies had to be performed to confirm both nuclearity and connectivity (Table 7.4).

Contrary to the mononuclear complex **4**, complex **5** is dinuclear with two hpp ligand bridging the two Sn atoms (Figure 7.5). The Sn(II) atoms exhibit geometries based on distorted tetrahedra with the coordination environment around each being defined by two nitrogen centers, a chloride ligand and a lone pair of electrons. As shown in Figure 7.5, there is no interaction of the lone pairs on the two Sn(II) centers as they are situated in mutually orthogonal directions. There were two independent molecules in the unit cell which differ only marginally in their bond lengths and angles.

Scheme 7.5

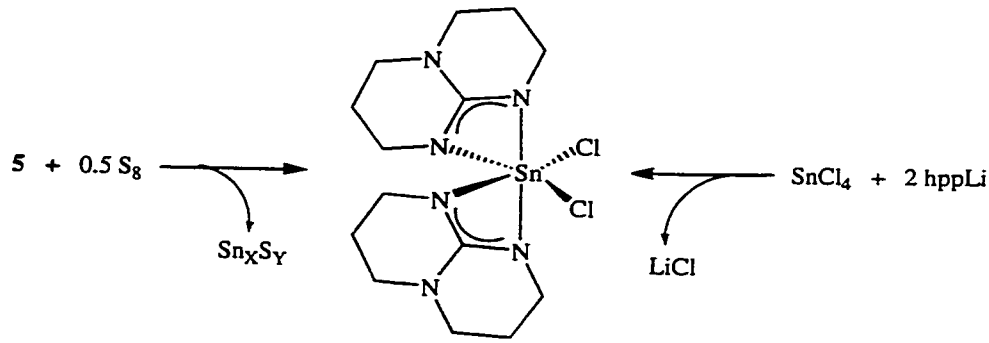

6

Complex **5** possesses a crystallographic inversion center which makes the two hpp ligands equivalent. The three N-C distances to the central sp^2 hybridized carbon are all equivalent within errors and correspond to a degree of N=C π bonding. The Sn-N distances are equivalent at 2.21Å.

In an effort to synthesize a polynuclear sulfido species of the dinuclear tin hpp complex, $(hppSnCl)_2$ was reacted with 0.5 equiv S_8 in THF according to Scheme 7.5. An insoluble yellow powder precipitated during the reaction. After filtration, we were somewhat surprised to isolate the mononuclear Sn(IV) complex $(hpp)_2SnCl_2$, **6**, as the product of this reaction.

Apparently, the starting complex **5** was oxidized by elemental sulfur to Sn(IV) at which point a ligand rearrangement occured to produce $(hpp)_2SnCl_2$ along with an insoluble tin sulfide byproduct, Sn_xS_y. The exact nature of the byproduct remains uncertain at this time.

X-ray diffraction studies were performed to confirm the structural features of **6** (Table 7.4). The structure is shown in Figure 7.6 with corresponding values for selected bond distances and angles provided in Table 7.7.

Figure 7.6. Molecular structure and atom numbering scheme for $\{CN[N(CH_2)_3]_2\}_2SnCl_2$ (**6**). Hydrogen atoms have been omitted for clarity.

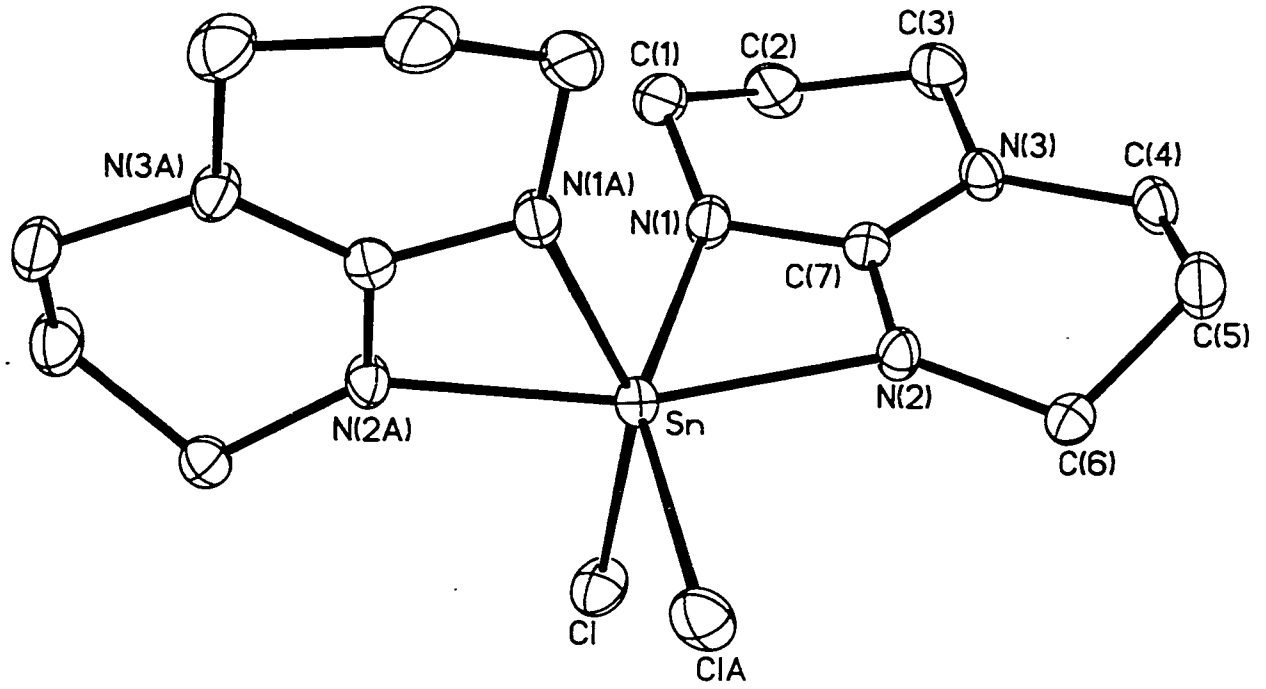

Complex **6** is a mononuclear Sn(IV) species with a coordination environment consisting of two bidentate hpp ligands along with two chloride ligands. The geometry is based on a cis-dichloro distorted octahedron with a crystallographic C_2 bisecting the Cl-Sn-Cl angle. Complex **6** is similar to reported bis(amidinato) Sn(IV) dichloride species.[9]

The hpp anion is bonded to the tin atom through the nitrogen atoms N(1) and N(2). The N-C bond distance to the central sp^2 carbon, C(7), for both nitrogen atoms is the same at 1.326(6)Å. The sum of the angles around these two atoms is 359° and 358° indicative of sp^2 character. The sum of angles around the ancillary third nitrogen, N(3), is exactly 360° while the N(3)-C(7) distance is 1.344(6)Å. As with complex 4, this indicates that all three nitrogen atoms in each ligand participate to some degree in π bonding to C(7). The π bond is thus delocalized between all three nitrogen atoms and the central carbon.

A more rational route to complex **6** was developed through addition of $SnCl_4$ to two equivalents of *in situ* prepared hppLi in THF according to Scheme 7.5.

Conclusion

These results show that direct protonation routes as well as lithiation routes provide a convenient methodology for the introduction of guanidinate mono-anions onto tin. Examples of guanidinato complexes of both Sn(II) and Sn(IV) are reported. All attempts to characterize a dianionic guanidinate complex were inconclusive. The best route to a dianionic guanidinate complex of tin appears to be through the use of the

dilithium salt of the guanidinate. However, the poor solubility of the resulting product has to date hampered purification and crystallization.

The first hpp complexes of tin were also prepared. Contrary to reported transition metal complexes, bis-hpp complexes of Sn(II) and Sn(IV) were mononuclear with bidentate hpp ligands. Reducing the coordination number and steric bulk about tin by preparing a mono hpp Sn(II) complex resulted in the formation of a dinuclear species with bridging hpp ligands. The difficulty with the hpp anion is the poor solubility of both the parent ligand and of the complexes formed. This limits reaction solvent choice and hinders further reactivity. A solution to this problem would be to make functionalized derivatives of Hhpp to increase solubility.

Experimental for Chapter Seven

General Procedure. All manipulations were carried out in either a Vacuum Atmospheres drybox or under nitrogen using standard Schlenk-line techniques. Diethyl ether, toluene and THF were purified by passing through drying columns developed by Anhydrous Engineering. CH_2Cl_2 and $CDCl_3$ were distilled under nitrogen from CaH. Deuterated benzene was distilled under nitrogen from Na/K alloy. 1,3,4,6,7,8-hexahydro-2H-pyrimido[1,2-a]pyrimidine (Hhpp), $SnCl_2$, $SnCl_4$ and MeLi (1.4M in diethyl ether) were purchased from Aldrich and used without further purification. N,N',N''-triisopropylguanidine and N,N',N''-tricyclohexylguanidine were prepared by literature procedures.

NMR spectra were run on a GEMINI 200 MHz spectrometer with deuterated benzene or $CDCl_3$ as a solvent and internal standard. All elemental analyses were run on a Perkin-Elmer PE CHN 4000 elemental analysis system. All melting points were determined on a Gallenkamp Melting Point Apparatus in sealed capillary tubes.

$\{[(CH_3)_2CHN]_2C[NHCH(CH_3)_2]\}SnCl_3$ (1). 0.500g N,N',N''-triisopropylguanidine (2.70 mmol) was disolved in toluene (50ml). 1 equiv $SnCl_4$ (0.703g, 2.70mmol) was added. The solution was stirred for 12h, filtered to remove the complex **3** precipitate and the solvent removed under vacuum. White crystals were obtained from diethyl ether at –34°C (0.54g, 49% yield). ^{1}H NMR (C_6D_6, ppm) : 3.20, (br, CH, 3H); 3.19 (br, NH, 1H); 1.20 (d, J_{HH}=6.6Hz, CH_3, 12H); 0.62 (d, J_{HH}=6.0Hz, CH_3, 6H). ^{13}C NMR (C_6D_6, ppm) : 160.1 (s, N<u>C</u>N); 48.2 (s, <u>C</u>$(CH_3)_2$); 46.4 (s, <u>C</u>$(CH_3)_2$); 23.4 (s, CH_3); 23.2 (s, CH_3). ^{119}Sn

NMR (C_6D_6, ppm *vs.* $SnMe_4$): -356.9. Anal. Calcd for $C_{10}H_{22}N_3SnCl_3$: C 29.34; H 5.42; N 10.27. Found: C 27.96; H 5.55; N 9.81. MP: 54-56 °C.

$[(CH_3)_2CHNH]_3C^+ SnCl_5^-$ (2). The precipitate from the formation of **2** in toluene was washed with toluene (3 x 5ml) and dried. White crystals were obtained from CH_2Cl_2 at –34°C (0.46g, 35% yield). ^1H NMR ($CDCl_3$, ppm) : 5.18 (d, J_{NH}=7.8Hz, NH, 3H); 3.88 (br, CH, 3H); 1.33 (d, J_{HH}=6.4Hz, CH_3, 18H). ^{13}C NMR ($CDCl_3$, ppm) : 152.1 (s, N$\underline{C}$N); 45.3 (s, $\underline{C}(CH_3)_2$); 22.7 (s, CH_3). Anal. Calcd for $SnCl_5C_{10}H_{24}N_3$·THF: C 30.33; H 5.82; N 7.58. Found: C 29.62; H 5.85; N 7.51. MP: 133-134 °C.

$\{[(C_6H_{11})N)_2C[NHC(C_6H_{11})]\}_2Sn$ (3). 0.500g N,N',N''-tricyclohexylguanidine (1.64 mmol) was disolved in diethyl ether (40ml). 1 equiv MeLi (1.17ml, 1.4M, 1.64mmol) was added dropwise. The solution was stirred for 30min and 0.5 equiv $SnCl_2$ (0.155g, 0.82mmol) was added. The solution was stirred for an additional 12h, filtered to remove the LiCl precipitate and the solvent removed under vacuum. Crystals were obtained from diethyl ether at –34°C (0.47g, 78% yield). ^1H NMR (C_6D_6, ppm) : 3.95, (br, C_6H_{11}, 2H); 3.40 (d, J_{NH}=11Hz, NH, 2H); 3.10 (br, C_6H_{11}, 2H); 2.90 (br, C_6H_{11}, 2H); 2.19-0.74 (m, C_6H_{11}, 60H). ^{13}C NMR (C_6D_6, ppm) : 148.4 (s, N$\underline{C}$N); 55.0, 52.0, 49.2, 35.9, 34.7, 34.0, 26.8, 26.6, 25.9, 25.6, 25.3 (11s, C_6H_{11}). Anal. Calcd for $C_{38}H_{68}N_6Sn$: C 62.72; H 9.42; N 11.55. Found: C 61.06; H 9.56; N 11.01. MP: 163-164 °C.

$\{CN[N(CH_2)_3]_2\}_2Sn$ (4). 0.300g Hhpp (2.16 mmol) was disolved in THF (35ml). 1 equiv MeLi (1.54ml, 1.4M, 2.16mmol) was added dropwise. The solution was stirred for 2h

and 0.5 equiv $SnCl_2$ (0.204g, 1.08mmol) was added. The solution was stirred for an additional 24h, filtered and the solvent removed under vacuum. White crystals were obtained from THF at –34°C (0.31g, 73% yield). ^{1}H NMR ($CDCl_3$, ppm) : 3.25, (br, CH_2, 16H); 1.85 (br, CH_2, 8H). Anal. Calcd for $C_{14}H_{24}N_6Sn$: C 42.56; H 6.12; N 21.27. Found: C 41.01; H 6.10; N 20.75. MP: 154-156 °C.

{CN[N(CH$_2$)$_3$]$_2$SnCl}$_2$ (5). 0.300g Hhpp (2.16 mmol) was disolved in THF (35ml). 1 equiv MeLi (1.54ml, 1.4M, 2.16mmol) was added dropwise. The solution was stirred for 2h and 1 equiv $SnCl_2$ (0.408g, 2.15mmol) was added. The solution was stirred for an additional 24h, filtered and the solvent removed under vacuum. White crystals were obtained from CH_2Cl_2 at –34°C (0.40g, 63% yield). ^{1}H NMR ($CDCl_3$, ppm) : 3.40, (br, CH_2, 8H); 3.20 (br, CH_2, 8H); 1.94 (br, CH_2, 8H). ^{13}C NMR ($CDCl_3$, ppm) : 144.9 (s, N<u>C</u>N); 47.4 (s, CH_2); 40.9 (br, CH_2); 23.6 (br, CH_2). Anal. Calcd for $C_{14}H_{24}N_6Sn_2Cl_2(CH_2Cl_2)$: C 26.91; H 3.91; N 12.55. Found: C 27.02; H 4.23; N 12.58. MP: 175 °C (dec).

{CN[N(CH$_2$)$_3$]$_2$}$_2$SnCl$_2$ (6). 0.654g of complex **5** (1.12 mmol) was disolved in THF (50ml). 0.5 equiv S_8 (0.144g, 0.561mmol) was added. There was an immediate formation of a yellow precipitate. The solution was stirred for 24h, filtered and the solvent removed under vacuum. Pale yellow crystals were obtained from THF at –34°C (0.253g, 24% yield based on Sn). ^{1}H NMR ($CDCl_3$, ppm) : 3.22, (br, CH_2, 8H); 3.10 (br, CH_2, 8H); 1.91 (br, CH_2, 8H). ^{13}C NMR ($CDCl_3$, ppm) : 155.4 (s, N<u>C</u>N); 46.2 (s, CH_2); 40.4 (br, CH_2); 23.7 (br, CH_2).

Direct preparation of $\{CN[N(CH_2)_3]_2\}_2SnCl_2$ (6) from $SnCl_4$. 0.500g Hhpp (3.59 mmol) was disolved in THF (50ml). 1 equiv MeLi (2.56ml, 1.4M, 3.58mmol) was added dropwise. The solution was stirred for 30 min and 0.5 equiv $SnCl_4$ (0.470g, 1.80 mmol) was added dropwise. The solution was stirred for an additional 24h, filtered and the solvent removed under vacuum. White crystals were obtained from THF at –34°C (0.40g, 48% yield).

Data Tables for Chapter Seven

Table 7.1. Crystal data and structure refinement for $\{[(CH_3)_2CHN]_2C[NHCH(CH_3)_2]\}SnCl_3$ (**1**) and $\{[(C_6H_{11})N)_2C[NHC(C_6H_{11})]\}_2Sn$ (**3**).

	1	**3**
empirical formula	C10 H22 Cl3 N3 Sn	C38 H60 N6 Sn
formula weight	409.35	719.61
temp (K),	203(2) K	298(2) K
λ(Å)	0.71073 A	0.71073 A
Crystal system, space group	Monoclinic, P2(1)/c	Monoclinic, C2/c
a (Å)	13.980(1)	17.542(7)
b (Å)	10.501(1)	12.284(7)
c (Å)	11.828(1)	18.584(9)
α (deg)	90	90
β (deg)	97.041(2)	93.36(1)
γ (deg)	90	90
V(Å^3),	1723.2(3)	3998(3)
Z	4	4
d_{calc} (g/cm^3),	1.578	1.196
μ (mm^{-1})	1.934	0.671
R1	0.0307	0.0626
wR2	0.0605	0.1185

Table 7.2. bond lengths(Å) and angles(°) for complex **1**

Distances			
Sn-N(1)	2.091(2)	N(2)-C(4)	1.474(4)
Sn-N(2)	2.137(2)	N(3)-C(7)	1.339(4)
Sn-Cl(1)	2.3188(9)	N(3)-C(8)	1.465(4)
Sn-Cl(2)	2.3221(9)	C(1)-C(2)	1.515(4)
Sn-Cl(3)	2.3897(9)	C(1)-C(3)	1.525(4)
Sn-C(7)	2.564(3)	C(4)-C(6)	1.512(4)
N(1)-C(7)	1.361(4)	C(4)-C(5)	1.523(5)
N(1)-C(1)	1.485(4)	C(8)-C(9)	1.524(5)
N(2)-C(7)	1.341(3)	C(8)-C(10)	1.531(5)

Angles			
N(1)-Sn-N(2)	63.48(9)	C(7)-N(2)-Sn	92.11(17)
N(1)-Sn-Cl(1)	121.87(7)	C(4)-N(2)-Sn	140.87(19)
N(2)-Sn-Cl(1)	96.13(7)	C(7)-N(3)-C(8)	127.3(3)
N(1)-Sn-Cl(2)	124.81(7)	N(1)-C(1)-C(2)	110.9(3)
N(2)-Sn-Cl(2)	97.18(7)	N(1)-C(1)-C(3)	111.1(3)
Cl(1)-Sn-Cl(2)	110.74(4)	C(2)-C(1)-C(3)	111.1(3)
N(1)-Sn-Cl(3)	96.34(7)	N(2)-C(4)-C(6)	108.4(3)
N(2)-Sn-Cl(3)	159.76(7)	N(2)-C(4)-C(5)	112.1(3)
Cl(1)-Sn-Cl(3)	93.47(4)	C(6)-C(4)-C(5)	111.9(3)
Cl(2)-Sn-Cl(3)	96.01(4)	N(3)-C(7)-N(2)	124.2(3)

N(1)-Sn-C(7)	31.98(9)	N(3)-C(7)-N(1)	124.9(3)
N(2)-Sn-C(7)	31.51(8)	N(2)-C(7)-N(1)	110.8(3)
Cl(1)-Sn-C(7)	111.18(7)	N(3)-C(7)-Sn	179.1(2)
Cl(2)-Sn-C(7)	114.65(7)	N(2)-C(7)-Sn	56.38(15)
Cl(3)-Sn-C(7)	128.27(7)	N(1)-C(7)-Sn	54.49(14)
C(7)-N(1)-C(1)	122.4(2)	N(3)-C(8)-C(9)	109.5(3)
C(7)-N(1)-Sn	93.53(17)	N(3)-C(8)-C(10)	110.2(3)
C(1)-N(1)-Sn	132.95(18)	C(9)-C(8)-C(10)	110.6(3)
C(7)-N(2)-C(4)	123.8(2)		

Table 7.3. selected bond lengths(Å) and angles(°) for complex **3**

Distances			
Sn-N(2)	2.152(6)	N(1)-C(6)	1.453(8)
Sn-N(2)#1	2.152(6)	N(2)-C(19)	1.344(8)
Sn-N(1)	2.424(6)	N(2)-C(12)	1.429(8)
Sn-N(1)#1	2.424(6)	N(3)-C(19)	1.435(9)
N(1)-C(19)	1.306(9)	N(3)-C(18)	1.473(9)
Angles			
N(2)-Sn-N(2)#1	99.4(3)	C(19)-N(1)-Sn	86.3(5)
N(2)-Sn-N(1)	58.1(2)	C(6)-N(1)-Sn	136.1(5)
N(2)#1-Sn-N(1)	95.1(2)	C(19)-N(2)-C(12)	122.8(7)
N(2)-Sn-N(1)#1	95.1(2)	C(19)-N(2)-Sn	97.4(5)
N(2)#1-Sn-N(1)#1	58.1(2)	C(12)-N(2)-Sn	139.8(5)
N(1)-Sn-N(1)#1	140.4(3)	C(19)-N(3)-C(18)	118.2(6)
C(19)-N(1)-C(6)	121.8(6)		

Table 7.4. Crystal data and structure refinement for $\{CN[N(CH_2)_3]_2\}_2Sn$ (**4**), $\{CN[N(CH_2)_3]_2SnCl\}_2$ (**5**) and $\{CN[N(CH_2)_3]_2\}_2SnCl_2$ (**6**).

	4	**5**	**6**
empirical formula	C14 H24 N6 Sn	C16 H28 Cl6 N6 Sn2	C18 H32 Cl2 N6 O Sn
formula weight	395.08	754.52	538.09
temp (K),	203(2)	238(2)	238(2) K
λ (Å)	0.71073	0.71073	0.71073
space group	Pbca	C2/c	C2/c
a (Å)	8.282(3)	17.270(2)	12.354(3)
b (Å)	16.129(6)	13.821(1)	13.778(3)
c (Å)	23.783(8)	23.395(2)	14.123(4)
α (deg)	90	90	90
β (deg)	90	105.361(2)	110.900(3)
γ (deg)	90	90	90
V(Å^3),	3177(2)	5385(1)	2246(1)
Z	8	8	4
d_{calc} (g/cm^3),	1.652	1.861	1.591
μ (mm^{-1})	1.613	2.467	1.397
R1	0.0496	0.0428	0.0316
wR2	0.0788	0.1006	0.0731

Table 7.5. selected bond lengths(Å) and angles(°) for complex **4**

Distances			
Sn-N(11)	2.171(8)	N(5)-C(6)	1.373(11)
Sn-N(1)	2.204(7)	N(5)-C(10)	1.456(12)
Sn-N(7)	2.327(8)	N(11)-C(16)	1.350(11)
Sn-N(17)	2.394(7)	N(15)-C(16)	1.343(12)
C(4)-N(5)	1.458(12)	C(16)-N(17)	1.324(11)
Angles			
N(11)-Sn-N(1)	102.2(3)	C(6)-N(7)-C(8)	120.6(9)
N(11)-Sn-N(7)	88.8(3)	C(6)-N(7)-Sn	89.9(6)
N(1)-Sn-N(7)	58.2(3)	C(8)-N(7)-Sn	144.7(7)
N(11)-Sn-N(17)	57.9(3)	C(16)-N(11)-C(12)	121.0(9)
N(1)-Sn-N(17)	90.5(3)	C(16)-N(11)-Sn	99.0(7)
N(7)-Sn-N(17)	129.6(3)	C(12)-N(11)-Sn	138.2(7)
C(6)-N(1)-C(2)	123.7(8)	C(16)-N(15)-C(14)	120.8(9)
C(6)-N(1)-Sn	96.5(6)	C(16)-N(15)-C(20)	118.3(9)
C(2)-N(1)-Sn	135.6(6)	C(14)-N(15)-C(20)	118.8(8)
C(6)-N(5)-C(10)	120.3(9)	N(17)-C(16)-N(11)	112.2(11)
C(6)-N(5)-C(4)	119.0(9)	N(17)-C(16)-N(15)	125.5(10)
C(10)-N(5)-C(4)	116.9(8)	N(11)-C(16)-N(15)	122.2(10)
N(1)-C(6)-N(7)	113.9(9)	C(16)-N(17)-C(18)	119.7(9)
N(1)-C(6)-N(5)	122.9(9)	C(16)-N(17)-Sn	89.8(7)
N(7)-C(6)-N(5)	123.2(10)	C(18)-N(17)-Sn	147.0(7)

Table 7.6. selected bond lengths(Å) and angles(°) for complex **5**

Distances			
Sn(1)-N(1)	2.208(4)	N(2)-C(7)	1.352(6)
Sn(1)-N(2)#1	2.213(4)	N(2)-Sn(1)#1	2.213(4)
Sn(1)-Cl(1)	2.5293(15)	N(3)-C(7)	1.344(6)
Sn(2)-N(4)	2.214(4)	N(4)-C(14)	1.341(6)
Sn(2)-N(5)#2	2.217(4)	N(5)-C(14)	1.344(6)
Sn(2)-Cl(2)	2.5316(14)	N(5)-Sn(2)#2	2.217(4)
N(1)-C(7)	1.350(6)	N(6)-C(14)	1.347(6)
Angles			
N(1)-Sn(1)-N(2)#1	92.50(14)	C(14)-N(4)-C(8)	117.0(4)
N(1)-Sn(1)-Cl(1)	91.71(11)	C(14)-N(4)-Sn(2)	106.7(3)
N(2)#1-Sn(1)-Cl(1)	91.96(11)	C(8)-N(4)-Sn(2)	127.5(3)
N(4)-Sn(2)-N(5)#2	92.84(14)	C(14)-N(5)-C(11)	114.3(4)
N(4)-Sn(2)-Cl(2)	89.27(11)	C(14)-N(5)-Sn(2)#2	111.0(3)
N(5)#2-Sn(2)-Cl(2)	92.01(10)	C(11)-N(5)-Sn(2)#2	122.4(3)
C(7)-N(1)-C(1)	116.2(4)	C(14)-N(6)-C(10)	123.1(4)
C(7)-N(1)-Sn(1)	108.1(3)	C(14)-N(6)-C(13)	122.3(4)
C(1)-N(1)-Sn(1)	126.0(3)	C(10)-N(6)-C(13)	114.6(4)
C(7)-N(2)-C(4)	116.0(4)	N(3)-C(7)-N(1)	122.4(4)
C(7)-N(2)-Sn(1)#1	107.3(3)	N(3)-C(7)-N(2)	122.8(4)

C(4)-N(2)-Sn(1)#1	127.5(3)	N(1)-C(7)-N(2)	114.8(4)
C(7)-N(3)-C(3)	122.5(4)	N(4)-C(14)-N(5)	115.2(4)
C(7)-N(3)-C(6)	122.4(4)	N(4)-C(14)-N(6)	121.8(4)
C(3)-N(3)-C(6)	114.9(4)	N(5)-C(14)-N(6)	123.0(4)

Table 7.7. selected bond lengths(Å) and angles(°) for complex **6**

Distances			
Sn-N(2)	2.104(4)	N(1)-C(7)	1.326(6)
Sn-N(2)#1	2.104(4)	N(1)-C(1)	1.448(6)
Sn-N(1)	2.191(4)	N(2)-C(7)	1.326(6)
Sn-N(1)#1	2.191(4)	N(2)-C(6)	1.456(6)
Sn-Cl	2.4202(14)	N(3)-C(7)	1.344(6)
Sn-Cl#1	2.4202(14)	N(3)-C(3)	1.455(7)
Sn-C(7)	2.582(5)	N(3)-C(4)	1.453(6)
Sn-C(7)#1	2.582(5)		

Angles			
N(2)-Sn-N(2)#1	164.1(2)	N(2)-Sn-C(7)#1	136.64(16)
N(2)-Sn-N(1)	61.64(15)	N(2)#1-Sn-C(7)#1	30.76(15)
N(2)#1-Sn-N(1)	106.43(16)	N(1)-Sn-C(7)#1	101.35(15)
N(2)-Sn-N(1)#1	106.43(16)	N(1)#1-Sn-C(7)#1	30.89(15)
N(2)#1-Sn-N(1)#1	61.64(15)	Cl-Sn-C(7)#1	122.62(12)
N(1)-Sn-N(1)#1	92.2(2)	Cl#1-Sn-C(7)#1	96.80(11)
N(2)-Sn-Cl	99.11(12)	C(7)-Sn-C(7)#1	123.0(2)
N(2)#1-Sn-Cl	91.87(12)	C(7)-N(1)-C(1)	119.1(4)
N(1)-Sn-Cl	93.50(12)	C(7)-N(1)-Sn	91.1(3)
N(1)#1-Sn-Cl	153.42(11)	C(1)-N(1)-Sn	148.8(3)
N(2)-Sn-Cl#1	91.87(12)	C(7)-N(2)-C(6)	119.6(4)
N(2)#1-Sn-Cl#1	99.11(12)	C(7)-N(2)-Sn	95.0(3)
N(1)-Sn-Cl#1	153.42(11)	C(6)-N(2)-Sn	143.2(3)
N(1)#1-Sn-Cl#1	93.50(12)	C(7)-N(3)-C(3)	120.8(4)
Cl-Sn-Cl#1	92.88(7)	C(7)-N(3)-C(4)	120.3(4)
N(2)-Sn-C(7)	30.76(15)	C(3)-N(3)-C(4)	118.9(4)
N(2)#1-Sn-C(7)	136.64(16)	N(2)-C(7)-N(1)	112.3(4)
N(1)-Sn-C(7)	30.89(15)	N(2)-C(7)-N(3)	123.6(4)
N(1)#1-Sn-C(7)	101.35(15)	N(1)-C(7)-N(3)	124.1(5)
Cl-Sn-C(7)	96.80(11)	N(2)-C(7)-Sn	54.3(2)
Cl#1-Sn-C(7)	122.62(12)	N(1)-C(7)-Sn	58.0(2)
N(3)-C(7)-Sn	177.6(4)		

References for Chapter Seven

[1] Bailey, P.J.; Gould, R.O.; Harmer, C.N.; Pace, S.; Steiner, A.; Wright, D.S. *Chem. Commun.* **1997**, 1161

[2] Bailey, P.J.; Blake, A.J.; Kryszczuk, M.; Parsons, S.; Reed, D. *J. Chem. Soc., Chem. Commun.*, **1995**, 1647

[3] Chivers, T.; Parvez, M., Schatte, G. *J. Organomet. Chem.* **1998**, *550*, 213

[4] Cotton, F.A.; Timmons, D.J. *Polyhedron* **1998**, *17*, 179

[5] Cotton, F.A.; Matonic, J.H.; Murillo, C.A. *J. Am. Chem. Soc.* **1997**, *119*, 7889

[6] Bear, J.L.; Li, Y.; Hen, B.; Kadish, K.M. *Inorg. Chem.* **1996**, *35*, 1395.

[7] Cotton, F.A.; Murillo, C.A.; Timmons, D.J. *Chem. Commun.* **1999**, 1427.

[8] Aeilts, S.L.; Coles, M.P.; Swenson, D.G.; Jordan, R.F.; Young, V.G. *Organometallics* **1998**, *17*, 3265

[9] Zhou, Y.; Richeson, D.S.; *Inorg. Chem.* **1997**, *36*, 501

[10] Tin, M.K.T.; Thirupathi, N.; Yap, G.P.A.; Richeson, D.S. *J Chem. Soc., Dalton Trans.* **1999**, 2947

[11] Similar structures have been noted for Sn(II) amidinato complexes. Zhou, Y.; Richeson, D.S. *J. Am. Chem. Soc.* **1996**, *118*, 10850

Alkylamidinato and Guanidinato Complexes of Iron

8

"do I feel lucky?"

Chapter Eight

Introduction

The preceding sections of this thesis have demonstrated the versatility of the $RNXNR^-$ (X = CR', NR'R") anion ligand framework with particular emphasis on the application of these ligands to main group metal species. Furthermore, the literature provides ample precedent for amidinates as supporting ligands for a variety of transition metal complexes and particularly for compounds of the early transition metals.[1] Guanidinates have received a much more limited attention as ligands in organometallic and coordination chemistry. In Chapter One we presented the common features and the anticipated differences between amidinate and guanidinate ligands (Chart 8.1). The obvious relation of guanidinates with amidinates first attracted us to the application of these ligands and the possibility that guanidinate ligands may exhibit alternative/unusual binding metal bonding modes was intriguing. We have chosen to focus on N, N', N"-trisubstituted guanidinates in order to fully exploit these potential novel interactions. For example, a trisubstituted guanidinate ligand can be further deprotonated to afford a dianionic species that may exhibit π delocalization (Y conjugation) of the lone pairs on the sp^2 hybridized nitrogen centers making it an analogue of the trimethylene methane dianion (Chart 8.2).

Chart 8.1

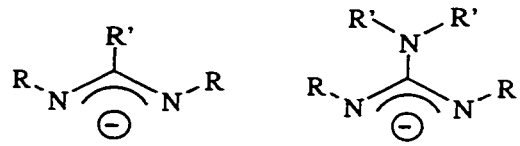

Amidinate Guanidinate

In this section of the thesis we report the extension of our efforts to encompass some fundamental aspects of the use of these ligands in the preparation of iron complexes. Among the features that attracted us to this area are that these species represent rather novel ancillary ligands in the organometallic chemistry of Fe, such ligands have the potential to generate novel complexes with Fe-Fe bonds, the target complexes may have applications to catalysis, and the chemistry of Fe carboxylates, an isoelectronic ligand, is particularly rich.

Chart 8.2

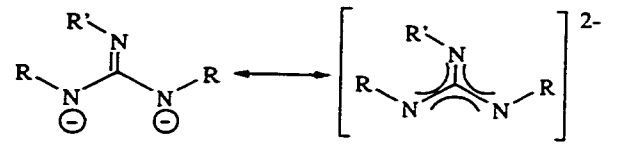

Iron may have more organometallic derivatives than any other transition metal.[2] Among the contributing factors for this feature are the ready availability of a range of suitable iron starting materials as well as the low cost and toxicity of Fe compounds. Due to the stereochemical stability exhibited by many of these compounds organoiron complexes have found various applications in organic synthesis. Particularly dominant supporting ligands in Fe organometallic chemistry are η^4- and η^5-diene, CO and Cp-based ligands.

Despite the growing interest in organometallic complexes bearing nitrogen ligands, few such compounds of iron have been made and these are largely limited to simple nitrogen bases such as pyridine or bipyridine and macrocyclic ligands such as porphyrins. Simple iron compounds with nitrogen donor bases are not very common.[2]

The first structurally characterized monomeric Fe(II) diamide $Fe[N(SiMe_3)]_2$ was only relatively recently synthesized.[3]

In dinuclear M-M bonded complexes of the heavy transition metals, lantern-type complexes are frequently found.[4] Amidinate and triazenate ligands ($RNXNR^-$; X = CR', N) have played an instrumental role in the formation of such species (**I**). In fact

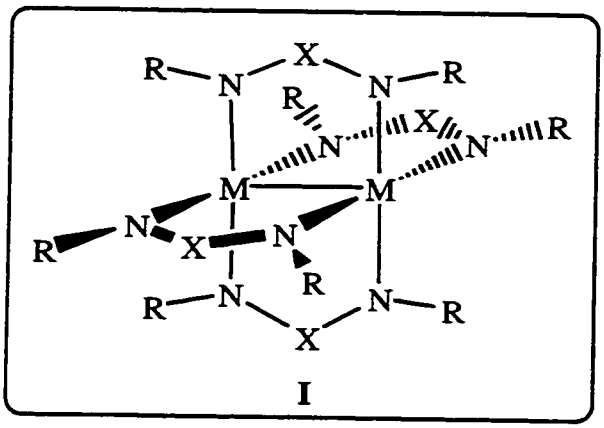

I

there are more metal-metal bonded complexes with more different metallic elements of these ligands than any other ligand type. Compounds possessing M-M bonds with lantern-type structures are less common for the 1st row transition metals. Furthermore, while short intermetallic distances with well-accepted metal-metal bonds have been described for a variety of transition metal species, Fe-Fe bonding is still rare and somewhat controversial. There are some binuclear Fe compounds that display features indicative of bonding (see below).

In terms of general reactivity, iron complexes have attracted attention as polymerization catalysts. Complexes of Fe(II) are reported to polymerize a range of monomers possessing a variety of functional groups (e.g. acrylonitrile, methyl methacrylate, acrolein). Recently, Fe(II) complexes bearing neutral iminopyridine ligands have been added to the growing number of non-metallocene olefin polymerization catalysts.[5]

Finally, carboxylate anions have been particulary important ligands in the chemistry of Fe. The relationship of carboxylates, amidinates and guanidinates was presented in Chapter 1.

Reported Fe Amidinate and Guanidinate Complexes

The literature regarding application of amidinate and guanidinate ligands to Fe complexes is surprisingly sparse. The study of amidinate complexes of iron has been limited by the reactivity features of the complexes. Iron(II) and iron(III) amidinate complexes have a tendency to be unreactive toward or be decomposed by reducing, electrophilic and nucleophilic reagents.[6] Attempts have been made to employ N,N'-di(aryl)acetamidinate (DAAc), N, N'-bis(trimethylsilyl)benzamidinate (TMSBz), N, N'-diphenylbenzamidinate (DPhBz), and N, N'-diphenylformamidinate (DPhF) in the preparation of Fe complexes with varying degrees of effort and success.

In an early investigation the reactions of several lithium amidinate salts with iron halides was explored. Reaction of N,N'-di(aryl)acetamidinate lithium (aryl = phenyl, p-tolyl) with $FeCl_3$ produced extremely air and moisture sensitive navy blue solids characterized as $Fe[ArNC(Me)NAr]_3$ (**II**) while a similar reaction with N,N'-di(phenyl)benzamidinate gave soluble red and air stable green products.[7] With N,N'-diphenylformamidinate lithium a red complex was

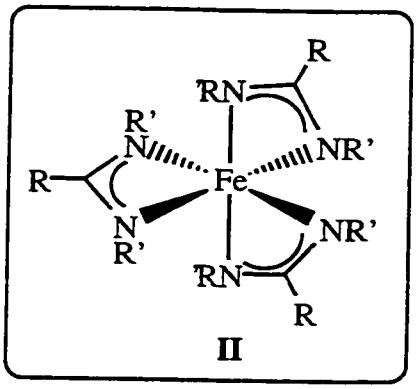

II

isolated. In all cases the complexes were formulated as Fe(amidinate)$_3$ but the properties indicated association which was speculated to occur through bridging groups. Iron (II) reacted with lithium N,N'-di(tolyl)acetamidinate in a 1:2 ratio to give a brown and a red product. All of the products of this study were characterized solely by elemental analysis and mass spectroscopy.

The only reported complex of N,N'-bis(trimethylsilyl)benzamidinate, PhC[N(SiMe$_3$)]$_2$FeCl (**III**), was prepared from the reaction of FeOCl with N, N, N'-tris(timethylsilyl)benzamidinate. Structural characterization of this compound was reported. Although this compound certainly represents an interesting precursor to

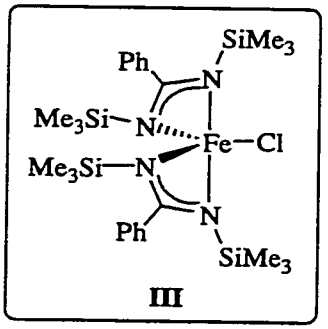

III

novel Fe(III) complexes, which might be accessible through a metathesis reaction of the Cl ligand, no reactivity has been reported. [1,8]

Cotton and coworkers have investigated several Fe(II) complexes of N, N'-diphenyl formamidinato and N, N'-diphenyl benzamidinato ligands. One of their goals was to investigate the ability of these systems to form M-M bonded complexes. The reaction of $FeCl_2$ with N,N' diphenylformamidine (HDPhF) generated $FeCl_2(HDPhF)_2$. Subsequent reaction with MeLi led to the formation of $Fe_2(DPhF)_4$, a complex which exhibited four bridging ligands that are highly distorted compared to analogous lantern type structures of the formula M_2(amidinato)$_4$ (Scheme 8.1).[9,10] In contrast, the reaction of $FeCl_2(HDPhF)_2$ with BuLi led to the formation of $Fe_2(DPhF)_3$ which contains a mixed valence dinuclear iron unit bridged by three

formamidinato groups with the shortest known Fe-Fe bond of 2.2318(18)Å (Scheme 8.1)[11].

The diphenyl(benzamidinate) ligand afforded a different product. Reaction of $FeCl_2(HDPhBz)_2$ (HDPhBz = N,N'-diphenylbenzamidine) with MeLi gave $Fe_2(\mu\text{-}DPhBz)_2(DPhBz)_2$ (**IV**) which exhibited an unusual dinuclear structure with two amidinato groups form bridges between the metal centers while the other two ligands each chelate to one of the iron centers.[9] The Fe coordination geometry in this complex is highly irregular with N-Fe-N angles ranging from 62.6 for the chelating group to 155.0 for the angle between the N atoms of the bridging groups. A fifth nitrogen "interacts" with each Fe center at a distance of 2.477(4)Å across the 8-membered ring formed by the bridging ligands. The nature of this interaction is unclear but it seems to cause a distortion of the bridging ligand. The authors of this study felt that this interaction was "too long for a bond and too short for a simple van der Waals interaction".[9] The Fe-Fe distance of 3.124(1)Å precludes

Scheme 8.1

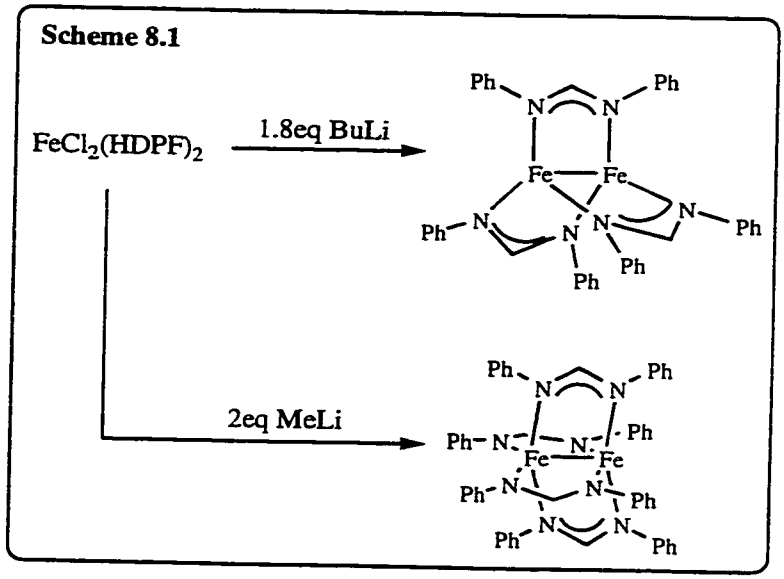

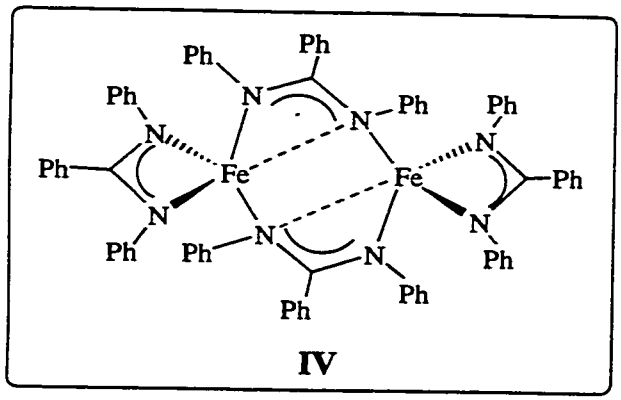

IV

the presence of an M-M bond. Furthermore, the reported magnetic data is consistent with two independent high-spin Fe atoms. A similar distortion has also been reported in a rhodium triazenide complex.[12]

Direct reaction of $FeCl_2$ with the formamidinate anions is reported to yield tris(chelate) complexes - $Fe(DPhF)_3$ and $Fe(DPhTA)_3^-$.[13] The complex $Fe(DPhF)_3$ will react with trace H_2O to produce a structurally characterized Fe(III) oxo species $Li_2(HDPhF)_2Fe_4O_4(DPhF)_6$ which has an eight membered ring of alternating iron and oxygen atoms where the iron atoms are bridged by amidinato groups.

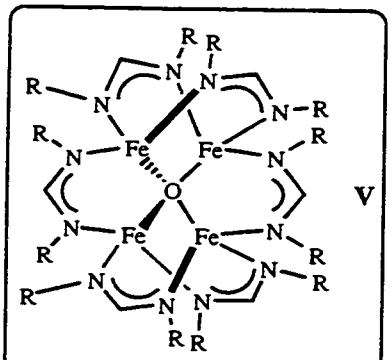

V

Two interesting oxo complexes exhibiting $(\mu^4\text{-}OFe_4)^{6+}$ cores , $Fe_4O(DPhF)_6$ and $Fe_4O(BBPhF)_6$ (BBPhF = N, N'-bis(biphenyl)formamidinate), are reported to arise from the controlled exposure of Fe_2L_3 complexes to O_2. The structure observed for $Fe_4O(DPhF)_6$ (**V**), somewhat related to basic beryllium acetate, exhibits an oxygen atom in a distorted tetrahedron of Fe atoms.[14] In addition to the oxo ligand, each metal is coordinated to three N atoms of three different amidinates. All of the formamidinate ligands are bridging but are not distributed evenly along the six edges of the metal tetrahedron which leads to three different sets of Fe-Fe distances. Two edges of the Fe_4 tetrahedron are bridged by two formamidinates (Fe-Fe approx. 2.85Å), two other edges are bridged only by one ligand (Fe-Fe approx. 3.17Å) and the remaining two edges are unbridged (Fe-Fe approx. 3.50Å). The room temperature magnetic moment of $3.38\mu_B$/Fe unit indicates some degree of antiferromagnetism is present.

Clearly the reported amidinate chemistry with Fe(II) and Fe(III) is very complex and products obtained show a dependence on choice of ligand, choice of starting material, and even the identity of the alkyl lithium reagent employed in the ligand deprotonation.[15]

Interestingly, the first transition metal complexes with dianionic guanidinate ligands are represented by a pair of related diiron complexes (Scheme 8.2). These species, $Fe[(NR)_3](CO)_3$ (R = ^{i}Pr, Cy) were formed by the reaction of dicyclohexylcarbodiimide and diisopropylcarbodiimide with $Fe(CO)_5$.[16] These complexes remained as unique examples of transition metal coordinated guanidinate dianions until 1996 when Pt[(NPh)2C=NPh](cod), cod = cyclooctadiene) was isolated and characterized.[17]

Scheme 8.2

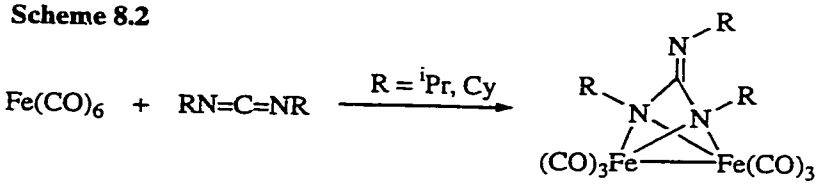

Given the limited application of amidinate and guanidinate ligands in Fe chemistry we set out to extend our investigations to include an exploration of the use of amidinates and trisubstituted guanidinates as supporting ligands with iron in both oxidations states (II) and (III). This was necessarily an exploratory effort and as such required the definition of methodologies for the introduction of these ligands into the iron coordination sphere as well as definition of the reactivity of these species. At the ouset we anticipated that the products of this study would be dominated by, and may be exclusively paramagnetic species. As a result there is a heavy reliance on single crystal

X-ray structural analysis for confirmation of connectivity of the complexes that were prepared from this effort.

Specifically, we present in this Chapter results regarding the use of N, N'-dicyclohexylformamidinate as a ligand with Fe(II) to yield $Fe_4(\mu_4\text{-}O)(\mu\text{-}Br)_2(\mu\text{-}CyNCHNCy)_4$ (**1**) and a comparison of these results with those obtained when the bulky alkyl amidinate, $CyNC^tBuNCy^-$, is employed with Fe(II). The only known mononuclear Fe(II) alkylamidinate species $Fe(CyNC^tBuNCy)_2$ (**2**) is reported. We further extended this chemistry to Fe(III) by introducing the $CyNC^tBuNCy^-$ into the coordination sphere of Fe(III) to form the monomeric species $(CyNC^tBuNCy)_2FeCl$ (**3**).

Our application of guanidinates as ligands with Fe(II) and (III) has led to a range of complexes. The preparation of these species as well as their reactivity, which is dominated by dinuclear complexes, is presented. For example, the use of trisubstituted guanidinates as ligands resulted in the formation of the dinuclear Fe(II) species $[\mu\text{-}(RN)_2C(HNR)]_2Fe_2[(RN)_2C(HNR)]_2$, R = iPr, Cy (**5** and **6**) as well as $[\mu\text{-}(CyN)_2C(HNCy)]_2Fe_2Br_2$ (**7**). With Fe(III), the mononuclear species $[(^iPrN)_2C(HN^iPr)]_2FeCl$ (**4**) is formed. The use of bulky tetrasubstituted guanidinates resulted in the formation of mononuclear species $[(^iPrN)_2C(N(SiMe_3)_2)]_2Fe$ (**11**). Subsequent alkylation attempts resulted in the formation of dianionic guanidinate complexes $[(^iPrN)_2C{=}N^iPr]_2Fe_2[(^iPrN)_2C(HN^iPr)Li]_2$ (**8**) and $Li_2(THF)Fe[(^iPrN)_2CN^iPr](CH_2SiMe_3)_2$ (**10**) as well as the rearrangement product $[\mu\text{-}(^iPrNCN^iPr)_2(HN^iPr)]Fe_2[(^iPrN)_2C(HN^iPr)]_2$ (**9**).

Results and Discussion

Amidinate Complexes:

Fe(II) Complexes of the (CyNCHNCy) Anion. Reaction of the lithium salt of N,N'-dicyclohexylformamidine with $FeBr_2$ in a 1:1 stoichiometry afforded, after crystallization from ether, the new species **1** (Scheme 8.3). Addition of a second

Scheme 8.3

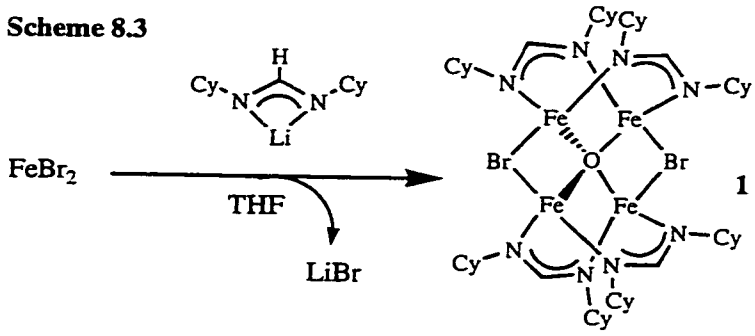

1

equivalent of the lithium salt produced no further reaction. The structure of **1** was determined by single-crystal X-ray diffraction analysis (Table 8.1). This species crystallized with two independent molecules in the asymmetric unit, both of these exhibited similar bonding parameters and the results of this analysis are presented in Figure 8.1 and Table 8.2.

As seen in Figure 8.1, compound **1** is a tetranuclear oxo species possessing the formula $Fe_4(\mu_4\text{-}O)(CyNCHNCy)_2Br_2$. The oxygen atom lies at the center of highly distorted tetrahedron of Fe(II) atoms. The Fe centers have a distorted tetrahedral coordination environment consisting of nitrogen atoms of two bridging formamidinates, the μ_4-O, and a bridging bromide. The Fe-O and Fe-N bond distances are regular and only deviate slightly from the average of 1.99 and 2.02Å respectively. The average Fe-Br distance is 2.58Å.

Figure 8.1. Molecular structure and atom numbering scheme for $Fe_4(\mu_4\text{-}O)(\mu\text{-}Br)_2(\mu\text{-}CyNCHNCy)_4$ (1). Hydrogen atoms have been omitted for clarity.

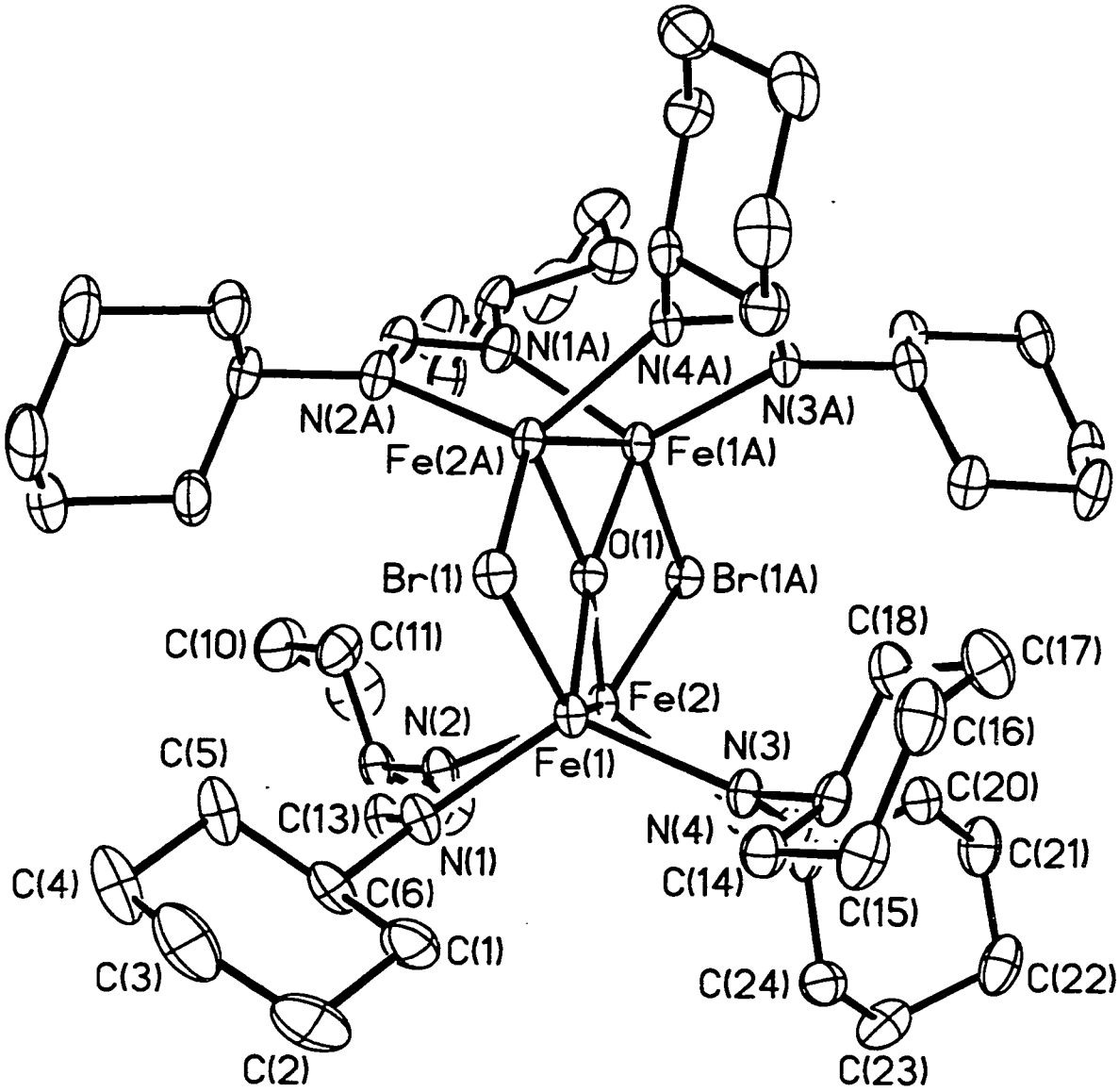

Despite the wealth of know iron-oxo complexes with carboxylate ligands,[18] **1** has only one analogue in the literature. This complex is obviously related to the previously reported species $Fe_4O(DPhF)_6$ (**V**). Like this complex the distribution of bridging ligands is not uniform and leads to three sets of Fe-Fe distances. In the case of **1**, two of the edges of the M_4 tetrahedron are bridged by two formamidinate ligands and exhibit a short average Fe-Fe distance (2.50Å), two of the edges are bridged by a Br atom and exhibit a longer average Fe-Fe distance (3.11Å), two of the edges remain unbridged and the resulting average Fe-Fe distance is quite long (3.91Å).

The source of the oxygen atom in **1** is, as yet, unknown. The results are however reproducible and all steps were taken to ensure an oxygen and moisture free environment. The reaction to produce **1** was easily repeated in THF and ether as reaction solvent with the identical results. However, reaction did not proceed if hexane or toluene was used as the reaction solvent. In the case of the reported complex $Fe_4O(DPhF)_6$ (**V**) the source of the O atom was presumed to be a small amount of molecular oxygen.

Fe(II) Complexes of CyNC(^{t}Bu)NCy Anion. Including complex **1**, all structurally characterized amidinate complexes of iron have been either formamidinate or benzamidinate species and other than the "tris" complexes all are polynuclear. In order to assess the effect of modification of the group on the central carbon atom of the amidinate we investigated the ability of the CyNC(^{t}Bu)NCy anion to generate stable Fe(II) species. ^{t}BuLi reacts quickly with an equivalent amount of dicyclohexylcarbodiimide at room

Scheme 8.4

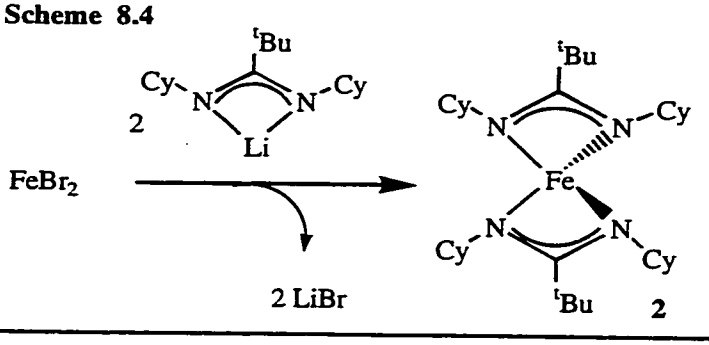

temperature. Subsequent addition of 0.5 eq $FeBr_2$ followed by recrystallization resulted in the monomeric Fe^{II} amidinate complex $Fe(CyN(^tBu)NCy)_2$ in 75% yield (Scheme 8.4).

Given the paramagnetic nature of **2**, the molecular structure of this complex was investigated by a single X-ray structure determination (Table 8.1). Structural analysis revealed a monomeric complex with two chelating bidentate amidinate ligands coordinated to the Fe (II) center, which was in a coordination environment based on a distorted tetrahedron (Figure 8.2 and Table 8.3). There were no anomalously short intermolecular contacts. The Fe-N bond lengths were regular (2.012, 2.028, 2.013 and 2.025 Å) and are slightly shorter than those reported for the iron(II) lantern type structure $Fe_2(DPF)_4$ which varied from 2.065 to 2.186 Å. The two nitrogen atoms and bridging carbon atom lie in a plane that includes the Fe atom where the sum of the internal angles equals 360°. The N-Fe-N angles fall into two groups the two ligand bite angles of 65.34(6)° and 65.29(6)° and the remaining four N-Fe-N angles that range from 124.79(6)°to 143.51(6)°. With an average for the six angles of 111.5° As might be expected, the sterically more demanding t-butyl group prevented bridging of the ligand.

Figure 8.2. Molecular structure and atom numbering scheme for $Fe(CyN(^tBu)NCy)_2$ (**2**). Hydrogen atoms have been omitted for clarity.

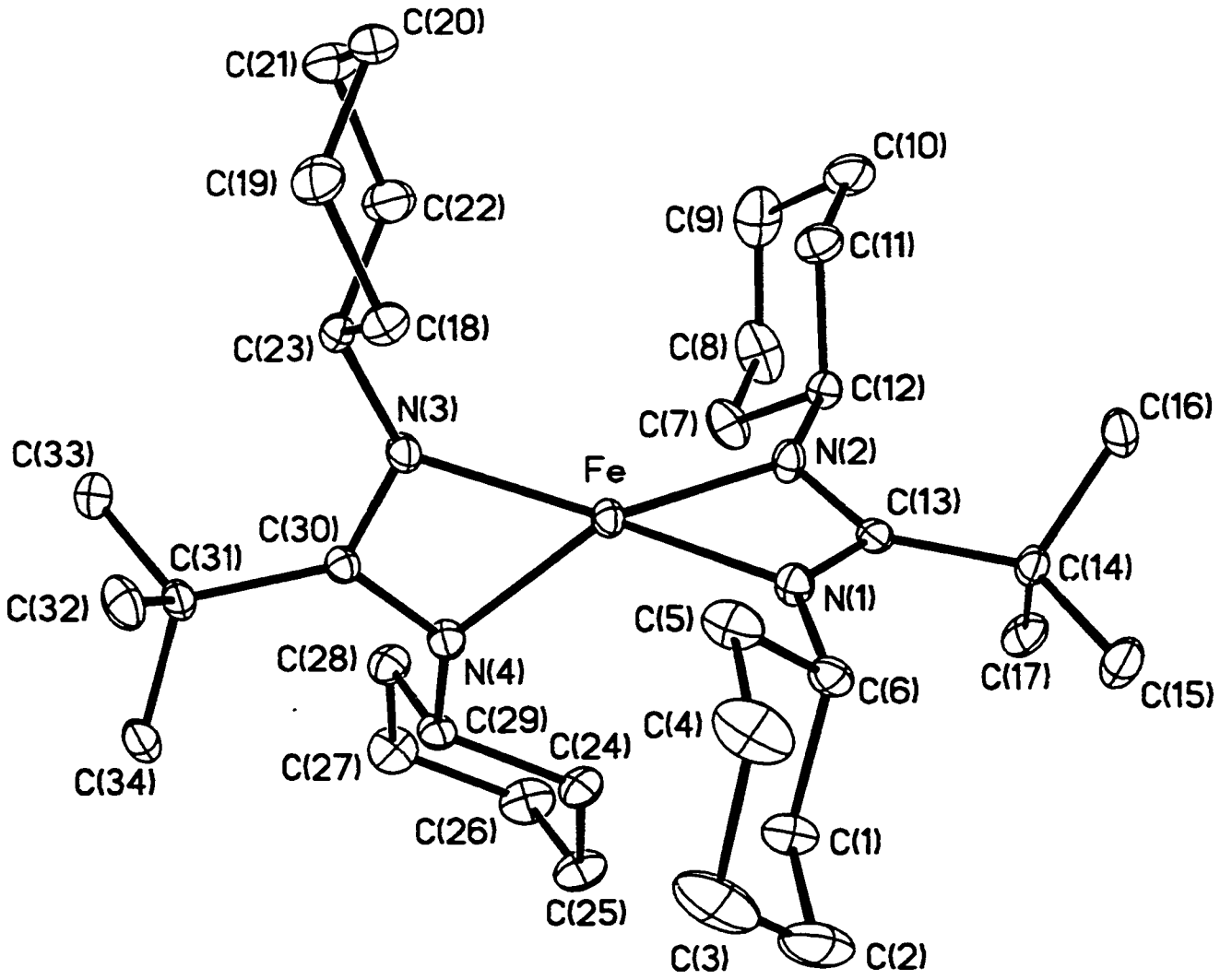

Fe(III) Complexes of the CyNC(^{t}Bu)NCy Anion. Prompted by the previous results we decided to extend the aforementioned methodology to the formation of new iron(III) amidinate complexes in order to investigate the effects of bulky amidinates on Fe(III) centers. Addition of $FeCl_3$ to two equivalents of the *in situ* generated alkylamidinate lithium salt in diethylether afforded the monomeric Fe(III) amidinate complex $(CyNC^tBuNCy)_2FeCl$ in 67% yield (Scheme 8.5).

Scheme 8.5

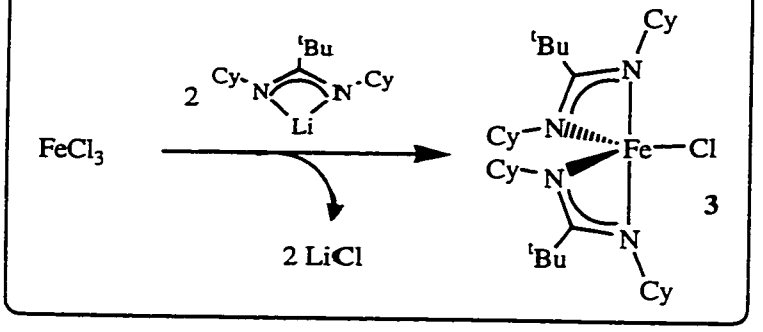

Blue crystals of **3** could be isolated from this solution upon removal of LiCl, concentration and cooling. A crystallographic structure determination was carried out to assess the detailed identity of this Fe complex (Table 8.1). As revealed in Figure 8.3 and Table 8.4, this analysis revealed a mononuclear species with two chelating bidentate amidinate ligands coordinated to an Fe(III) center in a distorted trigonal bipyramidal geometry where the coordination sphere of the metal is completed by a chloride anion. Each of the four Fe-N bond distances in **3** is unique but the values fell into a fairly narrow range (2.039(6), 2.050(7), 1.993(6) and 2.072(6)Å) with an average value of 2.039Å which correlates favourably with other reported iron amidinates. Interestingly, this Fe(III) complex actually has slightly longer Fe-N bond distances than **2** with an Fe(II) center. This is presumably an effect of the increased steric congestion in **3** compared with **2**. The

related complex $(Me_3SiNC(Ph)NSiMe_3)_2FeCl$ (**III**), the only other structurally characterized Fe(III) amidinate, displayed very similar bonding parameters to **3**.

Compound **3** certainly looks interesting as a starting material for Cl metathesis reactions. Unfortunately, several attempts to alkylate **3** with a variety alkyl lithium and alkyl Grignard reagents have not provided conclusive results. The inability to obtain a single pure product coupled with the paramagnetic nature of the products has frustrated efforts to develop this chemistry. Furthermore, as reported below, these reactions are likely complicated by the reduction of the Fe(III) center in **3** to Fe(II) products.

Figure 8.3. Molecular structure and atom numbering scheme for $(CyNC^tBuNCy)_2FeCl$ (**3**). Hydrogen atoms have been omitted for clarity.

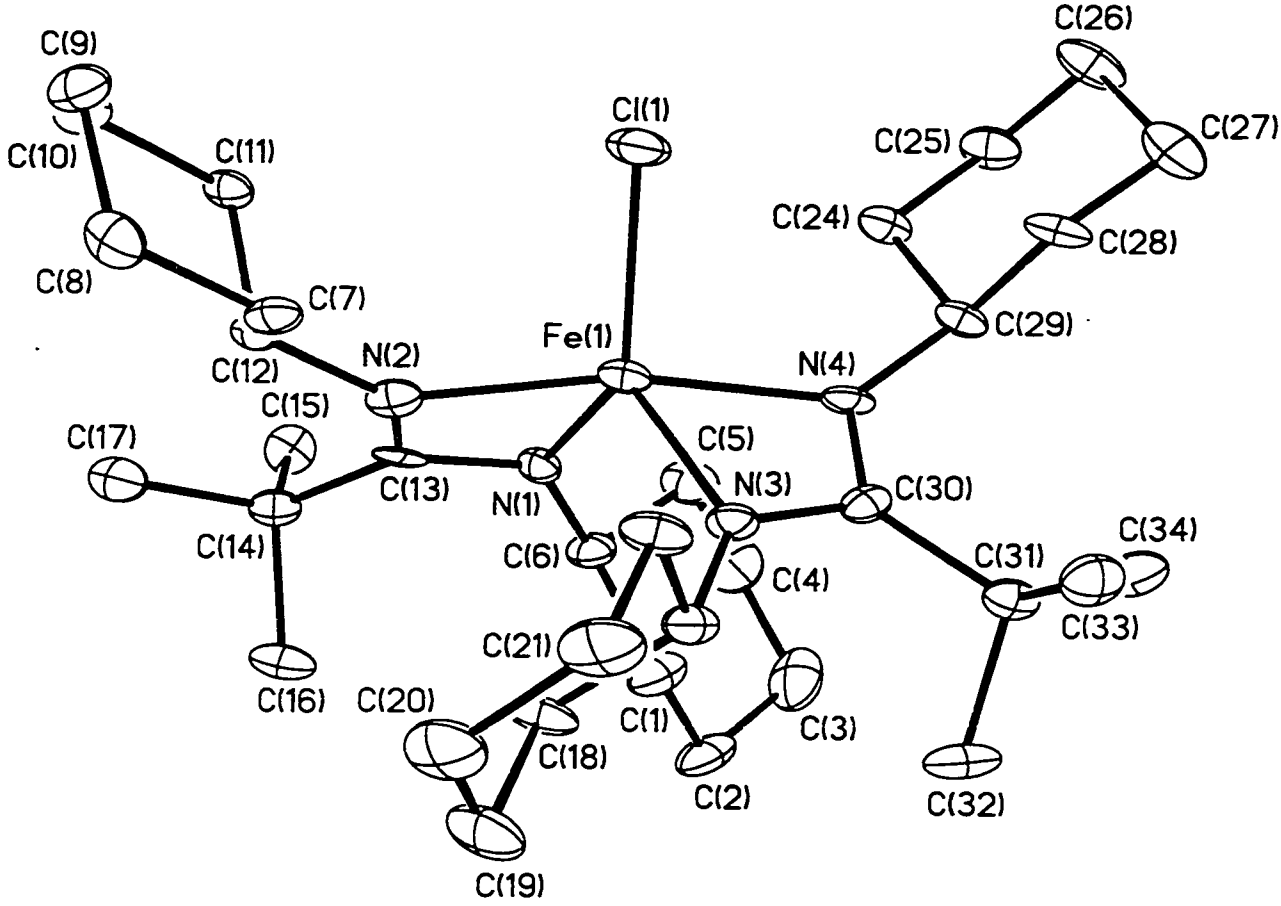

Guanidinate Complexes:

Our initial results for the application of amidinates as ligands for Fe(II/III) centers encouraged our initial foray into the guanidinate chemistry of iron. The chemistry that was observed is more complex than that of the group 14 metals. A strong dependence on both starting materials and choice of solvent was noted. The complexes are exceedingly air and moisture sensitive and the subsequent reactivity for Fe(III) complexes is dominated by reduction of the iron center to Fe(II).

Fe(II/III) Complexes of N, N', N"-Tri(alkyl)guanidinate Anions. The N,N',N"-tri(alkyl)guanidinato lithium [[$(RN)_2C(HNR)$]Li (R = ^{i}Pr, Cy) starting materials were formed by direct reaction of the guanidine with one equivalent of either MeLi or ^{n}BuLi. In all cases, metathesis reactions with iron halides (Scheme 8.6) were carried out with freshly prepared solutions of lithium guanidinate in ether or THF.

Addition of 0.5 equiv $FeCl_3$ to a solution of [(^{i}PrN)$_2$C(HN^{i}Pr)]Li followed by recrystallization from pentane resulted in isolation of the new bis(guanidinate) iron(III) chloride complex [(^{i}PrN)$_2$C(HN^{i}Pr)]$_2$FeCl, **4** (Scheme 8.6). We anticipated that complex would be analogous to amidinate complex (CyNC^{t}BuNCy)$_2$FeCl (**3**). Confirmation of this hypothesis and determination of the connectivity of **4** was provided by single X-ray diffraction analysis (Table 8.5) which revealed a monomer with two monoanionic chelating bidentate guanidinate ligands yielding planar M-N-C-N cycles as shown in Figure 8.4. The coordination sphere of the metal is completed by a terminal chloride to

yield a distorted pseudo-trigonal bipyramidal geometry for **4**. A list of selected bond distance and angles can be found in Table 8.6.

Figure 8.4. Molecular structure and atom numbering scheme for $[(^{i}PrN)_2C(HN^{i}Pr)]_2FeCl$ (**4**). Hydrogen atoms have been omitted for clarity.

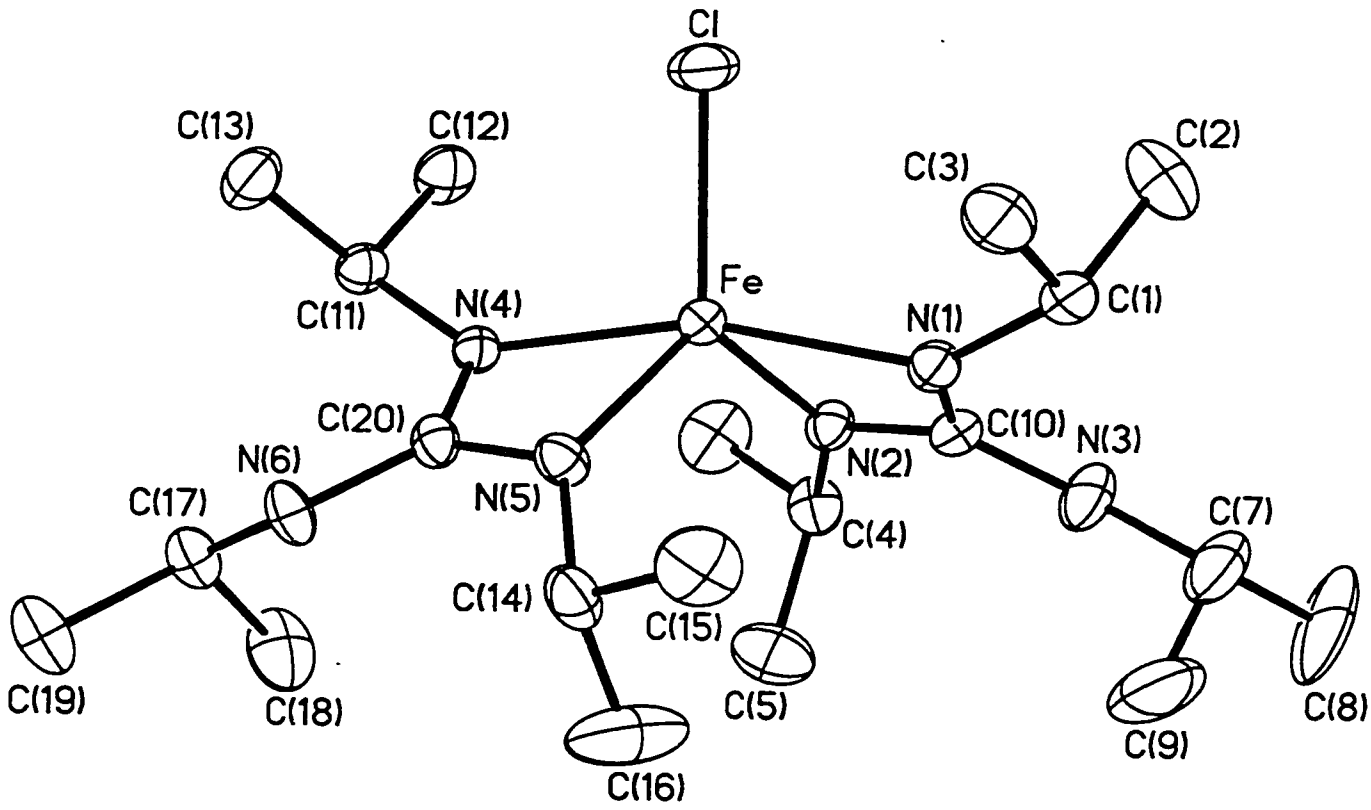

Scheme 8.6

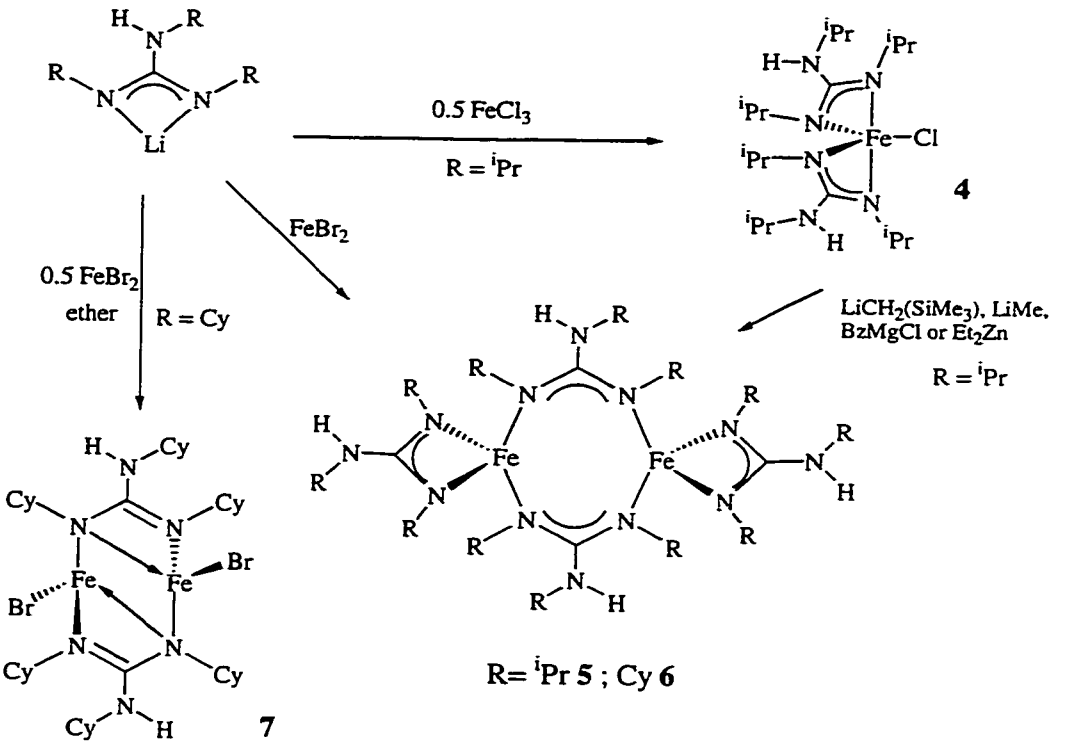

The point symmetry of **4** is approximately C_2 with the equatorial plane defined by Cl, N(2), and N(5) (Σ angles 360°) and the angle N(1)-Fe-N(4) of 162.05(12)° representing the pseudo-axial angle the termini of the guanidinate ligands can be divided into two types; the axial ^{i}PrN groups (N(1), N(4)) and the equatorial ^{i}PrN groups (N(2), N(3)). The average Fe-N_{axial} bond distances were 2.085(3)Å while the average equatorial bond distances were 2.008(3)Å.

The average C-N bond distances within the chelate ring are 1.34Å in one of the ligands and 1.36Å in the other. These bond distances are consistent with partial double bond character within the NCN moiety.

An alternative description of the coordination geometry of **4** is as a trigonal planar complex using the central C atoms (C(10) and C(20)) of the guanidinate ligands and the Cl ligand to define the three vertices. Consistent with this description, the angles defined by these atoms and the Fe center sum to 360°.

Attempts to exchange the chloride ligand of **4** with an alkyl group using a variety of alkylating reagents including RLi (R = Me, $CH_2(SiMe_3)$), $ZnEt_2$, and BzMgCl were examined. In all cases, reduction of the metal center from Fe(III) to Fe(II) was observed to yield complex **5** in 40-80% yields. This new product was determined to be a dinuclear species with two bridging guanidinate ligands and two chelating bidentate ligands with the formula $[\mu\text{-}(^i\text{PrN})_2\text{C}(\text{HN}^i\text{Pr})]_2\text{Fe}_2[(^i\text{PrN})_2\text{C}(\text{HN}^i\text{Pr})]_2$ (Scheme 8.6). Another route to the Fe(II) dinuclear species **5** was offered by direct reaction of $FeBr_2$ with 2 equiv of $[(^i\text{PrN})_2\text{C}(\text{HN}^i\text{Pr})]\text{Li}$ in THF followed by recrystallization from ether. This method led to isolation of **5** in 82% yield.

The formulation of complex **5** presented in Scheme 8.6 was confirmed through a single crystal X-ray diffraction study (Table 8.6). The results of the structural analysis of **5** are presented in Figure 8.5 and Table 8.7. and revealed a dinuclear Fe(II) complex with four monoanionic guanidinate ligands in two different coordination modes. Two of the guanidinates form bridges between the iron atoms while the other two groups are each chelating different iron atoms. The two chelating bidentate ligands are planar and exhibit bonding parameters reminiscent of other complexes with chelating monoanionic guanidinates such as **4**.

In contrast the bridging ligands appear to be quite distorted. The central C atoms (C(30), C(40)) of both of these groups are planar and the four N centers (N(7), N(8), N(10), N(11)) deviate only slightly from planarity. The CN bond distances within the bridging groups are indicative of delocalized π-bond (C(30)-N(7) 1.321(10)Å, C(30)-N(8) 1.330(10)Å, N(10)-C(40) 1.339(10)Å, N(11)-C(40) 1.340(10)Å). Furthermore, the average C-N(H)^{i}Pr distance of 1.41Å indicates a CN single bond. However, the ligand is far from planar and exhibits a decided twist. A measure of the ligand twist is provided by the Fe(1)-N(7)-N(8)-Fe(2) and the Fe(1)-N(10)-N(11)-Fe(2) dihedral angles (α, Chart 8.3) which have values of 67.2° and 70.3° respectively.

Chart 8.3

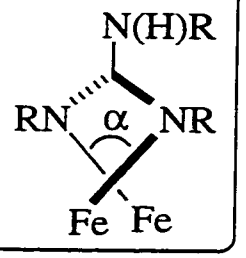

Figure 8.5. Molecular structure and atom numbering scheme for [μ-(^{i}PrN)$_2$C(HN^{i}Pr)]$_2$Fe$_2$[(^{i}PrN)$_2$C(HN^{i}Pr)]$_2$ (**5**). Hydrogen atoms have been omitted for clarity.

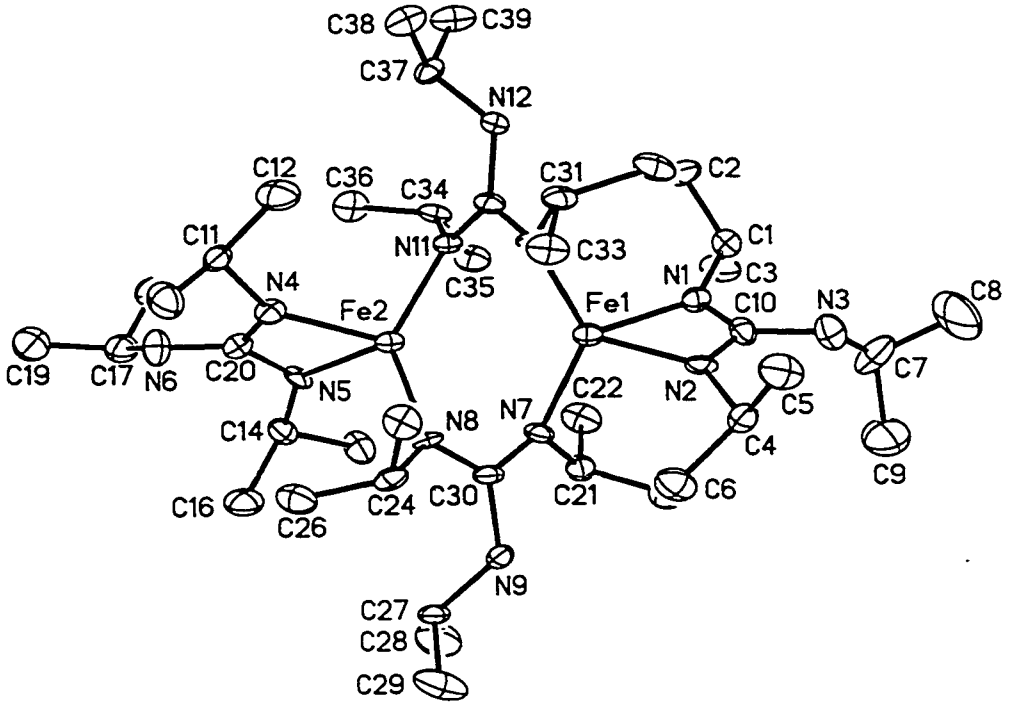

The coordination sphere for both Fe centers is composed of four nitrogen centers of the two different ligands. The N-Fe-N bond angles exhibit a broad range of values varying from 63.3° for the chelating ligands to 132.3° for the bridging ligands with average values of 106°. The Fe-N bond distances vary from 2.056(6) to 2.127(7)Å.

Complex **5** has many analogous structural features with $Fe_2(\mu\text{-DPhBz})_2(DPhBz)_2$ (**IV**) including a similar distortion of the bridging ligand.[19,12] In the case of **IV** the severe distortion of the bridging ligands was attributed to a weak intramolecular Fe···N interaction at a distance of 2.477(4)Å as depicted on page 180. In the case of **5** the closest non-coordinated N atoms to Fe(1) and Fe(2) are N(11) and N(7) at distances of 2.970Å and 3.007Å respectively. This distance is considerably further than in **IV** and not likely the result of an interaction between these atoms. The possibility of an Fe-Fe bond in **5** is excluded by the large iron-iron separation of 3.264 Å. It is worthwhile to note that the molybdenum complex $Mo_2[\mu\text{-}\eta^2\text{-}(NPh)_2CNHPh]_4$ has been prepared with trisubstituted guanidinate ligands.[20] All four guanidinate ligands bridge the two metal centers resulting in the formation of a metal-metal bond where none of the bridging ligands demonstrate the distortion exhibited by complexes **5** and **6**.

Reaction of $FeBr_2$ with 2 equiv of $[(CyN)_2C(HNCy]Li$ in ether was attempted in order to prepare the cyclohexyl analogue of **5**. This procedure led to the isolation of $[\mu\text{-}(CyN)_2C(HNCy)]_2Fe_2[(CyN)_2C(HNCy)]_2$, **6**. In order to confirm the metrical parameters of **6**, its structure was also determined (Table 8.5). Perhaps not surprisingly, complex **6**

displayed very similar structural features to **5** as shown in Figure 8.6 and presented in Table 8.8.

Figure 8.6. Molecular structure and atom numbering scheme for [μ-$(CyN)_2C(HNCy)]_2Fe_2[(CyN)_2C(HNCy)]_2$ (**6**). Hydrogen atoms have been omitted for clarity.

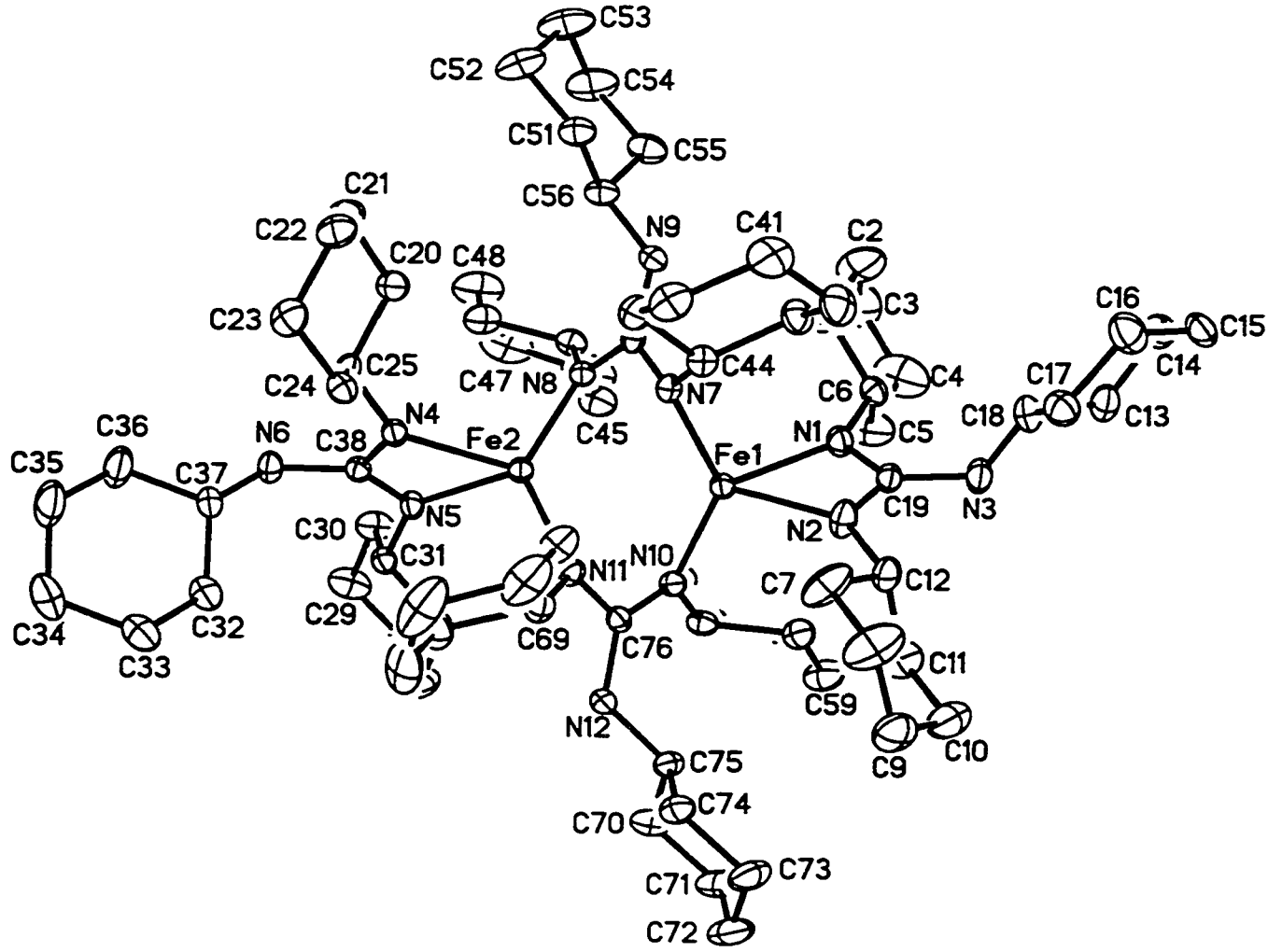

In addition to the obvious analogy in gross structural features, many of the structural details are similar between **5** and **6**. For example, the N-Fe-N bond angles vary from 63.1° for the nonbridging ligands to 134.1° for the bridging ligands with an average value of 106°. The Fe-N bond distances cover a range from 2.033 to 2.134 Å. The bridging ligands again exhibit a severe twist from planarity with the dihedral angles (α, Chart 8.3) defined by Fe(1)-N(10)-N(11)-Fe(2) and Fe(1)-N(7)-N(8)-Fe(2) exhibiting values of 70.0° and 73.6° respectively. The closest non-coordinated N centers for each Fe are even further away than in **5** (i.e. Fe(1)-N(8) 3.050Å, Fe(2)-N(10) 3.190Å) and the long Fe-Fe separation of 3.161Å indicates that there is no metal-metal bonding interaction in this compound.

A stepwise introduction of guanidinate ligand was investigated for the Cy species. Thus N, N', N"-tricyclohexylguanidinato lithium, $[(CyN)_2C(HNCy]Li$, was allowed to react in a ratio of 1:1 with $FeBr_2$ in ether. After work-up a new complex **7** could be crystallized from ether (Scheme 8.6). This compound was confirmed to be $[\mu\text{-}(CyN)_2C(HNCy)]_2Fe_2Br_2$ through examination of a single crystal by X-ray crystallography (Table 8.5).

From examination of the representation of **7** in Figure 8.7 and the selected bond distances and angles of this complex presented in Table 8.9, one can see that **7** is related to the dimers **5** and **6**. Figure 8.7 shows a dinuclear Fe(II) complex were the two metal centers are held in proximity by two bridging guanidinate monoanionic ligands. A

terminal bromide completes the coordination environment of each iron. The two halves of the molecule (the asymmetric unit) are related by an inversion center.

Figure 8.7. Molecular structure and atom numbering scheme for [μ-$(CyN)_2C(HNCy)]_2Fe_2Br_2$ (**7**). Hydrogen atoms have been omitted for clarity.

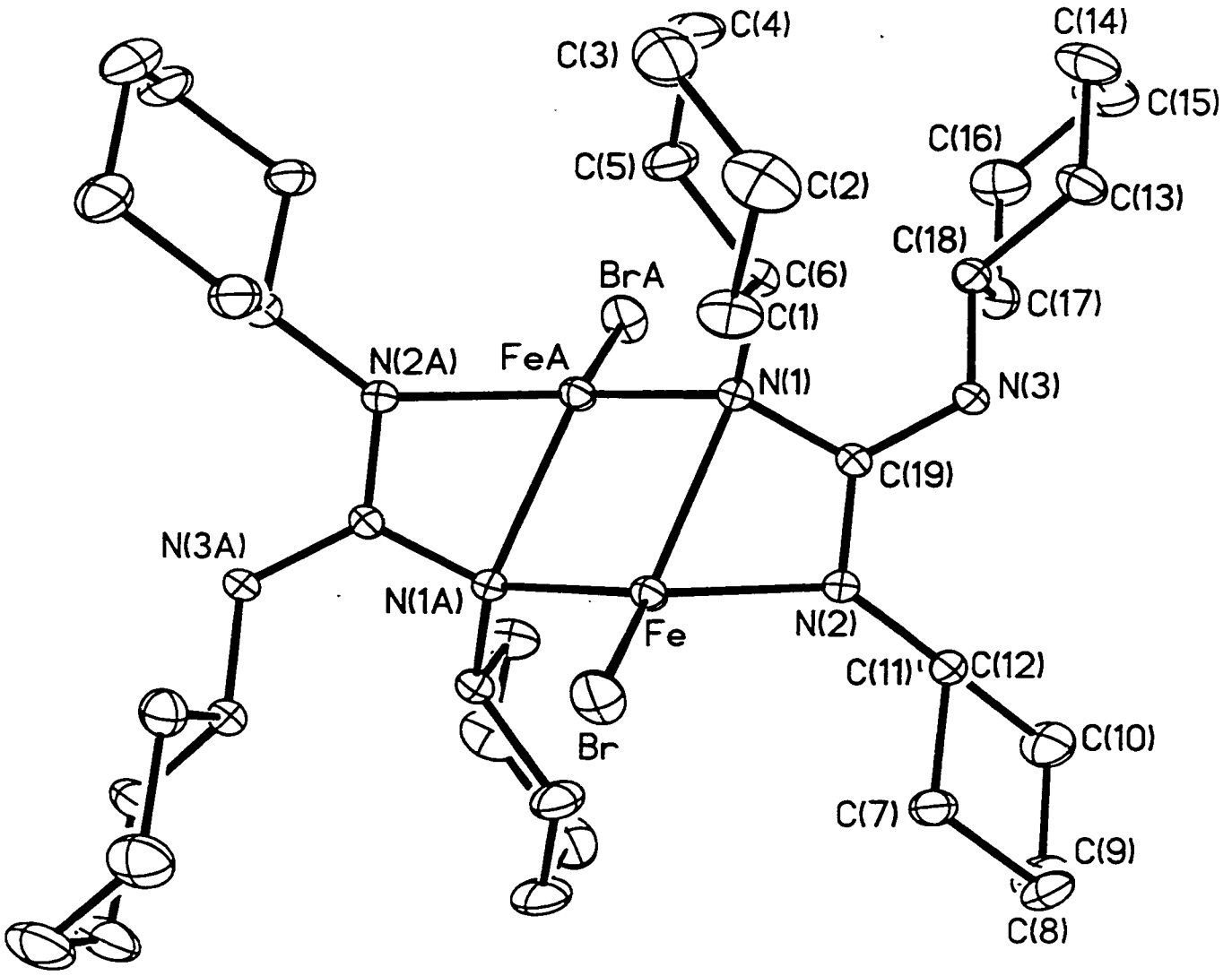

A similar twist is observed for the bridging guanidinate ligands in **7** as was seen with **5** and **6**. In the case of **7** the distortion does seem to be associated with the interaction of each Fe center with a third guanidinate nitrogen; an interaction with one of the nitrogen atoms that is coordinated to the other Fe atom of the dimer. While Fe-N(1) and Fe-N(2) are the shortest Fe-N distances in the molecule and are similar in length (2.0347(18)Å and 2.0363(18)Å respectively) the Fe-N(1A) distance of 2.2557(17)Å is certainly well within the van der Waals radii. This is much shorter than the comparable distances in **5** and **6** and even shorter than the similar interaction that was invoked for for $Fe_2(\mu\text{-DPhBz})_2(DPhBz)_2$ (**IV**). It appears that this additional nitrogen interaction with each metal center is an effort to preserve a pseudotetrahedral environment about each iron at the expense of the distortion of each ligand. As a result of this twist to the ligand the Fe-N(1)-Fe(1)-N(1A) atoms form a planar four-membered ring and, even though C(19) remains planar (Σ angles = 360), the twist along the bridging ligand can be seen in the angle of 62.6° that is formed between the mean planes defined by N(1)-N(2)-C(19)-Fe and Fe-Fe(1)-N(1). If significant, this third interaction should also lead to a localized π-bond within the chelating N-C-N group. This indeed seems to be the case with the C-N distance for the tetracoordinated nitrogen center (C(19)-N(1)) at 1.390(3)Å while the C(19)-N(2) bond distance of 1.315(3) Å corresponds to a C=N double bond. For comparison the C(19)-N(3) bond distance is 1.355(3)Å.

This interaction can be viewed as a result of an additional contributing resonance structure to **7** as depicted in Chart 8.4. It also brings the two Fe atoms in closer proximity

Chart 8.4

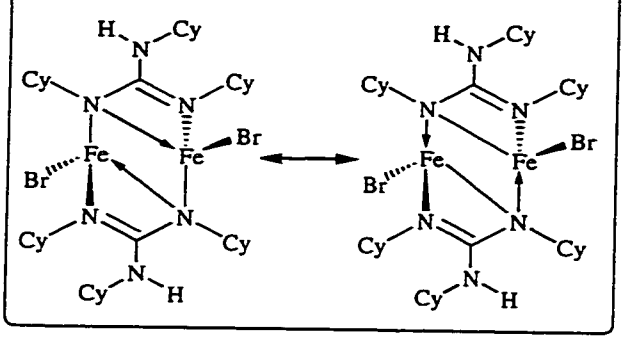

to each other than in **5** and **6**. However, the Fe-Fe distance of 2.8399(6)Å is too long to be considered a significant metal-metal interaction. The complex $Fe_2(DPhF)_4$ for example has a Fe-Fe distance of 2.462(2)Å.[9]

Other complexes possessing Fe-Fe bonds include the face sharing bioctahedral diamagnetic complex $Fe_2(CO)_9$ where two 17 electron irons share a single bond with an Fe-Fe distance of 2.523Å. Another group of compounds that have relatively short Fe-Fe interactions are $Fe_2(CO)_5(\mu\text{-}PR_2)$ with Fe-Fe distances of 2.46-2.48Å.[21] The dinuclear species (η^2- c(mes)=N^{t}Bu)$_2$Fe$_2$(μ-c(mes)=N^{t}Bu which was generated by reaction of Fe_2mes_2 with ^{t}BuNC exhibits an Fe-Fe bond distance of 2.371Å.[22,23]

Fe(II) Complexes of N, N', N''-Tri(alkyl)guanidinate Dianions. Trisubstituted guanidinate monoanions possess an additional N-H that may be susceptible to deprotonation. This possibility encouraged attempts to react the dinuclear complex **5** with strong bases. Complex **5** reacts rapidly with 2 equiv MeLi in THF, which, followed by recrystallization from pentane, results in the formation of [(^{i}PrN)$_2$C=N^{i}Pr]$_2$Fe$_2$[(^{i}PrN)$_2$C(HN^{i}Pr)Li]$_2$, **8**. (Scheme 8.7)

Again, X-ray crystallography provided the structural identity of this new material (Table 8.10). From Figure 8.8 and in conjunction with the structural parameters summarized in Table 8.11 one can see that this new dinuclear Fe(II) complex is derived

from the double deprotonation of complex **5**. The resultant complex exhibits two dianionic guanidinate ligands that bridge the two Fe centers while the remaining two monoanionic ligands have rearranged to exhibit a monodentate coordination to Fe. This deprotonation is not accompanied by any change in Fe oxidation state and thus requires the presence of two lithium cations for charge balance. These Li cations are coordinated to the monoanionic guanidinate in a bidentate mode.

Scheme 8.7

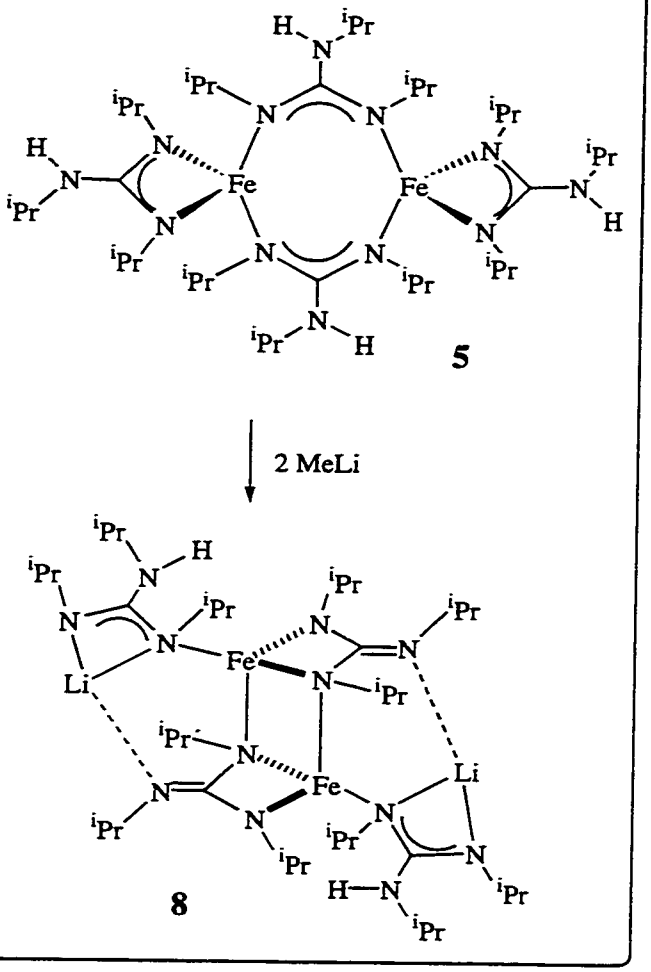

The structural core of **8** exhibits many similarities with that of compound **7** with the replacement of the monoanionic guanidinate for a dianionic analogue. Complex **8** also possesses a crystallographic inversion center that generates the other half of the molecule from the asymmetric unit. Other obvious similarities include the disposition of the bridging ligand with respect to the Fe_2 core and, in addition to the short bonding interactions of Fe-N(1) and Fe-N(2) (2.0931(18)Å and 2.0304(18)Å), each iron center has

an additional interaction with a third nitrogen Fe-N(1A) 2.2351(18)Å. This arrangement generates a four membered planar $(FeN)_2$ rectangle. The additional nitrogen interaction preserves a distorted pseudotetrahedral environment about each iron center.

The guanidinate ligands are planar and parallel to each other. The angle between Fe-N(1)-C(10)-N(2) mean plane and Fe-Fe(A)-N1 mean plane is 59.6° (β, Chart 8.5).

Figure 8.8. Molecular structure and atom numbering scheme for $[(^iPrN)_2C{=}N^iPr]_2Fe_2[(^iPrN)_2C(HN^iPr)Li]_2$ (**8**). Hydrogen atoms have been omitted for clarity.

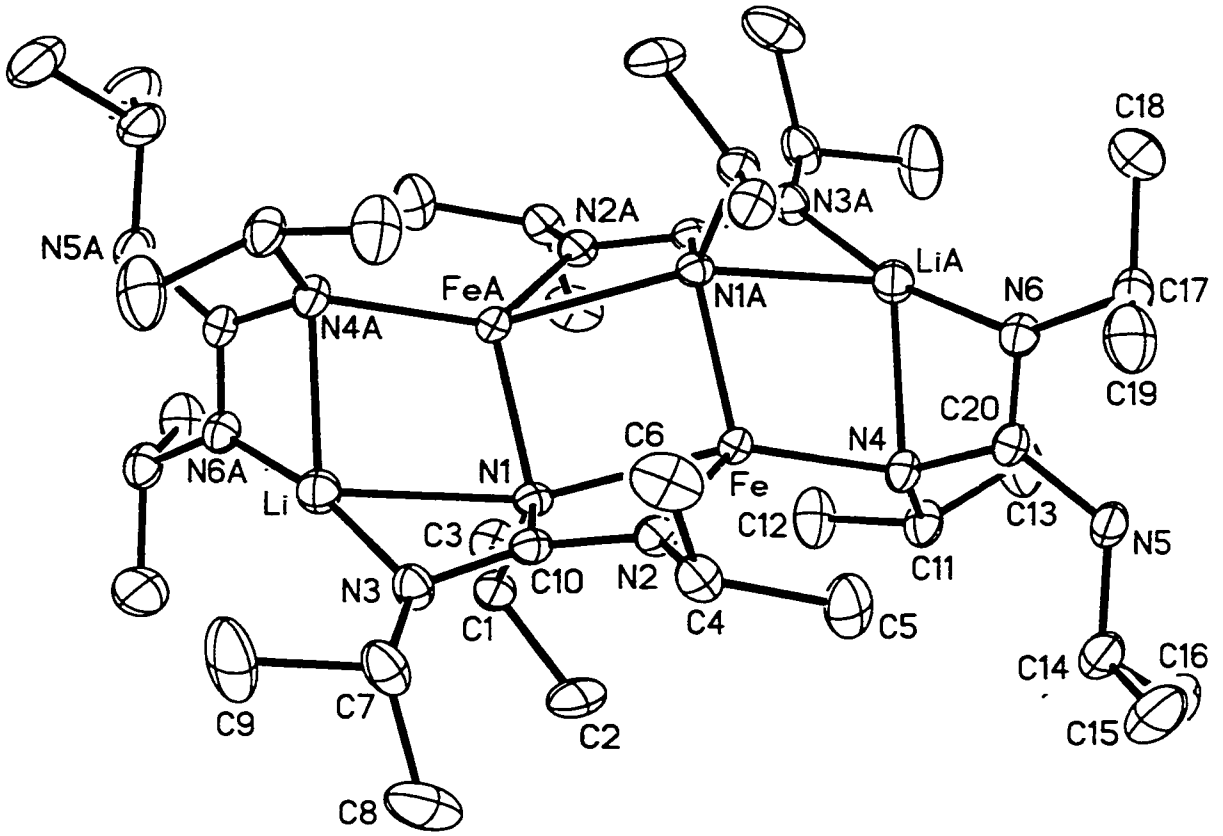

Chart 8.5

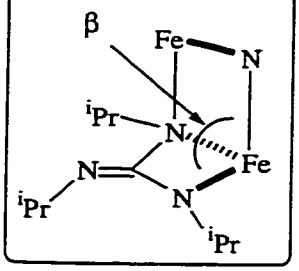

The interaction of the third interaction should also lead to a localized π-bond within the chelating N-C-N group. This indeed seems to be the case with the C-N distance for the tetracoordinated nitrogen center being consistent with a single bond (C(10)-N(1) 1.457(3)Å) while the CN bond distance of 1.315(3)Å for C(10)-N(3) corresponds to a C=N double bond. Some delocalization of the π bond does occur between C(10)-N(2) which exhibits a bod distance of 1.341(3)Å.

The Fe-Fe distance of 2.984Å is longer than in compound **7** (2.840Å) but shorter than in **5** (3.161Å) and is again too large for any metal-metal interaction to be considered.

The bonding parameters within the monodentate monoanion are consistent with other monoanionic guanidinates. The coordinated lithium guanidinate ligand has a C-$N_{ancillary}$ bond distance of 1.376Å while the C-$N_{termini}$ distances are 1.385 and 1.309 Å. The C-$N_{termini}$ bond distance of 1.385Å is longer due to coordination with the adjacent iron center.

Further reaction of **8** with 1 equiv $FeBr_2$ results only in crystallization of **9**. Presumably the $FeBr_2$ reacts with the coordinated $[(^iPrN)_2C(HN^iPr)]Li$ of **8** at which point the lithiated ligands dissociate from **8** to and react with $FeBr_2$ to form **5**. We remain unsure of what the other product becomes given its ability to thwart crystallization attempts.

Reactivity of 4 with alkyllithium reagents.

As noted above, the reaction of complex **4** with a variety of alkylating reagents led to the reduction of the Fe(III) center and formation of the dinuclear structure **5**. Complex 5 further reacts with two equiv of MeLi to produce complex **8**.

When $LiCH_2SiMe_3$ was employed in reactions with 4 using other stoichiometries different results were obtained (Scheme 8.8). Reaction of **4** with two equiv of $LiCH_2SiMe_3$ resulted in the formation of the Fe(II) complex **9**. Suitable crystals of **9** were obtained from ether and subjected to analysis by X-ray diffraction (Table 8.10). The results are summarized in Table 8.12 and presented pictorially in Figure 8.9.

Scheme 8.8

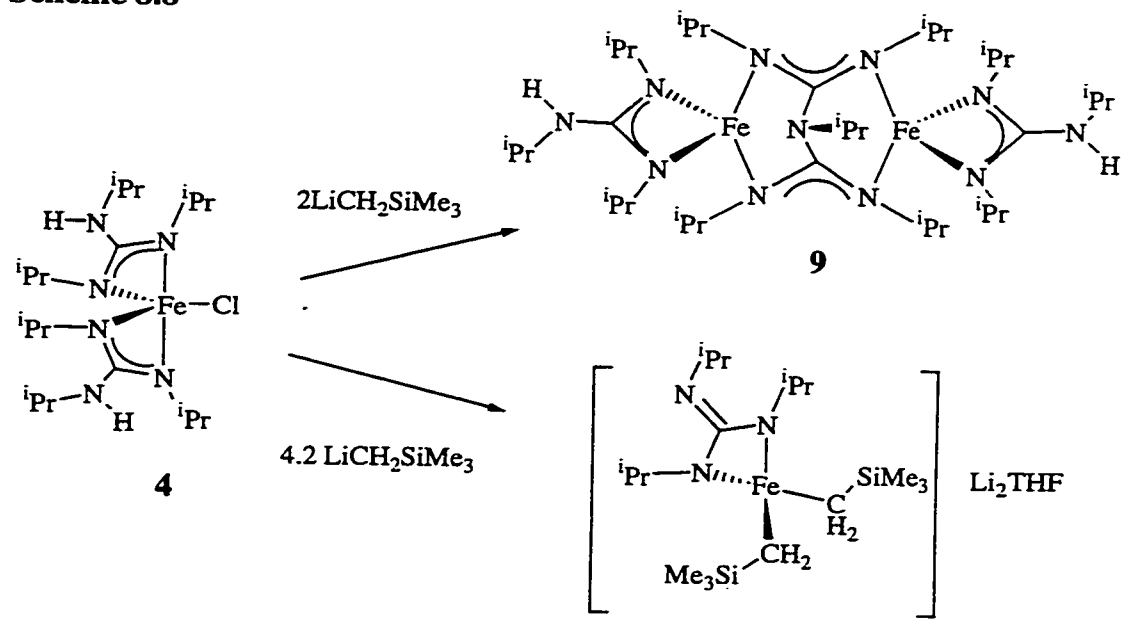

Examination of this structure discloses two obvious results from this reaction. First the Fe(III) center, as anticipated, has undergone reduction to Fe(II). Second, one guanidinate ligand on each of two different Fe centers engaged in a subsequent reaction

while one of them has remained intact. Note that the reaction with one equiv leads to reduction.

A proposed pathway for the formation of **9** is presented in Scheme 8.9. After reduction of **4** to generate **5** the second equivalent of lithium reagent removes a proton from one of the bridging ligands to generate a nitrogen centered anion. This nucleophilic center then attacks the second bridging ligand at the methyne carbon to release an amido anion and generate the observed dianionic ligand, $[(^{i}PrN_2C)_2N^{i}Pr]^{2-}$.

Figure 8.9. Molecular structure and atom numbering scheme for [μ-$(^{i}PrNCN^{i}Pr)_2(HN^{i}Pr)]Fe_2[(^{i}PrN)_2C(HN^{i}Pr)]_2$ (**9**). Hydrogen atoms have been omitted for clarity.

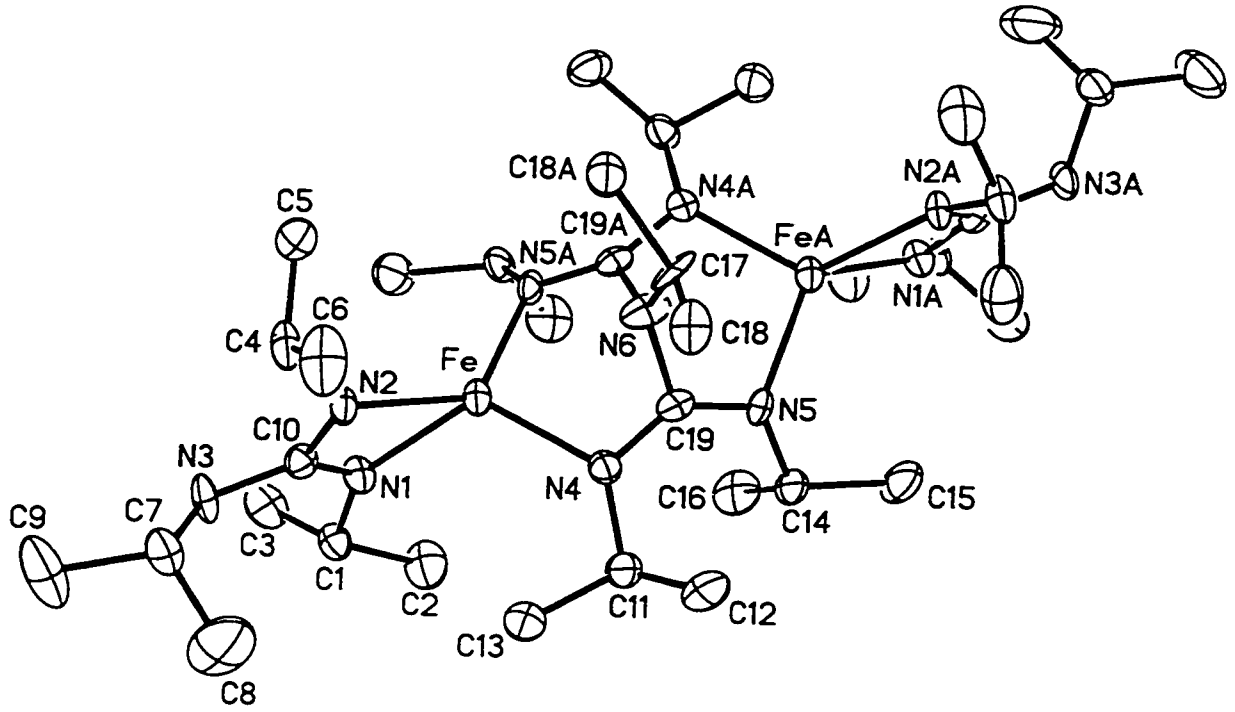

Scheme 8.9

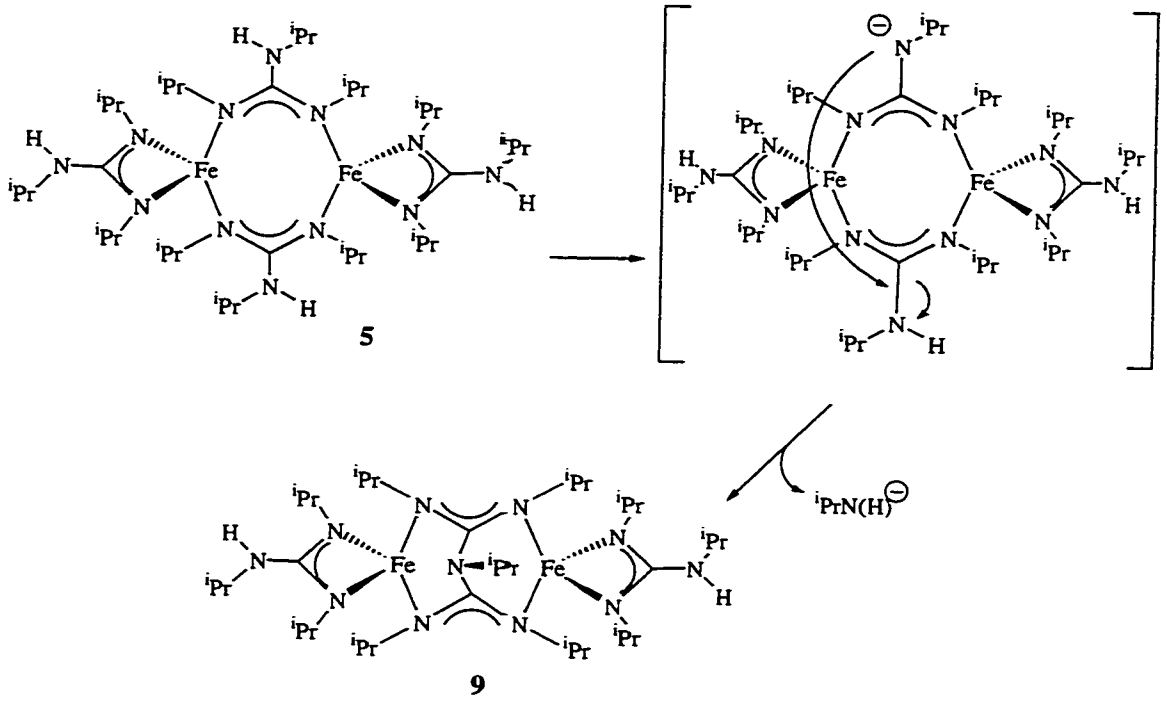

This proposal leaves a chelating bidentate guanidinate monoanion for completion of the coordination sphere for each of the Fe(II) centers in the dinuclear complex observed for **9** (Figure 8.9).

Due to the disorder observed for the ^{i}Pr group bonded to N(6) complex **9** exhibits an approximate C_2 axis passing through N(6) and perpendicular to the Fe-Fe vector. This disorder also gives the appearance that N(6) is a planar center.

Bonding parameters within the new ligand $[(^{i}PrN_2C)_2N^{i}Pr]^{2-}$ are consistent with the resonance representation in Scheme 8.9. In particular, the double bonds within the ligand appear to be localized in the N(4)-C(19)-N(5) framework (N(4)-C(19) = 1.336(7)Å , N(5)-C(19) = 1.311(7)Å and the N(6)-C(19) distance of 1.453(6)Å is similar to the other

single CN bond distances within the molecule. Furthermore, the methine C (C(19)) is planar ($\Sigma = 360°$) and N(4) and N(5) deviate only slightly from planarity ($\Sigma = 357°$). The two Fe atoms in **9** are separated by a distance of 4.945Å.

Reaction of **4** with four equivalents of $LiCH_2SiMe_3$ yields a different product. The paramagnetic nature of this species again required that we rely on single crystal structure determination in order clarify the consitution of this material (Table 8.13). The asymmetric unit for this material has the formula $Li_2(THF)Fe[(^iPrN)_2CN^iPr](CH_2SiMe_3)_2$ (**10**) shown in Figure 8.10 and the bond distances and angles summarized in Table 8.14.

The π bonding within the guanidinate ligand appears to be localized between N(3)-C(10), on the basis of the observed bond distance of 1.310(6)Å. The remaining two CN bond distances (N(2)-C(10) 1.381(6)Å, N(1)-C(10) 1.400(6)Å) are more consistent with a single bonds between an sp^2 C and an sp^3 based N atom. This treatment essentially localizes the two negative charges of the dianion on N(1) and N(2). Consistent with this assignment are the planar C(10) and N(3) centers and the coordination/ association of the Fe(II) and the two counter cations to N(1) and N(2) (Li(2) and Li(1)respectively).

With a +2 oxidation state assigned to the Fe atom, this $Fe[(^iPrN)_2CN^iPr](CH_2SiMe_3)_2^{2-}$ unit requires the presence of two Li^+ counterions to attain neutrality. Turning to the Li cations, Figure 8.10 shows that they exhibit different environments. One of the lithium centers (Li(1)) has a trigonal planar environment defined by the oxygen atom of an associated THF molecule, one of the negatively charged guanidinate nitrogen centers (N(2)), and a carbon of one of the CH_2SiMe_3 moieties (C(11). The second Li cation (Li(2)) "holds" the two asymmetric units together

by bonding to the other negatively charged guanidinate nitrogen (N(1)) and the lone pair on the imine nitrogen (N(3)) within one unit and a symmetry related nitrogen (N(1A)) and a carbon of one of the CH_2SiMe_3 moieties (C(15A)) in the other unit. There are also some longer interactions of the two Li cations with the guanidinate π-system. Specifically both Li(1) and Li(2) interact with C(10) at distances of 2.760(11)Å and 2.610(11)Å respectively.

Figure 8.10. Molecular structure and atom numbering scheme for $Li_2(THF)Fe[(^iPrN)_2CN^iPr](CH_2SiMe_3)_2$ (**10**). Hydrogen atoms have been omitted for clarity.

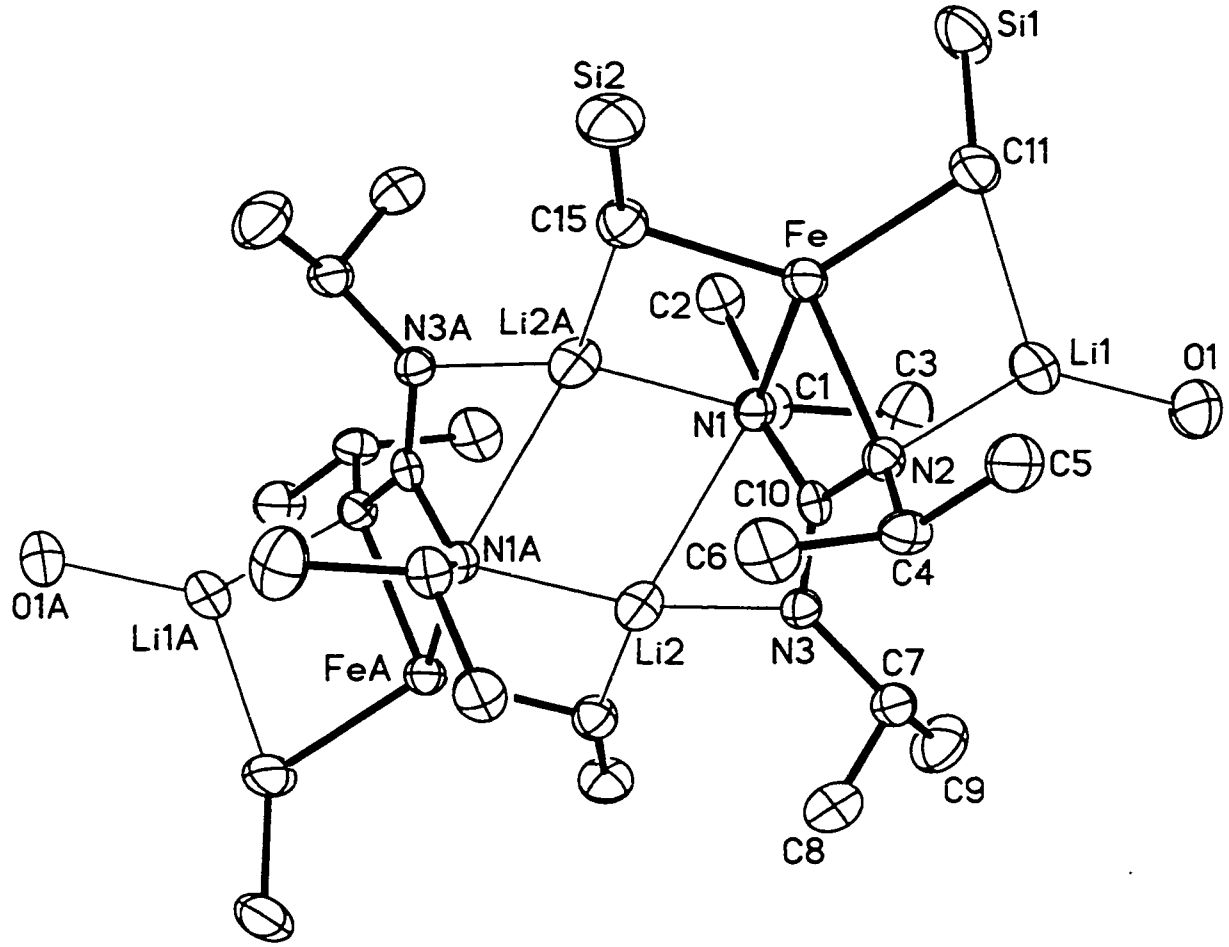

Fe(II) Complex of the tetrasubstitued guanidinate anion $CyNC(NSiMe_3)_2NCy$.

To further investigate the effects of modifying steric bulk and electronic properties of the ligands, a tetrasubstituted guanidinato iron(II) complex was prepared.

The lithium guanidinate was prepared *in situ* by direct reaction of $LiN(SiMe_3)_2$ with diisopropylcarbodiimide in ether. Reaction with 0.5 equiv $FeBr_2$ followed by recrystallization in ether resulted in isolation of the monomeric bisguanidinato iron(II) complex, $[(^iPrN)_2C(N(SiMe_3)_2)]_2Fe$, **11**. The molecular structure is shown in Figure 8.11 with bonding parameters given in Table 8.15. We anticipated that increasing the steric bulk of the ligand by using a tetrasubstituted in place of a trisubstituted guanidinate would result in preferential formation of a mononuclear species over a dinuclear species.

Scheme 8.10

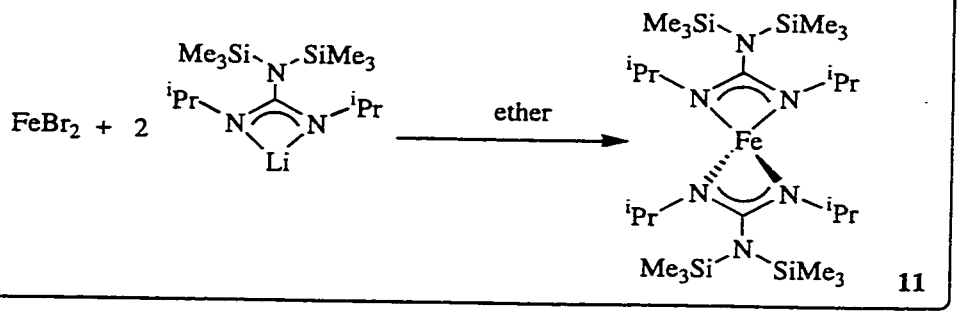

The complex is mononuclear with two tetrasubstituted guanidinates chelating to the metal center resulting in a distorted tetrahedral environment about the iron. This complex exhibits two Fe-N bond distances (2.013(3)Å and 2.031(3)Å) with an average Fe-N bond distance is 2.022 Å. The $C\text{-}N_{ancillary}$ bond distance is 1.438Å, consistent with a

single bond, while the two C-$N_{termini}$ distances are equivalent at 1.32Å, indicative of charge delocalization between the two nitrogen atoms.

Figure 8.11. Molecular structure and atom numbering scheme for $[(^{i}PrN)_2C(N(SiMe_3)_2)]_2Fe$ (**11**). Hydrogen atoms have been omitted for clarity.

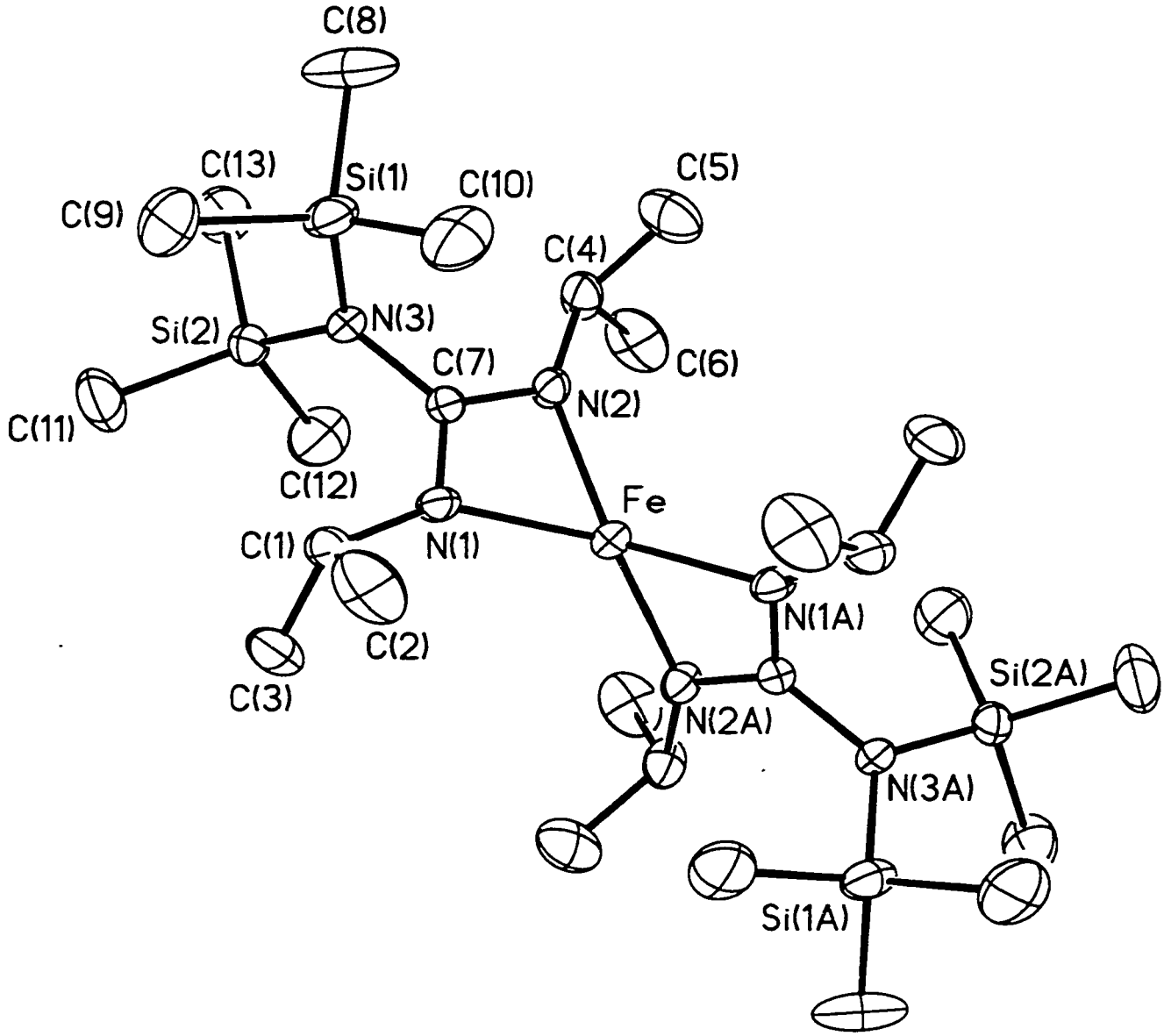

Conclusion

Amidinate ligands have proven useful in the preparation of new Fe(II/III) complexes. X-ray crystallographic studies confirm the steric effects that are expected to arise upon substitution of bulky groups in the bridgehead position of the amidinate ligand resulting in the only known Fe^{II} amidinate monomer.

The reactions of the lithium salts of N,N',N"-tricyclohexylguanidine and N,N',N"-triisopropylguanidine with Fe(II) and Fe(III) halides proceed smoothly at room temperature to give complexes **4-11**. With regard to the trisubstituted guanidinates, attempts to alkylate bis(guanidinato)iron(III)chloride unequivocally results in reduction of the Fe(III) center to Fe(II). Further reaction results in partial deprotonation of the ligands forming dianionic guanidinate complexes. Tetrasubstituted guanidinato complexes of Fe(II) and Fe(III) were also prepared to investigate the steric and electronic effects of having a fourth substituent present in place of a proton on the ancillary third nitrogen center, resulting in the formation of the mononuclear complex, **11**.

Experimental for Chapter Eight

General Procedure. All reactions were carried out in a nitrogen-filled drybox. Diethyl ether, THF, hexane, toluene and pentane were distilled under nitrogen from Na/K alloy. $FeBr_2$, $FeCl_3$, ^tBuLi (1.7M in hexane), MeLi (1.4M in hexane), $LiCH_2SiMe_3$, BzMgCl, Et_2Zn, diisopropylcarbodiimide and dicyclohexylcarbodiimide were purchased from Aldrich and used without further purification. Samples for magnetic susceptibility measurements were prepared inside a drybox and sealed in calibrated tubes; measurements were carried out with a Gouy balance (Johnson Matthey) at room temperature. Corrections for underlying diamagnetism were applied.

$Fe_4(\mu_4\text{-}O)(\mu\text{-}Br)_2(\mu\text{-}CyNCHNCy)_4$ (1). A schlenk flask was charged with lithium N,N'-dicyclohexylformamidinate (0.298g, 1.39mmol) and $FeBr_2$ (0.300g, 1.39mmol) to which THF (40ml) was added. The dark brown reaction mixture was stirred overnight and then filtered. The solution was condensed to 5 ml and then cooled to –25°C in a freezer. The resulting yellow crystals were collected and dried in vacuo (0.068g, 16%).

$Fe(CyN(^tBu)NCy)_2$ (2). A Schlenk flask was charged with dicyclohexylcarbodiimide (0.574g, 2.78mmol) and diethyl ether (30ml). To the stirring solution was added ^tBuLi (1.64ml, 1.7M, 2.78mmol) dropwise followed by $FeBr_2$ (0.300g, 1.39mmol). The dark brown solution was stirred overnight, concentrated to 5ml and then cooled to –25°C in a freezer. The resulting yellow crystals were collected and dried in vacuo (0.609g, 75%).

IR (nujol): 1657(w), 1619(w), 1487(m), 1409(vs), 1352(vs), 1339(vs), 1304(s), 1294(s), 1240(w), 1191(m), 1166(m), 1123(m), 1055(w), 990(m), 896(m), 845(w), 797(w), 654(w), 630(m) cm^{-1}. $\mu_{eff} = 5.105$ BM.

$(CyNC^tBuNCy)_2FeCl$ (3). A Schlenk flask was charged with dicyclohexylcarbodiimide (0.509g, 2.47mmol) and diethyl ether (60ml). To the stirring solution was added ^{t}BuLi (1.45ml, 1.7M, 2.47mmol) dropwise. After 30 min 0.5eq of $FeCl_3$ was added (0.200g, 1.23mmol). The dark blue solution was stirred for 16h, filtered, concentrated to 20ml and then cooled to –25°C. The resulting blue crystals were collected and dried in vacuo (0.509g, 67%). $\mu_{eff} = 5.610$ BM.

$[(^iPrN)_2C(HN^iPr)]_2FeCl$ (4). Triisopropylguanidine (1.212g, 6.55mmol) was dissolved in THF (50ml). MeLi (4.68ml, 1.4M) was added to the solution dropwise. The solution was stirred for 15min, followed by addition of 0.5 equiv $FeCl_3$ (0.531g, 3.27mmol). The purple solution was stirred for 24h at room temperature followed by removal of the solvent in vacuo. The product was extracted with pentane. Purple crystals were obtained from 15ml pentane at -30°C (0.63g, 42%yield). IR (nujol): 3419(m), 3376(s), 1612(w), 1527(vs), 1484(vs), 1328(s), 1303(s), 1214(s), 1180(m), 1125(m), 994(m), 736(m), 689(m) cm^{-1}. $\mu_{eff} = 5.667$BM.

$[\mu\text{-}(^iPrN)_2C(HN^iPr)]_2Fe_2[(^iPrN)_2C(HN^iPr)]_2$ (5). Triisopropylguanidine (0.500g, 2.70mmol) was dissolved in THF (40ml). MeLi (1.93ml, 1.4M) was added to the solution

dropwise. The solution was stirred for 15min, followed by addition of 0.5 equiv $FeBr_2$ (0.291g, 1.35mmol). The blue/green solution was stirred for 16h at room temperature followed by removal of the solvent in vacuo. The product was extracted with pentane. Pale green crystals were obtained from 5ml pentane at -30°C (0.47g, 82%yield). IR (nujol): 3426(m), 3397(w), 1650(m), 1532(vs), 1436(vs), 1311(s), 1176(m), 1133(m), 1075(w), 986(m), 838(w), 732(m) cm^{-1}. $\mu_{eff} = 7.490BM$.

Reduction of $[(^iPrN)_2C(HN^iPr)]_2FeCl$ (4) to $[\mu$-$(^iPrN)_2C(HN^iPr)]_2Fe_2[(^iPrN)_2C(HN^iPr)]_2$ (5). To a solution of **4** in THF was added an alkylating reagent (1eq BzMgCl, 0.5eq Et_2Zn, 1eq $LiCH_2SiMe_3$, or LiMe). The purple solutions were stirred overnight, filtered, and the solvent removed *in vacuo*. Crystals of **5** were obtained from pentane as the sole isolable product in yields from 40-80%. Confirmation of **5** was done through comparison of unit cell parameters.

$[\mu$-$(CyN)_2C(HNCy)]_2Fe_2[(CyN)_2C(HNCy)]_2$ (6). Tricyclohexylguanidine (1.00g, 3.28mmol) was dissolved in diethyl ether (30ml). ^nBuLi (1.31ml, 2.5M) was added to the solution dropwise. The solution was stirred for 15min, followed by addition of 0.5 equiv $FeBr_2$ (0.353g, 1.64mmol). The brown solution was stirred for 16h at room temperature followed by removal of the solvent in vacuo. The product was extracted with pentane. Pale green crystals were obtained from 5ml pentane at -30°C (0.80g, 73%yield). IR (nujol): 3458(m), 3420(w), 1652(m), 1534(vs), 1341(s), 1298(m), 1255(m), 1179(m), 1146(m), 1065(m), 1049(m), 978(w), 887(m) cm^{-1}. $\mu_{eff} = 7.277BM$.

[μ-(CyN)$_2$C(HNCy)]$_2$Fe$_2$Br$_2$ (7). Tricyclohexylguanidine (0.500g, 1.64mmol) was dissolved in diethyl ether (30ml). ^{n}BuLi (0.68ml, 2.5M) was added to the solution dropwise. The solution was stirred for 15min, followed by addition of 1 equiv $FeBr_2$ (0.353g, 1.64mmol). The brown/green solution was stirred for 16h at room temperature. Pale crystals were obtained from 5ml diethyl ether at -30°C (0.47g, 82%yield). IR (nujol): 3261(s), 3200(m), 1611(vs), 1248(m), 1151(m), 1099(m), 978(w), 890(m), 797(w), 713(w) cm^{-1}. μ_{eff} = 8.625BM.

[(^{i}PrN)$_2$C=N^{i}Pr]$_2$Fe$_2$[(^{i}PrN)$_2$C(HN^{i}Pr)Li]$_2$ (8). 0.570g (0.671mmol) of **5** was dissolved in THF (20ml). MeLi (0.97ml, 1.4M) was added to the solution dropwise. The green solution was stirred for 16h at room temperature followed by removal of the solvent in vacuo. The product was extracted with pentane. Pale yellow crystals were obtained from 3ml pentane at -30°C (0.39g, 68%yield). IR (nujol): 3429(m), 1614(m), 1560(vs), 1538(vs), 1364(s), 1357(s), 1330(m), 1305(s), 1173(m), 1117(m), 1064(w), 1051(w), 988(m), 951(w), 932(w), 894(m), 850(m), 753(w) cm^{-1}. μ_{eff} = 7.514BM.

[μ-(^{i}PrNCN^{i}Pr)$_2$(HN^{i}Pr)]Fe$_2$[(^{i}PrN)$_2$C(HN^{i}Pr)]$_2$ (9). 0.620g (1.35mmol) of **4** was dissolved in THF (50ml). 2 equiv LiCh2SiMe3 (2.70ml, 2.70mmol, 1.0M) was added to the solution. The brown solution was stirred for 24h at room temperature, filtered, followed by removal of the solvent *in vacuo*. Pale crystals were obtained from pentane -30°C (0.10g, 19%yield).

$Li_2(THF)Fe[(^iPrN)_2CN^iPr](CH_2SiMe_3)_2$ (10). 0.620g (1.35mmol) of **4** was dissolved in THF (50ml). 4.2 equiv $LiCH_2SiMe_3$ (5.68ml, 5.68mmol, 1.0M) was added to the solution. The dark red solution was stirred for 48h at room temperature, filtered, followed by removal of the solvent *in vacuo*. Pale crystals were obtained from pentane -30°C (0.182g, 27%yield).

$[(^iPrN)_2C(N(SiMe_3)_2)]_2Fe$ (11). Diisopropylcarbodiimide (0.300g, 2.38mmol) was dissolved in diethyl ether (40ml). $LiN(SiMe_3)_2$ (0.399g, 2.38mmol) was added to the solution. The solution was stirred for 30min, followed by addition of 0.5 equiv $FeBr_2$ (0.257g, 1.19mmol). The solution was stirred for 24h at room temperature. Crystals were obtained from 10ml diethyl ether at -30°C (0.46g, 62%yield). IR (nujol): 1638(m), 1417(m), 1358(w), 1321(s), 1252(s), 1216(s), 1116(w), 1064(s), 950(s), 840(s), 759(m), 685(m) cm^{-1}. $\mu_{eff} = 5.197BM$.

Data Tables for Chapter Eight

Table 8.1. Crystal data and structure refinement for Fe amidinate complexes **1-3**.

	1	2	3
empirical formula	C52 H90 Br2 Fe4 N8 O	C34 H62 Fe N4	C34.75 H62 Cl Fe N4
formula weight	1226.54	582.73	627.18
temp (K),	293(2)	293(2)	223(2) K
λ (Å)	0.71073	0.71073	0.71073 A
space group	P-1	P2(1)/n	P2(1)/c
a (Å)	15.980(3).	10.8890(5)	33.008(9)
b (Å)	16.003(3)	16.9823(8)	10.719(4)
c (Å)	23.466(5)	18.6572(9)	20.953(8)
α (deg)	86.114(4)	90	90
β (deg)	86.135(4)	93.745(1)	102.275(7)
γ (deg)	88.652(4)	90	90
V(Å^3),	5973(2)	3442.7(3)	7244(4)
Z	4	4	8
d_{calc} (g/cm^3),	1.364	1.124	1.150
absorption coefficient (mm^{-1})	2.331	0.465	0.517
R1[a]	0.0549	0.0334	0.0746
wR2[b]	0.1081	0.0962	0.1699

[a] $R1 = \sum \| F_o | - | F_c \| / \sum | F_o |$.

[b] $wR2 = \left(\sum w (| F_o | - | F_c |)^2 / \sum w | F_o |^2 \right)^{1/2}$

Table 8.2. Selected bond distances [Å] and angles [deg] for **1**.

Distances			
Fe(1)-O(1)	1.977(3)	Fe(8)-Br(4)	2.5520(10)
Fe(1)-N(3)	2.013(5)	N(1)-C(13)	1.320(6)
Fe(1)-N(1)	2.017(4)	N(1)-C(6)	1.477(6)
Fe(1)-Fe(2)	2.5074(12)	N(2)-C(13)	1.312(6)
Fe(1)-Br(1)	2.5822(11)	N(2)-C(12)	1.496(6)
Fe(2)-O(1)	1.994(4)	N(3)-C(26)	1.314(7)
Fe(2)-N(2)	2.009(4)	N(3)-C(19)	1.472(6)
Fe(2)-N(4)	2.035(5)	N(4)-C(26)	1.337(6)
Fe(2)-Br(2)	2.6032(10)	N(4)-C(25)	1.484(7)
Fe(3)-O(1)	2.000(4)	N(5)-C(52)	1.314(6)
Fe(3)-N(5)	2.010(5)	N(5)-C(45)	1.485(6)
Fe(3)-N(7)	2.040(4)	N(6)-C(52)	1.331(6)
Fe(3)-Fe(4)	2.5067(12)	N(6)-C(51)	1.469(6)
Fe(3)-Br(1)	2.6051(10)	N(7)-C(39)	1.308(7)
Fe(4)-O(1)	1.968(3)	N(7)-C(32)	1.468(7)
Fe(4)-N(8)	2.014(4)	N(8)-C(39)	1.310(7)
Fe(4)-N(6)	2.012(4)	N(8)-C(38)	1.485(7)
Fe(4)-Br(2)	2.5796(10)	N(9)-C(65)	1.311(7)

Fe(5)-O(2)	1.958(4)	N(9)-C(58)	1.479(7)
Fe(5)-N(9)	1.992(5)	N(10)-C(65)	1.334(7)
Fe(5)-N(11)	2.018(4)	N(10)-C(64)	1.483(6)
Fe(5)-Fe(6)	2.4879(12)	N(11)-C(78)	1.306(7)
Fe(5)-Br(3)	2.5533(10)	N(11)-C(71)	1.462(6)
Fe(6)-O(2)	1.996(4)	N(12)-C(78)	1.327(6)
Fe(6)-N(10)	2.011(5)	N(12)-C(77)	1.481(7)
Fe(6)-N(12)	2.028(4)	N(13)-C(91)	1.330(7)
Fe(6)-Br(4)	2.5914(11)	N(13)-C(84)	1.475(6)
Fe(7)-O(2)	2.001(4)	N(14)-C(91)	1.309(6)
Fe(7)-N(15)	2.005(4)	N(14)-C(90)	1.460(7)
Fe(7)-N(13)	2.029(4)	N(15)-C(104)	1.325(7)
Fe(7)-Fe(8)	2.4917(12)	N(15)-C(97)	1.493(7)
Fe(7)-Br(3)	2.5896(11)	N(16)-C(104)	1.315(7)
Fe(8)-O(2)	1.959(4)	N(16)-C(103)	1.462(7)
Fe(8)-N(14)	1.998(4)	C(1)-C(6)	1.483(7)
Fe(8)-N(16)	2.008(4)		

Angles			
O(1)-Fe(1)-N(3)	108.99(17)	O(2)-Fe(8)-Br(4)	92.18(11)
O(1)-Fe(1)-N(1)	114.95(16)	N(14)-Fe(8)-Br(4)	119.76(14)
N(3)-Fe(1)-N(1)	117.10(19)	N(16)-Fe(8)-Br(4)	103.65(13)
O(1)-Fe(1)-Fe(2)	51.15(11)	Fe(7)-Fe(8)-Br(4)	140.96(4)
N(3)-Fe(1)-Fe(2)	89.82(14)	Fe(1)-Br(1)-Fe(3)	73.64(3)
N(1)-Fe(1)-Fe(2)	84.98(13)	Fe(4)-Br(2)-Fe(2)	73.72(3)
O(1)-Fe(1)-Br(1)	92.25(11)	Fe(5)-Br(3)-Fe(7)	74.17(3)
N(3)-Fe(1)-Br(1)	118.87(14)	Fe(8)-Br(4)-Fe(6)	74.23(3)
N(1)-Fe(1)-Br(1)	102.25(13)	C(13)-N(1)-C(6)	117.3(4)
Fe(2)-Fe(1)-Br(1)	140.83(4)	C(13)-N(1)-Fe(1)	120.0(4)
O(1)-Fe(2)-N(2)	108.12(16)	C(6)-N(1)-Fe(1)	121.7(3)
O(1)-Fe(2)-N(4)	113.62(17)	C(13)-N(2)-C(12)	116.0(4)
N(2)-Fe(2)-N(4)	118.62(19)	C(13)-N(2)-Fe(2)	117.0(4)
O(1)-Fe(2)-Fe(1)	50.54(10)	C(12)-N(2)-Fe(2)	126.2(3)
N(2)-Fe(2)-Fe(1)	88.98(13)	C(26)-N(3)-C(19)	116.9(5)
N(4)-Fe(2)-Fe(1)	84.92(13)	C(26)-N(3)-Fe(1)	117.0(4)
O(1)-Fe(2)-Br(2)	90.70(10)	C(19)-N(3)-Fe(1)	125.7(4)
N(2)-Fe(2)-Br(2)	116.36(13)	C(26)-N(4)-C(25)	114.4(5)
N(4)-Fe(2)-Br(2)	106.15(14)	C(26)-N(4)-Fe(2)	120.2(4)
Fe(1)-Fe(2)-Br(2)	139.95(4)	C(25)-N(4)-Fe(2)	124.8(3)
O(1)-Fe(3)-N(5)	108.10(16)	C(52)-N(5)-C(45)	116.8(5)
O(1)-Fe(3)-N(7)	113.55(18)	C(52)-N(5)-Fe(3)	116.3(4)
N(5)-Fe(3)-N(7)	118.9(2)	C(45)-N(5)-Fe(3)	126.2(4)
O(1)-Fe(3)-Fe(4)	50.26(10)	C(52)-N(6)-C(51)	117.6(5)
N(5)-Fe(3)-Fe(4)	89.21(13)	C(52)-N(6)-Fe(4)	119.2(4)
N(7)-Fe(3)-Fe(4)	85.08(14)	C(51)-N(6)-Fe(4)	122.1(3)
O(1)-Fe(3)-Br(1)	91.04(10)	C(39)-N(7)-C(32)	115.7(5)
N(5)-Fe(3)-Br(1)	116.00(13)	C(39)-N(7)-Fe(3)	118.9(4)
N(7)-Fe(3)-Br(1)	106.02(13)	C(32)-N(7)-Fe(3)	125.1(4)
Fe(4)-Fe(3)-Br(1)	140.03(4)	C(39)-N(8)-C(38)	119.0(5)
O(1)-Fe(4)-N(8)	108.23(17)	C(39)-N(8)-Fe(4)	115.3(4)
O(1)-Fe(4)-N(6)	115.32(16)	C(38)-N(8)-Fe(4)	125.6(4)
N(8)-Fe(4)-N(6)	117.97(19)	C(65)-N(9)-C(58)	118.7(5)
O(1)-Fe(4)-Fe(3)	51.39(11)	C(65)-N(9)-Fe(5)	122.9(4)

N(8)-Fe(4)-Fe(3)	89.57(14)	C(58)-N(9)-Fe(5)	118.3(4)
N(6)-Fe(4)-Fe(3)	85.33(13)	C(65)-N(10)-C(64)	116.2(5)
O(1)-Fe(4)-Br(2)	91.99(11)	C(65)-N(10)-Fe(6)	114.7(4)
N(8)-Fe(4)-Br(2)	118.53(14)	C(64)-N(10)-Fe(6)	129.0(4)
N(6)-Fe(4)-Br(2)	102.13(13)	C(78)-N(11)-C(71)	119.8(5)
Fe(3)-Fe(4)-Br(2)	140.86(4)	C(78)-N(11)-Fe(5)	116.2(4)
O(2)-Fe(5)-N(9)	116.05(17)	C(71)-N(11)-Fe(5)	123.9(4)
O(2)-Fe(5)-N(11)	108.93(17)	C(78)-N(12)-C(77)	114.9(5)
N(9)-Fe(5)-N(11)	114.73(19)	C(78)-N(12)-Fe(6)	120.0(4)
O(2)-Fe(5)-Fe(6)	51.70(10)	C(77)-N(12)-Fe(6)	124.6(3)
N(9)-Fe(5)-Fe(6)	83.55(14)	C(91)-N(13)-C(84)	114.4(5)
N(11)-Fe(5)-Fe(6)	90.05(14)	C(91)-N(13)-Fe(7)	120.5(4)
O(2)-Fe(5)-Br(3)	92.38(11)	C(84)-N(13)-Fe(7)	124.9(4)
N(9)-Fe(5)-Br(3)	103.91(14)	C(91)-N(14)-C(90)	117.4(5)
N(11)-Fe(5)-Br(3)	119.13(14)	C(91)-N(14)-Fe(8)	117.9(4)
Fe(6)-Fe(5)-Br(3)	141.10(4)	C(90)-N(14)-Fe(8)	124.5(3)
O(2)-Fe(6)-N(10)	109.28(17)	C(104)-N(15)-C(97)	115.6(5)
O(2)-Fe(6)-N(12)	112.56(16)	C(104)-N(15)-Fe(7)	115.2(4)
N(10)-Fe(6)-N(12)	120.10(19)	C(97)-N(15)-Fe(7)	129.1(4)
O(2)-Fe(6)-Fe(5)	50.34(10)	C(104)-N(16)-C(103)	120.1(5)
N(10)-Fe(6)-Fe(5)	90.25(14)	C(104)-N(16)-Fe(8)	122.2(4)
N(12)-Fe(6)-Fe(5)	85.27(13)	C(103)-N(16)-Fe(8)	117.6(4)
O(2)-Fe(6)-Br(4)	90.17(11)	Fe(4)-O(1)-Fe(1)	165.28(19)
N(10)-Fe(6)-Br(4)	113.02(14)	Fe(4)-O(1)-Fe(2)	103.38(16)
N(12)-Fe(6)-Br(4)	107.76(14)	Fe(1)-O(1)-Fe(2)	78.31(13)
Fe(5)-Fe(6)-Br(4)	139.83(4)	Fe(4)-O(1)-Fe(3)	78.35(13)
O(2)-Fe(7)-N(15)	109.10(16)	Fe(1)-O(1)-Fe(3)	102.84(15)
O(2)-Fe(7)-N(13)	112.44(17)	Fe(2)-O(1)-Fe(3)	169.00(19)
N(15)-Fe(7)-N(13)	120.52(19)	Fe(8)-O(2)-Fe(5)	170.6(2)
O(2)-Fe(7)-Fe(8)	50.26(10)	Fe(8)-O(2)-Fe(7)	77.97(13)
N(15)-Fe(7)-Fe(8)	90.36(14)	Fe(5)-O(2)-Fe(7)	103.11(16)
N(13)-Fe(7)-Fe(8)	85.26(13)	Fe(8)-O(2)-Fe(6)	103.39(16)
O(2)-Fe(7)-Br(3)	90.32(11)	Fe(5)-O(2)-Fe(6)	77.96(13)
N(15)-Fe(7)-Br(3)	112.81(14)	Fe(7)-O(2)-Fe(6)	165.44(19)
N(13)-Fe(7)-Br(3)	107.61(13)	N(1)-C(13)-N(2)	125.6(5)
Fe(8)-Fe(7)-Br(3)	139.89(4)	N(3)-C(26)-N(4)	125.5(6)
O(2)-Fe(8)-N(14)	109.29(16)	N(7)-C(39)-N(8)	128.4(5)
O(2)-Fe(8)-N(16)	115.62(18)	N(5)-C(52)-N(6)	126.5(5)
N(14)-Fe(8)-N(16)	114.60(19)	N(9)-C(65)-N(10)	124.1(6)
O(2)-Fe(8)-Fe(7)	51.77(10)	N(11)-C(78)-N(12)	126.5(5)
N(14)-Fe(8)-Fe(7)	89.79(14)	N(14)-C(91)-N(13)	124.9(5)
N(16)-Fe(8)-Fe(7)	83.45(14)	N(16)-C(104)-N(15)	124.5(5)

Table 8.3. Bond lengths [Å] and angles [deg] for **2**.

Distances			
Fe-N(1)	2.0117(15)	C(9)-C(10)	1.505(3)
Fe-N(3)	2.0127(16)	C(10)-C(11)	1.518(3)
Fe-N(4)	2.0249(15)	C(11)-C(12)	1.523(3)
Fe-N(2)	2.0280(15)	C(13)-C(14)	1.547(3)
Fe-C(13)	2.4698(18)	C(14)-C(17)	1.530(3)
Fe-C(30)	2.4753(18)	C(14)-C(15)	1.539(3)
N(1)-C(13)	1.350(2)	C(14)-C(16)	1.539(3)
N(1)-C(12)	1.450(2)	C(18)-C(23)	1.529(3)
N(2)-C(13)	1.331(2)	C(18)-C(19)	1.530(3)
N(2)-C(6)	1.455(2)	C(19)-C(20)	1.503(3)
N(3)-C(30)	1.341(2)	C(20)-C(21)	1.515(3)
N(3)-C(23)	1.451(3)	C(21)-C(22)	1.529(3)
N(4)-C(30)	1.338(2)	C(22)-C(23)	1.518(3)
N(4)-C(29)	1.458(2)	C(24)-C(25)	1.520(3)
C(1)-C(2)	1.520(3)	C(24)-C(29)	1.527(3)
C(1)-C(6)	1.528(3)	C(25)-C(26)	1.516(3)
C(2)-C(3)	1.502(4)	C(26)-C(27)	1.515(3)
C(3)-C(4)	1.526(4)	C(27)-C(28)	1.521(3)
C(4)-C(5)	1.526(3)	C(28)-C(29)	1.524(3)
C(5)-C(6)	1.520(3)	C(30)-C(31)	1.545(3)
C(7)-C(12)	1.520(3)	C(31)-C(32)	1.531(3)
C(7)-C(8)	1.529(3)	C(31)-C(34)	1.536(3)
C(8)-C(9)	1.505(4)	C(31)-C(33)	1.537(3)

Angles			
N(1)-Fe-N(3)	143.51(6)	C(15)-C(14)-C(13)	107.78(15)
N(1)-Fe-N(4)	132.89(6)	C(16)-C(14)-C(13)	109.64(15)
N(3)-Fe-N(4)	65.34(6)	C(23)-C(18)-C(19)	111.82(18)
N(1)-Fe-N(2)	65.29(6)	C(20)-C(19)-C(18)	111.85(18)
N(3)-Fe-N(2)	137.09(7)	C(19)-C(20)-C(21)	111.42(17)
N(4)-Fe-N(2)	124.79(6)	C(20)-C(21)-C(22)	110.81(18)
N(1)-Fe-C(13)	33.10(6)	C(23)-C(22)-C(21)	111.47(17)
N(3)-Fe-C(13)	159.44(6)	N(3)-C(23)-C(22)	111.00(16)
N(4)-Fe-C(13)	134.26(6)	N(3)-C(23)-C(18)	108.65(16)
N(2)-Fe-C(13)	32.57(6)	C(22)-C(23)-C(18)	109.30(16)
N(1)-Fe-C(30)	153.59(6)	C(25)-C(24)-C(29)	112.02(16)
N(3)-Fe-C(30)	32.75(6)	C(26)-C(25)-C(24)	111.76(17)
N(4)-Fe-C(30)	32.67(6)	C(27)-C(26)-C(25)	110.90(18)
N(2)-Fe-C(30)	138.95(6)	C(26)-C(27)-C(28)	110.98(17)
C(13)-Fe-C(30)	165.26(6)	C(27)-C(28)-C(29)	111.98(16)
C(13)-N(1)-C(12)	129.79(15)	N(4)-C(29)-C(28)	111.42(15)
C(13)-N(1)-Fe	92.43(11)	N(4)-C(29)-C(24)	107.78(15)
C(12)-N(1)-Fe	137.37(12)	C(28)-C(29)-C(24)	109.53(15)
C(13)-N(2)-C(6)	133.02(16)	N(4)-C(30)-N(3)	108.91(15)
C(13)-N(2)-Fe	92.30(11)	N(4)-C(30)-C(31)	127.31(16)
C(6)-N(2)-Fe	134.00(12)	N(3)-C(30)-C(31)	123.60(16)
C(30)-N(3)-C(23)	130.91(15)	N(4)-C(30)-Fe	54.81(9)
C(30)-N(3)-Fe	92.95(11)	N(3)-C(30)-Fe	54.30(9)
C(23)-N(3)-Fe	135.91(12)	C(31)-C(30)-Fe	172.02(13)

C(30)-N(4)-C(29)	130.39(15)	C(32)-C(31)-C(34)	105.02(16)
C(30)-N(4)-Fe	92.52(11)	C(32)-C(31)-C(33)	107.65(16)
C(29)-N(4)-Fe	133.80(12)	C(34)-C(31)-C(33)	110.81(17)
C(2)-C(1)-C(6)	111.82(17)	C(32)-C(31)-C(30)	114.28(15)
C(3)-C(2)-C(1)	111.1(2)	C(34)-C(31)-C(30)	108.81(15)
C(2)-C(3)-C(4)	111.6(2)	C(33)-C(31)-C(30)	110.17(15)
C(5)-C(4)-C(3)	111.16(19)	N(1)-C(12)-C(7)	110.19(15)
C(6)-C(5)-C(4)	112.25(19)	N(1)-C(12)-C(11)	110.42(15)
N(2)-C(6)-C(5)	107.96(15)	C(7)-C(12)-C(11)	109.52(16)
N(2)-C(6)-C(1)	110.98(15)	N(2)-C(13)-N(1)	108.77(15)
C(5)-C(6)-C(1)	109.17(16)	N(2)-C(13)-C(14)	128.98(16)
C(12)-C(7)-C(8)	111.12(17)	N(1)-C(13)-C(14)	122.11(15)
C(9)-C(8)-C(7)	112.0(2)	N(2)-C(13)-Fe	55.13(9)
C(10)-C(9)-C(8)	111.37(19)	N(1)-C(13)-Fe	54.47(9)
C(9)-C(10)-C(11)	111.58(18)	C(14)-C(13)-Fe	167.92(13)
C(10)-C(11)-C(12)	111.77(17)	C(17)-C(14)-C(15)	105.80(16)
C(15)-C(14)-C(16)	112.29(17)	C(17)-C(14)-C(16)	105.66(16)
C(17)-C(14)-C(13)	115.72(15)		

Table 8.4. Bond lengths [A] and angles [deg] for **3.**

Distances			
Fe(1)-N(3)	1.993(6)	N(3)-C(23)	1.481(9)
Fe(1)-N(1)	2.039(6)	N(4)-C(30)	1.356(9)
Fe(1)-N(2)	2.050(7)	N(4)-C(29)	1.482(9)
Fe(1)-N(4)	2.072(6)	N(5)-C(47)	1.329(9)
Fe(1)-Cl(1)	2.272(2)	N(5)-C(40)	1.463(9)
Fe(1)-C(30)	2.503(8)	N(6)-C(47)	1.349(9)
Fe(2)-N(7)	1.991(7)	N(6)-C(46)	1.481(9)
Fe(2)-N(6)	2.031(6)	N(7)-C(64)	1.367(9)
Fe(2)-N(5)	2.071(6)	N(7)-C(57)	1.477(9)
Fe(2)-N(8)	2.080(6)	N(8)-C(64)	1.323(9)
Fe(2)-Cl(2)	2.263(3)	N(8)-C(63)	1.503(9)
N(1)-C(13)	1.341(9)	C(1)-C(6)	1.517(10)
N(1)-C(6)	1.476(9)	C(1)-C(2)	1.540(11)
N(2)-C(13)	1.350(9)	C(2)-C(3)	1.527(12)
N(2)-C(12)	1.487(9)	C(3)-C(4)	1.469(12)
N(3)-C(30)	1.324(9)		

Angles			
N(3)-Fe(1)-N(1)	109.7(2)	C(21)-C(20)-C(19)	111.9(8)
N(3)-Fe(1)-N(2)	113.2(3)	C(20)-C(21)-C(22)	110.8(7)
N(1)-Fe(1)-N(2)	64.3(2)	C(23)-C(22)-C(21)	111.0(7)
N(3)-Fe(1)-N(4)	64.5(2)	N(3)-C(23)-C(22)	109.7(6)
N(1)-Fe(1)-N(4)	100.5(2)	N(3)-C(23)-C(18)	109.6(6)
N(2)-Fe(1)-N(4)	163.6(2)	C(22)-C(23)-C(18)	110.2(7)
N(3)-Fe(1)-Cl(1)	115.78(19)	C(25)-C(24)-C(29)	111.2(7)
N(1)-Fe(1)-Cl(1)	134.49(18)	C(26)-C(25)-C(24)	110.8(6)
N(2)-Fe(1)-Cl(1)	98.19(18)	C(25)-C(26)-C(27)	110.9(7)
N(4)-Fe(1)-Cl(1)	97.10(17)	C(28)-C(27)-C(26)	109.7(7)

N(3)-Fe(1)-C(30)	31.8(2)	C(29)-C(28)-C(27)	110.4(6)
N(1)-Fe(1)-C(30)	107.4(2)	N(4)-C(29)-C(28)	112.2(6)
N(2)-Fe(1)-C(30)	142.4(2)	N(4)-C(29)-C(24)	108.1(6)
N(4)-Fe(1)-C(30)	32.8(2)	C(28)-C(29)-C(24)	107.3(6)
Cl(1)-Fe(1)-C(30)	110.04(18)	N(3)-C(30)-N(4)	108.2(7)
N(7)-Fe(2)-N(6)	110.5(3)	N(3)-C(30)-C(31)	123.9(7)
N(7)-Fe(2)-N(5)	116.5(2)	N(4)-C(30)-C(31)	127.8(7)
N(6)-Fe(2)-N(5)	63.8(2)	N(3)-C(30)-Fe(1)	52.4(4)
N(7)-Fe(2)-N(8)	64.4(2)	N(4)-C(30)-Fe(1)	55.8(4)
N(6)-Fe(2)-N(8)	102.2(3)	C(31)-C(30)-Fe(1)	174.2(5)
N(5)-Fe(2)-N(8)	165.7(2)	C(34)-C(31)-C(33)	107.1(7)
N(7)-Fe(2)-Cl(2)	111.28(19)	C(34)-C(31)-C(30)	115.5(6)
N(6)-Fe(2)-Cl(2)	138.1(2)	C(33)-C(31)-C(30)	110.7(6)
N(5)-Fe(2)-Cl(2)	98.76(19)	C(34)-C(31)-C(32)	103.8(6)
N(8)-Fe(2)-Cl(2)	93.72(18)	C(33)-C(31)-C(32)	110.5(6)
C(13)-N(1)-C(6)	126.1(6)	C(30)-C(31)-C(32)	109.0(6)
C(13)-N(1)-Fe(1)	94.2(5)	C(36)-C(35)-C(40)	112.0(6)
C(6)-N(1)-Fe(1)	135.8(5)	C(37)-C(36)-C(35)	110.5(7)
C(13)-N(2)-C(12)	125.4(7)	C(36)-C(37)-C(38)	112.4(7)
C(13)-N(2)-Fe(1)	93.5(5)	C(39)-C(38)-C(37)	110.9(7)
C(12)-N(2)-Fe(1)	137.6(5)	C(38)-C(39)-C(40)	111.8(7)
C(30)-N(3)-C(23)	129.0(6)	N(5)-C(40)-C(39)	109.9(6)
C(30)-N(3)-Fe(1)	95.9(5)	N(5)-C(40)-C(35)	111.7(6)
C(23)-N(3)-Fe(1)	135.0(5)	C(39)-C(40)-C(35)	110.3(7)
C(30)-N(4)-C(29)	128.2(7)	C(42)-C(41)-C(46)	111.9(7)
C(30)-N(4)-Fe(1)	91.4(5)	C(43)-C(42)-C(41)	111.0(7)
C(29)-N(4)-Fe(1)	136.9(5)	C(42)-C(43)-C(44)	111.0(8)
C(47)-N(5)-C(40)	127.6(7)	C(45)-C(44)-C(43)	110.9(7)
C(47)-N(5)-Fe(2)	93.4(5)	C(46)-C(45)-C(44)	110.9(7)
C(40)-N(5)-Fe(2)	135.1(5)	N(6)-C(46)-C(41)	111.7(6)
C(47)-N(6)-C(46)	126.7(6)	N(6)-C(46)-C(45)	111.3(6)
C(47)-N(6)-Fe(2)	94.6(5)	C(41)-C(46)-C(45)	108.4(7)
C(46)-N(6)-Fe(2)	135.1(5)	N(5)-C(47)-N(6)	108.2(7)
C(64)-N(7)-C(57)	128.0(7)	N(5)-C(47)-C(48)	130.2(7)
C(64)-N(7)-Fe(2)	95.4(5)	N(6)-C(47)-C(48)	121.6(7)
C(57)-N(7)-Fe(2)	134.8(5)	C(49)-C(48)-C(51)	104.8(6)
C(64)-N(8)-C(63)	127.4(7)	C(49)-C(48)-C(47)	116.0(7)
C(64)-N(8)-Fe(2)	92.7(5)	C(51)-C(48)-C(47)	112.6(7)
C(63)-N(8)-Fe(2)	134.6(5)	C(49)-C(48)-C(50)	103.5(7)
C(6)-C(1)-C(2)	110.3(7)	C(51)-C(48)-C(50)	111.8(7)
C(3)-C(2)-C(1)	112.1(8)	C(47)-C(48)-C(50)	107.9(6)
C(4)-C(3)-C(2)	111.5(8)	C(57)-C(52)-C(53)	109.2(7)
C(3)-C(4)-C(5)	112.5(8)	C(54)-C(53)-C(52)	111.5(8)
C(6)-C(5)-C(4)	111.0(7)	C(55)-C(54)-C(53)	111.6(7)
N(1)-C(6)-C(5)	111.6(6)	C(54)-C(55)-C(56)	109.4(7)
N(1)-C(6)-C(1)	110.9(6)	C(57)-C(56)-C(55)	110.4(7)
C(5)-C(6)-C(1)	110.5(7)	N(7)-C(57)-C(52)	108.1(6)
C(8)-C(7)-C(12)	108.8(6)	N(7)-C(57)-C(56)	108.8(6)
C(9)-C(8)-C(7)	112.7(6)	C(52)-C(57)-C(56)	110.7(6)
C(10)-C(9)-C(8)	111.0(6)	C(63)-C(58)-C(59)	110.2(7)
C(9)-C(10)-C(11)	112.8(6)	C(60)-C(59)-C(58)	109.9(7)
C(12)-C(11)-C(10)	111.4(6)	C(61)-C(60)-C(59)	110.1(8)
N(2)-C(12)-C(11)	110.8(6)	C(60)-C(61)-C(62)	112.0(7)

N(2)-C(12)-C(7)	108.7(6)	C(63)-C(62)-C(61)	110.6(7)
C(11)-C(12)-C(7)	110.1(6)	N(8)-C(63)-C(62)	108.5(6)
N(1)-C(13)-N(2)	108.0(7)	N(8)-C(63)-C(58)	109.5(6)
N(1)-C(13)-C(14)	123.3(7)	C(62)-C(63)-C(58)	109.0(7)
N(2)-C(13)-C(14	128.7(8)	N(8)-C(64)-N(7)	107.5(7)
C(17)-C(14)-C(13)	119.1(6)	N(8)-C(64)-C(65)	129.8(7)
C(17)-C(14)-C(15)	104.1(6)	N(7)-C(64)-C(65)	122.3(7)
C(13)-C(14)-C(15)	110.4(6)	C(67)-C(65)-C(64)	112.5(7)
C(17)-C(14)-C(16)	103.7(6)	C(67)-C(65)-C(66)	107.2(7)
C(13)-C(14)-C(16)	106.5(6)	C(64)-C(65)-C(66)	114.3(7)
C(15)-C(14)-C(16)	113.2(6)	C(67)-C(65)-C(68)	109.7(7)
C(23)-C(18)-C(19)	109.1(7)	C(64)-C(65)-C(68)	108.6(7)
C(20)-C(19)-C(18)	111.0(7)	C(66)-C(65)-C(68)	104.0(7)

Table 8.5. Crystal data for compounds **4** - **7**.

	4	**5**	**6**	**7**
empirical formula	$C_{20}H_{44}Cl$ Fe N_6	C41.50 H88 Fe2 N12	C82 H148 Fe2 N12 O1.50	C38 H68 Br2 Fe2 N6
formula weight	459.91	866.94	1437.82	880.50
temp (K)	238(2)	238(2)	203(2)	203(2)
λ (Å)	0.71073	0.71073	0.71073	0.71073
space group	P2(1)/c	P-1	P-1	P2(1)/c
a (Å)	9.631(2))	10.389(3)	14.283(1)	11.732(1)
b (Å)	14.350(2)	12.133(4)	14.437(1)	15.402(1)
c (Å)	19.259(3	21.766(7)	23.517(2)	12.893(1)
α (deg)		92.408(4)	86.821(2)	
β (deg)	98.581(3)	98.065(5	72.475(2)	113.110(1)
γ (deg)		106.481(4)	63.664(1)	
V(Å^3)	2631.9(7)	2595(2)	4127.1(7))	2142.7(3)
Z	4	2	2	2
d_{calc} (g/cm^3)	1.161	1.109	1.157	1.365
absorption coefficient (mm^{-1})	0.690	0.597	0.402	2.574
R1[a]	0.0470	0.0641	0.0508	0.0386
wR2[b]	0.0995	0.1489	0.1231	0.0750

[a] $R1 = \sum \| F_o | - | F_c \| / \sum | F_o |$.

[b] $wR2 = \left(\sum w (| F_o | - | F_c |)^2 / \sum w | F_o |^2 \right)^{1/2}$

Table 8.6. Selected bond lengths [Å] and angles [deg] for **4**.

Distances			
Fe-N(2)	2.006(3)	N(2)-C(4)	1.466(5)
Fe-N(5)	2.010(3)	N(3)-C(10)	1.361(5)
Fe-N(1)	2.087(3)	N(3)-C(7)	1.472(6)
Fe-N(4)	2.082(3)	N(4)-C(20)	1.335(5)
Fe-Cl	2.2796(13)	N(4)-C(11)	1.477(5)
Fe-C(10)	2.476(4)	N(5)-C(20)	1.349(5)
Fe-C(20)	2.481(4)	N(5)-C(14)	1.466(5)
N(1)-C(10)	1.342(5)	N(6)-C(20)	1.367(5)
N(1)-C(1)	1.456(5)	N(6)-C(17)	1.458(5)
N(2)-C(10)	1.336(5)		

Angles			
N(2)-Fe-N(5)	114.00(14)	C(11)-N(4)-Fe	139.5(2)
N(2)-Fe-N(1)	65.40(12)	C(20)-N(5)-C(14)	121.8(3)
N(5)-Fe-N(1)	103.66(13)	C(20)-N(5)-Fe	93.1(2)
N(2)-Fe-N(4)	104.88(13)	C(14)-N(5)-Fe	140.1(3)
N(5)-Fe-N(4)	65.41(13)	C(20)-N(6)-C(17)	126.2(3)
N(1)-Fe-N(4)	162.05(12)	N(1)-C(1)-C(3)	109.6(3)
N(2)-Fe-Cl	122.71(10)	N(1)-C(1)-C(2)	111.8(3)
N(5)-Fe-Cl	123.29(11)	N(2)-C(4)-C(6)	109.4(4)
N(1)-Fe-Cl	99.15(10)	N(2)-C(4)-C(5)	112.9(4)
N(4)-Fe-Cl	98.79(9)	N(3)-C(7)-C(8)	106.8(5)
N(5)-Fe-C(10)	111.85(14)	N(3)-C(7)-C(9)	111.3(5)
N(4)-Fe-C(10)	135.51(13)	N(2)-C(10)-N(1)	111.4(3)
Cl-Fe-C(10)	115.18(10)	N(2)-C(10)-N(3)	121.8(4)
N(2)-Fe-C(20)	112.85(13)	N(1)-C(10)-N(3)	126.8(4)
N(1)-Fe-C(20)	134.91(13)	N(3)-C(10)-Fe	175.5(3)
Cl-Fe-C(20)	114.89(10)	N(4)-C(11)-C(12)	109.2(3)
C(10)-Fe-C(20)	129.92(14)	N(4)-C(11)-C(13)	111.6(3)
C(10)-N(1)-C(1)	124.3(3)	N(5)-C(14)-C(16)	110.8(4)
C(10)-N(1)-Fe	89.7(2)	N(5)-C(14)-C(15)	109.9(4)
C(1)-N(1)-Fe	139.3(3)	N(6)-C(17)-C(19)	108.1(3)
C(10)-N(2)-C(4)	122.8(3)	N(6)-C(17)-C(18)	111.5(4)
C(10)-N(2)-Fe	93.4(2)	N(4)-C(20)-N(5)	111.0(3)
C(4)-N(2)-Fe	141.3(3)	N(4)-C(20)-N(6)	127.1(4)
C(10)-N(3)-C(7)	128.1(4)	N(5)-C(20)-N(6)	121.8(4)
C(20)-N(4)-C(11)	122.8(3)	N(6)-C(20)-Fe	175.8(3)
C(20)-N(4)-Fe	90.4(2)		

Table 8.7. Selected bond distances [Å] and angles [deg] for **5**.

Distances			
Fe(1)-N(10)	2.056(6)	N(5)-C(20)	1.359(11)
Fe(1)-N(7)	2.075(7)	N(5)-C(14)	1.474(10)
Fe(1)-N(2)	2.089(7)	N(6)-C(20)	1.367(11)
Fe(1)-N(1)	2.127(7)	N(6)-C(17)	1.466(12)
Fe(2)-N(8)	2.042(6)	N(7)-C(30)	1.321(10)
Fe(2)-N(11)	2.084(6)	N(7)-C(21)	1.482(10)
Fe(2)-N(4)	2.089(7)	N(8)-C(30)	1.330(10)
Fe(2)-N(5)	2.124(7)	N(8)-C(24)	1.464(10)
N(1)-C(10)	1.314(11)	N(9)-C(30)	1.420(10)
N(1)-C(1)	1.473(10)	N(9)-C(27)	1.481(10)
N(2)-C(10)	1.339(11)	N(10)-C(40)	1.339(10)
N(2)-C(4)	1.467(10)	N(10)-C(31)	1.471(10)
N(3)-C(10)	1.417(11)	N(11)-C(40)	1.340(10)
N(3)-C(7)	1.475(11)	N(11)-C(34)	1.478(10)
N(4)-C(20)	1.330(11)	N(12)-C(40)	1.406(10)
N(4)-C(11)	1.466(10)	N(12)-C(37)	1.448(10)

Angles			
N(10)-Fe(1)-N(7)	132.5(3)	C(30)-N(7)-Fe(1)	116.1(6)
N(10)-Fe(1)-N(2)	110.5(3)	C(21)-N(7)-Fe(1)	121.1(6)
N(7)-Fe(1)-N(2)	107.2(3)	C(30)-N(8)-C(24)	120.1(7)
N(10)-Fe(1)-N(1)	109.0(3)	C(30)-N(8)-Fe(2)	114.3(6)
N(7)-Fe(1)-N(1)	113.3(3)	C(24)-N(8)-Fe(2)	125.5(6)
N(2)-Fe(1)-N(1)	63.3(3)	C(30)-N(9)-C(27)	124.4(7)
N(8)-Fe(2)-N(11)	132.3(3)	C(40)-N(10)-C(31)	119.5(7)
N(8)-Fe(2)-N(4)	112.1(3)	C(40)-N(10)-Fe(1)	109.6(5)
N(11)-Fe(2)-N(4)	106.9(3)	C(31)-N(10)-Fe(1)	127.4(6)
N(8)-Fe(2)-N(5)	105.2(3)	C(40)-N(11)-C(34)	120.2(7)
N(11)-Fe(2)-N(5)	116.5(3)	C(40)-N(11)-Fe(2)	117.8(6)
N(4)-Fe(2)-N(5)	63.0(3)	C(34)-N(11)-Fe(2)	121.3(5)
C(10)-N(1)-C(1)	120.9(8)	C(40)-N(12)-C(37)	127.6(8)
C(10)-N(1)-Fe(1)	91.4(6)	N(1)-C(10)-N(2)	113.0(9)
C(1)-N(1)-Fe(1)	142.9(6)	N(1)-C(10)-N(3)	125.8(9)
C(10)-N(2)-C(4)	121.7(8)	N(2)-C(10)-N(3)	121.2(10)
C(10)-N(2)-Fe(1)	92.4(6)	N(4)-C(20)-N(5)	110.0(9)
C(4)-N(2)-Fe(1)	144.5(6)	N(4)-C(20)-N(6)	123.8(9)
C(10)-N(3)-C(7)	123.1(9)	N(5)-C(20)-N(6)	126.1(10)
C(20)-N(4)-C(11)	120.6(8)	N(7)-C(21)-C(22)	111.2(7)
C(20)-N(4)-Fe(2)	94.7(6)	C(29)-C(27)-C(28)	109.4(8)
C(11)-N(4)-Fe(2)	143.2(6)	N(7)-C(30)-N(8)	119.6(8)
C(20)-N(5)-C(14)	123.7(8)	N(7)-C(30)-N(9)	119.2(8)
C(20)-N(5)-Fe(2)	92.2(6)	N(8)-C(30)-N(9)	121.2(8)
C(14)-N(5)-Fe(2)	141.1(6)	N(10)-C(40)-N(11)	118.8(8)
C(20)-N(6)-C(17)	128.5(8)	N(10)-C(40)-N(12)	119.8(8)
C(30)-N(7)-C(21)	118.8(7)	N(11)-C(40)-N(12)	121.3(9)

Table 8.8. Selected bond distances [Å] and angles [deg] for **6**.

Distances			
Fe(1)-N(10)	2.050(2)	N(5)-C(38)	1.328(4)
Fe(1)-N(7)	2.050(2)	N(5)-C(31)	1.459(4)
Fe(1)-N(2)	2.112(3)	N(6)-C(38)	1.416(4)
Fe(1)-N(1)	2.122(2)	N(6)-C(37)	1.465(4)
Fe(2)-N(8)	2.033(2)	N(7)-C(57)	1.352(4)
Fe(2)-N(11)	2.056(2)	N(7)-C(44)	1.473(4)
Fe(2)-N(4)	2.123(2)	N(8)-C(57)	1.325(4)
Fe(2)-N(5)	2.134(2)	N(8)-C(50)	1.472(4)
N(1)-C(19)	1.322(4)	N(9)-C(57)	1.382(4)
N(1)-C(6)	1.459(4)	N(9)-C(56)	1.462(4)
N(2)-C(19)	1.327(4)	N(10)-C(76)	1.323(3)
N(2)-C(12)	1.458(4)	N(10)-C(63)	1.478(4)
N(3)-C(19)	1.402(4)	N(11)-C(76)	1.343(4)
N(3)-C(18)	1.414(5)	N(11)-C(69)	1.470(4)
N(4)-C(38)	1.321(4)	N(12)-C(76)	1.393(3)
N(4)-C(25)	1.469(4)	N(12)-C(75)	1.475(4)

Angles			
N(10)-Fe(1)-N(7)	134.05(9)	N(1)-C(19)-N(3)	123.1(3)
N(10)-Fe(1)-N(2)	108.20(11)	N(2)-C(19)-N(3)	123.4(3)
N(7)-Fe(1)-N(2)	109.40(11)	C(38)-N(6)-C(37)	118.0(2)
N(10)-Fe(1)-N(1)	115.93(10)	C(57)-N(7)-C(44)	124.2(2)
N(7)-Fe(1)-N(1)	104.18(10)	C(57)-N(7)-Fe(1)	111.52(19)
N(2)-Fe(1)-N(1)	63.09(10)	C(44)-N(7)-Fe(1)	119.42(18)
N(8)-Fe(2)-N(11)	129.10(9)	C(57)-N(8)-C(50)	122.0(2)
N(8)-Fe(2)-N(4)	107.52(9)	C(57)-N(8)-Fe(2)	111.38(19)
N(11)-Fe(2)-N(4)	117.01(9)	C(50)-N(8)-Fe(2)	126.58(19)
N(8)-Fe(2)-N(5)	114.35(9)	C(57)-N(9)-C(56)	128.8(3)
N(11)-Fe(2)-N(5)	107.18(9)	C(76)-N(10)-C(63)	120.7(2)
N(4)-Fe(2)-N(5)	63.07(9)	C(76)-N(10)-Fe(1)	107.72(19)
C(19)-N(1)-C(6)	123.4(3)	C(63)-N(10)-Fe(1)	129.80(18)
C(19)-N(1)-Fe(1)	91.56(18)	C(76)-N(11)-C(69)	118.8(2)
C(6)-N(1)-Fe(1)	145.0(2)	C(76)-N(11)-Fe(2)	118.36(18)
C(19)-N(2)-C(12)	122.2(3)	C(69)-N(11)-Fe(2)	121.07(18)
C(19)-N(2)-Fe(1)	91.86(19)	C(76)-N(12)-C(75)	126.0(2)
C(12)-N(2)-Fe(1)	145.0(2)	N(4)-C(38)-N(5)	114.4(3)
C(19)-N(3)-C(18)	120.8(3)	N(4)-C(38)-N(6)	122.9(3)
C(38)-N(4)-C(25)	121.8(2)	N(5)-C(38)-N(6)	122.7(3)
C(38)-N(4)-Fe(2)	91.64(18)	N(8)-C(57)-N(7)	116.0(3)
C(25)-N(4)-Fe(2)	142.89(18)	N(8)-C(57)-N(9)	124.4(3)
C(38)-N(5)-C(31)	121.9(2)	N(7)-C(57)-N(9)	119.6(3)
C(38)-N(5)-Fe(2)	90.93(17)	N(10)-C(76)-N(11)	117.5(3)
C(31)-N(5)-Fe(2)	143.85(19)	N(10)-C(76)-N(12)	123.1(3)
N(1)-C(19)-N(2)	113.5(3)	N(11)-C(76)-N(12)	119.3(2)

Table 8.9. Selected bond distances [Å] and angles [deg] for **7**.

Distances			
Br-Fe	2.3891(4)	N(1)-C(6)	1.495(3)
Fe-N(1)#1	2.0347(18)	N(1)-Fe#1	2.0347(17)
Fe-N(2)	2.0363(18)	N(2)-C(19)	1.315(3)
Fe-N(1)	2.2557(17)	N(2)-C(12)	1.473(3)
Fe-Fe#1	2.8399(6)	N(3)-C(19)	1.355(3)
N(1)-C(19)	1.390(3)	N(3)-C(18)	1.465(3)
Angles			
N(1)#1-Fe-N(2)	116.91(7)	C(6)-N(1)-Fe#1	119.28(13)
N(1)#1-Fe-N(1)	97.28(6)	C(19)-N(1)-Fe	85.57(12)
N(2)-Fe-N(1)	63.44(7)	C(6)-N(1)-Fe	126.63(13)
N(1)#1-Fe-Br	116.55(5)	Fe#1-N(1)-Fe	82.72(6)
N(2)-Fe-Br	122.37(5)	C(19)-N(2)-C(12)	121.39(18)
N(1)-Fe-Br	127.45(5)	C(19)-N(2)-Fe	97.08(13)
N(1)#1-Fe-Fe#1	51.99(5)	C(12)-N(2)-Fe	141.51(14)
N(2)-Fe-Fe#1	88.23(5)	C(19)-N(3)-C(18)	125.31(19)
N(1)-Fe-Fe#1	45.29(5)	N(2)-C(19)-N(3)	124.6(2)
Br-Fe-Fe#1	143.44(2)	N(2)-C(19)-N(1)	113.61(18)
C(19)-N(1)-C(6)	115.68(17)	N(3)-C(19)-N(1)	121.76(19)
C(19)-N(1)-Fe#1	118.76(14)		

Table 8.10. Crystal data and structure refinement for **8** and **9**.

	8	**9**
empirical formula	C40 H86 Fe2 Li2 N12	C37 H79 Fe2 N11
formula weight	860.79	789.81
temp (K),	238(2)	238(2),
λ (Å)	0.71073	0.71073
space group	P-1	Pccn
a (Å)	9.944(3)	19.572(6),
b (Å)	9.946(3)	12.747(4),
c (Å)	13.775(4)	18.649(6),
α (deg)	73.201(5)	90
β (deg)	82.316(5)	90
γ (deg)	73.183(5)	90
V(Å^3),	1246.5(7)	4653(3)
Z	1	4
d_{calc} (g/cm^3),	1.147	1.128
absorption coefficient (mm^{-1})	0.620	0.659
R1	0.0480	0.0488
wR2	0.1107	0.1076

Table 8.11. Selected bond distances [Å] and angles [deg] for **8**.

Distances			
Fe-N(2)	2.0304(18)	N(3)-C(7)	1.464(3)
Fe-N(4)	2.0524(18)	N(3)-Li	1.952(5)
Fe-N(1)#1	2.0931(18)	N(4)-C(20)	1.385(3)
Fe-N(1)	2.2351(18)	N(4)-C(11)	1.484(3)
Fe-Li#1	2.764(4)	N(4)-Li#1	2.214(4)
N(1)-C(10)	1.457(3)	N(5)-C(20)	1.376(3)
N(1)-C(1)	1.494(3)	N(5)-C(14)	1.455(3)
N(1)-Fe#1	2.0931(17)	N(6)-C(20)	1.309(3)
N(1)-Li	2.298(4)	N(6)-C(17)	1.469(3)
N(2)-C(10)	1.341(3)	N(6)-Li#1	1.976(5)
N(2)-C(4)	1.467(3)	Li-N(6)#1	1.976(5)
N(3)-C(10)	1.315(3)	Li-N(4)#1	2.214(4)

Angles			
N(2)-Fe-N(4)	126.71(7)	C(11)-N(4)-Li#1	113.26(19)
N(2)-Fe-N(1)#1	119.39(7)	Fe-N(4)-Li#1	80.66(11)
N(4)-Fe-N(1)#1	106.01(7)	C(20)-N(5)-C(14)	128.5(2)
N(2)-Fe-N(1)	64.21(7)	C(20)-N(6)-C(17)	121.36(19)
N(4)-Fe-N(1)	142.31(7)	C(20)-N(6)-Li#1	92.74(19)
N(1)#1-Fe-N(1)	92.91(6)	C(17)-N(6)-Li#1	143.2(2)
N(2)-Fe-Li#1	148.15(10)	N(3)-C(10)-N(2)	136.6(2)
N(4)-Fe-Li#1	52.23(10)	N(3)-C(10)-N(1)	114.79(18)
N(1)#1-Fe-Li#1	54.38(9)	N(2)-C(10)-N(1)	108.64(17)
N(1)-Fe-Li#1	140.15(10)	N(6)-C(20)-N(5)	122.1(2)
C(10)-N(1)-C(1)	110.15(16)	N(6)-C(20)-N(4)	116.31(19)
C(10)-N(1)-Fe#1	117.62(12)	N(5)-C(20)-N(4)	121.48(19)
C(1)-N(1)-Fe#1	123.67(14)	N(6)-C(20)-Li#1	54.58(15)
C(10)-N(1)-Fe	87.34(11)	N(5)-C(20)-Li#1	160.59(19)
C(1)-N(1)-Fe	124.13(13)	N(4)-C(20)-Li#1	64.57(15)
Fe#1-N(1)-Fe	87.09(6)	N(3)-Li-N(6)#1	168.7(2)
C(10)-N(1)-Li	78.48(15)	N(3)-Li-N(4)#1	125.3(2)
C(1)-N(1)-Li	84.38(15)	N(6)#1-Li-N(4)#1	65.94(14)
Fe#1-N(1)-Li	77.86(11)	N(3)-Li-N(1)	66.11(13)
Fe-N(1)-Li	151.29(13)	N(6)#1-Li-N(1)	115.8(2)
C(10)-N(2)-C(4)	124.53(18)	N(4)#1-Li-N(1)	94.38(15)
C(10)-N(2)-Fe	99.46(13)	N(3)-Li-Fe#1	101.59(16)
C(4)-N(2)-Fe	135.69(14)	N(6)#1-Li-Fe#1	86.45(15)
C(10)-N(3)-C(7)	124.71(19)	N(4)#1-Li-Fe#1	47.11(9)
C(10)-N(3)-Li	95.91(18)	N(1)-Li-Fe#1	47.76(8)
C(7)-N(3)-Li	138.52(19)	C(20)#1-Li-Fe#1	69.37(11)
C(20)-N(4)-C(11)	115.60(17)	C(10)-Li-Fe#1	71.25(11)
C(20)-N(4)-Fe	117.89(14)	C(1)-Li-Fe#1	72.27(11)
C(11)-N(4)-Fe	126.20(14)		
C(20)-N(4)-Li#1	81.05(16)		

Table 8.12. Selected bond distances [Å] and angles [deg] for **9**.

Distances			
Fe-N(2)	2.054(4)	N(3)-C(7)	1.469(7)
Fe-N(4)	2.056(5)	N(4)-C(19)	1.336(7)
Fe-N(5)#1	2.093(5)	N(4)-C(11)	1.477(7)
Fe-N(1)	2.119(4)	N(5)-C(19)	1.311(7)
Fe-C(10)	2.499(6)	N(5)-C(14)	1.466(7)
N(1)-C(10)	1.327(7)	N(5)-Fe#1	2.093(5)
N(1)-C(1)	1.465(7)	N(6)-C(17)	1.407(13)
N(2)-C(10)	1.331(7)	N(6)-C(19)	1.453(6)
N(2)-C(4)	1.454(7)	N(6)-C(19)#1	1.453(6)
N(3)-C(10)	1.394(6)		

Angles			
N(2)-Fe-N(4)	121.32(19)	C(19)-N(4)-Fe	103.2(4)
N(2)-Fe-N(5)#1	127.99(18)	C(11)-N(4)-Fe	130.8(4)
N(4)-Fe-N(5)#1	103.21(18)	C(19)-N(5)-C(14)	121.4(5)
N(2)-Fe-N(1)	64.18(18)	C(19)-N(5)-Fe#1	109.4(4)
N(4)-Fe-N(1)	118.2(2)	C(14)-N(5)-Fe#1	126.1(4)
N(5)#1-Fe-N(1)	118.24(18)	C(17)-N(6)-C(19)	115.1(13)
N(2)-Fe-C(10)	32.14(17)	C(17)-N(6)-C(19)#1	131.0(15)
N(4)-Fe-C(10)	124.95(19)	C(19)-N(6)-C(19)#1	113.4(7)
N(5)#1-Fe-C(10)	130.84(18)	N(1)-C(10)-N(2)	113.2(5)
N(1)-Fe-C(10)	32.06(16)	N(1)-C(10)-N(3)	123.6(6)
C(10)-N(1)-C(1)	121.9(5)	N(2)-C(10)-N(3)	123.3(6)
C(10)-N(1)-Fe	89.9(3)	N(1)-C(10)-Fe	58.0(3)
C(1)-N(1)-Fe	145.5(4)	N(2)-C(10)-Fe	55.2(3)
C(10)-N(2)-C(4)	123.8(5)	N(3)-C(10)-Fe	177.5(5)
C(10)-N(2)-Fe	92.7(3)	N(5)-C(19)-N(4)	136.8(6)
C(4)-N(2)-Fe	137.5(4)	N(5)-C(19)-N(6)	112.2(5)
C(10)-N(3)-C(7)	122.1(5)	N(4)-C(19)-N(6)	111.0(4)
C(19)-N(4)-C(11)	123.0(5)		

Table 8.13. Crystal data and structure refinement for **10** and **11**.

	10	**11**
empirical formula	C44 H102 Fe2 Li4 N6 O2 Si4	C26 H64 Fe N6 Si4
formula weight	999.14	629.04
temp (K),	238(2)	203(2)
λ (Å)	0.71073	0.71073
space group	$P2_1/n$	C2/c
a (Å)	16.410(9)	17.438(2)
b (Å)	11.398(6)	8.6336(9)
c (Å)	17.380(9)	26.222(3)
α (deg)		
β (deg)	107.013(7)	94.141(2)
γ (deg)		
V(Å^3),	3108(3)	3937.5(7)
Z	2	4
d_{calc} (g/cm^3),	1.068	1.061
absorption coefficient (mm^{-1})	0.578	0.527
R1	0.0525	0.0577
wR2	0.1381	0.1985

Table 8.14. Bond lengths [A] and angles [deg] for **10**.

Distances			
Fe-C(15)	2.097(5)	N(3)-C(10)	1.310(6)
Fe-C(11)	2.110(6)	N(3)-C(7)	1.475(6)
Fe-N(1)	2.122(4)	C(1)-C(2)	1.517(7)
Fe-N(2)	2.148(4)	C(1)-C(3)	1.545(7)
Li(1)-O(1)	1.864(11)	C(4)-C(5)	1.522(7)
Li(1)-N(2)	1.954(10)	C(4)-C(6)	1.525(7)
Li(1)-C(10)	2.760(11)	C(7)-C(8)	1.484(8)
Li(2)-N(3)	1.948(10)	C(7)-C(9)	1.521(8)
Li(2)-N(1)#1	2.053(10)	C(11)-Si(1)	1.825(6)
Li(2)-C(10)	2.610(11)	C(12)-Si(1)	1.838(8)
Li(2)-N(1)	2.712(10)	C(13)-Si(1)	1.870(9)
N(1)-C(10)	1.400(6)	C(14)-Si(1)	1.855(7)
N(1)-C(1)	1.477(6)	C(15)-Si(2)	1.827(5)
N(1)-Li(2)#1	2.053(10)	C(16)-Si(2)	1.739(11)
N(2)-C(10)	1.381(6)	C(17)-Si(2)	1.764(11)
N(2)-C(4)	1.472(6)	C(18)-Si(2)	1.721(11)

Angles			
C(15)-Fe-C(11)	125.1(2)	Fe-N(1)-Li(2)	147.8(3)
C(15)-Fe-N(1)	104.49(18)	C(10)-N(2)-C(4)	122.3(4)
C(11)-Fe-N(1)	123.4(2)	C(10)-N(2)-Li(1)	110.5(5)
C(15)-Fe-N(2)	122.17(19)	C(4)-N(2)-Li(1)	115.0(5)
C(11)-Fe-N(2)	103.40(19)	C(10)-N(2)-Fe	93.5(3)

N(1)-Fe-N(2)	63.64(16)	C(4)-N(2)-Fe	128.7(3)
C(15)-Fe-Li(1)	163.5(3)	Li(1)-N(2)-Fe	77.9(3)
C(11)-Fe-Li(1)	57.5(3)	C(10)-N(3)-C(7)	122.0(4)
N(1)-Fe-Li(1)	83.0(3)	C(10)-N(3)-Li(2)	104.8(4)
N(2)-Fe-Li(1)	47.7(2)	C(7)-N(3)-Li(2)	132.3(4)
C(15)-Fe-Li(2)#1	57.0(2)	N(1)-C(1)-C(2)	108.2(4)
C(11)-Fe-Li(2)#1	152.7(3)	N(1)-C(1)-C(3)	111.7(4)
N(1)-Fe-Li(2)#1	47.6(2)	C(2)-C(1)-C(3)	109.9(5)
N(2)-Fe-Li(2)#1	94.0(2)	N(2)-C(4)-C(5)	107.6(4)
Li(1)-Fe-Li(2)#1	129.7(3)	N(2)-C(4)-C(6)	111.2(4)
O(1)-Li(1)-N(2)	134.9(6)	C(5)-C(4)-C(6)	110.9(5)
O(1)-Li(1)-Fe	166.8(6)	N(3)-C(7)-C(8)	111.3(5)
N(2)-Li(1)-Fe	54.4(3)	N(3)-C(7)-C(9)	108.4(5)
O(1)-Li(1)-C(10)	123.8(5)	C(8)-C(7)-C(9)	110.6(5)
N(2)-Li(1)-C(10)	28.0(2)	N(3)-C(10)-N(2)	132.3(5)
Fe-Li(1)-C(10)	58.7(2)	N(3)-C(10)-N(1)	119.6(4)
N(3)-Li(2)-N(1)#1	137.2(5)	N(2)-C(10)-N(1)	108.1(4)
N(3)-Li(2)-C(10)	29.0(2)	N(3)-C(10)-Li(2)	46.2(3)
N(1)#1-Li(2)-C(10)	115.4(4)	N(2)-C(10)-Li(2)	157.4(4)
N(3)-Li(2)-N(1)	57.6(3)	N(1)-C(10)-Li(2)	78.8(3)
N(1)#1-Li(2)-N(1)	99.2(4)	N(3)-C(10)-Li(1)	131.0(4)
C(10)-Li(2)-N(1)	30.42(17)	N(2)-C(10)-Li(1)	41.6(3)
N(3)-Li(2)-Fe#1	161.6(5)	N(1)-C(10)-Li(1)	92.0(4)
N(1)#1-Li(2)-Fe#1	49.8(2)	Li(2)-C(10)-Li(1)	161.0(4)
C(10)-Li(2)-Fe#1	165.2(4)	Si(1)-C(11)-Fe	118.8(3)
N(1)-Li(2)-Fe#1	140.4(4)	Si(2)-C(15)-Fe	120.0(3)
N(3)-Li(2)-Li(2)#1	91.0(5)	O(1)-C(19)-C(20)	106.5(8)
N(1)#1-Li(2)-Li(2)#1	58.8(3)	C(21)-C(20)-C(19)	104.6(8)
C(10)-Li(2)-Li(2)#1	62.2(3)	C(20)-C(21)-C(22)	107.6(7)
N(1)-Li(2)-Li(2)#1	40.4(3)	O(1)-C(22)-C(21)	107.6(7)
Fe#1-Li(2)-Li(2)#1	104.1(4)	C(18)-Si(2)-C(16)	108.0(10)
C(19)-O(1)-C(22)	107.4(6)	C(18)-Si(2)-C(17)	105.1(10)
C(19)-O(1)-Li(1)	125.7(5)	C(16)-Si(2)-C(17)	101.4(9)
C(22)-O(1)-Li(1)	126.8(5)	C(18)-Si(2)-C(15)	113.8(4)
C(10)-N(1)-C(1)	116.4(4)	C(16)-Si(2)-C(15)	113.9(4)
C(10)-N(1)-Li(2)#1	119.4(4)	C(17)-Si(2)-C(15)	113.5(4)
C(1)-N(1)-Li(2)#1	110.2(4)	C(11)-Si(1)-C(12)	112.0(4)
C(10)-N(1)-Fe	94.1(3)	C(11)-Si(1)-C(14)	113.1(3)
C(1)-N(1)-Fe	130.5(3)	C(12)-Si(1)-C(14)	108.9(4)
Li(2)#1-N(1)-Fe	82.6(3)	C(11)-Si(1)-C(13)	109.9(4)
C(10)-N(1)-Li(2)	70.8(3)	C(12)-Si(1)-C(13)	107.6(5)
C(1)-N(1)-Li(2)	81.3(3)	C(14)-Si(1)-C(13)	105.1(4)
Li(2)#1-N(1)-Li(2)	80.8(4)		

Table 8.15. Selected bond distances [Å] and angles [deg] for **11**.

Distances			
Fe-N(1)#1	2.013(3)	Si(2)-C(13)	1.860(6)
Fe-N(1)	2.013(3)	Si(2)-C(11)	1.864(5)
Fe-N(2)#1	2.031(3)	N(1)-C(7)	1.320(5)
Fe-N(2)	2.031(3)	N(1)-C(1)	1.449(5)
Fe-C(7)	2.432(4)	N(2)-C(7)	1.322(5)
Fe-C(7)#1	2.432(4)	N(2)-C(4)	1.449(5)
Si(1)-N(3)	1.752(3)	N(3)-C(7)	1.438(5)
Si(1)-C(10)	1.849(6)	C(1)-C(3)	1.508(7)
Si(1)-C(9)	1.855(6)	C(1)-C(2)	1.528(7)
Si(1)-C(8)	1.866(6)	C(4)-C(6)	1.515(8)
Si(2)-N(3)	1.752(3)	C(4)-C(5)	1.522(7)
Si(2)-C(12)	1.844(6)		

Angles			
N(1)#1-Fe-N(1)	137.93(19)	N(3)-Si(2)-C(11)	112.2(2)
N(1)#1-Fe-N(2)#1	65.80(12)	C(12)-Si(2)-C(11)	109.6(3)
N(1)-Fe-N(2)#1	129.78(13)	C(13)-Si(2)-C(11)	107.1(3)
N(1)#1-Fe-N(2)	129.78(13)	C(7)-N(1)-C(1)	125.4(3)
N(1)-Fe-N(2)	65.80(12)	C(7)-N(1)-Fe	91.3(2)
N(2)#1-Fe-N(2)	142.6(2)	C(1)-N(1)-Fe	143.2(3)
N(1)#1-Fe-C(7)	145.53(12)	C(7)-N(2)-C(4)	125.8(3)
N(1)-Fe-C(7)	32.86(12)	C(7)-N(2)-Fe	90.4(2)
N(2)#1-Fe-C(7)	148.56(12)	C(4)-N(2)-Fe	143.5(3)
N(2)-Fe-C(7)	32.93(12)	C(7)-N(3)-Si(1)	116.9(2)
N(1)#1-Fe-C(7)#1	32.86(12)	C(7)-N(3)-Si(2)	116.9(2)
N(1)-Fe-C(7)#1	145.53(12)	Si(1)-N(3)-Si(2)	126.04(19)
N(2)#1-Fe-C(7)#1	32.93(12)	N(1)-C(1)-C(3)	110.4(4)
N(2)-Fe-C(7)#1	148.56(12)	N(1)-C(1)-C(2)	108.8(4)
C(7)-Fe-C(7)#1	177.51(16)	C(3)-C(1)-C(2)	108.9(5)
N(3)-Si(1)-C(10)	109.2(2)	N(2)-C(4)-C(6)	108.6(4)
N(3)-Si(1)-C(9)	110.9(3)	N(2)-C(4)-C(5)	110.9(4)
C(10)-Si(1)-C(9)	108.0(3)	C(6)-C(4)-C(5)	108.7(4)
N(3)-Si(1)-C(8)	111.4(2)	N(1)-C(7)-N(2)	112.5(3)
C(10)-Si(1)-C(8)	109.2(4)	N(1)-C(7)-N(3)	124.2(3)
C(9)-Si(1)-C(8)	108.0(3)	N(2)-C(7)-N(3)	123.3(3)
N(3)-Si(2)-C(12)	109.5(2)	N(1)-C(7)-Fe	55.8(2)
N(3)-Si(2)-C(13)	110.4(2)	N(2)-C(7)-Fe	56.6(2)
C(12)-Si(2)-C(13)	108.0(3)	N(3)-C(7)-Fe	179.8(3)

References for Chapter Eight

[1] a) Edelmann, F.T. *Coord. Chem. Rev.* **1994**, *137*, 403
b) Barker, J.; Kilner, M. *Coord. Chem. Rev.* **1994**, *133*, 219

[2] E.W. Abel, F.G.A. Stone, G.Wilkinson, *Comprehensive Organometallic Chemistry*, Pergamon, Vol.7, **1997**

[3] R.A. Anderson, K. Faegri, J.C. Green, A. Haaland, M.F. Lapert, W. Leung, K. Krypdal, *Inorg. Chem.* **1988**, *27*, 1782

[4] F.A. Cotton, R.A. Walton, *Multiple Bonds Between Metal Atoms*, Oxford University Press, UK, 2nd Ed, **1993**

[5] Small, B.L.; Brookhart, M.; Bennett, A.M.A. *J. Am. Chem. Soc.* **1998**, *120*, 4049

[6] Barker, J.; Kilner, M. *Coord. Chem. Rev.* **1994**, *133*, 219

[7] Clark, J. A.; Kilner, M.; Pietrzykowski, A. *Inorg. Chim. Acta.* **1984**, *82*, 85.

[8] Zinn, A.; von Arnim, H.;Massa, W.; Shafer, M.; Pebler, J.; Dehnicke, K. *Z. Naturforsch.* **1991**, *46B*, 1300.

[9] Cotton, F.A. ;Daniels, L. M.; Murillo, C.A.; *Inorg. Chim. Acta,* **1994**, *224*, 5.

[10] F.A. Cotton, L.M. Daniels, J.C. Matonic, C.A. Murillo, *Inorg. Chim. Acta,* **1997**, *256*, 277

[11] F.A. Cotton, L.M. Daniels, L.R. Falvello, C.A. Murillo, *Inorg. Chim. Acta,* **1994**, *219*, 7

[12] Connelly, N.G.; Hopkins, P.M.; Orpen, A.G.; Rosair, G.M.; Viguri, F. *J. Chem. Soc. Dalton. Trans.* **1992**, 2907

[13] F.A. Cotton, L.M. Daniels, Maloney C.A. Murillo *Inorg. Chim. Acta,* **1996**, *242*, 31

[14] F.A. Cotton, L.M. Daniels, J.C. Matonic, C.A. Murillo, X. Wang, H. Zhou, *Inorg. Chim. Acta,* **1997**, *266*, 91

[15] F.A. Cotton, L.M. Daniels, D.J. Maloney, C.A. Murillo, *Inorg. Chim. Acta,* **1996**, *252*, 293

[16] Bremer, N.J.; Cutcliffe, A.B.; Farona, M.F. *Chem. Commun.* **1970**, 932.

[17] Dinger, M.B.; Henderson, W. *Chem. Commun.* **1996**, 212.

[18] see for example:Mikuriya, M.; Hashimoto, Y.; Nakshima, S. *Chem. Commun.* **1996**, 295. Menage, S.; Fujii, H.; Hendrich, M. P.; Que Jr., L. *Angew. Chem,.Int. Ed. Engl.*, **1994**, *33*, 1660. Taft, K. L.; Papaefthymiou, G. C.;Caneschi, A.; Pence, L. E.; Delfs, C. D.; Lippard, S. *J. Am. Chem. Soc.* **1993**, *115*, 11753.; Taft, K. L.; Papaefthymiou, G. C.; Lippard, S *Inorg. Chem.* **1994**, *33*, 1510.; Sessler, J. L.; Hugdahl, J. D.; Lyanch, V.; Davis, B. *Inorg. Chem,.* **1991**, *30*, 334.; Sessler, J. L.; Sibert, J. N.; Lyanch, V.. *Inorg.Chem.*, **1990**, *29*, 4143.

[19] Cotton, F.A.; Daniels, L.M.; Matonic, J.H.; Murillo, C.A. *Inorg. Chim. Acta* **1997**, *256*, 277.

[20] Bailey, P.J.; Bone, S.F.; Mitchell, L.A.; Parsons, S.; Taylor, K.J.; Yellowlees, L.J. *Inorg. Chem.* **1997**, *36*, 867

[21]Walther, B.; Harting, H.; Reinhold, J.; Jones, P. G.; Mealli, C.; Böttcher, H.-C.; Baumeister, U.; Krug, A.; Möckel, A. *OrganometallicsI, 1992*, 11, *1542.*

[22] Cotton, F. A.; Daniels, L. M.; Falvello, L. R.; Matonic, J. H.; Murillo, C. A. *Inorg. Chim. Acta*, **1997**, *256*, 269.

[23] Klose, A.; Solari, E.; Floriani, C.; Chiesi-Villa, A.; Rizzoli, C.; Re, N. *J. Am. Chem. Soc.*, **1994**, *116*, 9123. Klose, A.; Solari, E.; Ferguson, R.; Floriani, C.; Chiesi-Villa, A.; Rizzoli, C. *Organometallics*, **1993**, *112*, 2414.

Epilogue

"well do ya punk?"

Epilogue

There can hardly be an overall conclusion to the work presented here as much of it can and hopefully will be expanded upon in the future (albeit *sans* the author of this thesis). As such, this epilogue will hopefully serve as a prologue to future works from within our group (and yes, I am aware that there are conclusions at the end of each chapter). The body of work you are holding in your hand began with a desire to make terminal chalcogenido species of heavy group 14 elements and investigate chalcogen atom exchange reactions between them. To this end the work went surprisingly well. A variety of terminal chalcogenides were discovered and atom exchange reactions between tin and germanium were studied. However, only sulfur atom exchange reactions could be studied as only the terminal sulfide of tin could be prepared.

The chemistry was then extended into the cleavage of chalcogen-chalcogen bonds. Cyclotetrasulfides, sulfur bridged species and diphenyldichalcogenido complexes of tin and germanium were prepared. It was during this work when we discovered that these complexes exhibit a remarkable catalytic tendency towards the trimerization of aryl isocyanates resulting in the formation of isocyanurates.

Extending the NCN ligand motif through the inclusion of guanidinates resulted in the formation of the first reported guanidinate complexes of tin. Contrary to reported transition metal complexes, use of the hpp anion in the preparation of tin complexes usually resulted in the formation of mononuclear species. An exception was observed in

the formation of the mono ligand complex where a dinuclear species with bridging hpp ligands resulted.

Concurrent with these results were investigations into the formation of amidinate and guanidinates complexes of both Fe(II) and Fe(III). The transition metal chemistry was originally motivated by a lack of terminal chalcogenido complexes of the first row transition metals Cr, Mn and Fe. While isolation of a terminal chalcogenido complex of iron is unlikely, we were interested in the formation of sulfur bridged species. Unfortunately, we were unable to isolate any such complexes. Thus the iron work serves as an introduction into the formation amidinate and guanidinate complexes of iron. Subsequent reactivity of the Fe(III) complexes was dominated by reduction to Fe(II) followed by, in the case of guanidinates, deprotonation of the guanidinate anion to form dianionic guanidinate complexes. These iron complexes may have applications in catalytic formation of polyolefins and polyisocyanates.

I have nothing to put in my stew, you see,
Not a bone or a bean or a black-eyed pea,
So I'll just climb in the pot to see
If I can make a stew out of me.
I'll put in some pepper and salt and I'll sit
In the bubbling water - I won't scream a bit.
I'll sing while I simmer, I'll smile while I'm stewing,
I'll taste myself often to see how I'm doing.
I'll stir me around with this big wooden spoon
And serve myself up at a quarter to noon.
So bring out your stew bowls,
You gobblers and snackers.
Farewell - and I hope you enjoy me with crackers!